Molecular characterization and functional analysis of poor-prognosis B-cell leukemias

Nadia Bougacha

SCIENCES SORBONNE UNIVERSITÉ

DOCTORAL THESIS

Presented to the Faculty of Sciences of Sorbonne Université
In Candidacy for the Degree of Doctor of Philosophy (PhD)

Specialty: Physiology, Physiopathology and Therapeutics (ED394)

Molecular characterization and functional analysis of poor-prognosis B-cell leukemias

Nadia BOUGACHA

Defended on Friday December 20, 2019
Pierre and Marie Curie Campus, Paris

Before a jury comprising:
Pr. Xavier HOUARD – Thesis advisor
Pr. Fawzia LOUACHE - Rapporteur
Pr. Eric SOLARY - Rapporteur
Pr. Muriel UMBHAUER – Jury President

Abstract

The overall aim of this thesis consisted of expanding the current understanding of the genetic basis and physiopathology of aggressive B-cell leukemias, namely in chronic lymphocytic leukemia (CLL) subtypes and in B-cell prolymphocytic leukemia (B-PLL).

CLL, the most common form of adult leukemia in the West, is characterized by an accumulation of monoclonal B cells (CD20+, CD5+ and CD23+) in the peripheral blood, bone marrow, and secondary lymphoid organs. CLL is a highly heterogeneous disease, with a large panel of genetic alterations leading to variable clinical outcomes.

Gain of the short arm of chromosome 2 (2p gain) is a frequent chromosomal abnormality in CLL and in other malignancies. Our group has reported that 2p gain was associated with drug refractoriness and poor prognosis factors such as unmutated *IGHV* and 11q deletion. Using cytogenetic and molecular analyses, we have notably identified a minimal region of gain which encompasses among others *XPO1* and ***REL***. In my main thesis project, functional analysis of the role of ***REL***, using three complementary strategies of pharmacological inhibition, gene knockout and transcriptional activation, led to its identification as a key player driving cell survival in CLL. Moreover, I developed several CLL cellular models that allow the overexpression of any gene, alone or in combination, in order to further investigate the roles of ***REL*** and *XPO1* in CLL and identify potential oncogenic cooperation driving phenotypic features of 2p gain CLL. Finally, we have analyzed the hierarchy and the clonal evolution of the chromosomal abnormalities in 2p gain CLL.

CLL with 17p deletion, del(17p), is associated with a lack of response to standard treatment and thus the worst clinical outcome. Our findings showed that del(17p) and 8q24 gain have a synergistic impact on outcome, therefore patients with this "double-hit" CLL have a particularly poor prognosis.

B-PLL is an aggressive leukemia, usually resistant to standard chemo-immuno therapy, defined by the presence of prolymphocytes in peripheral blood exceeding 55% of lymphoid cells. We described the cytogenetic and molecular features of a large cohort of 34 B-PLL cases, as well as their *in vitro* response to novel targeted drugs.

Altogether, this work enabled a better understanding of CLL and B-PLL, as well as paving the way for the development of novel therapeutic strategies.

Key words: chronic lymphocytic leukemia, ***REL***, NF-κB, XPO1, del(17p), 2p gain, drug resistance, B-cell prolymphocytic leukemia.

Résumé

L'objectif général de cette thèse a été d'approfondir la compréhension actuelle des bases génétiques et de la pathophysiologie de leucémies B agressives, à savoir deux sous-types de leucémie lymphoïde chronique (LLC) et la leucémie prolymphocytaire B (LPLB).

La LLC, qui est la forme de leucémie adulte la plus fréquente en Occident, est caractérisée par une accumulation de lymphocytes B monoclonaux (CD20+, CD5+ and CD23+) dans le sang périphérique, la moelle osseuse ainsi que les organes lymphoïdes secondaires. La LLC est une maladie très hétérogène, où un large panel d'altérations génétiques mènent à des résultats cliniques variables.

Le gain du bras court du chromosome 2 (gain 2p) est une anomalie chromosomique récurrente dans la LLC et d'autres cancers. Notre groupe avait décrit l'association du gain 2p avec la résistance aux traitements et des facteurs de mauvais pronostic comme l'*IGHV* non-muté et la délétion 11q. Des analyses cytogénétiques et moléculaires nous ont notamment permis d'identifier une région minimale de gain incluant entre autres les gènes *XPO1* et *REL*. Dans la partie principale de ma thèse, l'analyse fonctionnelle du rôle de *REL*, par trois stratégies complémentaires d'inhibition pharmacologique, d'inactivation du gène et d'activation transcriptionelle, a permis l'identification de *REL* comme un acteur central de la survie cellulaire dans la LLC. De plus, j'ai développé plusieurs modèles cellulaires de LLC permettant la surexpression de n'importe quel gène, seul ou en combinaison, pour approfondir les études sur *REL* et *XPO1*, et identifier de potentielles coopérations oncogéniques menant au phénotype des LLC avec gain 2p. Enfin, nous avons analysé la hiérarchie et l'évolution clonale des anomalies chromosomiques dans les LLC avec gain 2p.

La LLC avec délétion 17p est associée avec une absence de réponse aux traitements standards et donc avec la pire issue clinique possible. Nous avons montré que la délétion 17p et le gain 8q24 ont un impact synergique sur le résultat clinique, et que les patients ayant cette LLC « double-hit » ont un pronostic particulièrement défavorable.

La LPLB est un lymphome agressif, habituellement résistant aux chimio-immunothérapies standard, et défini par la présence de prolymphocytes dans le sang périphérique excédant 55% des cellules lymphoïdes. Nous décrivons les aspects cytogénétiques et moléculaires d'une large cohorte de 34 cas de LPLB, ainsi que leurs réponses aux nouveaux inhibiteurs spécifiques *in vitro*.

In fine, notre travail a permis une meilleure compréhension de la LLC et de la LPLB, et d'ouvrir la voie au développement de nouvelles stratégies thérapeutiques.

Mots-clés : leucémie lymphoïde chronique, *REL*, NF-κB, *XPO1*, del(17p), gain 2p, résistance aux traitements, leucémie prolymphocytaire B.

A ma famille,
Innée et acquise

« Being stupid is like being dead:
It is only painful for others" – Ricky Gervais

Acknowledgements

Ce doctorat est le fruit d'un dur labeur, de dévouement et d'efforts incessants durant plus de 4 années. Je tiens à remercier chaleureusement toutes les personnes qui y ont contribué, que ce soit par le partage de leurs connaissances et compétences, de bons moments passés ensemble au labo ou ailleurs, et surtout par leur soutien indéfectible.

Je tiens à remercier les membres de mon jury de thèse, qui m'ont fait l'honneur d'évaluer mon travail : merci au Pr Xavier Houard, qui a accepté d'être mon directeur de thèse, pour son suivi et pour la préparation de la soutenance, merci au Pr Muriel Umbhauer d'avoir accepté la Présidence du jury, et merci infiniment aux rapporteurs, Pr Fawzia Louache et Pr Eric Solary, qui ont pris le temps d'étudier mon manuscrit et de proposer des suggestions pertinentes m'ayant permis de l'améliorer.

Je remercie les services de Sorbonne Université, l'ensemble des collaborateurs de l'équipe « Mort cellulaire et résistance aux traitements dans les hémopathies malignes » au Centre de recherche des Cordeliers, ainsi que ceux du service Hématologie Clinique de la Pitié-Salpêtrière, et enfin ceux de l'unité « Hématopoïèse normale et pathologique » à l'Institut Gustave Roussy. Merci aussi aux patients et à leurs familles, ainsi qu'aux donneurs de sang.

En particulier, je remercie mes co-équipiers Dr (Hussein) Ghamlouch, Dr Michela Esposito, Dr Cécile Herate, Dr Véronique Della Valle, Dr Camille Decaudin, Dr Laure Delestré, Dr Cyril Quivoron, Dr Muriel David, Dr Cécile Thirant, Dr Zakia Aid, Dr Cécile Lopez, Dr Mira Khoury, Dr Claire Marceaux, Aurélie Siret, Dr Enguerran Mouly et Khadija Diop pour tout ce qu'ils m'ont appris, pour leurs conseils avisés et leur aide précieuse. Merci beaucoup à Christine Muamba pour son soutien et son humanité. Je tiens à exprimer ma profonde gratitude envers Pr em Najet Debili, Dr Julie Rivière, Dr Christel Guillouf, Dr Salima Benbarche et Dr Natalie Droin pour leurs conseils et aide technique sur des questions pointues, ainsi que pour leur bienveillance. Je remercie mes amis doctorants Tracy Dagher, Rameez Ishaq, Dr Deshan Ren, Sebastian Gregoricchio, Esteve Noguera, Dr Shoutang Wang et David Brandao pour avoir en plus été mes compagnons dans cette aventure incroyable, merci pour votre amitié, pour les fous rires autour d'un café ou d'un brunch, merci pour les conseils, l'écoute et le soutien. Je remercie tous les scientifiques que j'ai eu la chance d'écouter en congrès ou de lire dans les revues, qui m'inspirent et éveillent continuellement ma curiosité.

Enfin je remercie du fond du cœur mes proches : votre soutien, vos encouragements, votre confiance en mes capacités m'ont permis de persévérer et de dépasser les obstacles pour toujours avancer. Je vous aime de tout mon être et je vous dois toutes mes réussites.

Table of contents

Abstract 3

Résumé 4

Acknowledgements 6

Abbreviations 10

List of figures 15

List of tables 16

Introduction 17

Chapter I: Hematopoiesis *18*
1. Generating and regenerating the blood system 18
2. An evolutionarily conserved process 20
3. Regulation of hematopoiesis 21

Chapter II: B lymphocytes *23*
1. Physiological functions of B cells 23
2. B-cell development and regulation 23
3. Structure and function of immunoglobulins 26
   3.1. VDJ recombination 26
   3.2. Clonal selection and affinity maturation 28
4. Deregulation of B cell pathways and cancer 30

Chapter III: Chronic Lymphocytic Leukemia (CLL) *31*
1. Hallmarks of CLL 31
2. Diagnosis and clinical staging 32
3. The genomic and epigenomic landscape of CLL 35
   3.1. Chromosomal abnormalities 35
   Deletion 13q14 37
   Trisomy 12 37
   Deletion 11q22-23 38
   Deletion 17p13 38
   2p gain 38
   Other chromosomal abnormalities 38
   3.2. Somatic mutations 39
   3.3. Epigenetic alterations 41
4. CLL metabolism and microenvironment dependency 42
5. Cell of origin 45
6. Convergent evolution, clonal evolution and Richter syndrome 46
7. Clinical management of CLL 49
   7.1. Chemo-immunotherapy 49
   7.2. Targeted therapies 50
   7.3. Emergence of drug resistance 51
   7.4. Combination strategies 52

Chapter IV: Gain of the short arm of chromosome 2 (2p gain) *53*
1. Prevalence of 2p gain/amplification in cancer 53
   1.1. Non-hematological cancers 53
   1.2. Hematological cancers 53
2. Incidence and evolution of 2p gain in CLL 53
3. Impact of 2p gain on CLL disease progression 55
4. Putative oncogenic drivers in 2p gain CLL 56

4.1. Candidate oncogenes 56
XPO1 (2p15) 57
REL (2p16.1) 58
PAPOLG (2p16.1) 58
BCL11A (2p16.1) 58
MSH2 (2p21) 60
ALK (2p23) 60
NCOA1 (2p23.3) 62
MYCN (2p24.3) 62
ROCK2 (2p25.1) 63
ACP1 (2p25.3) 64
CAV1 (7q31.1) 64
4.2. Strategies for targeting of 2p genes 64
XPO1 64
REL 65
BCL11A 65
MYCN 65
ROCK2 66
4.3. Possible oncogenic cooperation within the 2p 66
REL-BCL11A 66
ALK-MYCN 66
2p oncogenes – TP53 67
2p oncogenes – BCL2 67

Chapter V: REL/NF-κB *68*
1. The NF-κB genes and pathways 68
1.1. Canonical/Classical pathway 69
1.2. Non-canonical/Alternative pathway 69
2. NF-κB: a "double-edged sword' in health and disease 69
2.1. REL/ NF-κB deregulation in cancer 70
2.2. REL/ NF-κB deregulation in CLL 70
3. The c-Rel subunit 72
3.1. Direct targets of c-Rel 74
3.2. Knockout phenotype and physiological functions of c-Rel 74
3.3. Functions of c-Rel in oncogenesis 75
3.3.1. Transforming abilities 76
3.3.2. REL gains/amplifications 76
3.3.3. REL mutations 77
3.3.4. Interactions with oncogenic REL 78
3.3.5. Reports of c-Rel implication in drug resistance 78
4. Targeting NF-κB 78
4.1. Pan- NF-κB inhibitors 78
4.2. Targeting c-Rel 79

Chapter VI: Programmed cell death *82*

1. Apoptosis *82*
1.1. Bcl-2 family of proteins 82
1.2. Caspases 83
1.3. Extrinsic apoptotic pathway 84
1.4. Intrinsic apoptotic pathway 85
1.5. Tumour resistance to apoptosis 86

2. Autophagic cell death *86*

3. Necrosis *86*

4. Pyroptosis *88*

5. Oncosis *88*

Chapter VII: CRISPR-Cas gene editing *90*
1. CRISPR-Cas defense systems 90
2. CRISPR/Cas9-mediated targeted genome editing 92
3. Designing CRISPR/Cas-based genome editing experiments with their specific caveats in mind 94
3.1. Targeting specificity 94
3.2. Cas9 integration and expression 95
3.3. Genome editing efficacy 95
3.4. Detection of on-target mutations 96
4. CRISPR/Cas9-mediated transcriptional regulation 97
4.1. CRISPRi: transcriptional repression 98
4.2. CRISPRa: transcriptional activation 98
5. Applications of CRISPR/Cas9 systems 99

Thesis objectives **101**

Results and discussion **105**

I - Gain in the short arm of chromosome 2 (2p+) induces gene overexpression and drug resistance in chronic lymphocytic leukemia: analysis of the central role of XPO1 ..... *106*

II – Functional Analysis of the role of REL in Chronic Lymphocytic Leukemia (CLL) cell survival and in 2p gain-associated drug resistance *123*

III - The Gain of the Short Arm of Chromosome 2 (2p gain) Plays an Important Role in CLL Drug Resistance, and Has to be Systematically Considered before Deciding an Adapted Therapy *145*

IV - "Double-hit" chronic lymphocytic leukemia: An aggressive subgroup with 17p deletion and 8q24 gain *148*

V – Genetic Characterization of B-Cell Prolymphocytic Leukemia (B-PLL): A Hierarchical Prognostic Model Involving MYC and TP53 Abnormalities. on Behalf of the Groupe Francophone De Cytogenetique Hematologique (GFCH) and the French Innovative Leukemia Organization (FILO) Group *160*

Conclusions and future perspectives **163**

Characterizing 2p gain in the era of precision medicine *164*

Multidrug resistance phenotype *165*

Developing relevant 2p gain CLL models *166*

Genome-scale screens *166*

Annex **169**

Bibliography **170**

Abbreviations

ADCC, antibody-dependent cellular cytotoxicity
AHSA2, AHA1 activator of heat shock 90 kDa protein ATPase homolog 2
AIF, apoptosis-inducing factor
ALCL, anaplastic large-cell lymphoma
ALL, acute lymphoid leukemia
AML, acute myeloid leukemia
ANGPTL5, angiopoietin like 5
ANKHD1, ankyrin repeat and KH domain containing 1
APAF1, apoptotic protease activating factor-1
ARID1A, AT-rich interaction domain 1A
ASPP, apoptosis stimulating protein of p53
ASXL1, additional sex combs like 1
ATLL, adult T-cell leukemia/lymphoma
ATM, ataxia telangiectasia mutated
ATP, adenosine triphosphate
ATRX, alpha thalassemia/mental retardation syndrome X-linked

BAD, Bcl-2-associated agonist of cell death
BAFF, B cell-activating factor
BAK1, Bcl-2 homologous antagonist/killer 1 (encodes BAK).
BAX, Bcl-2-associated X protein
BAZ2A, bromodomain adjacent to zinc finger domain 2A
BCL2, B-cell lymphoma 2 (encodes Bcl-2)
BCL11A, B-cell lymphoma/leukemia 11A
BCR, B cell receptor
BCOR, BCL6 co-repressor
BH, Bcl-2 homology
BID, BH3-interacting domain death agonist
BIM, BH3-interacting mediator (Bcl-2-like 11)
BIRC3, baculoviral IAP repeat containing 3
bp, base pair(s)
BRD4, bromodomain-containing 4
BTK, Bruton's tyrosine kinase

C11orf70, chromosome 11 open reading frame 70
Cas(9), CRISPR-associated protein (9)
CARD, caspase activation and recruitment domain
CCND2, cyclin D2
CDC, complement-dependent cytotoxicity
CDKN, cyclin-dependent kinase inhibitor
CDP, common dendritic progenitor
CGH, comparative genomic hybridization
CHD2, chromodomain helicase DNA binding protein 2
CLL, chronic lymphocytic leukemia
CLP, common lymphoid progenitor
CMP, common myeloid progenitor

CNOT3, CCR4–NOT transcription complex subunit 3
CREBBP, CREB-binding protein
CRISPR, Clustered Regularly Interspaced Short Palindromic Repeats
CRM1, chromosomal region maintenance 1 (XPO1)

DAMP, damage-associated molecular pattern
DcR3, decoy receptor 3
DD, death domains
DDX3X, DEAD box helicase 3, X-linked
DIABLO, Direct IAP-binding protein with low pI (SMAC)
DLBCL, diffuse large B-cell lymphoma
DNA, deoxyribonucleic acid
DNA-PK, DNA-dependent protein kinase
DSB, double strand break

EGR2, early growth response 2
ELP, early lymphoid progenitor
ER, endoplasmic reticulum
ERK, Extracellular signal-regulated kinase

FADD, FAS-associated protein with Death Domains
FBXW7, F-box and WD repeat domain containing 7
FC(R), fludarabine cyclophosphamide (rituximab)
FISH, fluorescent *in situ* hybridization
FL, follicular lymphoma
FLICE, FAS-associated DD protein-like interleukin-1β-converting enzyme-like protease
FLIP, FLICE-inhibitory protein
FR-CLL; fludarabine-resistant CLL
FUBP1, far upstream element (FUSE) binding protein 1

GMP, granulocyte–macrophage progenitor
GVHD, graft-versus-host-disease

H(D)R, homology (-directed) repair
HIST1H1B, histone cluster 1, H1b
HL, Hodgkin lymphoma
HSC, hematopoietic stem cell

IAP, inhibitor of apoptosis proteins
Ig, immunoglobulin
IGHV (-M or -UM), immunoglobulin heavy chain variable (-mutated or -unmutated)
IκB, inhibitor of NF-kappa B
IKK, IκB kinase
IKZF3, IKAROS family zinc finger 3
IRAK1, interleukin 1 receptor-associated kinase 1
IRF4, interferon regulatory factor 4
IT-, intermediate-term repopulating

KLHL6, kelch like family member 6

LLC, leucémie lymphoïde chronique
LN, lymph node
LMPP, lymphoid-primed MPP
LT-, long-term repopulating
LTβ, lymphotoxin-β
LUC7L2, LUC7-like 2 pre-mRNA splicing factor

MAPK, mitogen-activated protein kinase
MBL, monoclonal B lymphocytosis
MCL1, myeloid cell leukemia sequence 1
mDC, myeloid dendritic cell
MDP, monocyte–dendritic cell progenitor
MDR(1), multi-drug resistance (protein-1)
MED, mediator complex subunit
MEP, megakaryocyte–erythrocyte progenitor
MGA, MAX dimerization protein
ML-IAP, melanoma IAP
MLL2, mixed-lineage leukemia 2
MMP, matrix metalloproteinase
MOI, multiplicity of infection
MOMP, mitochondrial outer membrane permeabilization
MPP, multipotent progenitor
MSH2, MutS protein homolog 2
MYD88, myeloid differentiation primary response 88

NB, neuroblastoma
NF-κB, nuclear factor-κB
NFKBIE, NFκ light polypeptide gene enhancer in B cells inhibitor-ε
NGS, next-generation sequencing
NHL, non-Hodgkin lymphoma
NIK, NF-κB-inducing kinase
NK, natural killer cell
NKAP, NF-κB activating protein
NLS, nuclear localization signal
NPM, nucleophosmin (nucleolar protein)
nt, nucleotide(s)
NXF1, nuclear RNA export factor 1

OS, overall survival

PAPOLG, poly(A) polymerase gamma
PARP, poly(ADP-ribose) polymerase
PCLBCL, primary cutaneous large B-cell lymphoma
pDC, plasmacytoid dendritic cell
PEX13, peroxisomal biogenesis factor 13

PFS, progression-free survival
PI, propidium iodide
PI3K, phosphatidylinositol 3-kinase
PI-9/SPI-6, protease inhibitor 9/serine protease inhibitor 6
PMB(C)L, primary mediastinal B cell lymphoma
POLR3B, polymerase (RNA) III (DNA directed) polypeptide B
POT1, protection of telomeres 1
PS, phosphatidylserine
PTPN11, protein tyrosine phosphatase, non-receptor type 11
PUS10, pseudouridylate synthase 10

RANK, receptor activator of NF-κB
RHD, Rel homology domain
RID, REL inhibitory domain
RIP3, receptor interacting protein kinase 3
RNA, ribonucleic acid
ROS, reactive oxygen species
RPS15, ribosomal protein S15
RS, Richter syndrome

SCC, squamous cell carcinoma
SDS-PAGE, sodium-dodecyl sulfate polyacrylamide gel electrophoresis
SETD, SET domain containing
SF3B1, splicing factor 3b subunit 1
(s)gRNA, (single) guide RNA
shRNA, short-hairpin RNA
SINE, specific inhibitors of nuclear export
siRNA, small interfering RNA
SKIV2L2, superkiller viralicidic activity 2-like 2
SLL, small lymphocytic lymphoma
SMAC, second mitochondria-derived activator of caspases (DIABLO)
SNP, single-nucleotide polymorphism
ST-HSC, short-term repopulating HSC
STAT, signal transducer and activator of transcription
SYNE1, spectrin repeat containing, nuclear envelope 1

TAD1/2, transactivation domain 1/2
TALE, transcription activator-like effector
TCR, T-cell receptor
TIR, Toll/IL-1 receptor
TLR, Toll-like receptor
TLR2, Toll-like receptor 2
TMEM123, transmembrane protein 123
TNF(R), tumour necrosis factor (receptor)
TRAF3, TNF receptor-associated factor 3
TRAIL, tumor-necrosis factor-related apoptosis-inducing ligand
TSS, transcription start site
TTFT, time to first treatment

UBA, ubiquitin-associated domain
USP34, ubiquitin specific peptidase 34

WM, Waldenström's macroglobulinemia

XAF1, XIAP-associated factor 1
XIAP, X-linked inhibitor of apoptosis
XPO1, exportin 1

YAP1, yes-associated protein 1

ZAP-70, Zeta-associated protein of 70 kDa
ZF, zinc finger
ZMYM3, zinc finger, MYM-type 3
ZNF292, zinc finger protein 292

List of figures

Figure 1: Types of leukocytes in innate and adaptive immunity....20
Figure 2: Hierarchical models of hematopoiesis....21
Figure 3: Hematopoiesis in humans....22
Figure 4: Networks motifs for induction and maintenance of lineage commitment....24
Figure 5: B-cell development....25
Figure 6: Regulation of lineage commitment throughout B Cell Development....28
Figure 7: Representation of the chromosomal organization of the Ig H, κ, and λ gene clusters....29
Figure 8: V(D)J recombination of the heavy chain immunoglobulin (IgH) from germ line gene segments....30
Figure 9: B-cell differentiation in the GC reaction....31
Figure 10: Morphological appearances of CLL and CLL/PL....35
Figure 11: Recurrent cytogenetic abnormalities and genetic mutations in CLL....38
Figure 12: Chromosomal abnormalities and genetic mutations refine prognosis and risk classification....39
Figure 13: Clinical implications of gene mutations in CLL....42
Figure 14: Putative core CLL pathways....43
Figure 15: Methylation disorder and clonal selection in CLL....44
Figure 16: Cellular origin of human B-cell lymphomas....47
Figure 17: Clonal evolution is a major driving force in cancer progression and drug resistance....49
Figure 18: Coevolution of cancer and host-immune cells in CLL....50
Figure 19: Mechanism of action of venetoclax....53
Figure 20: Inferred evolutionary history of CLL....56
Figure 21: Gain of the short arm of chromosome 2p....59
Figure 22: Human BCL11A locus and predicted protein isoforms....61
Figure 23: The five mammalian NF-κB subunits....70
Figure 24: Canonical and non-canonical NF-κB signaling pathways....72
Figure 25: NF-κB pathway mutations in CLL....73
Figure 26: Structure and genomic location of human c-Rel....75
Figure 27: c-Rel interactome....77
Figure 28: Comparisons of domain structures of Bcl-2-family proteins....85
Figure 29: The caspase protein family....86
Figure 30: Extrinsic and intrinsic apoptotic signaling pathways....87
Figure 31: Progression of a normal cell, to an oncotic and necrotic cell....90
Figure 32: Genomic loci architecture of the components of class 1 and class 2 CRISPR-Cas systems and schematic representation of target interference for the different subtypes....93
Figure 33: Genome editing technologies exploit endogenous DNA repair machinery....95
Figure 34: Model of AcrIIC1 and AcrIIC3 Inhibition of Cas9....98
Figure 35: dCas9-mediated transcriptional modulation....100
Figure 36: the expanding CRISPR toolbox....102
Figure 37: REL could be a central piece of the CLL drug resistance puzzle....104

List of tables

Table 1: Structure and function of transcription factors implicated in the networks controlling B cell development....26
Table 2. The revised Matutes/Moreau scoring system....36
Table 3. The Rai staging system....36
Table 4. The Binet staging system....37
Table 5: Mechanisms of tumor resistance to apoptosis....89
Table 6: PCR-based methods for the detection of on-target mutations induced by sequence specific nucleases....99

Introduction

Chapter I: Hematopoiesis

1. Generating and regenerating the blood system

The blood system contains various blood cell types (or lineages) exerting different functions (Rieger and Schroeder, 2012):

- Erythrocytes, commonly known as red blood cells, provide O_2 and CO_2 transport.
- Megakaryocytes generate platelets for blood clotting and wound healing.
- Leukocytes, or white blood cells, embody several specialized cell types involved in innate and adaptive immunity: namely neutrophils, monocytes/macrophages, B and T lymphocytes… (**Figure 1**)

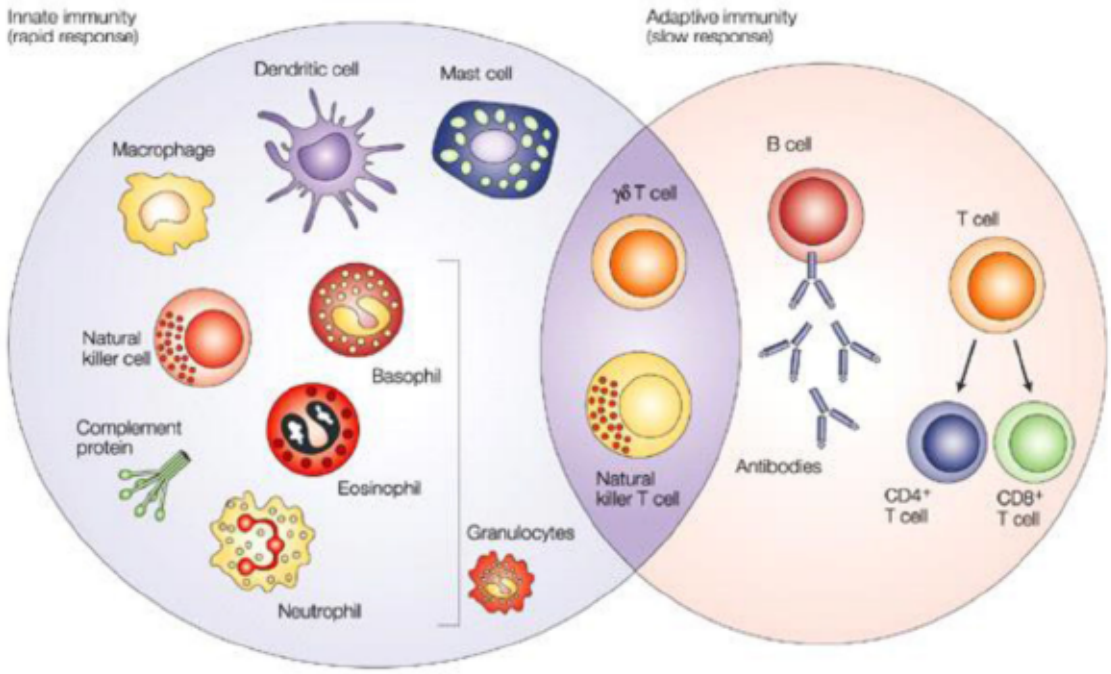

Figure 1: Types of leukocytes in innate and adaptive immunity (Dranoff, 2004).

Hematopoiesis designates the highly complex and dynamic process by which all these blood cells are formed, which occurs during embryonic development and throughout adulthood to generate and replace the blood cellular components (Jagannathan-Bogdan and Zon, 2013). Indeed, every second during life, millions of "old" blood cells are replaced with new ones. In response to stress situations such as anemia or infections, blood cell counts rapidly increase, then decrease back to normal following resolution (Rieger and Schroeder, 2012).

In adults, these components are formed from hematopoietic stem cells (HSCs), through an exquisitely intricate series of proliferation and differentiation events (Tavian et al., 2010).

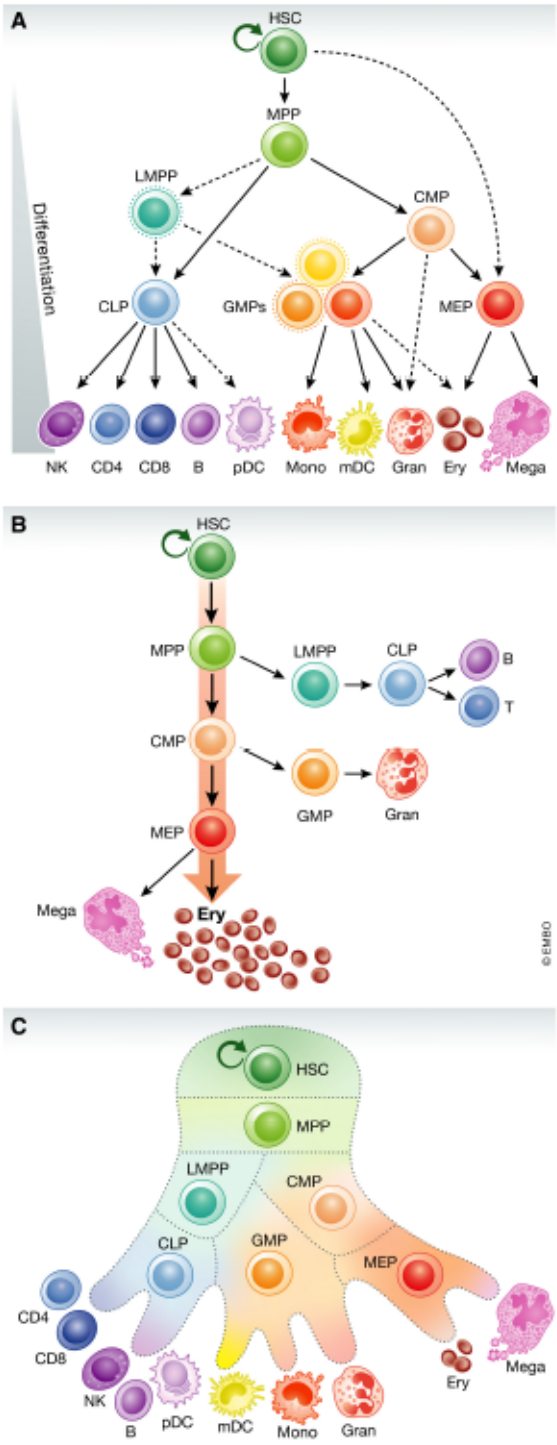

Figure 2: Hierarchical models of hematopoiesis. (A) Schematic of the human hematopoietic hierarchy. Dashed lines indicate recently discovered differentiation paths. mono, monocyte; gran, granulocyte; ery, erythroid; mega, megakaryocyte; CD4, CD4+ T cell; CD8, CD8+ T cell; B, B cell. (B) Quantitative depiction of hematopoietic hierarchy, in which erythroid commitment is the predominant and default pathway of differentiation. (C) Visualization of hematopoietic hierarchy in which lineage commitment occurs on a continuum rather than in punctuated stages, a perspective motivated by recent single-cell transcriptomic studies (Bao et al., 2019).

In fact, long-term (LT-) self-renewing HSCs are at the top of a cascade of multiple progenitor cell stages, which sequentially lose multilineage potential and commit to unilineage, ultimately yielding one of the mature blood cell types (Rieger and Schroeder, 2012).

Modelization of the hematopoietic differentiation hierarchy is constantly subject to evolution due to novel findings. Around the year 2000, HSCs were visualized as a homogeneous population downstream of which the first lineage bifurcation divides the myeloid and lymphoid branches via the CMP and CLP populations. During the years 2005 to 2015 this visualization integrated new findings: the HSC pool was now acknowledged to be more heterogeneous both in terms of self-renewal and differentiation properties, the myeloid and lymphoid branches remain associated further down in the hierarchy via the LMPP population, the GMP compartment is shown to be rather heterogeneous. From 2016 onwards, results gathered from single cell transcriptomics studies indicate a continuum of differentiation (Laurenti and Göttgens, 2018) (**Figure 2**).

Indeed, recent experiments where HSCs were barcoded and traced *in situ* in mice confirmed a treelike model of hematopoiesis with main myeloerythroid and common lymphoid arms (Höfer and Rodewald, 2018).

HSCs are identified by expression of high amounts of the receptor for stem cell factor, c-kit (CD117), and the absence of cell-surface proteins expressed on differentiated myeloid, erythroid, and T lineage cells. This lineage-negative (Lin–), CD117hi fraction of BM cells is highly enriched for long-term repopulating HSCs (Hardy et al., 2007; Spangrude et al., 1988).

2. An evolutionarily conserved process

This process is quite conserved among vertebrates, and the study of several model systems has allowed its fundamental understanding (Höfer and Rodewald, 2018).

In vertebrates, hematopoiesis occurs in two waves: the primitive wave and the definitive wave (Jagannathan-Bogdan and Zon, 2013).

The primitive wave, which occurs transiently during early embryonic development, primarily aims at producing red blood cells that can enable tissue oxygenation during rapid embryo growth (Galloway and Zon, 2003). Indeed, this phase implicates non-renewable erythroid progenitors that produce erythrocytes (red blood cells) and macrophages (Orkin and Zon, 2008).

The definitive wave occurs later in development, at different time points in different species. In most organisms, definitive hematopoiesis first involves erythroid-myeloid progenitors (EMPs) (Palis and Yoder, 2001), then hematopoietic stem cells (HSCs), which are multipotent cells that can produce all blood lineages of the adult organism. Definitive HSCs emerge in the aorta-gonad-mesonephros (AGM) region of

the developing embryo (Bertrand et al., 2007; McGrath et al., 2011), then colonize the fetal liver, the spleen and finally the bone marrow, which is the location for HSCs in adults (Ivanovs et al., 2011).

Specifically, in humans, hematopoiesis is initiated in the yolk sac and migrates into the liver momentarily, then definitively settles in the bone marrow and thymus (**Figure 3**).

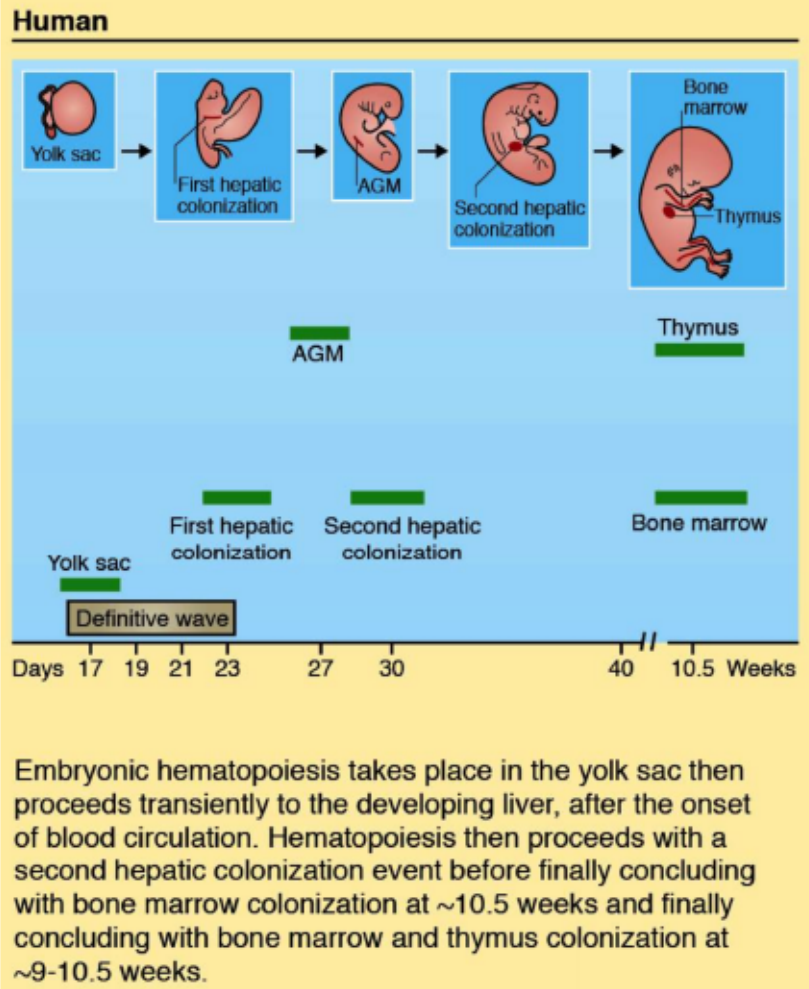

Figure 3: Hematopoiesis in humans (Jagannathan-Bogdan and Zon, 2013).

3. Regulation of hematopoiesis

The stem cell's decision to either self-renew or undergo differentiation must be tightly regulated to allow both the production of functioning mature cells and the precise maintenance of the right HSC count. Owing to its highly complex nature, a myriad of intrinsic and extrinsic factors have been reported to play important roles for HSC self-renewal and differentiation (Jagannathan-Bogdan and Zon, 2013).

Importantly, the microenvironment or niche is known to play a crucial role in the function of stem cells, by providing ligands that activate various signaling pathways in HSCs. Although still debated, it is generally admitted that signaling pathways such as the cytokine receptor c-Kit, Wnt, which is critical for embryonic development and Notch, involved in cell fate specification and pattern regulation, play

an important role in the regulation of HSC self-renewal (Rieger and Schroeder, 2012). For instance, activation of Notch pathway has been shown to stimulate expansion and self-renewal of both murine and human HSCs in adult hematopoiesis (Jagannathan-Bogdan and Zon, 2013). Examples of HSC intrinsic regulatory factors include transcription factors, signaling modulators, epigenetic modifiers, cell cycle regulators, microRNAs and RNA-binding proteins (Guruharsha et al., 2012).

Induction and propagation of a stable lineage commitment is orchestrated in a regulatory network of major transcription factors. Simplified examples are shown in figure (**Figure 4**).

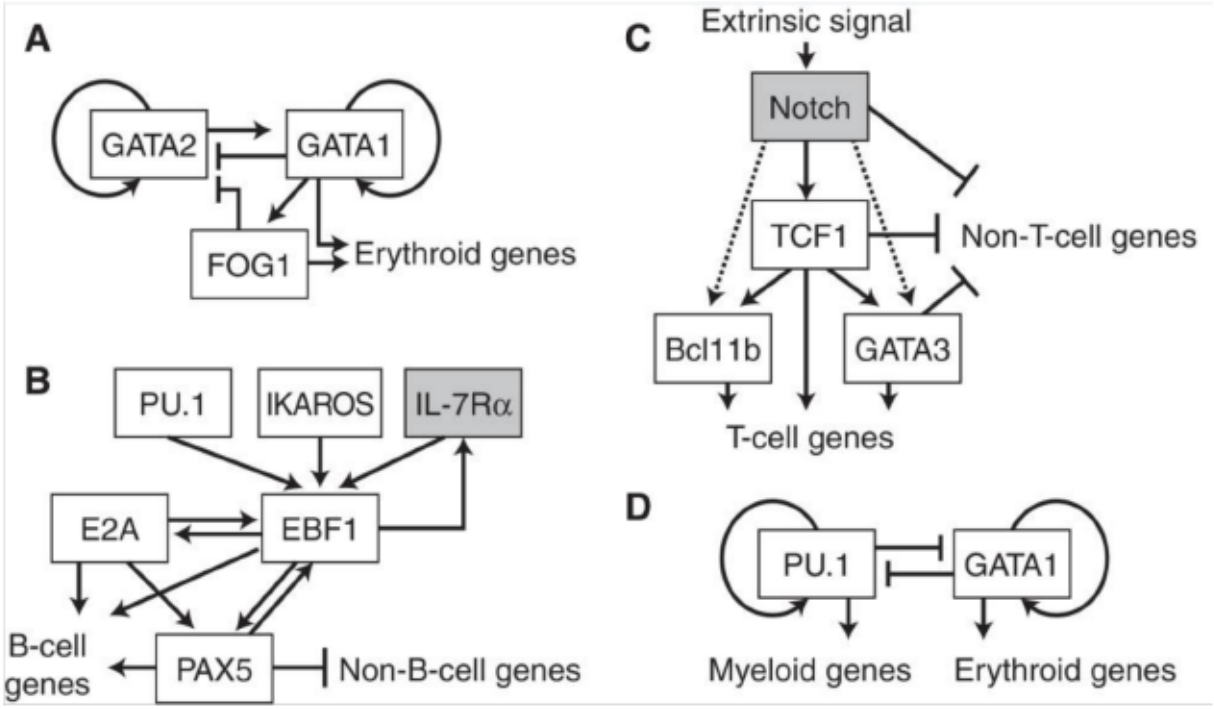

Figure 4: Networks motifs for induction and maintenance of lineage commitment in erythroid (A), B-lymphoid (B), T-lymphoid (C), and myeloid (D) cells. Direct or indirect activation (arrows) and repression (barred lines) of individual factor expression are indicated. Transcription factors are depicted in white, surface receptors in gray. Dashed lines represent indirect interactions (Rieger and Schroeder, 2012).

Chapter II: B lymphocytes

1. Physiological functions of B cells

B lymphocytes are key components of the adaptive immune system. Mature B cells, which are located in the spleen, lymph nodes and peripheral blood, are able to recognize a single antigen with high specificity. Naïve mature B cells, *i.e.* cells that have not encountered their antigen yet, scan all passing cells and particles, and will be activated upon antigen recognition. Activated cells subsequently undergo final differentiation into antibody-producing plasma cells and memory B cells.

2. B-cell development and regulation

Upon unilineage commitment of the common lymphoid progenitor, pro-B cells undergo a series of maturation stages to produce mature naïve B cells (**Figure 5**).

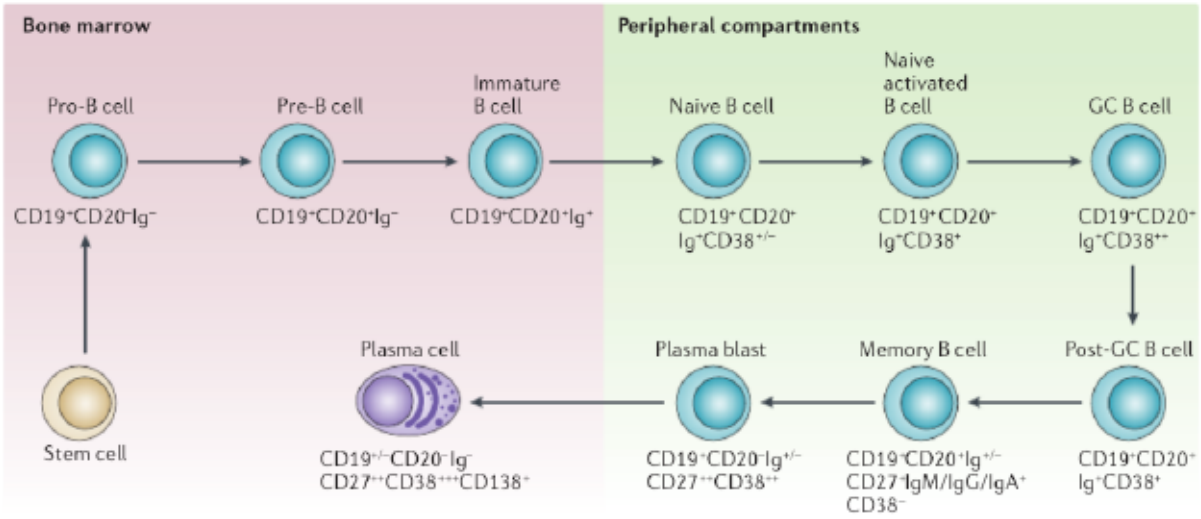

Figure 5: B-cell development. Stages of B cell maturation are indicated by their anatomical site and the expression of cell-surface markers (Edwards and Cambridge, 2006).

Regulation of lineage commitment in B-cell development relies on key transcription factors with feed-forward regulatory pathways. These complex and strongly regulated networks involve several factors (detailed in **Table 1**), acting in various contexts and combinations. Importantly, PU.1 and E2A are crucial for lymphoid cell-fate determination and induce specific B-lineage commitment factors such as early B-cell factor 1 (EBF1) and Pax5. The B-cell fate is stabilized by a feedback loop of Pax5 and IKAROS to maintain EBF1 expression (Decker et al., 2009; Nutt and Kee, 2007; Pridans et al., 2008; Rieger and Schroeder, 2012) (**Figures 4B and 6**).

Table 1: Structure and function of transcription factors implicated in the networks controlling B cell development (adapted from (Nutt and Kee, 2007)).

Transcription Factor (Gene Symbol)	DNA-Binding Motif (Consensus-Binding Sequence)	Ectopic Expression Phenotype	B Cell Phenotype of Mouse Germline (KO) and Conditional (cKO) Deficiency
PU.1 (*Sfpi1*)	Ets (A GGAAGT)	In PU.1 $^{-/-}$ fetal-liver cells graded amounts of PU.1 rescue B cell and macrophage development.	KO: lack fetal B cells and CLPs; cKO: normal B2 and expansion of B1 cells.
Ikaros (*Ikzf1*)	Zinc finger (T GGGAA)	N.D.	KO: lack all stages of B cell differentiation.
E2A (*Tcfe2a*)	bHLH (CANNTG, prefers ACACCTGC)	Induces cell-cycle arrest and apoptosis in T or B cell lines, in the 70Z/3 macrophage line induces B cell-lineage conversion.	KO: block prior to pre-pro-B cells; cKO: reduced survival in pre-B cell lines. Ectopic E protein antagonist: pro-B cell-growth arrest, decreased pro-B cell gene expression.
Early B cell factor, EBF1 (*Ebf1*)	Zinc knuckle (ATTCCCNNG GGAAT)	Induces B cell differentiation in multipotent progenitors, rescues B lymphopoiesis in PU.1 $^{-/-}$, E2A $^{-/-}$ or IL-7R $^{-/-}$ progenitors .	KO: arrest at CLP to pre-pro-B cell transition, no cells with *Igh* gene rearrangement.
Pax5 (*Pax5*)	Paired domain ($^{A/}{}_{G}$NCNANT $^{C/}{}_{G}$A $^{T/}{}_{A}$GCG $^{G/}{}_{T}$ $^{A/}{}_{G}$ $^{T/}{}_{A}$ $^{A/}{}_{C}$)	Impairs T cell development and promotes T cell-lymphoma formation. Variably affects myeloid and erythroid differentiation.	KO: Fetal liver lacks B lineage cells. Adult bone marrow block at pro-B cell stage but have D-J $_{H}$ but only a few proximal V-DJ $_{H}$ rearrangements; cKO: required for the maintenance of B cell fate and repression of plasma-cell differentiation.

Table 1 (continued)

Transcription Factor (Gene Symbol)	DNA-Binding Motif (Consensus-Binding Sequence)	Ectopic Expression Phenotype	B Cell Phenotype of Mouse Germline (KO) and Conditional (cKO) Deficiency
Aiolos (*Ikzf3*)	Zinc finger (T GGGAA)	N.D.	KO: regulates B cell activation and differentiation to effector stage. Represses λ5 in pre-B cells.
Sox4 (*Sox4*)	HMG-box (CCTTTGAA)	N.D.	KO: lethal at e13.5, pro-B cells fail to expand in IL-7 and few pro-B after fetal-liver transfer into irradiated adults.
Lymphoid enhancer factor, Lef1 (*Lef1*)	HMG-box (CCTTTGA/T A/T)	N.D.	KO: decreased pro-B cells in fetal liver and neonatal bone marrow, pro-B cells respond to IL-7 but not Wnt3a.
Bcl11a (*Evi9*)	Zinc finger (GGCCGG)	N.D.	KO: no B lineage cells.
GABP (*gabpa*)	Ets (A GGAAGT)	N.D.	Hypomorphic gene trap allele lethal between E12.5-14.5. Impaired B cell development and *Pax5* expression after fetal-liver transfer into irradiated adults.

All these factors function in a collaborative way in pro-B cells to warrant the repression of myeloid genes and hence warrant stability of B-cell commitment (Edwards and Cambridge, 2006).
Cells committed to the B cell lineage can be identified by expression of CD19, a target of the lineage-commitment factor Pax5 (Nutt and Kee, 2007).

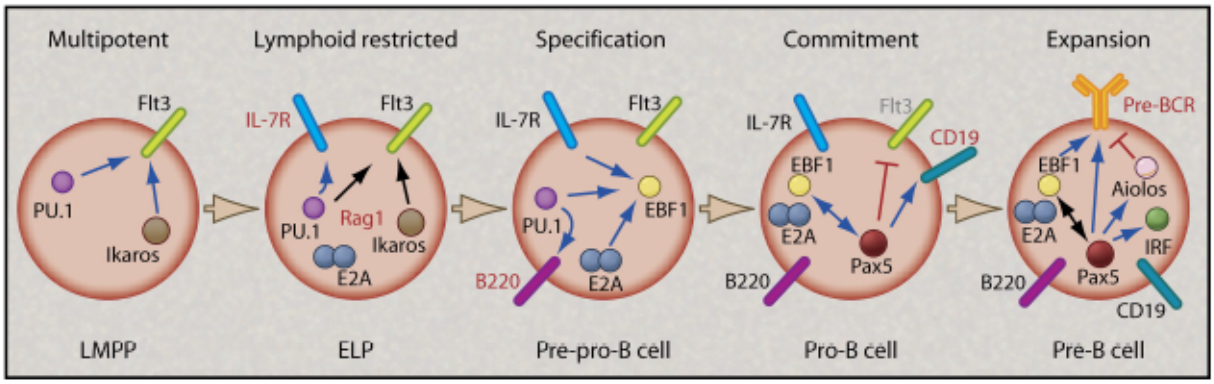

Figure 6: Regulation of lineage commitment throughout B Cell Development. Consecutive steps of differentiation from the LMPP (lymphoid-primed multipotent progenitor), ELP (early lymphoid progenitor), pre-pro-B cell, and committed pro- and pre-B cell are shown. Developmental capacities of the successive stages are indicated. Main transcription factors, growth-factor receptors, and cell-surface markers are shown, with important events started at a particular stage shown in blue. An arrow pointing upward indicates positive interactions, and ⊥ indicates gene repression. RAG1 expression is initiated in the ELP and is continued until throughout the remaining stages depicted. IRFs: interferon regulatory factor-4 and -8 (Nutt and Kee, 2007).

3. Structure and function of immunoglobulins

Mature naïve B cells express immunoglobulins at their surface. Each immunoglobulin (Ig) is a heterodimeric protein consisting of two identical heavy (H) chains and two identical light (L) chains, both of which harbor constant and variable regions. The L chain can consist of either a κ or a λ chain.

Functionally, variable domains on H and L chains specify the antigen binding site, while constant domains define effector functions such as complement activation or binding to Fc receptors (Schroeder et al., 2010).

Massive pools of specific B cells with unique Igs are produced in the bone marrow, collectively and virtually recognizing any given molecule. How is this diversity generated?

3.1. VDJ recombination

Igs are encoded by the Ig gene locus, which is organized in gene segments: the variable (V), diversity (D), joining (J) and constant (C) gene segments. V, D and J segments constitute the variable region. C gene segments encode the five main classes of heavy C domains, defining five main Ig isotypes with distinct biological properties: IgG ($C\gamma_{1\text{-}4}$), IgA ($C\alpha_{1\text{-}2}$), IgD ($C\delta$), IgM ($C\mu$) or IgE ($C\varepsilon$) (**Figure 7**).

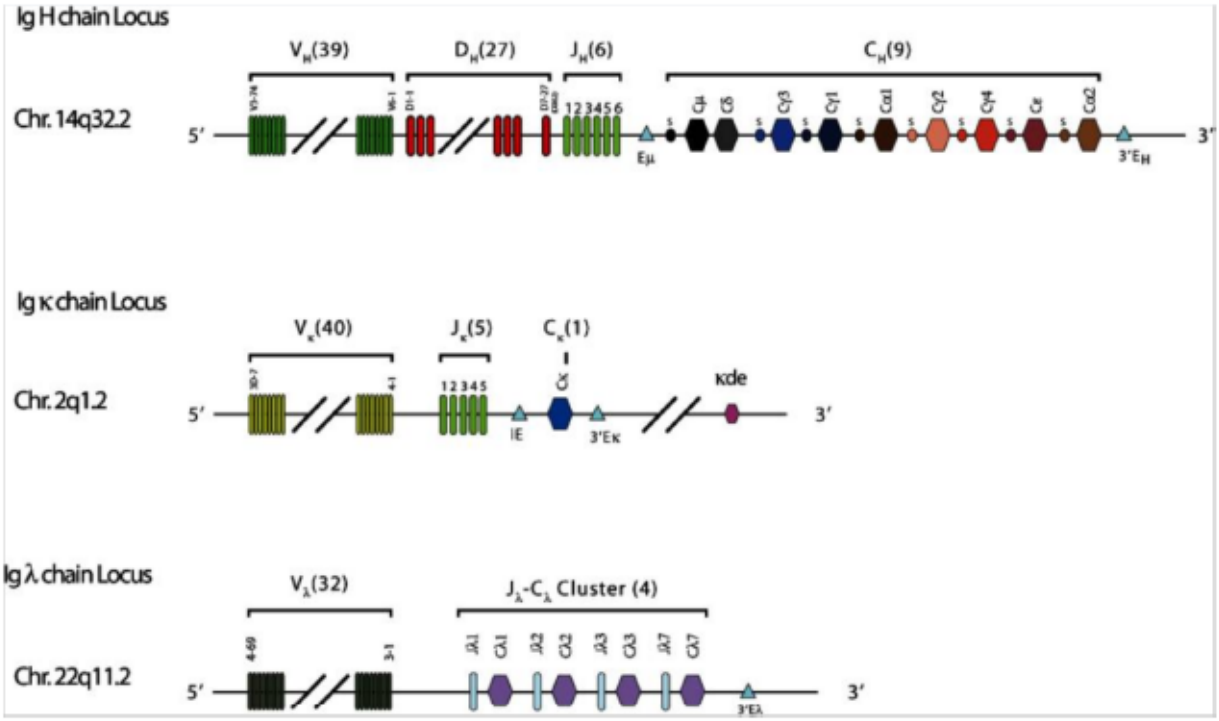

Figure 7: Representation of the chromosomal organization of the Ig H, κ, and λ gene clusters. The typical numbers of functional gene segments are shown. The κ gene cluster includes a κ deleting element that can rearrange to sequences upstream of Ck in cells that express λ chains, reducing the likelihood of dual κ and λ light chain expression (Schroeder et al., 2010).

VDJ recombination designates the process undergone by B (and T) lymphocytes (**Figure 8**), where each Ig is generated by random recombination of V, +/-D and J sequences to form the variable region, and thus generate a unique antigen receptor. Recombination is started by the lymphoid-specific RAG1 and RAG2 proteins, which cooperate to create double-strand breaks at specific recognition sequences (recombination signal sequences, RSSs). The adjacent coding DNA is converted to a hairpin during breakage. Broken ends are then processed and joined through the cooperation of numerous factors (DNA-dependent protein kinase (DNA-PK) and the Ku, Artemis, DNA ligase IV, Xrcc4 proteins…). V(D)J recombination is tightly regulated by limiting access to RSS sites within chromatin, so that particular sites are available only in certain cell types and developmental stages (Gellert, 2002).

Generation of immunoglobulin diversity is hierarchical and occurs at specific stages of B cell development (**Figure 5**). In pro-B cells, $D_H \rightarrow J_H$ joining is followed by $V_H \rightarrow DJ_H$ rearrangement. In-frame, functional VDJ_H rearrangement permits the production of μ H chains in pre-B cells, and $V_L \rightarrow J_L$ joining takes place at the late pre-B cell stage. Successful production of a complete κ or λ light chain allows expression of conventional IgM B cell receptor on the cell surface (sIgM), which is a hallmark of immature B cells. Maturation involves the extension of transcription of the H chain locus to include the Cδ exons downstream of Cμ. Alternative splicing authorizes co-production of IgM and IgD. These newly mature IgM+IgD+ B lymphocytes enter the blood and migrate to the spleen and the other secondary lymphoid organs where they form the majority of the B cell pool. The IgM and IgD on each of these cells

harbor the same variable domains, i.e. the same antigen specificity (Schroeder et al., 2010).

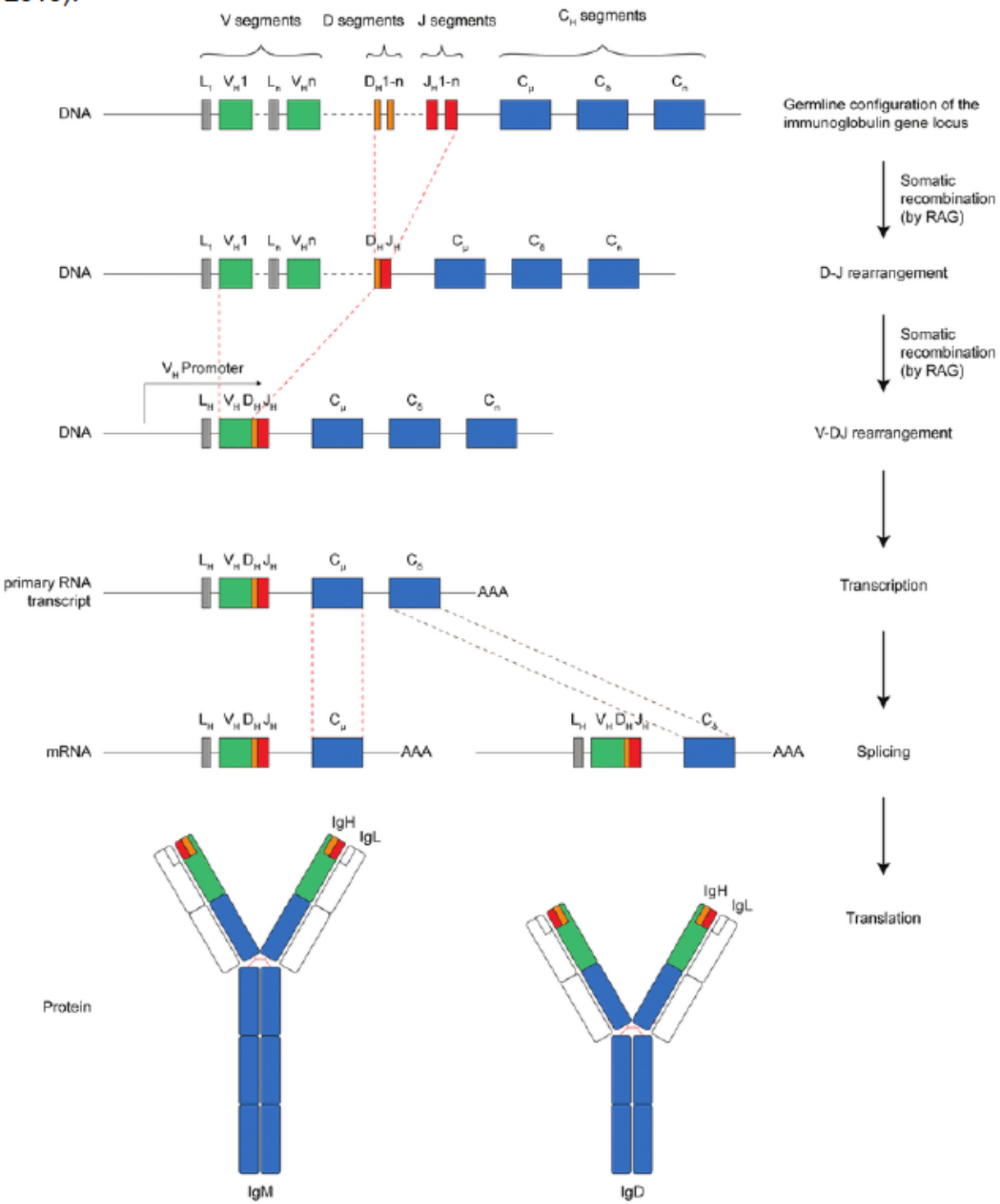

Figure 8: V(D)J recombination of the heavy chain immunoglobulin (IgH) from germ line gene segments (Backhaus, 2018)**.** L = leader sequence.

3.2. Clonal selection and affinity maturation

Upon maturation, lymphocytes are subject to stringent Darwinian selection. After leaving the bone marrow, mature unstimulated IgM+IgD+ B cells only live for a

few days or a few weeks. Recognition of their specific antigen leads to activation, which rescues them from programmed cell death. The activation method is critical:

- T cell independent stimulation of B cells prompts differentiation into short-lived plasma cells with limited class switching.
- T cell dependent stimulation typically induces the germinal center (GC) response, consisting of somatic hypermutation of the variable domains, thus enabling affinity maturation, class switching to the other isotypes, and differentiation into long-lived plasma cells or into a broad diversity of mutated memory B cells (Schroeder et al., 2010).

The GC reaction is a critical part of the antibody response (**Figure 9**): indeed, it corresponds to a delayed but sustained phase responsible for generating high-affinity antibodies of the IgG, IgA and/or IgE isotypes. Activated B cells in the GC undergo re-iterative cycles of somatic hypermutation of Ig gene variable regions, rapid cellular proliferation (clonal expansion) and Darwinian selection for cells expressing higher-affinity antibody variants (DeFranco, 2016). Both somatic hypermutation and class-switch recombination are initiated by activation-induced cytidine deaminase (AID), an enzyme that converts cytidine in DNA to uridine and that is strongly upregulated in GC B cells (Di Noia and Neuberger, 2007).

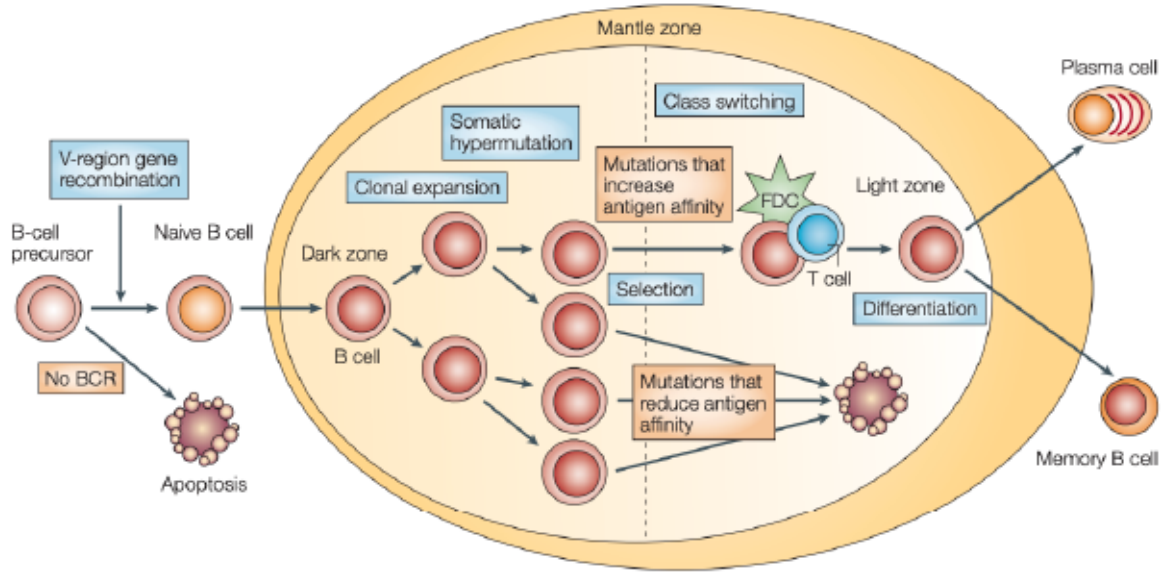

Figure 9: B-cell differentiation in the GC reaction. Mature (naïve, IgM+IgD+) antigen-activated B cells that receive signals from helper T cells are driven into primary B-cell follicles in secondary lymphoid organs such as lymph nodes, where they establish GCs (lightest yellow region). GC B cells are proliferating and relocate to the outside of the follicle, where they form a mantle zone around the GC. In the GC, a dark zone (left) and a light zone (right) can be distinguished. The dark zone primarily comprises proliferating GC B cells, whereas the GC B cells in the light zone are resting. In proliferating GC B cells, the process of somatic hypermutation is activated, which leads to the introduction of mutations at a high rate into the rearranged Ig variable region genes of the B cells. Most mutations are disadvantageous for the cells— such as those that lead to reduced affinity of the BCR for antigen and cause cells to undergo apoptosis. A few GC B cells will acquire

mutations in the BCR that increase their affinity for antigen, and these cells will be positively selected. The selection process presumably takes mainly place in the light zone, where the GC B cells are in close contact with CD4+ T cells and follicular dendritic cells (FDCs). A fraction of these GC B cells undergo class-switch recombination. Finally, GC B cells differentiate into memory B cells or antibody-producing plasma cells and leave the GC microenvironment (Küppers, 2005).

4. Deregulation of B cell pathways and cancer

Alterations in the regulatory pathways regulating B cell development and function lead to diseases such as immune deficiency, autoimmunity, and cancer (Nutt and Kee, 2007).
Importantly, subtle variations and deregulation of individual transcription factors will have a direct impact on normal differentiation and can induce leukemia (Backhaus, 2018). B cell tumors can arise from cells at various developmental stages and will maintain some characteristics of the normal B cell counterpart. Specifically, the oncogenesis and pathophysiology of chronic lymphocytic leukemia, and to a lesser extent, of prolymphocytic leukemia, will be discussed in **Chapter III**.

Chapter III: Chronic Lymphocytic Leukemia (CLL)

1. Hallmarks of CLL

Chronic Lymphocytic Leukemia (CLL) is the most common adulthood leukemia in Western countries, accounting for approximately 40% of adult leukemias and 25% of all leukemias. CLL is nearly twice as common in men as in women, and its incidence increases with age, the median age at diagnosis being of approximately 70 years (Rosenbauer et al., 2006).

CLL is a malignancy of mature-appearing, clonal B cells that accumulate in the blood, bone marrow and secondary lymphoid tissues. This accumulation is thought to be the result of both defective apoptosis (Fabbri and Dalla-Favera, 2016; Hernández et al., 1995; Hallek, 2019) as well as deregulated proliferation (Chiorazzi et al., 2005).

Immunophenotypically, CLL cells co-express the surface T cell marker CD5 together with the B cell antigens CD19, CD20 and CD23. Each clone of leukemia cells is restricted to expression of either kappa or lambda immunoglobulin light chains (Calissano et al., 2009).

The clinical course of CLL is highly variable, ranging from an indolent condition, with an almost normal life expectancy, to rapidly progressing, aggressive disease. The transformation of CLL to aggressive lymphoma is a rare but critical complication termed Richter syndrome (RS) (Fama et al., 2014; Landau et al., 2017; Woyach et al., 2014) (discussed in **Section III. 6**). This variability in outcome reflects a highly heterogeneous landscape of genetic abnormalities, which will be the main focus of this chapter (detailed in **Section III. 3**).

The load of somatic hypermutation of the rearranged immunoglobulin heavy-variable genes (*IGHV*) is one of the most important prognostic factors in CLL, as it defines two biologically and clinically distinct subgroups. Indeed, CLLs with unmutated *IGHV* genes (*IGHV*-UM, 40%) are linked with disease progression, whereas mutated *IGHV* genes (*IGHV*-M, 60% of CLL cases) tend to confer a favorable prognosis (Damle et al., 1999; ten Hacken et al., 2019; Hamblin et al., 1999).

These differences in clinical outcome between the two subtypes could reflect disparities in underlying mutagenic mechanisms: it was recently shown that *IGHV*-UM CLL is dominated by coding mutations in driver genes and an aging signature, while *IGHV*-M CLL has a high occurrence of promoter and enhancer mutations due to aberrant AID activity (Burns et al., 2018).

Usually, VDJ rearrangement generates one productive *IGHV*, but some CLL cells lack allelic exclusion and yield two productive rearrangements. Although there were no significant differences in survival and disease progression between patients with single or double (3-5% of samples) *IGHV* gene rearrangement, the presence of at least one mutated *IGHV* gene conferred a better prognosis (Hamblin et al., 1999).

Noteworthily, a cut-off of 2% deviation or 98% sequence identity to germline in *IGHV* sequence is currently used to classify CLL patients into mutated and unmutated groups. However, recent data indicated that *IGHV*% was rather a continuous variable significantly associated with survival. Indeed, higher *IGHV*% levels were incrementally associated with favorable PFS and OS in CLL patients treated with FCR (Jain et al., 2018).

Importantly, around 30-35% of CLL patients (with two thirds being UM-*IGHV*) express a largely skewed Ig repertoire, with quasi-identical BCRs, the so-called "stereotyped" receptors. Stereotyped subsets are associated with clinical features and outcome. BCR "stereotypy" denotes the existence of common antigenic determinants, which may favor CLL disease initiation and progression (ten Hacken et al., 2019).

Although the vast majority of CLLs occur sporadically, in 5-10% of cases, CLL develops in individuals with a family history of CLL, with a 7,5-fold increased risk in first degree relatives (Heyman et al., 2016; Rassenti and Kipps, 1997; Visco et al., 2013). Moreover, CLL predominantly affects individuals of European descent. However, the basis for this inherited predisposition remains ill-defined, even though several susceptibility loci were identified (Goldin et al., 2004); there are no major differences in terms of phenotype and clinical outcome between sporadic and familial CLL (Speedy et al., 2014).

Despite efficient treatments (discussed in **Section III. 7**), CLL remains incurable, with inevitable relapses. Identifying deregulated genes is therefore crucial for a better understanding of CLL pathogenesis and evolution, and hence for the development of novel targeted therapies.

2. Diagnosis and clinical staging

The international workshop on CLL, which recently published updated guidelines for the clinical management of CLL (Hallek et al., 2018, Hallek, 2019), provides that diagnosis of CLL requires the presence of $\geq 5x10^9$ B lymphocytes/L in the peripheral blood, sustained for at least 3 months.

Importantly, the presence of a clonal B lymphocyte population in the blood below that threshold, i.e. $< 5x10^9$ B lymphocytes/L, in otherwise healthy individuals, is termed monoclonal B cell lymphocytosis (MBL). MBL is viewed as a precursor state of CLL: the majority of MBL cases have the immunophenotype of CLL, and each year, 1-2% of MBLs progress to overt CLLs, probably as a result of progressive accumulation of genetic and epigenetic alterations as well as environmental factors (Hallek et al., 2018).

Circulating CLL cells display a characteristic and typical morphology in the majority of cases **(Figure 10A)**: most cells are small with normal mature morphological features (regular nucleus with clumped chromatin and no nucleoli, minimal cytoplasm), sometimes associated with smudge or basket cells (also called Gumprecht shadows), which correspond to remainders of fragile lymphocytes

disrupted by the smearing of the blood sample on a glass slide. The proportion of prolymphocytes defines distinct morphological classes of CLL and is associated with clinical features (Matutes and Polliack, 2000). 'Typical' CLL morphology is defined by < 10% prolymphocytes.

However, in 15% of cases, either at diagnosis or during disease progression, CLL cells display atypical morphology reflected by either:

- an increased (> 10%) number of circulating prolymphocytes, designated CLL/PL **(Figure 10B)**
- or an increased (> 15%) number of circulating lymphoplasmacytic and cleaved cells, designated 'atypical' CLL (Matutes and Polliack, 2000).

A cytological analysis showing a majority of prolymphocytes rules out CLL from the diagnosis. Indeed, this would rather be indicative of B-cell prolymphocytic leukemia (B-PLL), a distinct malignancy that is defined by ≥ 55% of prolymphocytes. These cells are large, have condensed non-clumped chromatin and a single vesicular nucleolus **(Figure 10D)** (Oscier et al., 2016).

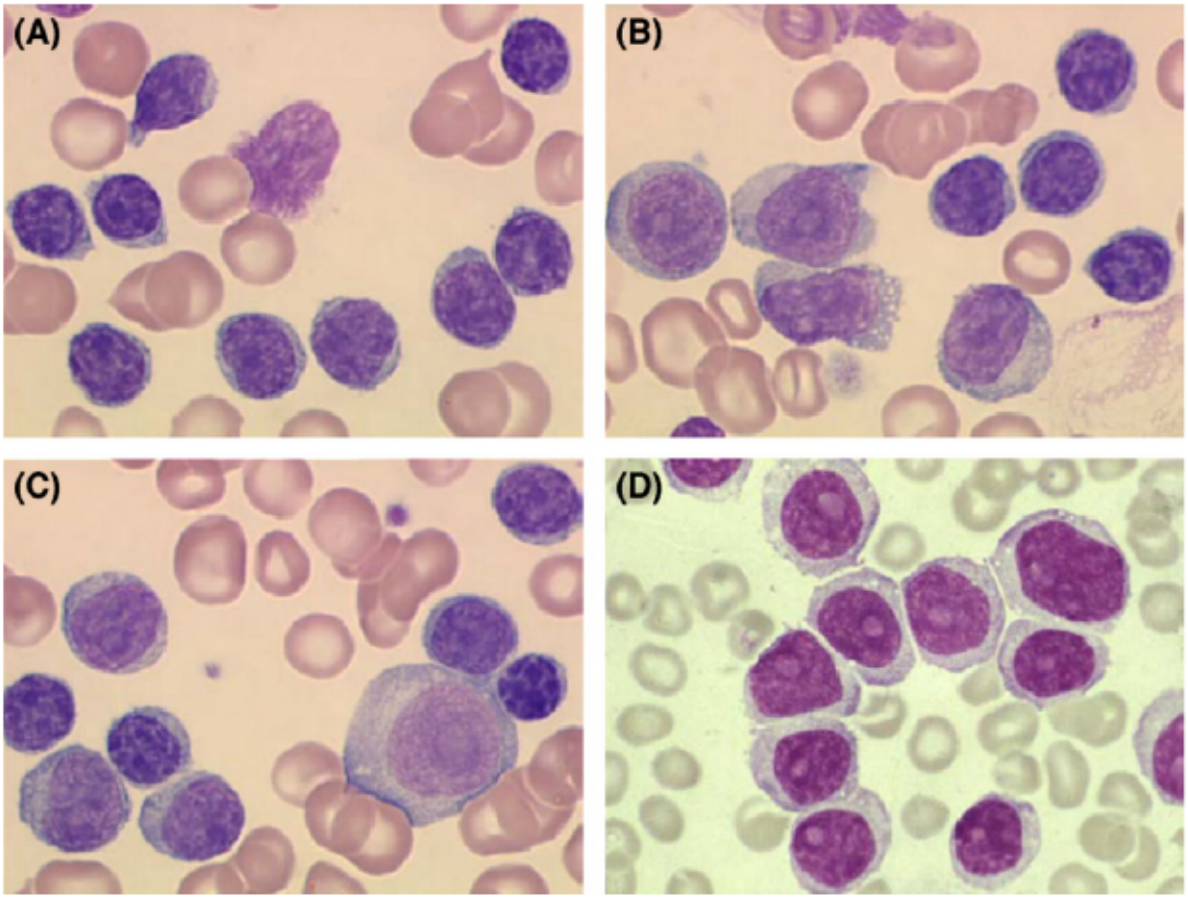

Figure 10: Morphological appearances of CLL and CLL/PL (>10% circulating prolymphocytes). (A) Typical CLL. (B) CLL/PL. There is a mixture of prolymphocytes and typical CLL lymphocytes. (C) CLL/ PL showing small lymphocytes, prolymphocytes and an immunoblast. (D) Typical B-cell prolymphocytic leukemia (B-PLL) (Oscier et al., 2016).

Moreover, a scoring system, termed the Matutes-Moreau score, was devised to aid the differential diagnosis of CLL, i.e. to distinguish CLL from other B-cell lymphoproliferative disorders. Based on the analysis of five immunological markers by flow cytometry (**Table 2**), this scoring system attributes for each of these five markers a value of 1 or 0 according to whether it is typical or atypical for CLL: a score of 4-5 corresponds to typical CLL, a score of 3 to atypical CLL while a score <3 excludes CLL from the diagnosis (Matutes et al., 1994; Moreau et al., 1997).

Table 2. The revised Matutes/Moreau scoring system (Matutes et al., 1994; Moreau et al., 1997)

Immunological marker	1 point	0 point
CD5	+	-
CD23	+	-
FMC7	-	+
Surface Igs expression	weak (+/-)	strong
CD79b (SN8) expression	weak (+/-)	strong

Noteworthily, replacing weak surface Igs expression by CD200 positivity kept high sensitivity but significantly increased specificity in differentiating CLL from non-CLL cases (Köhnke et al., 2017).

Upon diagnosis, two staging systems help stratify patients according to the disease risk, Rai (Rai and Montserrat, 1987; Rai et al., 1975) (**Table 3**) and Binet (Binet et al., 1981) (**Table 4**). Both classifications, based on physical examination and standard laboratory tests, describe 3 major prognostic groups with distinct clinical outcomes. Notably, the development of anemia and/or thrombocytopenia, indicating progressive bone marrow failure, is associated with high-risk disease (Binet et al., 1981).

Table 3. The Rai staging system (Rai and Montserrat, 1987; Rai et al., 1975)

Stage (original system)	Disease risk (revised system)	Criteria	Median survival (years)
0	low	Lymphocytosis (blood ± marrow)	> 10
I, II	intermediate	Lymphocytosis + lymphadenopathy + splenomegaly ± hepatomegaly	7-9
III, IV	high	Lymphocytosis + lymphadenopathy + splenomegaly ± hepatomegaly + Anemia ± thrombocytopenia	1,5-5

Lymphadenopathy refers to the enlargement of lymph nodes, anemia is defined by a hemoglobin (Hb) level < 1g/dL, and thrombocytopenia by a platelet count of < $100x10^9$/L.

Table 4. The Binet staging system (Binet et al., 1981)

Stage	Criteria	Median survival (years)
A	Hb ≥ 10g/dL + Platelets ≥ $100x10^9$/L + ≤ 2 areas involved	> 10
B	Hb ≥ 10g/dL + Platelets ≥ $100x10^9$/L + ≥ 3 areas involved	7
C	Hb < 10g/dL ± Platelets < $100x10^9$/L	5

Areas of involvement considered for Binet staging include enlarged lymph nodes (head and neck, axillae or groins) or organomegaly (palpable liver or spleen).

Patients who present with lymphadenopathy, organomegaly, and presence of infiltrating monoclonal B cells with the same immunophenotype as CLL cells, but without peripheral blood lymphocytosis, are diagnosed with small lymphocytic leukemia (SLL). CLL and SLL are presently considered as two faces of the same disease (Tees and Flinn, 2017).

CLL cells expressed significantly higher levels of CXCR3/CXCR4 (leukocyte trafficking/migration and homing receptors) and diminished CD49d levels (cell adhesion integrin alpha4 chain) compared to SLL cells, explaining why the majority of CLL malignant cells circulate in the blood, while SLL cells reside in tissues. Noteworthily, SLL is typically considered as a more progressive disease with a more complex genotype (Tooze et al., 2017).

3. The genomic and epigenomic landscape of CLL

Recent advances in massively parallel sequencing technologies allowed the identification of a vast number of genetic lesions in CLL (Puente et al., 2011). These studies have revealed a tremendous inter- and intra-patient heterogeneity, with a small number of "mountains" (i.e. frequently altered genes) and a relatively larger number of "hills" (i.e. infrequently altered genes) (Fabbri et al., 2011, 2013; Landau et al., 2013; Puente et al., 2011; Ramsay et al., 2013; Vogelstein et al., 2013) (**Figure 11**). However, importantly, no unifying genetic event accounting for all cases has been identified so far.

3.1. Chromosomal abnormalities

Recurrent chromosomal alterations are detected in more than 80% of CLL patients at diagnosis, and constitute important independent predictors of disease progression and survival (Guièze and Wu, 2015). Cytogenetic (and mutational) analyses are therefore crucial to refine prognosis and guide clinical practice (**Figure 12**). In addition to their prognostic relevance, the minimal deleted/gained region of some of these abnormalities have been found to contain within them putative CLL drivers.

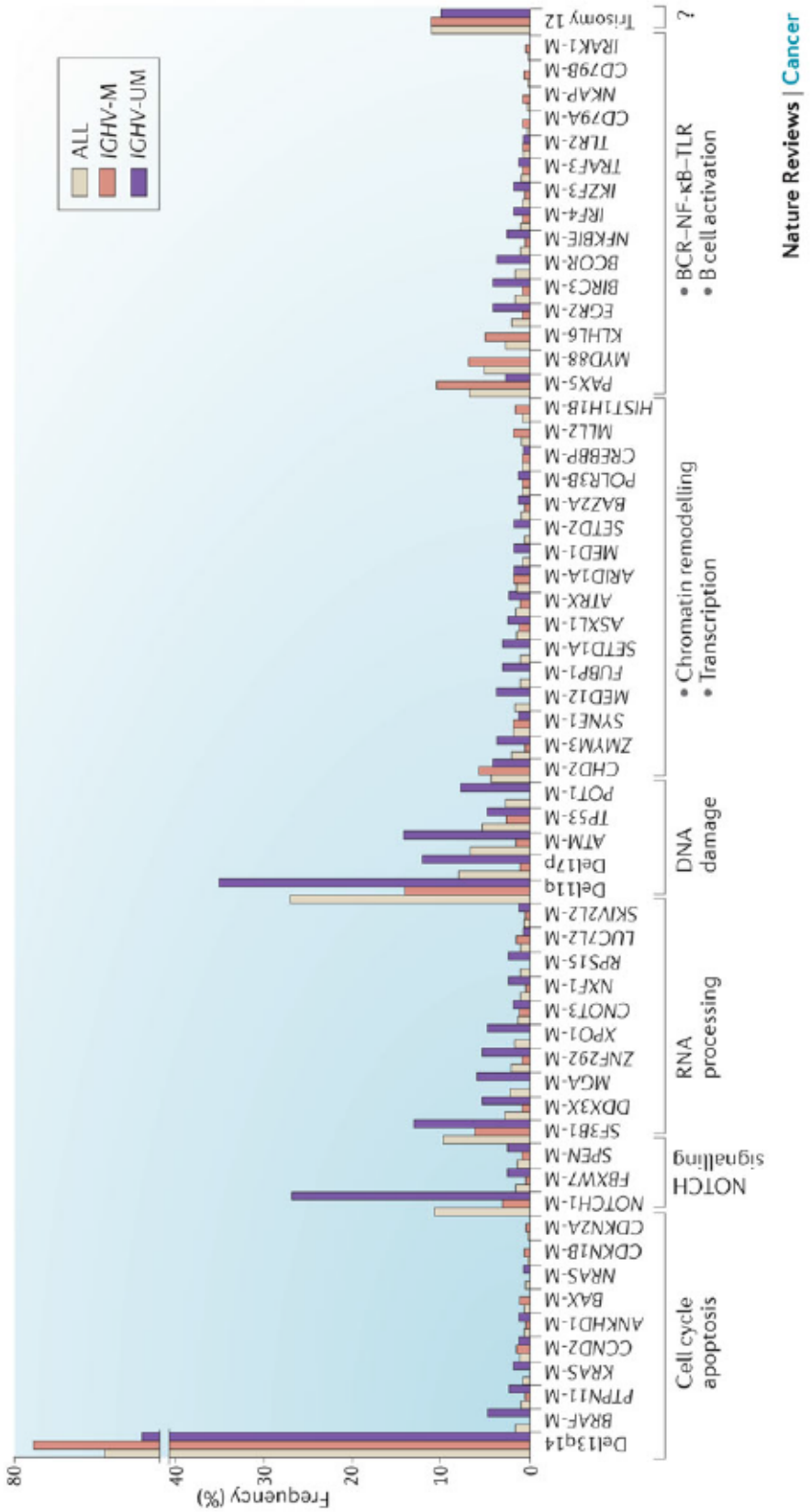

Figure 11: Recurrent cytogenetic abnormalities and genetic mutations in CLL, grouped according to the core cellular pathway in which they are involved (Fabbri and Dalla-Favera, 2016).

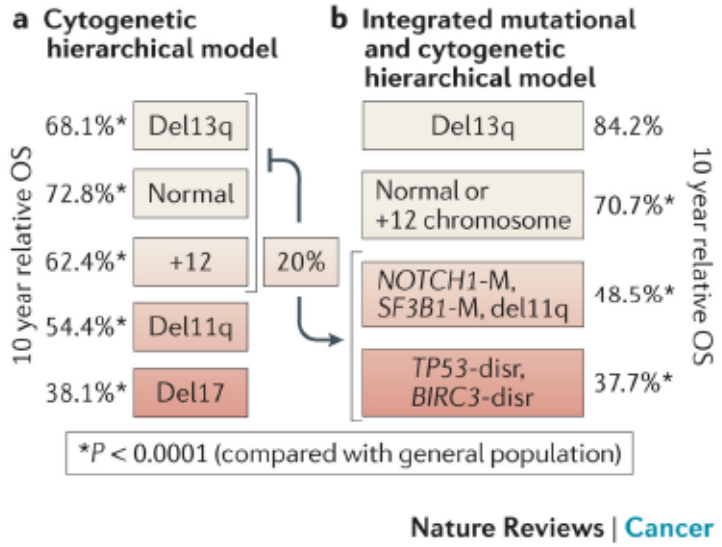

Figure 12: Chromosomal abnormalities and genetic mutations refine prognosis and risk classification (Fabbri and Dalla-Favera, 2016).

Deletion 13q14

Deletions involving chromosome band 13q14, or del(13q), are the most frequent genetic abnormality in CLL, occurring in 50-60% of patients (Döhner et al., 2000). Deletions are often monoallelic (80%) and heterogeneous in size, and the minimal region of deletion harbors the *DLEU2/MIR15A/MIR16-1* cluster (Calin et al., 2002). When functional, miR15A and miR16-1 are known to inhibit the expression of several genes, including the anti-apoptotic gene *BCL2* and genes controlling cell cycle entry (Calin et al., 2002). Deletion of the *MIR15A* and *MIR16-1* cluster alone is sufficient to generate CLL in mice, however, concurrent deletion of the *DLEU2* locus or larger deletions encompassing additional genetic elements were shown to increase the aggressiveness of the disease, suggesting that the loss of other tumor suppressors located on the 13q may contribute to CLL pathogenesis (Klein et al., 2010).

Del(13q) occur more frequently in *IGHV*-M patients and is generally associated with a favorable outcome. Specifically, in approximately 25% of CLL patients, del(13q) is the sole genetic lesion (i.e. occurring in the absence of any concomitant driver genetic abnormality), which is associated with an excellent prognosis, with a 10-year survival of 69,3% similar to a matched general population (Klein et al., 2010; Lia et al., 2012).

Trisomy 12

An extra copy of chromosome 12, or tri12, is detected in approximately 15-20% of CLL patients (Döhner et al., 2000; Roos-Weil et al., 2018). Tri12 is generally considered as an intermediate risk genetic lesion (Rossi et al., 2013). The co-occurrence of *NOTCH1* mutations confers an adverse prognosis and shifts the disease to higher-risk classes (Del Giudice et al., 2012). It was reported that tri12 is associated with a higher prevalence of thrombocytopenia, RS transformation and secondary cancers (Strati et al., 2015). However, the mechanisms by which tri12 contributes to CLL pathogenesis remain elusive.

Deletion 11q22-23

Deletion of 11q22-23, or del(11q), often encompasses *ATM* and *BIRC3* genes (Rossi et al., 2013). *ATM* is included in the minimally deleted region, and *BIRC3* deletion is always co-existing with *ATM* deletion. *BIRC3* deletion and/or mutation does not seem to have an impact on overall and progression-free survival (Rose-Zerilli et al., 2014).

ATM is a gene encoding a nuclear serine/threonine kinase which is induced by chromosomal double strand breaks (DSBs) and either activates the DNA repair pathways or induce apoptosis if the DNA damage cannot be repaired (Shiloh and Ziv, 2013).

In CLL, the *ATM* gene may be inactivated by deletion, mutation or both. *ATM* abnormalities are detected at diagnosis in approximately 6% of stage A patients and 20% of stages B/C patients, but their incidence increases to nearly 35% at the time of first line treatment (Rossi and Gaidano, 2016a; Skowronska et al., 2012).

Del(11q) is characterized by extensive lymph node involvement (Döhner et al., 1997) and is generally considered as an unfavorable factor associated with disease progression and poor response to chemotherapy (Rossi et al., 2013). In particular, biallelic *ATM* alterations are associated with significantly reduced survival and increased risk of death compared with patients with del(11q) alone or *ATM* mutation alone, and independently of treatment or *IGHV* status (Lozano-Santos et al., 2017; Skowronska et al., 2012).

Deletion 17p13

Deletion of 17p13, or del(17p), implicates *TP53*, a gene coding for a major tumor suppressor. In normal cells, *TP53* is a central regulator of the DNA damage response pathway, rebranding it as the "guardian of the genome". The latter pathway induces apoptosis in response to chemotherapy.

In CLL, *TP53* may be inactivated by deletion, mutation or both. Indeed, *TP53* mutations are often accompanied by the loss of the second allele through del(17p) (Rossi et al., 2009). *TP53* abnormalities are detected in 4-8% of newly diagnosed patients, mostly in IGHV-UM CLLs, but their occurrence increases with disease progression, reaching 10-12% at the time of first line treatment, 40% in fludarabine-refractory CLL and 50-60% in Richter syndrome (Döhner et al., 2000; Rossi and Gaidano, 2016a).

Importantly, *TP53* defects are associated with poor survival and resistance to chemo +/- immunotherapy, hence representing an indication to targeted therapies (Rossi et al., 2013). As a consequence, current guidelines recommend to assess the presence of del(17p) by FISH and *TP53* mutations by gene sequencing in CLL patients at each disease progression requiring treatment (Hallek et al., 2018).

2p gain

Gain of the short arm of chromosome 2, denoted as 2p gain or amp(2p), is a recurrent chromosomal abnormality in CLL and will be the focus of **Chapter IV**.

Other chromosomal abnormalities

Several less frequent genomic aberrations have been reported, such as trisomy 8q24, 18 and 19, as well as deletions of 6q21, 8p, 14q, 15q15.1, 2q37, 3p21 and 10q24 (Edelmann et al., 2012). In most cases, target genes and prognostic

values of these abnormalities are not fully understood. However, our group has recently demonstrated that **gain of 8q24** (5% of patients), a region harboring the *MYC* gene, was a significant predictor of poor survival. In particular, "double-hit" CLL combining 17p deletion and 8q24 gain, have a particularly poor clinical outcome (Chapiro et al., 2018). Moreover, deletions of chromosome region 6q21, or **del(6q21)**, detected in 5-7% of CLL cases, are associated with poor prognosis (Jarosova et al., 2017).

Recurrent balanced chromosomal translocations are rather rare in CLL, being found in less than 5% of all cases at diagnosis. They are generally associated with an unfavorable prognosis (DE Braekeleer et al., 2016), except for the t(14;18) translocation involving the *BCL2* gene, usually associated with lymphomas of a follicular center cell origin, but which has been reported in approximately 2% of CLL patients, all of them *IGHV*-M (Cavazzini et al., 2008; Puente et al., 2015).

Complex karyotype, or CK, is defined by 3 or more chromosomal abnormalities. Leukemia cells with highly complex karyotypes are linked with an adverse prognostic significance (Baliakas et al., 2014; Cavallari et al., 2018; Herling et al., 2016; Jarošová et al., 2019; Thompson et al., 2015). Specifically, it was recently demonstrated that patients with ≥5 abnormalities, defined as high-CK, exhibit the worst prognosis, independently of clinical stage, *TP53* aberrations and mutational status of *IGHV* genes. On the other hand, CK with 3 (low-CK) or 4 aberrations (intermediate-CK) were not independent predictors of unfavorable outcome (Baliakas et al., 2019).

Near tetraploidy (i.e., 4 copies of most chromosomes within a cell) is detected in 3% of CLLs, and was found to be associated with aggressive disease features such as advanced stages, del(17p) and complex karyotype, and with Richter transformation in ibrutinib-treated patients (Miller et al., 2017).

Complex DNA rearrangements like chromotripsis and chromoplexis are also extremely uncommon (Puente et al., 2015).

3.2. Somatic mutations

Comparably to other hematological malignancies, CLL is characterized by an overall low somatic mutation rate (0,6/Mb). For comparison, this rate is approximately at 15/Mb for melanoma (Lawrence et al., 2014). The median number of nonsynonymous mutations per tumor in CLL is 12 (Vogelstein et al., 2013).

Numerous recurrent somatic mutations have been described in CLL (**Figure 11**), generally disturbing the coding sequence of the targeted gene. Gene deregulation can also arise from mutations within non-coding regions. For instance, aberrant activation of *NOTCH1* can occur from either mutations within exon 34 or non-coding mutations affecting the 3'UTR region of the gene; while inactivating mutations in the enhancer of *PAX5* result in a decreased expression of the corresponding transcription factor (Puente et al., 2015).

In addition to the aforementioned *TP53* and *ATM* lesions, several genetic lesions were shown to significantly impact prognosis (**Figure 13**). For instance, mutations affecting *NOTCH1* (found in 12-15% of patients), *SF3B1* (9-10%) and *XPO1* (2,4-3,4%) are highly correlated to unmutated *IGHV* genes (Jeromin et al.,

2014; Puente et al., 2011; Quesada et al., 2012). All *XPO1* mutations were missense mutations in exon 15 resulting in protein alteration in codon 571 : the most frequent mutation was p.E571K, followed by p.E571V, p.E571G and p.E571Q (Jain et al., 2016).

Specifically, CLL patients with *NOTCH1* and *SF3B1* mutations have faster disease progression and shorter overall survival, independently of other prognostic factors (Jeromin et al., 2014; Quesada et al., 2012). Furthermore, *NOTCH1* mutations are linked with trisomy 12 and resistance to anti-CD20 monoclonal therapy (Jeromin et al., 2014; Puente et al., 2015; Stilgenbauer et al., 2014).

Importantly, the prevalence of these mutations in newly diagnosed or unselected CLL patients is increased in advanced disease stages. For example, the frequency of *XPO1* mutations rises from approximately 3% to 14,9% in refractory/relapsed CLL (Guièze and Wu, 2015). In relapsed/refractory CLL, concomitant mutations of the *TP53, ATM* and/or *SF3B1* genes are frequent and negatively impact clinical outcome (Guièze and Wu, 2015). On the other hand, *MYD88 mutations* (1,5-2,9%), which are associated with mutated *IGHV* status, are generally linked with a favorable outcome (Jeromin et al., 2014; Puente et al., 2011). Consistently, the frequency of *MYD88* mutations is rarely affected at relapse (Guièze and Wu, 2015).

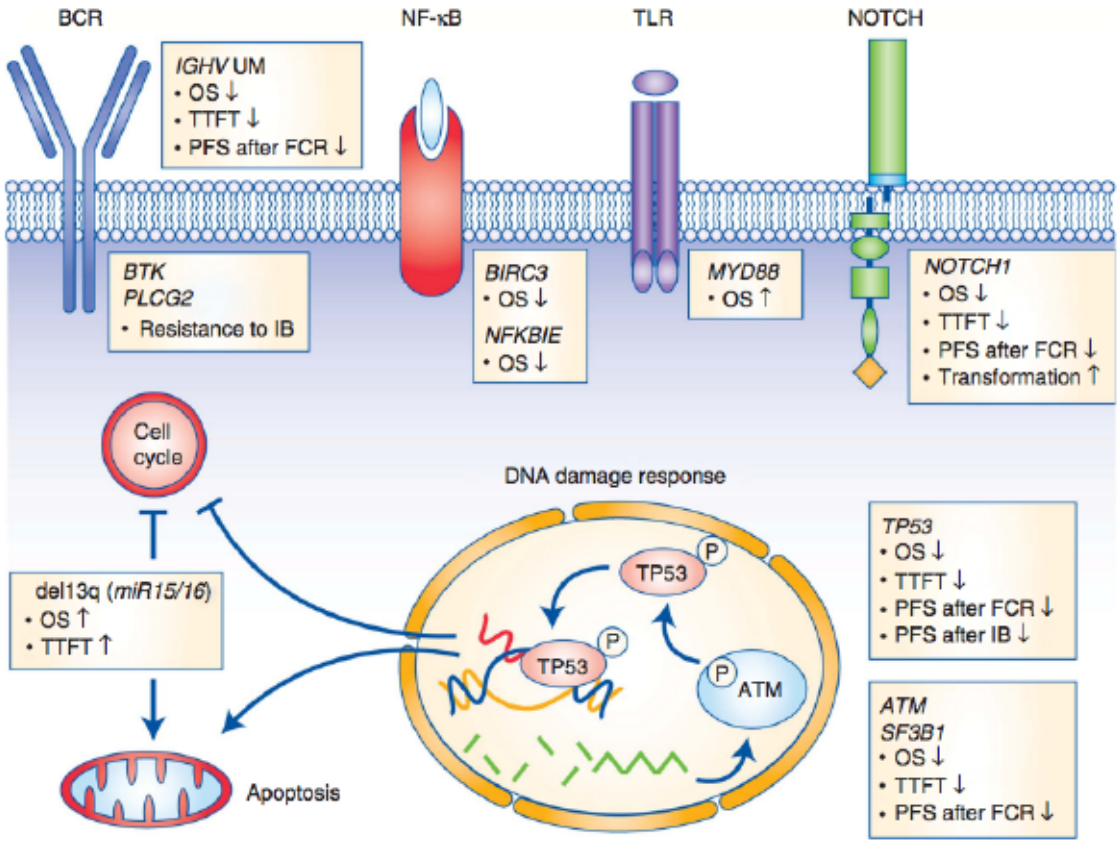

Figure 13: Clinical implications of gene mutations in CLL (Rossi and Gaidano, 2016a).

Recurrent alterations consistently affect genes playing central roles in essential cellular programs, suggesting that these are core CLL pathways. As depicted in **Figure 14**, these pathways include DNA damage response, mRNA processing, chromatin remodeling, NOTCH signaling and BCR signaling. Genetic and functional studies have implicated the latter pathway as a pivotal player in CLL pathophysiology. In particular, several genetic lesions lead to NF-κB activation, and will be thoroughly reviewed in **Chapter V**: namely mutations in the *NFKBIE*, *BIRC3*, *MYD88* and *NOTCH1* genes.

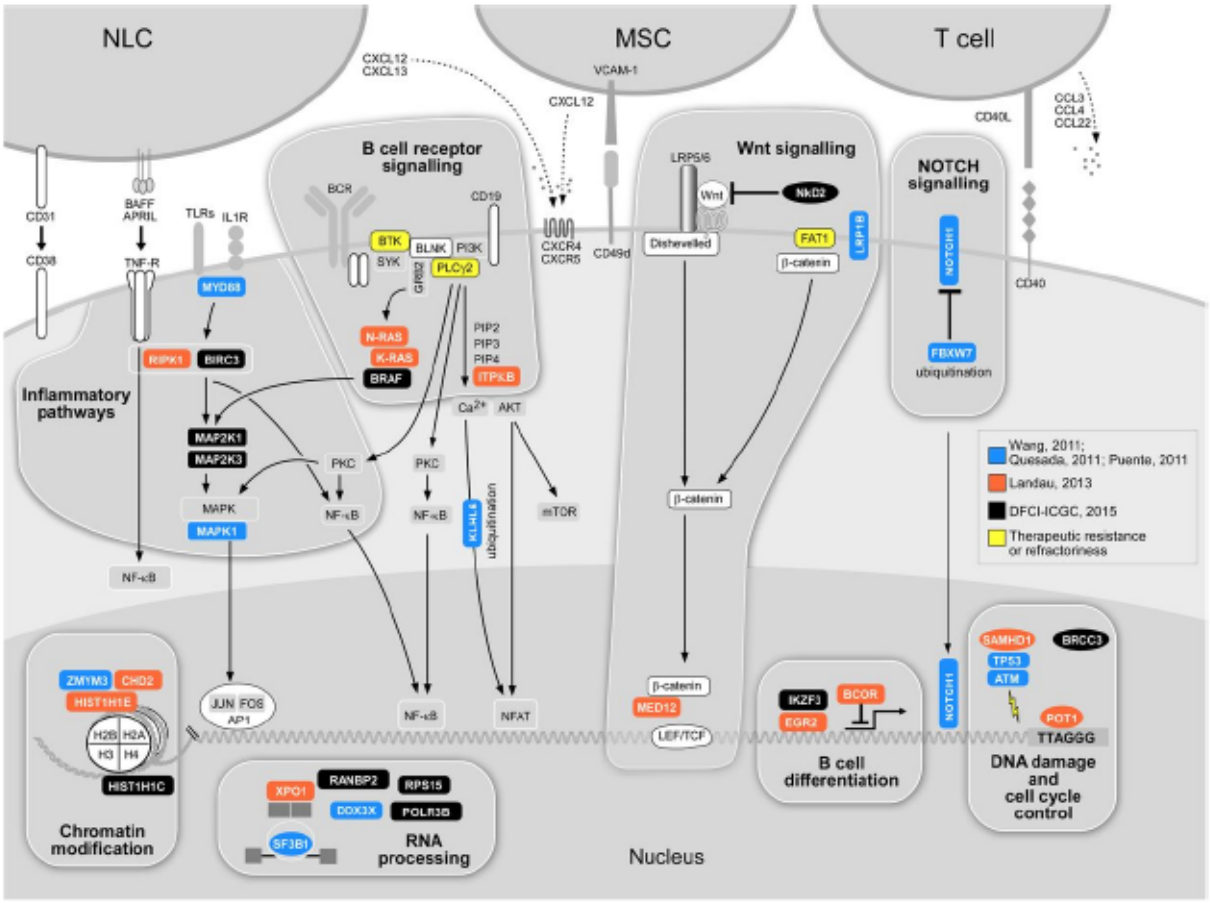

Figure 14: Putative core CLL pathways (Guièze and Wu, 2015).

Recently, mutations in *LCP1* and *WNK1* were proposed as novel CLL drivers using integrated single-cell genetic and transcriptional analysis (Wang et al., 2017b).

3.3. Epigenetic alterations

Epigenetic lesions also play a role in the deregulation of gene expression in cancer (Baylin and Jones, 2011). Comprehensive methylation profiling studies have provided an unbiased picture of the CLL epigenome, which displays a high degree of heterogeneity across samples (Cahill et al., 2013; Kanduri et al., 2010; Kulis et al., 2012; Landau et al., 2014; Oakes et al., 2014). These studies have shown that the CLL methylome is remarkably stable over time, with few changes between resting

(G0 or early G1 phase of the cell cycle) and proliferating compartments of CLL (Cahill et al., 2013).

Moreover, the CLL epigenome is characterized by a global genome-wide hypomethylation, combined with localized regions of hypermethylation (Kulis et al., 2012). It has been reported that high levels of intra-tumoral methylation heterogeneity were associated with high-risk genetic lesions, clonal evolution and poor prognosis, advocating for the assessment of epigenetic changes in CLL (Landau et al., 2014; Oakes et al., 2014) (**Figure 15**).

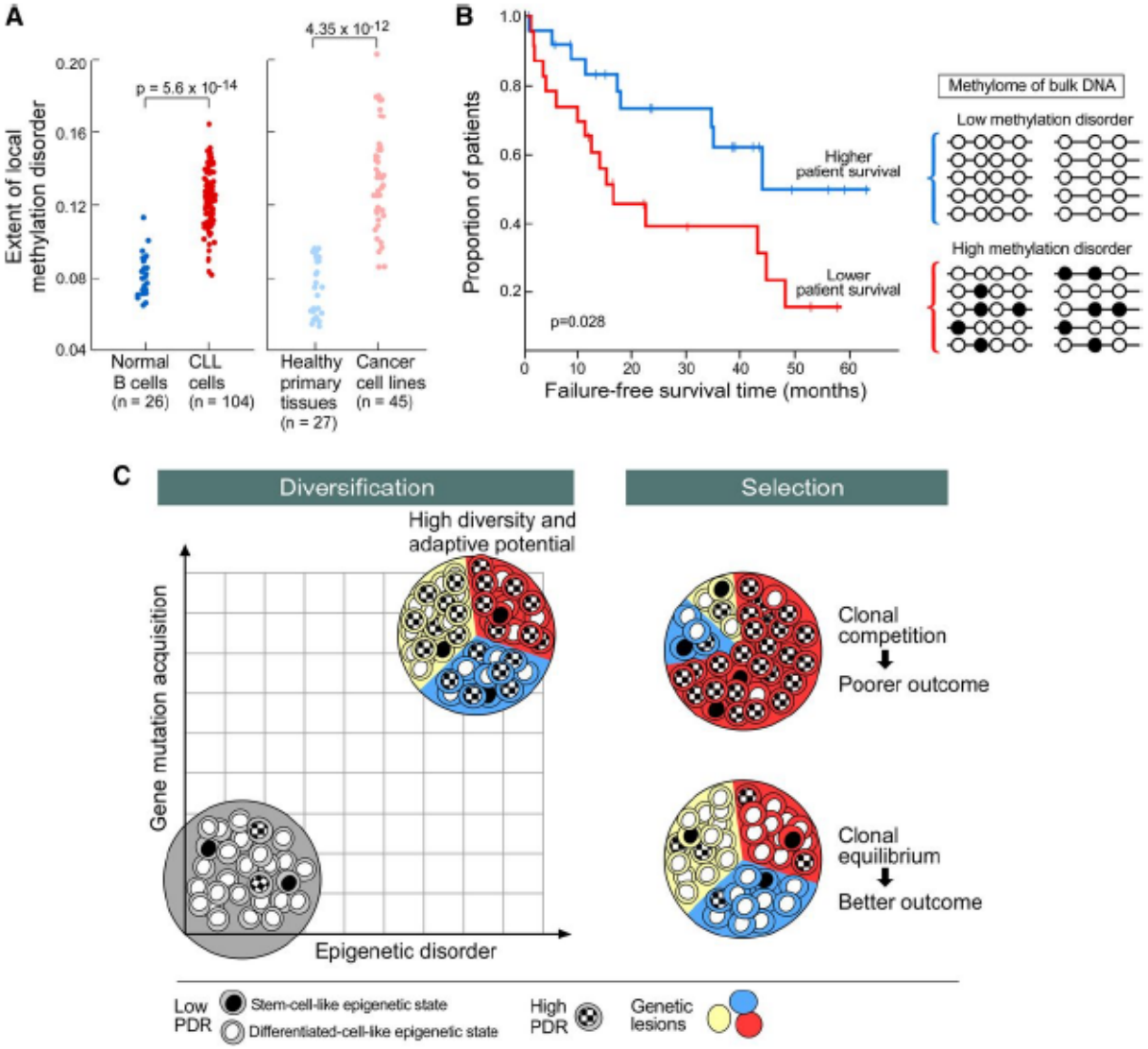

Figure 15: Methylation disorder and clonal selection in CLL (Guièze and Wu, 2015).

4. CLL metabolism and microenvironment dependency

The aforementioned inherent factors (namely, chromosomal abnormalities, somatic mutations and epigenetic alterations) are far from being the sole players

accounting for CLL pathogenesis. Indeed, external signals from the leukemia microenvironment play crucial roles in this process. Ultimately, CLL disease progression is determined by cross-talks between leukemia-intrinsic and environmental factors (Burger, 2011).

While lymph nodes are the main site of active cell proliferation, from which newly born cells are released into other compartments (Herndon et al., 2017), peripheral blood CLL cells are replicationally quiescent, i.e. in a resting state (Soma et al., 2006).

CLL cells have been reported to be more prone than normal B cells to spontaneous apoptosis (Douglas et al., 1997), and those expressing *IGHV*-UM more than those expressing *IGHV*-M genes (Coscia et al., 2011).

CLL cells spontaneously and rapidly die by apoptosis *in vitro*, because they lack essential signals provided by the natural microenvironment (Douglas et al., 1997). Indeed, CLL cells are exquisitely sensitive to microenvironmental cues and depend on them for their survival (Guièze and Wu, 2015).

The sensitivity of freshly isolated CLL cells to spontaneous apoptosis is highly variable across patients and is negatively correlated with constitutive activation of STAT3 and NF-κB (see **Section V. 1.2**). CLL cells with higher susceptibility to *in vitro* spontaneous apoptosis showed the greatest chemo-responsiveness. (Liu et al., 2016a).

A plethora of cellular and molecular players in the CLL microenvironment promote the survival and evolution of CLL cells. CLL cells interact with bone marrow stromal cells, and with T cells, antigen-presenting cells and dendritic cells within the lymph node proliferation centers (or pseudofollicles). Cytokines, chemokines, integrins, and other ligands and receptors play key roles in proliferation and survival within these cellular niches (Burger and Chiorazzi, 2013).

The lymph node (LN) microenvironment is indeed a central actor in CLL pathogenesis, promoting activation of BCR and NF-κB signaling pathways and tumor cell proliferation. In cancer cells, NF-κB encourages tumor growth both by contributing to maintenance/expansion of tumor initiating cells and by modeling the tumor microenvironment (Bradford and Baldwin, 2014). Specifically, gene expression profiling of LN-derived tumor cells exhibited an increased phosphorylation of IκBa as well as an upregulation of several NF-κB target genes, such as the *CCND2* and *BCL2A1* genes, involved in cell cycle regulation and inhibition of apoptosis (Herishanu et al., 2011).

In particular, BCR signaling is a central pathomechanism (ten Hacken and Burger, 2014). For instance, modeling of microenvironment *in vitro* induces resistance dependent on LYN and BTK (Nguyen et al., 2016; Purroy et al., 2014). Furthermore, the proliferation of Mec1 and JVM-3 cell lines was inhibited by Src and Abl kinase inhibitor dasatinib (Veldurthy et al., 2008).

BCR-crosslinking with anti-IgM antibodies *in vitro* mimics antigen recognition and is followed by calcium mobilization and phosphorylation of several tyrosine kinases (including ZAP-70 when expressed), leading *in fine* to the activation of NF-κB and PI3K/Akt kinase pathways. Immobilized anti-IgM ligation leads to cell proliferation/survival whereas soluble anti-IgM cross-linking leads to cell apoptosis (Perrot et al., 2011). IgM stimulation results in BCR pathway activation in *IGHV*-UM CLLs, but not in *IGHV*-M CLL cells (Guarini et al., 2008).

Expression of ZAP-70 is associated with increased BCR signaling (Chen et al., 2002) and was shown to act as an amplifier of NF-κB signaling in CLL cells (Pede et al., 2013), which may participate in the more aggressive clinical course associated with CLL cells that express *IGHV*-UM genes.

Functional features of chronic active BCR signaling are displayed in other B cell neoplasms such as DLBCL (Davis et al., 2010) and Waldenström's macroglobulinemia (WM) (Argyropoulos et al., 2016).

A combination of cytokines (IL-2, 4, 6, 10, 12, 15, 21, BAFF and APRIL) significantly improved CLL survival. Among these cytokines, IL-4 is sufficient to rescue CLL cells from spontaneous apoptosis *in vitro* (Ghamlouch et al., 2013). Interleukin-4 (IL-4) is a cytokine secreted by activated T cells, NK-T cells, basophils, eosinophils and mast cells. IL-4 induces signaling cascades leading to maturation of B-cell precursors, proliferation of activated B cells, and induction of isotype switching toward IgE (Thomson and Lotze, 2003). In B cells, IL-4 induces preferentially the non-canonical NF-κB pathway (Thieu et al., 2007). IL-4 efficiently protects CLL cells from spontaneous apoptosis or killing with agents such as fludarabine and chlorambucil (Dancescu et al., 1992; Douglas et al., 1997; Steele et al., 2010). Consistently, inhibition of NF-κB counteracts cytoprotection by IL-4 (Ruiz-Lafuente et al., 2014). In a nutshell, NF-κB activation is anti-apoptotic in CLL (Cuní et al., 2004; Furman et al., 2000).

Moreover, PKCbeta-dependent activation of NF-κB in bone marrow stromal cells is indispensable for the survival of CLL B cells *in vivo* (Lutzny et al., 2013).

Finally, oxidative phosphorylation (OxPhos) is a major pathway for energy production in CLL cells and is further enhanced in the presence of the stromal microenvironment. In short-term cultures, supporting stromal cells can confer a survival advantage to CLL cells by increasing OxPhos and bioenergy, allowing them to maintain transcription and translation, without however affecting proliferation (Vangapandu et al., 2017).

Accordingly, inhibition of reactive oxygen species limits expansion of CLL cells (Yigit et al., 2017), although recent data suggest that CLL cells adapt and compensate through glycolysis when OxPhos is inhibited (Vangapandu et al., 2018a).

5. Cell of origin

Several findings have suggested that CLL may develop from pluripotent hematopoietic stem cells (HSCs). Indeed, HSCs from CLL patients were able to engraft efficiently in immunodeficient mice, giving rise to clonal CD5+ B cell populations of B cells resembling MBL, the precursor state of CLL (Kikushige et al., 2011). Moreover, CLL-associated somatic mutations, namely ***BRAF***, ***NOTCH1***, ***SF3B1***, ***NFKBIE*** and ***EGR2***, have been found in multipotent hematopoietic progenitors from CLL patients (Damm et al., 2014).

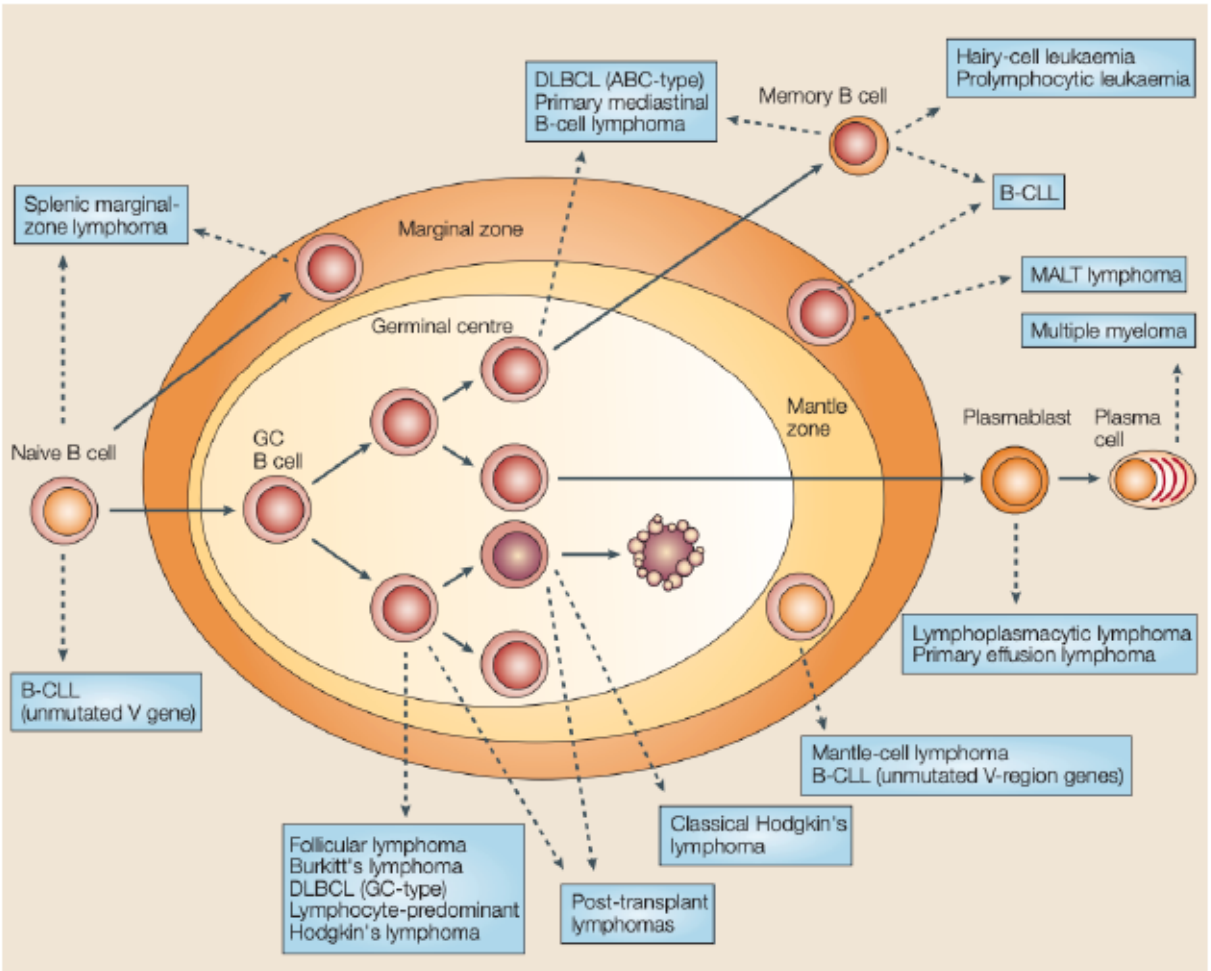

Figure 16: Cellular origin of human B-cell lymphomas. Human B-cell lymphomas are assigned to their proposed normal B-cell counterpart. Solid arrows denote B-cell differentiation steps and broken arrows assign the various lymphomas to their proposed normal counterpart. The origin of B-cell chronic lymphocytic leukemia (CLL) cells has been debated. About half of the cases of CLL carry mutations in V-region genes. Both subsets of CLL have been proposed to derive either from CD5+ B cells, memory B cells or marginal-zone B cells (Küppers, 2005).

Although the precise cell of origin of CLL is still debated, comparison of gene expression and DNA methylation profiles between normal B cells and CLL cells,

showed that all CLL cells resemble memory B cells (Klein et al., 2001; Oakes et al., 2016).

Specifically, results from gene expression profile studies suggested that *IGHV*-M CLL may derive from post-germinal center (GC), T-cell dependent CD5+ CD27+ memory B cells, whereas *IGHV*-UM CLL seem to arise either from naïve pre-GC CD5+ CD27- B cells or from a minor fraction of CD5+ CD27+ GC-independent memory B cells (Fabbri and Dalla-Favera, 2016; Klein et al., 2001; Milpied et al., 2015; Rosenwald et al., 2001; Seifert et al., 2012) (**Figure 16**).

It has been reported that, in rare cases (1,3%), CLL arises from two distinct populations. This biclonal CLL led to faster disease progression compared to monoclonal CLL (Kern et al., 2014).

6. Convergent evolution, clonal evolution and Richter syndrome

Progressive accumulation of additional genetic and epigenetic defects, BCR stimulation and microenvironmental factors lead to clonal selection of the cell of origin, giving rise to MBL, and eventually to overt monoclonal CLL (Fabbri and Dalla-Favera, 2016).

Despite the tremendous genetic heterogeneity, CLL cells display a relatively homogeneous and specific gene expression profile, which clearly distinguish them from B cells of other related pathologic entities and from normal B cells (Dürig et al., 2003; Jelinek et al., 2003; Klein et al., 2001; Rosenwald et al., 2001; Stratowa et al., 2001; Wang et al., 2004; Zheng et al., 2002). This signature is largely independent of their *IGHV* genotype, even though a limited number of genes (30) have been identified whose differential expression can distinguish *IGHV*-M from *IGHV*-UM cases (Klein et al., 2001).

Longitudinal deep sequencing studies identified convergent evolution as a recurrent event in the CLL genome whereby independent genetic lesions in the same gene were acquired in different subclones (Ojha et al., 2015). More broadly speaking, convergent evolution engenders cells with distinct genetic backgrounds to display similar phenotypes, thereby generating a consistent expression profile in each CLL sample despite the genetic heterogeneity (Wang et al., 2017b).

Despite highly effective treatments, CLL remains an incurable disease as it invariably evolves and recurs (Fabbri et al., 2013; Landau and Wu, 2013; Landau et al., 2014).

The evolutionary dynamics of CLL follows two general patterns: clonal equilibrium, in which the relative sizes of each subclone remain stable, and clonal evolution, in which some fitter subclones emerge as dominant (Landau et al., 2013). Presence of subclonal driver mutations negatively impact clinical outcome. The diversity of subclones predicts disease progression and persistence in CLL (Leeksma et al., 2019).

Importantly, chemotherapy and targeted agents (discussed in **Section III. 7**) have been identified as accelerator of clonal evolution (Landau et al., 2013) by exerting strong selective pressures for the emergence of resistant subclones (Landau et al., 2017) (**Figure 17**).

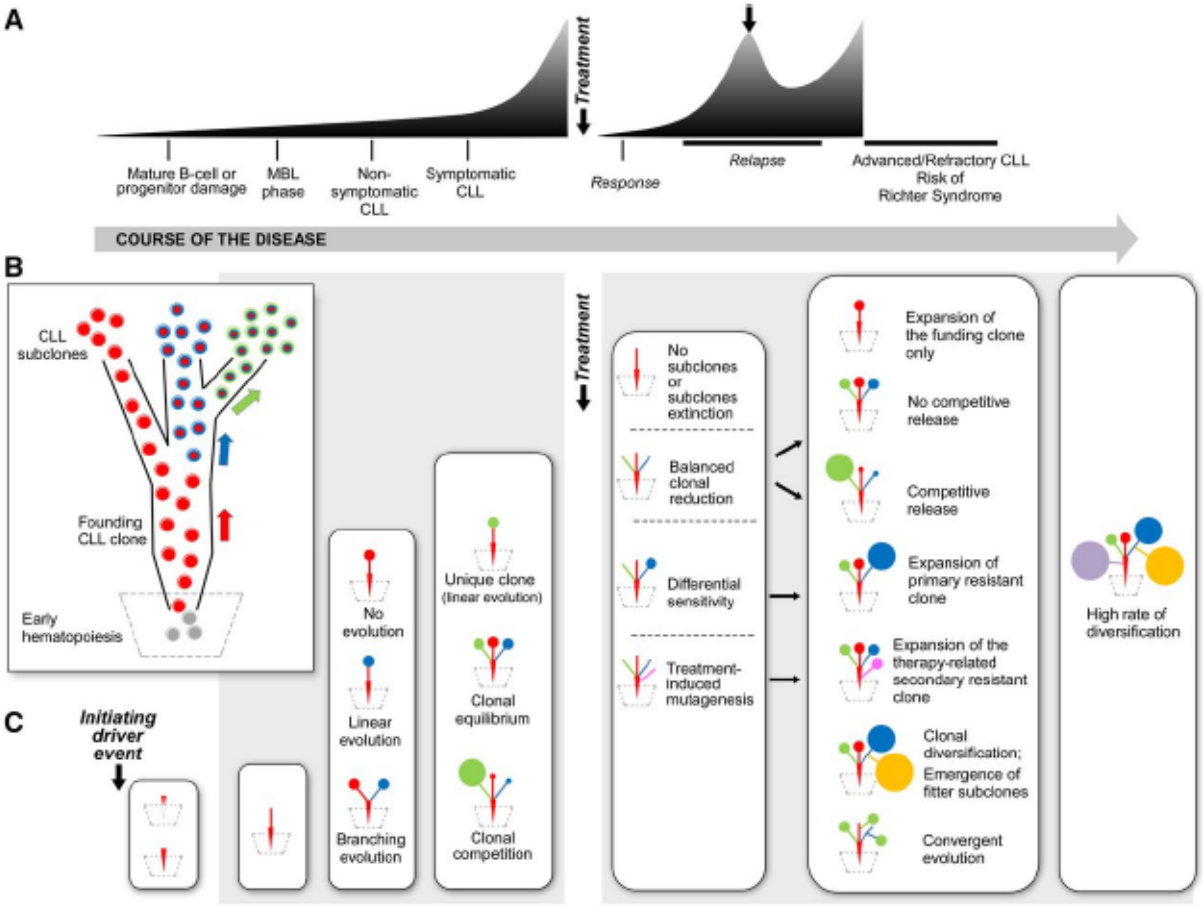

Figure 17: Clonal evolution is a major driving force in cancer progression and drug resistance (Guièze and Wu, 2015).

Indeed, longitudinal data analysis of chemo-immunotherapy-treated CLL showed that treatment, in the majority of cases, leads to large clonal shifts between pre-treatment and relapse samples, resulting in the expansion of previously minor subclones (Landau et al., 2013, 2015). In particular, another longitudinal study in a homogeneously treated cohort of 12 patients found clonal competition between 2 or more genetic subclones in 70% of the patients with relapse, and stable clonal dynamics in the remaining 30% (Ojha et al., 2015).

Moreover, drug-induced selective pressure can also lead to the appearance of ibrutinib resistant mutations. For instance, mutations affecting the *BTK* binding site of ibrutinib and gain-of-function mutations in *PLCG2*, undetectable before ibrutinib treatment, were reported, further highlighting the dynamic nature of CLL genome (Fama et al., 2014; Landau et al., 2017; Woyach et al., 2014).

In addition to genetic evolution arising from therapeutic pressure and interactions between tumoral subclones, it is becoming clear that reciprocal interactions between the tumor cell and cellular components of the microenvironment further apply selective pressures on specific clones that can influence the equilibrium between tumor immunity and immunologic evasion and escape (Purroy and Wu, 2017) (**Figure 18**).

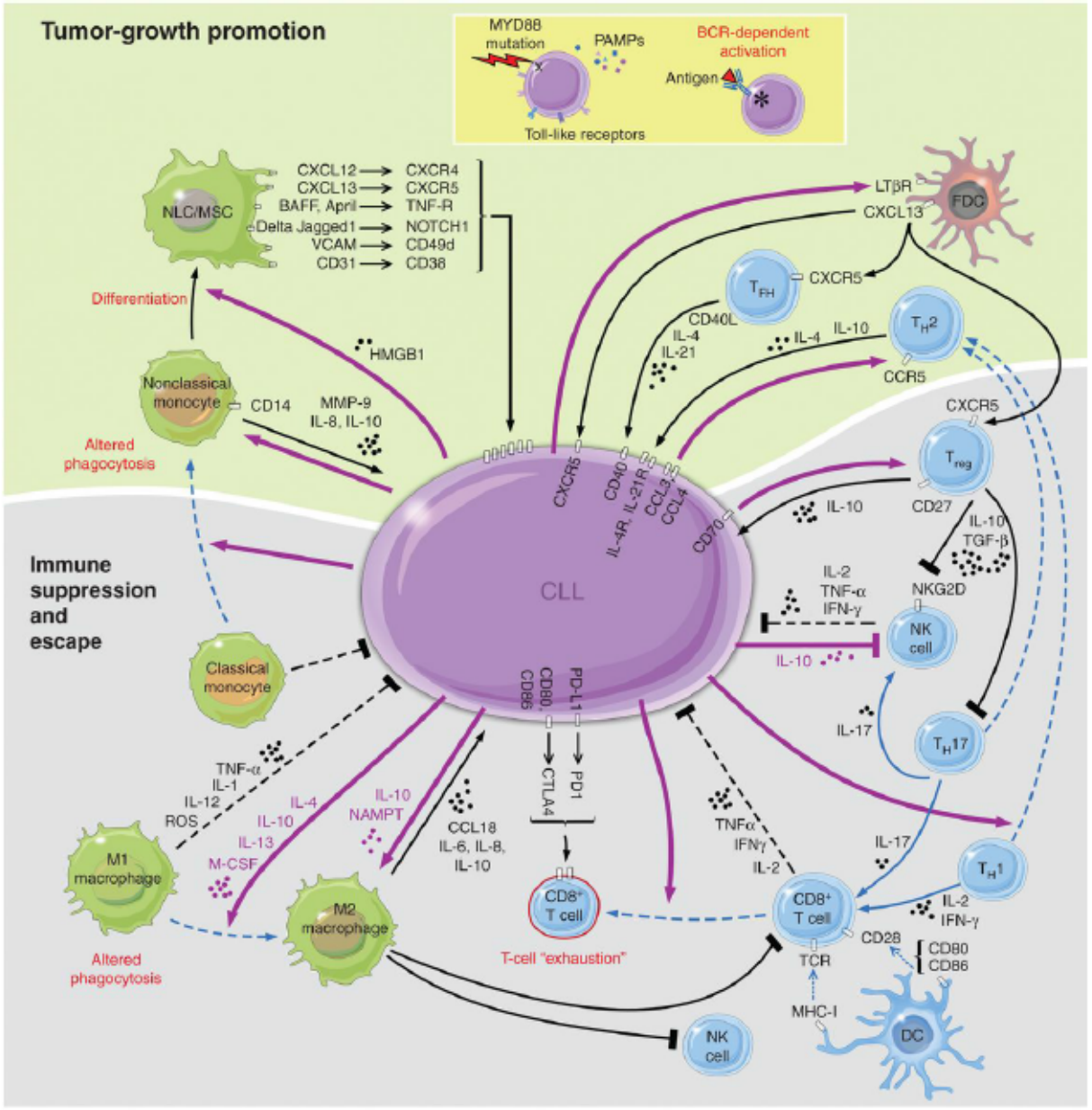

Figure 18: Coevolution of cancer and host-immune cells in CLL. Cellular components and mechanisms of tumor-growth promotion, and of immune suppression and escape (magenta arrows, activating signals from CLL cells toward immune cells; black arrows, activating signals from immune cells toward CLL cells; dashed black arrows, mechanisms of immunosurveillance; blue arrows, activating signals between immune cells; dashed blue arrows, mechanisms of immune suppression and escape). NLC, Nurse-like cell; MSC, mesenchymal stromal cell; PAMP, pathogen-associated molecular pattern; TLR, Toll-like receptor; BCR, B-cell

receptor; FDC, follicular dendritic cell; DC, dendritic cell; T_{FH}, follicular helper T cell (Purroy and Wu, 2017).

Notably, a small fraction of CLL (5-10%) undergoes transformation into aggressive forms of clonally related malignancies, a complication termed Richter syndrome (RS). These malignancies are most commonly of the diffuse large B cell lymphoma (DLBCL) type (~ 90% of cases) or Hodgkin variant RS (HVRS) (~ 5-10%) (Allan and Furman, 2018; Rossi et al., 2013; Solh et al., 2013).

RS usually derives from the main CLL clone through a linear evolution pattern implicating the acquisition of an average of 20 genetic lesions/case (Fabbri et al., 2013). These lesions are heterogeneous among patients, although the most frequent ones involve ***TP53*** disruption (approximately 60% of RS cases), ***NOTCH1*** mutations (30%), ***MYC*** activation (30%) and ***CDKN2A/B*** loss (30%) genes (Allan and Furman, 2018; Fabbri et al., 2013). Furthermore, a recent next-generation sequencing study performed in 11 RT patients identified for the first time ***TET2*** and ***CREBBP*** as two of the most commonly mutated genes in RT (Chitalia et al., 2019).

The prognosis of RS is highly unfavorable, with a median survival of a few months because of limited therapeutic options and responses (Allan and Furman, 2018; Rossi and Gaidano, 2009, 2016b; Tsimberidou and Keating, 2005).

Importantly, Rossi and colleagues showed, using longitudinal analysis, that small ***TP53*** mutated subclones identified before treatment became the predominant population at the time of CLL relapse and anticipated the development of chemorefractoriness. This study provides a proof-of-principle that very minor leukemia subclones detected at diagnosis are an important driver of the subsequent disease course (Rossi et al., 2014).

Indeed, such minor ***TP53*** mutated subclones were shown to have the same adverse prognostic impact as clonal ***TP53*** abnormalities. Since conventional Sanger sequencing can miss mutations of low clonal abundance (<10% of the alleles), this advocates for the use of deep next-generation sequencing to assess genetic lesions in a comprehensive manner prior to treatment, even though the current cost and time of analysis seem difficult to render it systematic (Rossi et al., 2014).

7. Clinical management of CLL

As outlined by the 2018 International Workshop on CLL guidelines (Hallek et al., 2018), the CLL treatment paradigm for managing asymptomatic patients consists of a "watch and wait" strategy. When symptoms appear and/or disease progresses, numerous effective therapeutic approaches are available, which can be used either as single agents or in combinations to constitute individually tailored treatment plans (Sharma and Rai, 2019).

7.1. Chemo-immunotherapy

Chemo-immunotherapy is an effective first-line treatment for CLL patients without ***TP53*** abnormalities and is especially beneficial for young (aged < 65 years) and fit patients. A broad range of drugs have been approved:

Bendamustine, chlorambucil and cyclophosphamide are alkylating agents, which counteract cell division by cross-linking DNA strands.

Fludarabine and pentostatin are purine analogs that affects DNA synthesis by inhibiting DNA polymerase.

Monoclonal antibodies (rituximab, obinutuzumab, ofatumumab) bind to the CD20 antigen, expressed on the surface of pre–B-lymphocytes and mature B-lymphocytes, and activate complement-dependent cytotoxicity (CDC) and antibody-dependent cell-mediated toxicity (ADCC) towards these cells. Anti-CD20 antibodies can be used alone or in combination with chemotherapy as well as with targeted drugs (discussed below).

Several combinations have proven their efficacy in a frontline setting (Ghia and Hallek, 2014):

i) chlorambucil with an anti-CD20 antibody,
ii) bendamustine-based regimens, or
iii) fludarabine and cyclophosphamide with rituximab (FCR).

FCR is considered the most effective option for front-line treatment in young, fit patients who have *IGHV* mutation and without del(17p) (Sharma and Rai, 2019).

7.2. Targeted therapies

Therapies targeting the B-cell-receptor (BCR) signaling pathway, such as the Bruton tyrosine kinase (BTK) inhibitor ibrutinib and the phosphoinositide 3-kinase δ (PI3Kδ) inhibitor idelalisib, have demonstrated high efficacy (Byrd et al., 2014).

Duvelisib (also known as IPI-145) is a dual inhibitor of PI3Kδ and PI3Kγ approved for use in all patients with relapsed/refractory CLL who have received at least 2 prior lines of therapy (Flinn et al., 2018).

In vivo, ibrutinib inhibits BCR and NF-κB signaling and reduces tumor proliferation in LN and BM resident CLL cells (Herman et al., 2014). Studies showed that these patients rather significantly benefited from targeted therapies (Brown et al., 2016; Wiestner, 2015). Indeed, these orally bioavailable inhibitors induced high rates of durable responses (Wiestner, 2015) and have demonstrated impressive results, even in relapsed or refractory CLL (Byrd et al., 2013; Farooqui et al., 2015; Furman et al., 2014), and are hence approved for clinical use.

Recently, selective inhibition of BCL-2 through the BH3 mimetic venetoclax demonstrated a high efficacy in relapsed or refractory patients, including those with high-risk genetic lesions such as del(17p), indicating a major role for BCL-2 in the pathogenesis of CLL (Roberts et al., 2016). Venetoclax acts by selectively binding to BCL-2, displaces proapoptotic proteins, which results in activation of caspases and apoptosis (Konopleva et al., 2016) (**Figure 19**) (see **Section VI. 1**).

Novel therapeutic regimes are constantly being developed.

Acalabrutinib is a BTK inhibitor phase II trial in CLL currently underway, approved for mantle cell lymphoma (Niemann et al., 2017).

A first in human phase 1 study in relapsed or refractory CLL using the BTK inhibitor GDC-0853, a selective reversible and non-covalent inhibitor of BTK that

does not require interaction with the Cys481 residue for activity, showed a generally well tolerated antitumor activity (Byrd et al., 2018).

The CXCR4 inhibitor BL-8040 (synthetic peptide antagonist) induces the apoptosis of AML blasts by downregulating ERK, BCL-2, MCL-1 and cyclin-D1 via altered miR-15a/16-1 expression (Abraham et al., 2017), and might be useful in CLL. Bispecific CAR (chimeric antigen receptor) T cells with binding domains for CD19 and CD20, efficiently killed patients CLL cells *in vitro*, and may avoid the risk of relapse associated with single specificity CAR T cells, through leukemic cells which lack the CAR targeted antigen (Martyniszyn et al., 2017).

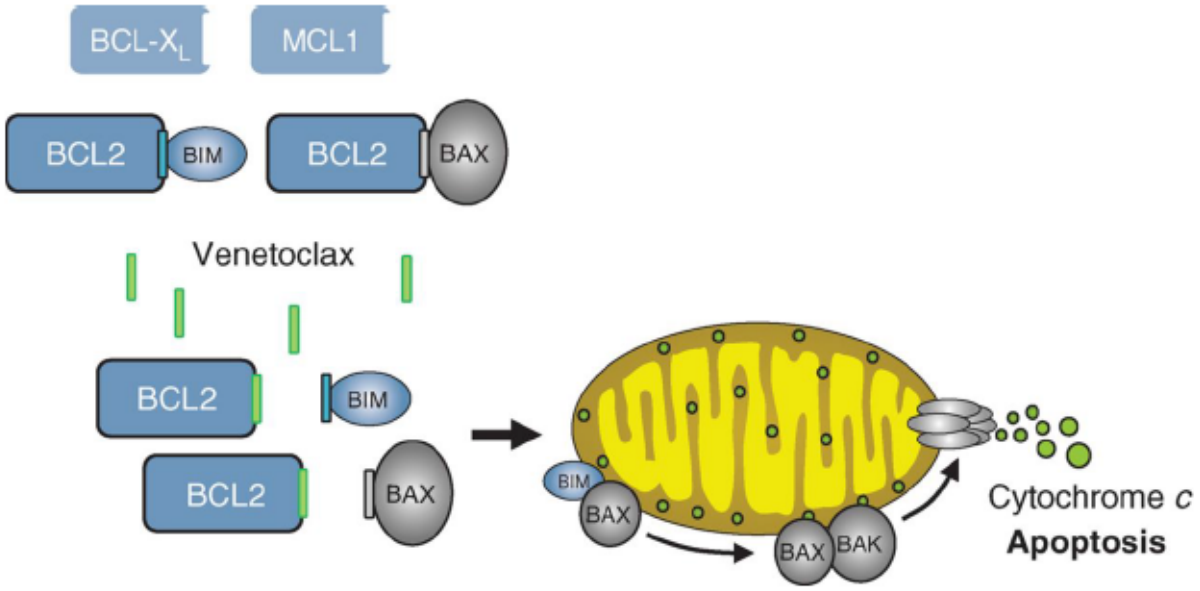

Figure 19: Mechanism of action of venetoclax. Venetoclax acts as a specific inhibitor of BCL-2 and upon binding, releases proapoptotic proteins to induce apoptosis (Konopleva et al., 2016).

Various selective inhibitors have been tried in CLL cells, some of which will be discussed in **Chapter IV**.

However, indefinite treatment seems required with single agent therapy and drug resistance inevitably develops in a subset of patients (Burger et al., 2016; Byrd et al., 2015; Maddocks et al., 2015; Woyach et al., 2014).

7.3. Emergence of drug resistance

Although targeting the BCR pathway with single agent BTK or PI3Kδ inhibitors has proven clinically effective in CLL, the majority of responses are partial and indefinite treatment is currently required, while resistance to single agent therapy and toxicity with chronic therapy is a concern.

Complete remissions, without minimal residual disease, are rare with single-agent therapy, and occur only after prolonged treatment leading to an increased risk of progression for high-risk patients (Byrd et al., 2015; Farooqui et al., 2015).

This is further supported by data on subclonal development in CLL (Landau et al., 2015), the development of pathway specific mutations upon BTK inhibition (Ahn et al., 2017; Komarova et al., 2014; Woyach et al., 2014).

In venetoclax-treated patients, the emergence of Gly101Val point mutation in *BCL2* reduces its affinity for venetoclax by ~180-fold, thereby conferring acquired resistance in cell lines and primary patient cells (Blombery et al., 2019). Moreover, whole-exome sequencing of venetoclax-treated patients found mutations in *BTG1*, *CDKN2A/B*, *BRAF* as well as high-level focal amplification of *CD274* (*PD-L1*) (Herling et al., 2018).

Interestingly, CLL cases refractory to fludarabine (FR-CLL) were significantly enriched in *FAT1* mutations. Indeed, the frequency of *FAT1*-mutated cases was significantly higher in FR-CLL than in unselected CLLs at diagnosis (10.3% vs 1.1%), suggesting a role in the development of a high-risk phenotype (Messina et al., 2014).

7.4. Combination strategies

In order to circumvent the emergence of secondary resistance to drugs, combination strategies involving two or more molecules have been developed.

Despite the limited efficacy of sequential BTK/PI3K targeting after clinical progression on one agent in CLL patients (Mato et al., 2016), combined BTK and PI3K inhibition exhibited synergistic effects on DLBCL lymphoma cell survival *in vitro* (Mathews Griner et al., 2014). *In vivo*, combined inhibition of BTK and PI3Kδ with acalabrutinib and ACP-319 significantly reduced tumor burden, improved survival by nearly two-fold and reduced NF-κB signaling, compared with single agents, in the CLL mouse model TCL1-192 (Niemann et al., 2017).

Furthermore, combination of ibrutinib and venetoclax was designed to overcome resistance to ibrutinib. However, CLL samples displayed resistance to this combination as well in *ex vivo* experiments. Microenvironmental agonists (IL-10, CD40L, CpG-ODN) induced a robust activation of NF-κB signaling which enhanced expression of MCL1, BCLXL and survivin, thus decreasing dependence on BCL2 and causing drug resistance. Consistently, inhibitors of NF-κB signaling overcame this resistance and showed a synergistic benefit with ibrutinib/venetoclax combination (Jayappa et al., 2017).

Nevertheless, the best combinations of these agents, with or without chemotherapy, remain to be established and tailored to each patient (Brander, 2017).

Chapter IV: Gain of the short arm of chromosome 2 (2p gain)

Gains and amplifications of 2p have been described in various types of hematological and non-hematological neoplasms. However, their impact on harbored genes and their involvement in disease progression remain ill-defined. Here I propose a comprehensive review of the literature regarding 2p gain or amplification, with a focus on CLL and an in-depth study of putative oncogenic drivers and their reported impact on pathogenesis and survival.

1. Prevalence of 2p gain/amplification in cancer

Noteworthily, even though a gain is normally defined by a median copy number 3-6, and an amplification by a median copy number > 6, authors seem to use gain and amplification in an interchangeable manner regarding 2p.

1.1. Non-hematological cancers

Copy number aberrations of 2p are recurrent in medulloblastoma, although 2p gain/amplifications were not associated with shorter overall (OS) nor progression-free survival (PFS) (De Bortoli et al., 2006).

Neuroblastomas (NBs) are pediatric solid tumors that develop from the neural crest, with heterogeneous clinical courses. Amplifications of 2p are also frequent in NBs (discussed in **Section IV. 4**).

1.2. Hematological cancers

Gains of 2p have been reported in 20% of extranodal B-cell non-Hodgkin lymphomas (B-NHL), in follicular and mediastinal B-NHL (or PMBCL), and in Hodgkin lymphoma (HL) (Satterwhite et al., 2001).

Specifically, 2p gain is recurrent in 54% of classical HL (Joos et al., 2002). Analysis of four HL cell lines (KM-H2, HDLM-2, L428, L1236) identified frequent 2p gain including ***REL*** in 3 of 4 cell lines (Joos et al., 2003).

Gain of 2p is reported in 17% of DLBCL samples, regardless of subgroup. This frequency is increased in refractory DLBCL, where 2p gain is detected in 2 of 5 patients (Park et al., 2016). In particular, primary mediastinal B cell lymphoma (PMBCL), a subtype of DLBCL, is characterized by frequent gains/amplifications of 2p14-p16 found in up to 47% of cases (Bea et al., 2005).

2. Incidence and evolution of 2p gain in CLL

Longitudinal studies have outlined the paths of clonal evolution and their close link to therapy-induced selective pressure. Gain of 2p was identified as

predominantly subclonal, suggesting that it may mainly be a late driver event in CLL evolution (Landau et al., 2015) (**Figure 20**).

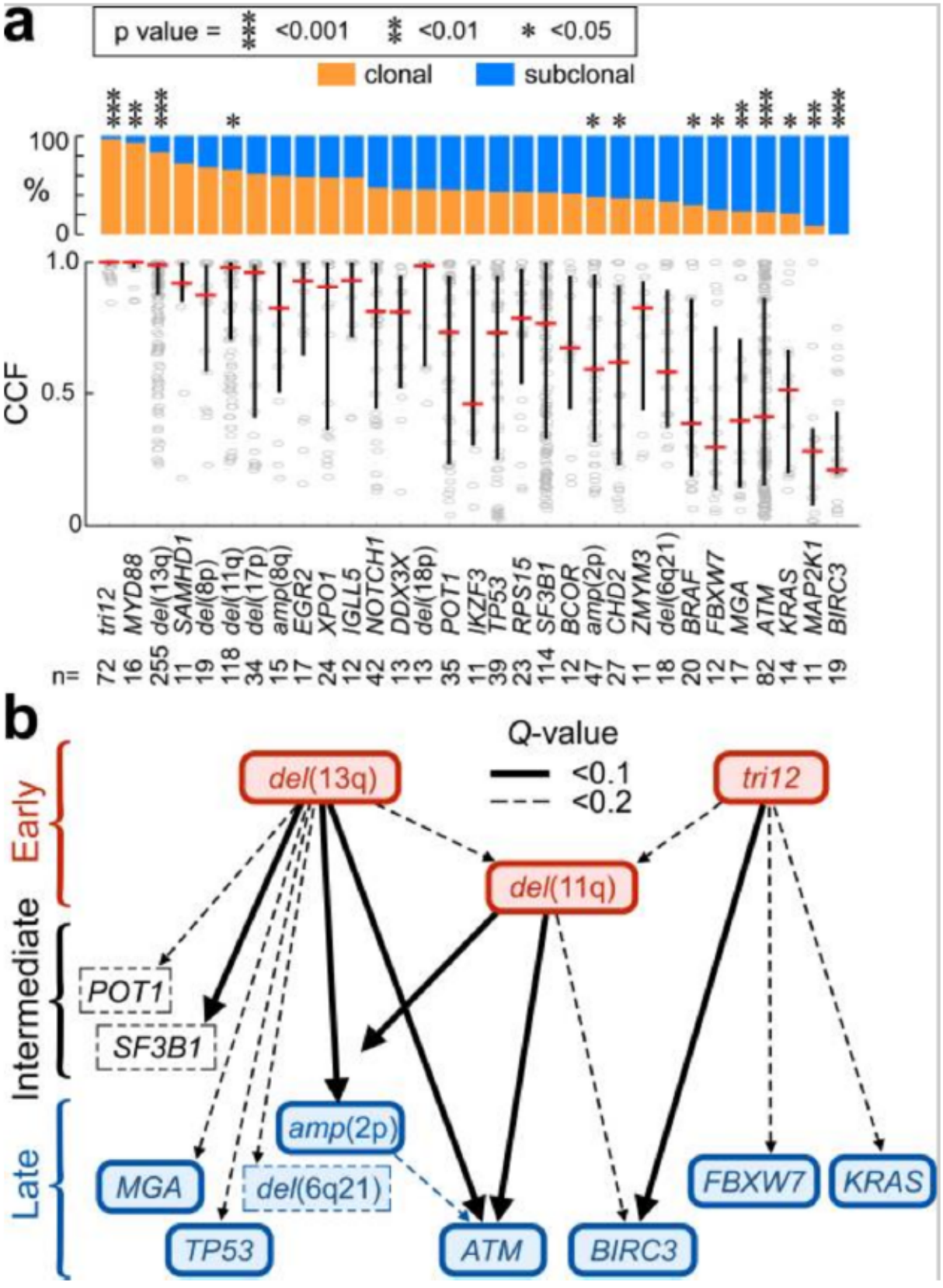

Figure 20: Inferred evolutionary history of CLL (Landau et al., 2015).

In CLL, gain of 2p is found in different frequencies depending on the patient cohorts as well as on the detection technique.

For instance, by SNP-array, gain of 2p16.1-2p15 is detected in 1,9% of newly diagnosed cases (Gunnarsson et al., 2011). Similarly, in a series of 176 newly diagnosed CLL representative of all disease stages, gain of 2p was detected by FISH in 2,3 to 3,4% of cases (Deambrogi et al., 2010).

This prevalence is of 7% in a series of previously untreated patients, mostly Binet stages B/C patients (Edelmann et al., 2012). The 2p gain was detected by FISH and SNP-array in 7,3% early stage Binet A CLL patients and, interestingly, in 1,4% of clinical MBL cases (Fabris et al., 2013).

Using array-based CGH, gain of 2p was detected in 8% of unsorted CLL cases (Jarosova et al., 2010). Using the same technique, our group has identified 2p gain in 28% of untreated Binet stages B/C CLL patients (Chapiro et al., 2010). Similarly, 2p gains constituted 30% of a cohort of mixed treated/untreated patients, and ranged from a small 29-kb region to large segments involving the entire short arm. Interestingly, gain of the telomeric region 2p25.3 harboring the acid phosphatase 1 *ACP1* gene is recurrent and found in 25% of patients (Ma et al., 2011) (discussed in **Section IV. 4**).

3. Impact of 2p gain on CLL disease progression

Gain/amplification of 2p is associated with various outcomes in numerous malignancies. In CLL, our group has shown that 2p gain is linked with refractoriness to treatments (Cosson et al., 2017). Refractory disease is defined as failure to respond to treatment or as progression within 6 months from the last dose of therapy (Hallek et al., 2018).

Gain of 2p is associated with unfavorable prognosis factors. Indeed, amp(2p) was significantly enriched in *IGHV*-UM CLL vs *IGHV*-M CLL and in Binet B/C stages. Mutated *ATM*, del(11q) and del(17p), as well as CD38 and ZAP70 positive expression, significantly co-occurred with 2p gain (Chapiro et al., 2010; Cosson et al., 2017; Edelmann et al., 2012; Fabris et al., 2013; Landau et al., 2015; Ma et al., 2011). Moreover, 2p gain cases had significantly higher utilization of stereotyped BCR compared with CLL without 2p gain (Fabris et al., 2013).

Gains of 2p also reportedly determined a higher risk of RS transformation (Rinaldi et al., 2011), however, no enrichment of 2p amplification was observed in RS. Indeed, gains of the 2p16.1-2p15 locus occurred at an analogous frequency in RS and in unselected CLLs (Fabbri et al., 2013).

Importantly, while 2p gain is generally found with concurrent genetic lesions, most notably del(11q) (Deambrogi et al., 2010; Jarosova et al., 2010; Ma et al., 2011), 2p gain could be detected as the sole genetic abnormality in a few stage A CLL cases (Fabris et al., 2013), which might suggest an additional role in early disease progression. Interestingly, there was no significant difference in time to first treatment (TTFT) between early 2p gain and 2p normal CLLs (Fabris et al., 2013).

Furthermore, no 2p gain was reported in 39 fludarabine-resistant CLL (FR-CLL) patients, indicating that 2p gain might not play a role in the development of this particular phenotype (Messina et al., 2014).

4. Putative oncogenic drivers in 2p gain CLL

Identifying drivers of treatment resistance is essential to precisely tailor therapeutic intervention and circumvent its failure.

As previously discussed, the target genes of some recurrent chromosomal abnormalities in CLL have already been identified, but genes involved in 2p gain pathogenesis remain unknown (Fabbri et al., 2013).

Several putative oncogenes have been and might be considered for study in order to gain insight into the genetic basis of drug resistance in 2p gain CLL. Owing to the subclonal nature of 2p gain, identifying drivers of treatment resistance is a challenge.

Conversely to gain/amplification of the 2p, a 2p15-p16.1 microdeletion syndrome was reported as a novel, rare disorder characterized by developmental delay, growth retardation, facial abnormalities, and other medical problems. The microdeletion involved *BCL11A*, *PAPOLG*, and *REL*, and one long non-coding RNA gene *FLJ16341* (Hancarova et al., 2013).

4.1. Candidate oncogenes

The rationale for selecting the candidate oncogenes discussed in this section requires said genes to meet at least one of the following criteria:

i. The candidate gene is contained in the minimal region of gain, which corresponds to a 1.28 Mb region harboring nine genes (*BCL11A, PAPOLG, REL, PUS10, PEX13, KIAA1841, AHSA2, USP34* and *XPO1)* (Cosson et al., 2017)

ii. A documented impact of their gain and/or overexpression on clinical features of other neoplasms, particularly on drug resistance.

iii. Increased expression of the corresponding mRNA or protein in 2p gain CLL as compared with CLL without 2p gain.

A transcriptional profiling analysis in early stage CLL and MBL identified several genes significantly upregulated in 2p gain CLLs: *NCOA1* and *ROCK2* on 2p and *CAV1* at 7q31.1. Importantly, in this cohort, there were no differences in *BCL11A*, *REL*, *ALK* nor *MYCN* expression levels between 2p gain and 2p normal patients (Fabris et al., 2013).

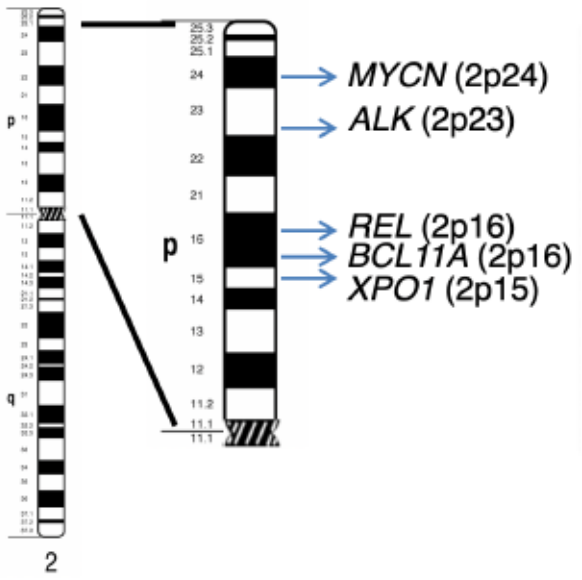

Figure 21: Gain of the short arm of chromosome 2p. Localization of the main candidate 2p oncogenes is depicted.

Gene localization on the chromosome is indicated between brackets (position in GRCh37/hg19) (**Figure 21**).

XPO1 (2p15)

The *XPO1/CRM1* gene encodes Exportin-1, which is the sole exporter of over 200 known cargos bearing leucine-rich nuclear export sequences (Fornerod et al., 1997), including major tumor suppressor proteins such as p53, BRCA1/2 and IκBa (Turner and Sullivan, 2008).

Increased Exportin-1 expression is observed in many hematological and solid tumor malignancies and is generally correlated with poor prognosis. Overexpression of Exportin-1 increases the export of tumor suppressor proteins to the cytoplasm, preventing them from conducting their normal cell cycle checkpoint regulation in the nucleus (Kashyap et al., 2016).

The Exportin-1 protein is overexpressed in cervical cancer and was shown to be critical for cancer cell survival and proliferation: inhibition of Exportin-1 induced cancer cell death (van der Watt et al., 2009). Exportin-1 is also expressed in a subpopulation of ovarian carcinomas with aggressive behavior and is linked to poor clinical outcome (Noske et al., 2008).

High Exportin-1 expression was a significant prognostic indicator for PFS as well as OS in pancreatic cancer (Huang et al., 2009) as well as in osteosarcoma (Yao et al., 2009). Specifically, in pancreatic cancer, Exportin-1 expression was reportedly associated with tumor size, lymphadenopathy and liver metastasis (Huang et al., 2009).

Mutations in *XPO1* have been reported in several hematological malignancies: in CLL (**Section III.3.2**), as well as in relapsed/refractory DLBCL, PMBL (Dubois et al., 2016; Jardin et al., 2016) and HL (Camus et al., 2016). Although frequently

associated with UM-*IGHV*, survival of CLL cases with *XPO1* mutations were reportedly similar to CLL without *XPO1* (nor *TP53*) mutations, as well as linked with favorable responses to ibrutinib (Jain et al., 2016).

REL (2p16.1)

REL encodes for c-Rel (see **Chapter V**).

PAPOLG (2p16.1)

The *PAPOLG* gene is responsible for post-transcriptional 3′ adenylation of mRNA precursors and small RNAs (Kyriakopoulou et al., 2001).

BCL11A (2p16.1)

The *B-cell lymphoma/leukemia 11A (BCL11A/EVI9/CTIP1)* gene encodes a zinc-finger Krüppel-like transcription repressor protein, BCL-11A, implicated in early B lymphopoiesis, essential for normal lymphoid development. Indeed, *Bcl11a* knockout mice die shortly after birth and embryos have no B cells and present alterations in T cells (Liu et al., 2003).

BCL-11A is normally expressed at high levels only in the fetal brain and in germinal center B-cells (Satterwhite et al., 2001).

BCL-11A is a DNA-sequence-specific transcriptional repressor, which is a critical component of a transcriptional network that regulates B cell fate: BCL-11A functions upstream of Ebf1 and Pax5 in the B cell pathway, and controls V(D)J recombination (Lee et al., 2017).

Alternative splicing of *BCL11A* pre-mRNA produces multiple isoforms sharing a common N-terminus. The most abundant isoform in human lymphoid samples is *BCL11A*-XL (Liu et al., 2006) (**Figure 22**).

Gain or amplification of *BCL11A* was reported in hematological as well as non-hematological neoplasms, but was linked with various clinical outcomes.

Overexpression of *BCL11A*, resulting from the t(2;14)(p13;q.32.3) translocation which consists of its fusion to the *IGH* locus, is a rare but recurrent observation in human B cell malignancies (Dyer, 2003). Specifically, translocation of the *BCL11A* gene into the *IGH* locus in a subset of CLL cases is associated with aggressive disease (Satterwhite et al., 2001) and poor prognosis (Cavazzini et al., 2008).

In a series of 20 cases of PMBL, 75% of cases showed an increased *BCL11A* gene copy number as detected by FISH. Immunolabeling identified nuclear BCL11A-XL protein in 87.5% of PMBLs. However, there was no overall correlation between genomic, transcript and protein levels in PMBLs (Weniger et al., 2006).

Consistently, downregulation of *BCL11A* by siRNA induces apoptosis in B lymphoma cell lines SUDHL6 and EB1. Interestingly, the combination with BCL2

siRNA produced a greater inhibitory effect on cell proliferation of these two cell lines, compared to each siRNA given separately (Gao et al., 2013).

High BCL-11A expression levels was correlated with lower complete response rate and shorter overall survival worse clinical outcome in adult acute myeloid leukemia (AML) patients (Dong et al., 2017).

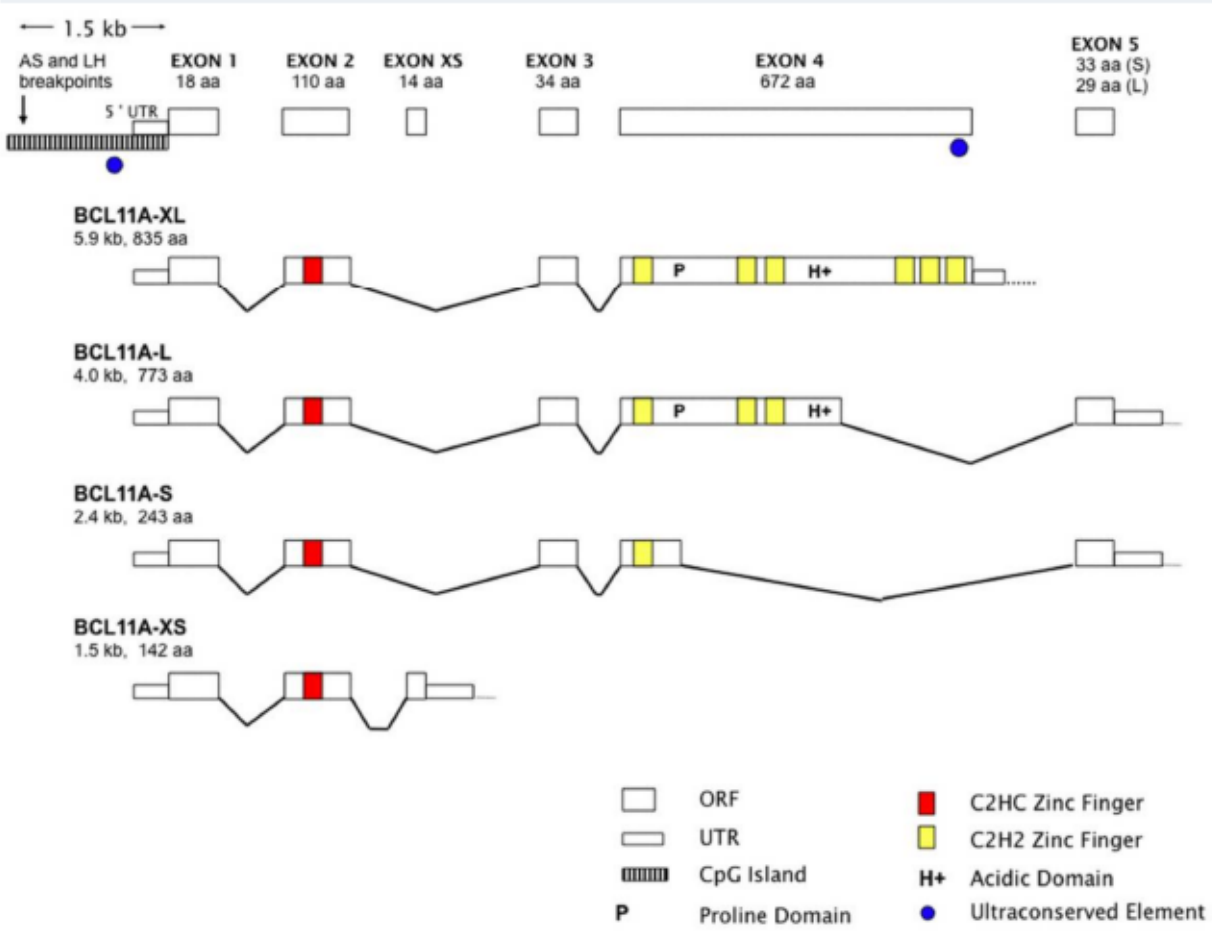

Figure 22: Human *BCL11A* locus and predicted protein isoforms (Liu et al., 2006)

In non-small cell lung cancers, BCL-11A protein expression levels were specifically upregulated in cancer tissues, compared to adjacent healthy lung tissues. The survival analysis found that patients with increased BCL-11A expression had better outcomes and *BCL11A* was proposed as an independent prognostic factor for disease-free survival as well as overall survival (Jiang et al., 2013).

In mice, *Bcl11a* is activated by retroviral insertions in some myeloid leukemias (Dong et al., 2017). *Bcl11a* can transform mouse 3T3 cells (Nakamura et al., 2000) but has not been shown to transform human lymphoid cells.

Bcl11a is also required for normal T cell development and loss of *Bcl11a* expression induces murine T cell leukemia, implying a function of T cell tumor suppressor gene for *Bcl11a* in mice (Liu et al., 2003).

MSH2 (2p21)

DNA mismatch repair (MMR) is a highly conserved biological pathway that plays a crucial role in maintaining genomic stability. MMR enzymes ensure DNA replication fidelity and maintain genomic integrity; they are highly expressed in normal cells (Li, 2008).

Unsurprisingly, defects in this pathway predispose to several human cancers. For instance, somatic deletions of genes regulating MSH2 protein stability cause DNA mismatch repair deficiency and drug resistance in human leukemia cells (Diouf et al., 2011). Indeed, MMR deficient cells display resistance to some chemotherapeutic agents (Karran, 2001). Interestingly, NPM-ALK mediates phosphorylation of MSH2 at tyrosine 238, which impairs MSH2 function and blocks MMR (Bone et al., 2015).

However, overexpression of *MSH2* in cancer cells can promote rapid repair of DNA damage, hence leading to disease progression and chemotherapy resistance (Ding et al., 2006; Marcelis et al., 2001). In ovarian carcinoma, MSH2 expression is associated with drug resistance, and inhibition of MSH2 *in vitro* reestablishes drug sensitivity (Zhang et al., 2014).

ALK (2p23)

ALK encodes the ALK tyrosine kinase receptor for pleiotrophin (PTN), a growth factor involved in embryonic brain development. The expression of *ALK* is normally restricted to neural tissues (Iwahara et al., 1997): it is highly expressed during perinatal development of the nervous system and is then down-modulated in adult tissues (Iwahara et al., 1997; Stoica et al., 2001).

The 6226 bp ALK cDNA encodes a 1620-amino acid (aa) protein of predicted mass 177 kDa, that undergoes post-translational N-linked glycosylation to a fully mature form of 220 kDa (Morris et al., 1997).

Aberrant activation of ALK can stem from numerous genetic mechanisms (including translocations or structural rearrangements, *ALK* gene amplification, mutations, and overexpression) and is usually associated with unfavorable clinical features.

In particular, *ALK* amplification is a common genetic event in several cancers and generally associated with poor outcome and more aggressive behavior (Zito Marino et al., 2016).

Anaplastic large-cell lymphomas (ALCL) constitute a distinct subset within the spectrum of mature T-cell neoplasms/lymphomas (Swerdlow et al., 2016). Although the majority of *ALK*+ (positive: presence of chromosomal rearrangements of *ALK)* ALCL is generally associated with favorable response to treatment and overall survival, some patients can have a highly aggressive disease. Furthermore, 20–30%

of *ALK*+ ALCL patients relapse and eventually require high-dose chemotherapies and bone marrow transplantation (Abate et al., 2015; Ferreri et al., 2012; Savage et al., 2008; Schmitz et al., 2010).

In a NB cohort with no *ALK* amplification and rare *ALK* mutation (4,1%), ALK protein expression was frequent (found in 56% of patients) and was correlated with advanced stage and high-risk NB. *ALK* mutations consisted of two somatically acquired missense mutations (F1174L and R1275Q) (Lee et al., 2018).

In NB, 2p gains including the *ALK* locus (91,8%) were associated with a significantly increased ALK expression, which was correlated with poor survival. Combined occurrence of *MYCN* amplification and *ALK* mutations was associated with a particularly poor outcome (De Brouwer et al., 2010) (see **Section IV. 4.2**).

Deregulation of *ALK* can also occur with genomically intact *ALK* locus. Alternative transcription initiation leads to expression of an aberrant *ALK* transcript, that is expressed in 11% of melanomas and sporadically in other human cancer types, but not in normal tissues. The novel *ALK* transcript, ALK^{ATI}, initiates from a *de novo* initiation site in *ALK* intron 19, and encodes three proteins consisting primarily of the intracellular tyrosine kinase domain. ALK^{ATI} drives cell proliferation *in vitro* and promotes tumorigenesis *in vivo* in mouse models (Wiesner et al., 2015).

Another aberrant *ALK* transcript with retention of the entire intron 19 (~2 kb) was detected in 4/4 NB cell lines and 38% of NB tumors at diagnosis. *ALK-I19* was more common in cases with gain of *MYCN*, and combination of *ALK-I19* and *MYCN* amplification was linked with a poor outcome (see **Section IV. 4.2**). *ALK-I19* significantly correlated with stage 4 disease and with the high-risk group (Alshareef et al., 2018).

ALK signaling can be activated by the formation of oncogenic fusions of the *ALK* gene at chromosomal band 2p23 with a variety of partners through chromosomal translocation events, generating oncogenic *ALK* fusion genes and their encoded proteins (Nava et al., 2008).

The t(2;5)(p23;q35) chromosomal translocation occurs in most (70-80%) *ALK*+ ALCL cases. Fusion of the nucleolar protein gene *NPM* on chr 5q35 to *ALK* on chr 2p23 generates a hybrid protein where the amino terminus of NPM is linked to the catalytic domain of ALK (Morris et al., 1994). NPM is a ubiquitously expressed nuclear protein responsible for protein shuttling between the cytoplasm and nucleus (Borer et al., 1989). Since ALK is normally not expressed in lymphoid cells, unscheduled expression of the truncated protein may contribute to malignant transformation in these lymphomas (Morris et al., 1994).

Indeed, the chimeric oncoprotein NPM-ALK has transforming capacity through its tyrosine kinase activity (Bai et al., 1998; Bischof et al., 1997) : NPM-ALK was able to transform fibroblasts (Wellmann et al., 1997), and to induce a T cell lymphoma and plasma cell tumors in mice (Chiarle et al., 2003).

NPM-ALK is typical of ALCL, but was not reported in classical HL, where constitutive activation of NF-κB appears to be a basis for the characteristic clinical

features. Noteworthily, NPM-ALK transduction into HL cell lines abolished NF-κB activation by blocking recruitment and aggregation of TRAF proteins, inducing an ALCL-like morphology and phenotype (Horie et al., 2004).

Interestingly, translocation causing the fusion of the *TRAF1* and *ALK* genes was reported in one chemorefractory patient who presented with a leukemic *ALK*+ ALCL. TRAF1-ALK induced the constitutive activation of ALK and NF-κB pathways (Abate et al., 2015).

The *TFG-ALK* fusion, implicating *TFG* (TRK-fused gene), also led to the activation of NF-κB pathway (Hernández et al., 1999).

ALK was recognized as a major familial NB predisposition gene. The presence of aberrant *ALK* copy number status (gain or amplification) strongly correlated with an aggressive clinical course, including metastasis at diagnosis, and death from disease (Mossé et al., 2008).

A distinct *ALK* oncogenic fusion protein involving *ALK* and echinoderm microtubule-associated protein like 4 (*EML4)* has been reported in non-small cell lung cancer (NSCLC) samples (3-7%), and in some cases of lung adenocarcinoma. Similarly to the aforementioned ALK fusion oncoproteins, the amino-terminal region of EML4 is fused to the kinase domain of ALK (Rikova et al., 2007; Soda et al., 2007; Takeuchi et al., 2008).

NCOA1 (2p23.3)

NCOA1 encodes the nuclear receptor coactivator 1, that directly binds nuclear receptors and stimulates the transcriptional activities in a hormone-dependent way.

Next-generation sequencing, performed in tumor tissue of one treatment-responsive lung adenocarcinoma patient, allowed the identification of a novel fusion form of an *ALK* rearrangement: *NCOA1-ALK* (Cao et al., 2019).

Several recent large-scale genome-wide association studies have identified *NCOA1* as a genetic risk factor associated with NHL, and recently as a susceptibility gene for multiple myeloma (Peng et al., 2017).

MYCN (2p24.3)

The *MYCN* gene encodes a 64-kDa nuclear phosphoprotein, N-Myc (Hansford et al., 2004). *MYCN* is a member of the *MYC* family of proto oncogenes, encodes a transcription factor involved in the control of fundamental processes during embryonal development (Ruiz-Pérez et al., 2017). Accordingly, the expression of N-Myc is normally high in embryonic tissues but low in adult tissues (Zimmerman et al., 1986).

Gain of the *MYCN* gene and high N-Myc expression were reported in several malignancies, mainly with a childhood onset such as NB, but were also linked, albeit less frequently, to adult cancers such as prostate and lung cancer (Beltran, 2014; Ruiz-Pérez et al., 2017).

In NB, *MYCN* gene amplifications strongly correlate with poor prognosis and treatment failure (Fix et al., 2008; Ruiz-Pérez et al., 2017; Seeger et al., 1985).

Indeed, NB patients with 2p gain had a significantly worse survival rate than patients with no such gain; all of the 2p gain samples were associated with segmental and/or numerical alterations, which were identified as a strong predictor of relapse in NB (Jeison et al., 2010). A genome-scale CRISPR-Cas9 screening of *MYCN*-amplified neuroblastoma revealed that *MYCN* upregulates ***EZH2***, leading to inactivation of a tumor suppressor program in NB (Chen et al., 2018).

Novel protein-coding genes can be generated by rearrangement of non-genic DNA. *NCYM*, a cis-antisense gene of *MYCN*, originally considered to be a large non-coding RNA, encodes a *de novo* evolved protein that stabilizes N-Myc protein by impairing the activity of GSK3β, a kinase that supports N-Myc degradation. In primary human NBs, *NCYM* is 100% co-amplified and co-expressed with *MYCN*, and *NCYM* mRNA expression is associated with poor clinical outcome. Interestingly, tumors developed in *Mycn/Ncym* double transgenic mice exhibited drug resistance (Suenaga et al., 2014).

Furthermore, N-Myc expression was elevated in a majority of human primary AML samples (Hirvonen et al., 1991). In mice, overexpression of N-Myc promptly induced AML, although N-Myc–overexpressing AML cells were oligoclonal or monoclonal, indicating that N-Myc overexpression alone is not sufficient to cause full leukemic transformation and other genetic events are needed (Kawagoe et al., 2007).

Patients with erythroleukemia showed higher expression of N-Myc than normal controls. Overexpression of N-Myc, acting through EZH2-mediated epigenetic repression of p21, promoted cell proliferation and induced erythroid differentiation block as well as, importantly, resistance to etoposide-induced apoptosis (Liu et al., 2017).

MYCN was also reportedly involved in a chromosomal translocation t(2;14)(p24;q32) that features the IGH gene in nodal marginal zone B cell lymphoma (Brown et al., 2019).

In CLL, our group and others have proposed that poor prognosis associated with 2p gain might be heralded by gain of *MYCN*. Indeed, CLL harboring *MYCN* gain at diagnosis have a significantly lower survival probability compared with CLL without *MYCN* gain (Deambrogi et al., 2010) and 2p gain correlated with increased *MYCN* transcript levels (Chapiro et al., 2010).

Although no enrichment of 2p amplification was observed in Richter syndrome (Fabbri et al., 2013), *MYCN* was reported to be recurrently gained in RS (Scandurra et al., 2010).

ROCK2 (2p25.1)

ROCK2 codes for the Rho-associated protein kinase 2, which is a major regulator of actin cytoskeleton and cell polarity.

In mantle cell lymphoma, immunohistochemical studies displayed significant increases in ROCK2 protein expressions in patients when compared with controls. However they found no significant change in *ROCK2* gene expression (Yanardağ Açık et al., 2016).

In gastric cancer, high expression of *ROCK2* predicted poor prognosis. Upregulated *ROCK2* promoted proliferation, metastasis and invasion of GC cells, while *ROCK2* knockdown led to the opposite results in vitro (Li et al., 2017).

ACP1 (2p25.3)

The *ACP1* gene encodes the low molecular weight phosphotyrosine protein phosphatase, or LMW-PTPase.

As previously mentioned, the *ACP1* gene is gained in about 25% of CLL cases (Ma et al., 2011), with frequent co-amplifications of *MYCN*. ACP1 regulates TCR signaling through activation of ZAP-70 (Ma et al., 2011).

In a chemoresistant leukemia cell line (Lucena-1), the LMW-PTPase is about 20-fold more active than in its susceptible counterpart (K562). Resistant leukemia cells present lower levels of oxidative metabolism and higher expression levels of glucose transporter 1 and higher production of lactate. It was shown, that LMW-PTPase superactivation is a pivotal mechanism of metabolic reprogramming towards glucose addiction that confers survival advantages to leukemia cells against death stimuli (Faria et al., 2017).

CAV1 (7q31.1)

The *CAV1* gene encodes the Caveolin-1 protein, which is implicated in the costimulatory signal necessary for TCR-mediated T-cell activation (Ohnuma et al., 2007). *CAV1* is not located on the 2p, but its transcription was significantly upregulated in 2p gain CLL patients (Fabris et al., 2013).

CAV1 seems to play a critical role in CLL-tumor microenvironment interactions, specifically in tumor-induced immunosuppression during CLL progression (Gilling et al., 2012). Caveolin-1 mRNA and protein levels were upregulated in CLL cells after interaction with bone marrow stromal cell (Vangapandu et al., 2018b). Consistently, knockdown of Caveolin-1 in primary CLL cells displayed a significant reduction in cell migration and immune synapse formation. *In vivo*, decreased Caveolin-1 in Eμ-TCL1 mice significantly delayed the onset of CLL and reduced leukemic progression by inhibiting MAPK-Erk signaling (Shukla et al., 2016).

4.2. Strategies for targeting of 2p genes

XPO1

Selective inhibitors of nuclear export (SINE) compounds covalently bind to cysteine 528 in the cargo-binding groove of Exportin-1 to inhibit nuclear export.

In CLL, Exportin-1 inhibition by the SINE compound KPT-185 impaired tumor growth *in vivo* in the murine Emu-TCL1-SCID model: importantly, KPT-185 induced apoptosis of tumor cells but not of normal B cells (Lapalombella et al., 2012).

The first-generation SINE KPT-185 analog, named selinexor (or KPT-330), has demonstrated anti-leukemic activity in CLL patient cells *in vitro* (Cosson et al., 2017; Lapalombella et al., 2012).

Experiments using CRISPR-Cas9 genome editing allowed the validation of Exportin-1 as the prime target of KPT-330: introduction of a homozygous (Neggers et al., 2015) or even a heterozygous (Neggers et al., 2016) mutation of cysteine 528 residue inside the XPO1 cargo-binding pocket conferred resistance to selinexor.

A novel second-generation inhibitor of Exportin-1-mediated nuclear export, KPT-8602, showed superior anti-leukemic efficacy and better tolerability than selinexor in AML (Etchin et al., 2017) and in CLL (Hing et al., 2016).

Combination treatment of selinexor with proteasome inhibitors decreased NF-κB activity, sensitized SINE resistant cells and showed synergistic cytotoxicity *in vitro* and *in vivo* (Kashyap et al., 2016).

In CLL, the concomitant targeting of Exportin-1 by selinexor and BTK by ibrutinib provoked a synergistic effect both *in vitro* in primary cells and *in vivo* in the Eμ-TCL1 mouse model, and bypassed ibrutinib resistance due to the C481S BTK mutation (Hing et al., 2015).

REL

Strategies to target ***REL*** are detailed in **Chapter V**.

BCL11A

miR-146a induces apoptosis in neuroblastoma cells by targeting BCL11A.

The miR-146a acts as a potential tumor suppressor gene in NB by targeting the 3'UTR of ***BCL11A*** and inhibiting its mRNA and protein expression. Upregulation of BCL-11A by miR-146a inhibition can promote human NB cells growth and protect them against apoptosis *in vitro* (Li et al., 2018).

MYCN

Robust correlation between *MYCN* amplification and sensitivity to bromodomain inhibition was reported. In NB, bromodomain-mediated inhibition of *MYCN* suppressed its gene transcription and downregulated the *MYCN* transcriptional program, resulting in diminished growth and apoptosis (Puissant et al., 2013).

Targeting BET proteins was previously shown to have specific antitumoral efficacy against *MYCN*-amplified NB. The BET inhibitor, OTX015, displayed therapeutic efficacy in preclinical *in vitro* and *in vivo* models of human and murine *MYCN*-driven NB. However, ectopic N-Myc expression, did not abolish effects of OTX015, implying that N-Myc repression is not the only target of BET proteins in NB (Henssen et al., 2016).

The c-Myc inhibitor 10058-F4 was demonstrated to also interfere with the transcriptional function of N-Myc *in vitro* and to convey anti-tumorigenic effects in N-Myc-overexpressing NB tumor models (Müller et al., 2014). This is not surprising, given the homology between c-Myc and N-Myc. Indeed, *MYCN* was originally identified as a gene amplified in human NB cells that showed high homology with *MYC*, the gene encoding c-Myc (Kato et al., 1990). N-Myc can substitute for c-Myc in murine development, cellular growth and differentiation (Malynn et al., 2000).

Receptor tyrosine kinases (RTKs) are involved in N-Myc protein stabilization and angiogenesis regulation. Sunitinib, an inhibitor of several RTKs, showed potent

antitumor activity on NB cells, through induction of apoptosis and cell cycle arrest. Treatment with sunitinib decreased N-Myc protein levels and significantly inhibited both angiogenesis *in vivo* as well as the growth of *MYCN*-amplified NB xenografts in nude mice (Calero et al., 2014).

The microRNA miR-204 was identified as a tumor suppressor that negatively regulates N-Myc expression in NB tumorigenesis. miR-204 directly bound *MYCN* mRNA and inhibited N-Myc expression. Overexpression of miR-204 significantly inhibited NB cell proliferation *in vitro* and tumorigenesis *in vivo* (Ooi et al., 2018).

A novel dual inhibitor allows the concomitant inhibition of ALK and BRD4 (Watts et al., 2019).

ROCK2

Inhibition of ROCK by small molecule ROCK1/2 inhibitors impaired growth and induced apoptosis in T cell leukemia cells *in vitro* (Oku et al., 2014).

4.3. Possible oncogenic cooperation within the 2p

REL-BCL11A

BCL11A is coamplified with ***REL*** in B-NHL cases and HL cell lines with gains and amplifications of 2p13 (Satterwhite et al., 2001).

Whole exome sequencing and transcriptome sequencing in DLBCL patients revealed a ***REL-BCL11A*** fusion, found in two refractory patients, with one having both fusion and copy gain (Park et al., 2016).

Transformation of FL to DLBCL is often accompanied by treatment resistance and poor survival. A high level of 2p15-16.1 amplification was found in the FL stage prior to transformation. Fusion or gain of ***REL*** and ***BCL11A*** was reported to be enriched in transformed lymphoma compared to *de novo* DLBCL, and this may be a genomic marker for disease progression to clinically more aggressive forms. Specifically, a higher level of amplification of ***REL*** and other NF-κB related genes ***USP34*** and ***COMMD1*** was reported, compared with ***BCL11A***, suggesting a driver role for the NF-κB pathway in this transformation (Kwiecinska et al., 2014; Martinez-Climent et al., 2003).

ALK-MYCN

ALK is a direct transcriptional target of *MYCN* (Hasan et al., 2013).

The kinase ERK5, also known as big mitogen-activated protein kinase (MAPK) 1 (BMK1), is required for ALK-induced transcription of *MYCN* and stimulation of cell proliferation in NB (Umapathy et al., 2014).

As previously mentioned, combined occurrence of *MYCN* amplification and *ALK* mutations was associated with a particularly poor outcome in NB, suggesting cooperative effect between the two alterations (De Brouwer et al., 2010).

For instance, the *ALK(F1174L)* mutation, one of the oncogenic *ALK* variants identified in primary NBs, is associated with inherent and acquired resistance to crizotinib and co-segregates with *MYCN* in NB. In mice co-overexpressing *Alk(F1174L)* and *Mycn* in the neural crest, NBs developed with earlier onset, higher penetrance, and enhanced lethality compared with expression of each oncogene alone (Berry et al., 2012; Schulte et al., 2013). Interestingly, tumor cells remained susceptible to the Myc-inhibitor, NBT-272, suggesting that cell growth depended on functional N-Myc (Schulte et al., 2013).

2p oncogenes – TP53

High-risk NBs are often near-di/tetraploid. *MYCN*-amplification synergizes with loss of *TP53* function in NB cells to induce overexpression of mitotic spindle regulatory genes and support survival of tetraploid NBs cells (Gogolin et al., 2013).

In NB, resistance to ionizing radiation-induced cell death has been linked to a combination of p53 loss of function and enhanced N-Myc expression (Yogev et al., 2016).

Mutant p53 augmented tumor promoting anti-apoptotic activities of the NF-κB subunit p65 (Schneider et al., 2010).

2p oncogenes – BCL2

Small cell lung cancer (SCLC) is a clinically aggressive cancer with very poor prognosis. Co-targeting of N-Myc and Bcl-2 by JQ1 and ABT-263 resulted in marked synergistic antitumor effects in *MYCN*-amplified SCLC (Wang et al., 2017a).

Chapter V: REL/NF-κB

The nuclear factor "kappa-light-chain-enhancer" of activated B cells (NF-κB) transcription factor plays a crucial role in a plethora of cellular processes, ranging from cell growth to apoptosis and immunity, and even learning and memory (Kaltschmidt and Kaltschmidt, 2009; Perkins, 2007; Sen and Baltimore, 1986b, 1986a).

NF-κB is ubiquitously expressed and responds to diverse stimuli, particularly including infectious agents, cytokines, or growth factors (Hayden and Ghosh, 2012; Kaltschmidt and Kaltschmidt, 2015).

1. The NF-κB genes and pathways

The NF-κB family is composed of five subunits, namely p65 (encoded by *RELA*), RelB (*RELB*), c-Rel (*REL*), p105/p50 (*NFKB1*), and p100/p52 (*NFKB2*), all comprising a conserved REL homology domain (RHD) near the N-terminus. This domain is crucial for DNA-binding (N-terminal part of RHD), dimerization of NF-κB family members, as well as interaction with the inhibitors of κB (IκBs) (C-terminal part of RHD). Via the RHD, NF-κB family members can form homo- or heterodimers, such as p50/p65, RelB/p50, p52/c-Rel, or p65/p65. RelB has an amino-terminal leucine zipper (LZ)-like motif. In addition, the subunits p65, RelB and c-Rel contain a C-terminal transactivation domain (TAD) (**Figure 23**). The subunits p52 and p50 are derived from proteolysis of their precursor proteins p100 and p105, respectively. (Chen et al., 1998; Kaltschmidt et al., 2018; Oeckinghaus and Ghosh, 2009). A more detailed view of c-Rel structure is shown in **Figure 26** and discussed in **Section V. 3**.

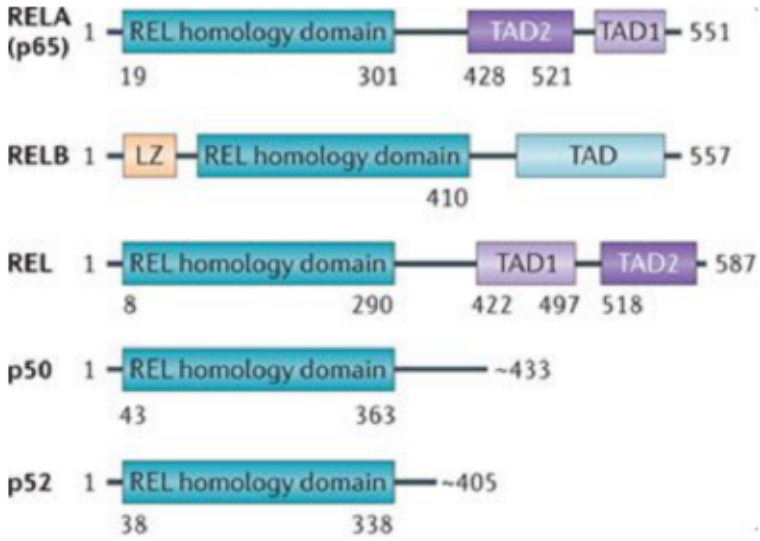

Figure 23: The five mammalian NF-κB subunits, adapted from (Perkins, 2012).

The RHD harbors a nuclear localization signal (NLS). Without stimulation, the NLS is masked by IκBs, which results in the retention of inactive NF-κB dimers within the cytoplasm.

Two major pathways leading to NF-κB activation have been described, namely the canonical and alternative pathways, which engage common and distinct components (Hayden and Ghosh, 2004). Both pathways are usually considered to be independent, however the non-canonical pathway may attenuate activities of the canonical pathway (Jin et al., 2014).

In mature B cells, BCR triggering results in canonical NF-κB activity, whereas ligation of the BAFF-receptor activates both pathways. Notably, NF-κB mediates B cell survival through upregulation of antiapoptotic proteins of the Bcl-2 family (Lam et al., 1997; Ng et al., 2005; Sasaki et al., 2006; Siebenlist et al., 2005).

1.1. Canonical/Classical pathway

During canonical NF-κB signaling, binding of ligands such as cytokine, growth factors, or lipopolysaccharides to their respective receptors leads to the phosphorylation of the IκB kinase (IKK) complex, consisting of IKK1/IKK2 (IKKα/IKKβ) and the regulatory subunit NEMO (NF-κB essential modulator, or IKKγ). Phosphorylated IKKs, in particular IKK2, in turn phosphorylates IκBα, which subsequently undergoes polyubiquitylation and proteasome-mediated degradation. Degradation of IκBα leads to demasking of the NLS of the NF-κB dimer, which leads to its translocation into the nucleus. This results in the expression of NF-κB target genes via binding to the respective target sites. This pathway activates predominantly heterodimers consisting of p50, p65, and c-Rel (Kaltschmidt and Kaltschmidt, 2009; Oeckinghaus and Ghosh, 2009) (**Figure 24**).

1.2. Non-canonical/Alternative pathway

On the contrary, non-canonical NF-κB signaling induced by distinct members of the tumor necrosis factor (TNF) family like lymphotoxin-β relies on the phosphorylation of IKK1 via NIK (NF-κB-inducing kinase), independently of NEMO. IKK1 mediates the phosphorylation of p100, associated to RelB, inducing the proteasomal processing of p100 to p52. The p52/RelB heterodimer is able to enter the nucleus and activate specific target genes via binding to selective κB sites (**Figure 24**). The alternative pathway induces mostly RelB-containing complexes (Senftleben et al., 2001).

2. NF-κB: a "double-edged sword' in health and disease

NF-κB is usually under tight control, with a variety of negative feedback loops finely regulating the magnitude and duration of NF-κB responses. However in many human diseases, NF-κB is aberrantly active and either causes or contributes to the pathology of the disease (Perkins, 2012).

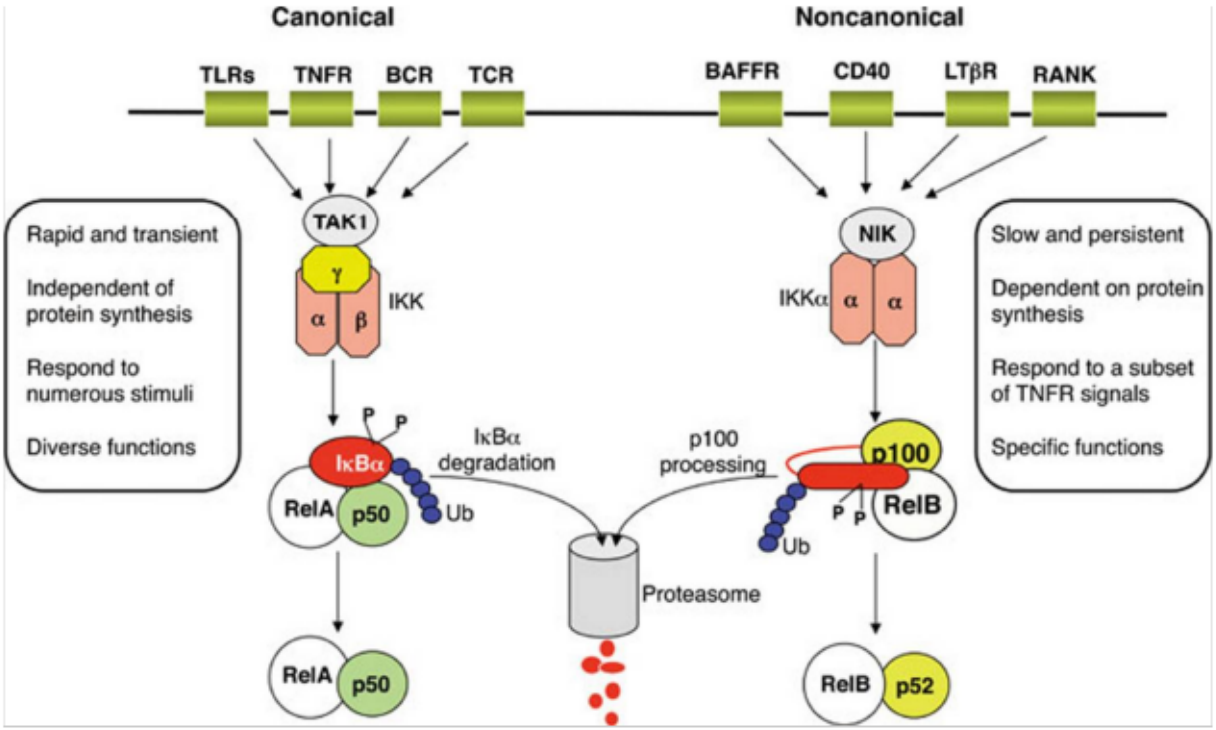

Figure 24: Canonical and non-canonical NF-κB signaling pathways. Canonical pathway is triggered by numerous signals, including those mediated by innate and adaptive immune receptors. It involves activation of IKK complex by Tak1, IKK-mediated IκBα phosphorylation, and subsequent degradation, resulting in rapid and transient nuclear translocation of the prototypical NF-κB heterodimer RelA/p50. Non-canonical NF-κB pathway relies on phosphorylation-induced p100 processing, which is triggered by signaling from a subset of TNFR members. This pathway is dependent on NIK and IKKα, but not on the trimeric IKK complex, and mediates the persistent activation of RelB/p52 complex (Sun, 2011).

2.1. REL/ NF-κB deregulation in cancer

In particular, consistent with its various cellular functions, deregulation of NF-κB signaling is strongly associated with cancer formation and progression (Ben-Neriah and Karin, 2011; Karin, 2006; Xia et al., 2014). Both the canonical and the non-canonical pathway have been described to be closely linked to cancer formation and progression (Hoesel and Schmid, 2013). In addition, atypical NF-κB pathways as in the case of epidermal growth factor receptor (EGFR) tyrosine kinase-dependent NF-κB activation, were likewise described to promote cancer (Alberti et al., 2012).

2.2. REL/ NF-κB deregulation in CLL

Several CLL-associated genetic lesions seem to converge on the activation of the NF-κB signaling pathway, either through activation of positive regulators or by disruption of negative ones (**Figure 25**).

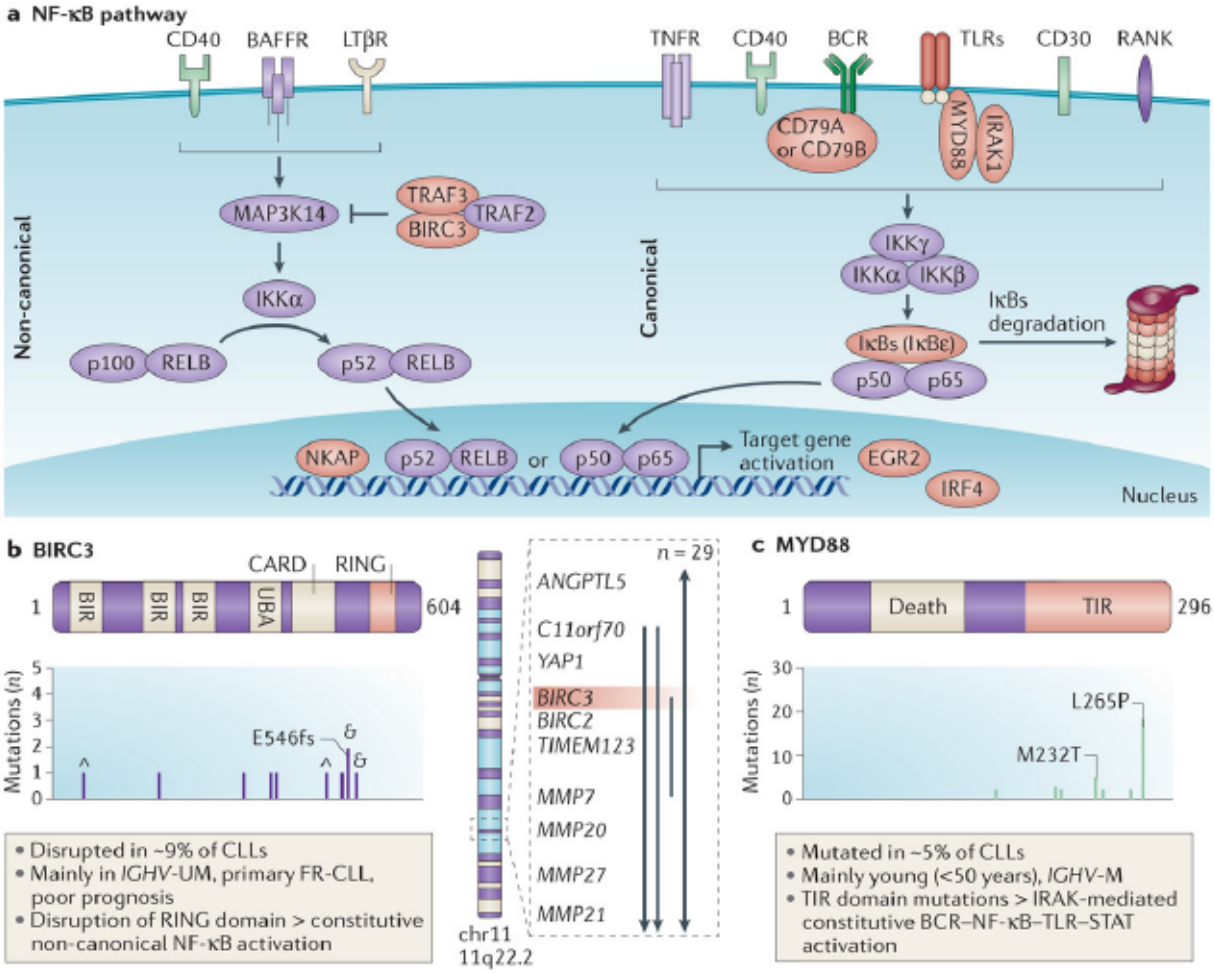

Nature Reviews | Cancer

Figure 25: NF-κB pathway mutations in CLL (Fabbri and Dalla-Favera, 2016).

For instance, disruptions of the Baculoviral IAP repeat containing 3 (***BIRC3***) gene (9% of CLLs), a negative regulator of non-canonical NF-κB signaling, lead to constitutive NF-κB activation. Disruption of ***BIRC3***, which can occur either by truncating mutations (2% of CLLs) and/or by monoallelic 11q deletions (see **Section III. 3**), lead to the deletion of the C-terminal RING domain, which is required for proteasomal degradation of a MAP3K14/NIK, a key activator of the non-canonical NF-κB pathway. Lesions in ***BIRC3*** are associated with poor prognosis factors (*IGHV*-UM, primary fludarabine-resistance) (Fabbri and Dalla-Favera, 2016; Rossi et al., 2011, 2012, 2013).

Genetic lesions in the NF-κB inhibitor epsilon ***NFKBIE***, found in approximately 5-7% of CLL cases, are generally associated with clonal evolution and rapid disease progression. These lesions are monoallelic mutations resulting in truncation of the ankyrin repeat domain, which leads to increased NF-κB nuclear translocation and subsequent target transcription (Alves et al., 2014; Mansouri et al., 2015).

The myeloid differentiation primary response 88 (***MYD88***) gene is a cytosolic adaptor protein of the Toll-like receptor (TLR) pathway, which upon stimulation by various ligands, lead to the activation of several signaling pathways in B cells,

including NF-κB (Rawlings et al., 2012). Mutations in *MYD88*, found in 2-5% of CLLs, all of them carrying *IGHV*-M genes, are generally associated with a favorable clinical outcome (Baliakas et al., 2015; Martinez-Trillos et al., 2014; Puente et al., 2011, 2015). The predominant lesion affecting *MYD88* in CLL is the L265P activating mutation, which is also recurrent in other malignancies (Ngo et al., 2011) such as DLBCL and WM (Treon et al., 2012). This mutation in the TIR domain leads to increased binding of MYD88 to IRAK1, inducing enhanced downstream phosphorylation and subsequent target activation, leading to enhanced NF-κB activity and cytokine secretion (Puente et al., 2011).

Furthermore, *NOTCH1* mutations constitutively activate the NF-κB signaling pathway: mutant cells displayed elevated *RELA* mRNA and increased apoptosis in the presence of NF-κB inhibitor PDTC (Xu et al., 2015).

CLL cells exhibit high constitutive NF-κB activation compared to normal B lymphocytes, with the p65 subunit being the most active and relevant for transcription (Cuní et al., 2004; Furman et al., 2000; Hewamana et al., 2008, 2009), while c-Rel is usually expressed and active at very low levels (Vaisitti et al., 2017). CD40 ligation further augmented NF-κB activity and prolonged CLL cell survival *in vitro*. The principle NF-κB proteins in CD40-stimulated CLL cells appear to be quite similar to those in nonmalignant human B cells and include p50, p65, and c-Rel (Furman et al., 2000).

Indeed, *RELA* DNA binding was strongly associated with *in vitro* survival, resistance to fludarabine (Hewamana et al., 2008) and advanced Binet stage (Hewamana et al., 2009), and was hence proposed as a predictive marker of response to treatment and predictor of overall survival. Expression of p65 is constitutively elevated in patients with more aggressive disease and is induced by chemotherapy (Hewamana et al., 2009). Moreover, RelB, together with p65, was shown to sustain cell survival and confer sensitivity to proteasome inhibitor in CLL cells (Xu et al., 2014).

3. The c-Rel subunit

c-Rel is mainly expressed in hematopoietic cells, and at low levels in endothelial and epithelial cells (Gilmore and Gerondakis, 2011).

In B cells, c-Rel is among the first transcription factors activated by BCR signaling (Gilmore and Gerondakis, 2011). Expression of c-Rel occurs at every stage of B cell development but is lowest in B cell precursors and highest in immature/mature B cells: during the developmental transition from a pre-B cell to a naïve mature B lymphocyte, upregulation of c-Rel (and p50) expression causes p50/c-Rel to be the predominant NF-κB dimers in mature B cells. In most cells, c-Rel exists either as a homodimer or a heterodimer with p50, but c-Rel can also form dimers with p65 and p52 (Grumont and Gerondakis, 1994; Liou et al., 1994).

As previously mentioned, the human *REL* gene encodes the 587-amino acid c-Rel transcription factor. *REL* contains the highly conserved N-terminal RHD domain

(Gilmore, 2006), a transactivation REL inhibitory domain (RID) (Leeman et al., 2008) and two C-terminal transactivation subdomains TAD1 and TAD2 (Martin and Fresno, 2000; Martin et al., 2001; Starczynowski et al., 2003) (**Figure 26**).

c-Rel can also subject to posttranscriptional modifications: phosphorylation, acetylation and ubiquitination, although their precise functional relevance remain unclear (Gilmore and Gerondakis, 2011).
Alternative splicing can remove part of the RID, which increases DNA binding and transactivating activities. This alternatively spliced form of ***REL*** mRNA is overexpressed in B lymphoma cell lines (Leeman et al., 2008) (**Figure 26A**) (see **Section V. 3.3**).

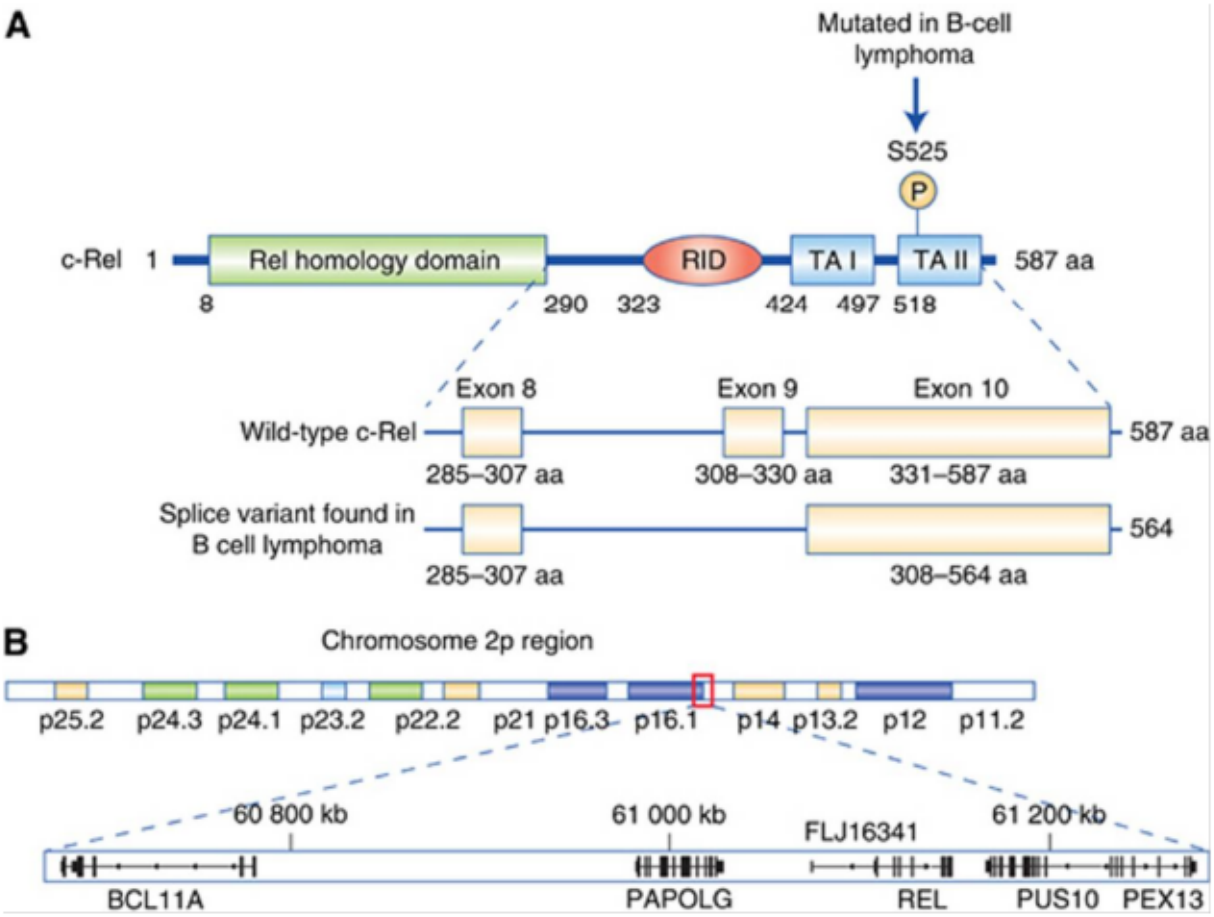

Figure 26: Structure and genomic location of human c-Rel. A: Schematic diagram showing the structure of c-Rel and amino-acid positions of different regulatory motifs. A putative IKK phosphorylation site found mutated in some B-cell lymphoma patient samples together with a splice variant that removes 23 amino acids from the ***REL*** inhibitory domain (RID) also found in some B-cell lymphoma cell lines and patient samples are shown. TA I (TAD1) and TA II (TAD2) are c-Rel transcriptional activation domains. B: Diagram demonstrating the close proximity of the ***REL*** gene to the ***BCL11A*** proto-oncogene and the pseudouridine kinase ***PUS10*** on human chromosome 2. Both genes therefore have the potential to be co-amplified in human cancers. Figure compiled using the Integrated Genomics Viewer and the hg19 build of the human genome (Hunter et al., 2016).

3.1. Direct targets of c-Rel

Context-specific gene regulation by NF-κB is determined by various factors, namely the selective activation of different dimers, their different DNA binding and transactivation properties, as well as post-translational modifications (Perkins, 2012). Although its differential regulation relatively to other NF-κB subunits remain poorly understood, c-Rel is certainly a unique NF-κB member, exhibiting both nonredundant and overlapping functions (Li et al., 2015). Particularly, c-Rel seems to harbor a unique oncogenic activity among the Rel/NF-κB family (Gilmore et al., 2004) (see **Section V. 3.3**).

Indeed, despite the considerable overlap in the DNA sequences and genes bound by the various NF-κB dimers, some genes appear to be preferred direct targets for c-Rel, as reviewed in (Gilmore and Gerondakis, 2011). Specifically, c-Rel promotes cell survival by transactivating genes involved in:

i. cell proliferation/growth, such as *MYC* (Grumont et al., 2002), *IRF4* (Grumont and Gerondakis, 2000), *E2F3* (Cheng et al., 2003)
ii. apoptosis inhibition, namely *BCL2* (Bureau et al., 2002; Grossmann et al., 2000), *BCLX/BCL2L1*, *BCL2A1*, *XIAP*, *BIRC2* (Banerjee et al., 2008; Bureau et al., 2002; Chen et al., 2000; Gilmore and Gerondakis, 2011; Kaileh and Sen, 2012)
iii. adhesion/cell structure: *Selectin*, *MMP1* (De Siervi et al., 2009)
iv. immune cell function: *TNFA* (Bunting et al., 2007), *CD40L* (Pham, 2005), *BAFF* (Fu et al., 2006), *FOXP3* (Son et al., 2011)
v. DNA repair/damage: *ATM* (De Siervi et al., 2009) (see **Section III. 3**).

Importantly, c-Rel is able bind to the *REL* promoter and modulate its own expression (Grumont et al., 1993).

The polycomb group protein EZH2 is a histone methyltransferase that alters chromatin structure to modify gene expression during embryonic development and lymphocyte activation. Loss of *EZH2* was shown to confer multidrug resistance in multiple myeloma (Göllner et al., 2017). c-Rel, but not other NF-κB members, was shown to be an activator of *EZH2* transcription in human lymphoid cells (Neo et al., 2014).

3.2. Knockout phenotype and physiological functions of c-Rel

c-Rel knockout mice are viable with an overall normal hematopoiesis, but have deficiencies in specialized immune functions: for instance, although they display normal numbers of mature B cells, these cells do not proliferate in response to mitogenic stimulation (Gerondakis et al., 2006; Gilmore and Gerondakis, 2011; Köntgen et al., 1995). Studies using knockout mice have also shown that c-Rel is required for both B cell activation during formation and maintenance of the GC reaction (Heise et al., 2014) as well as for T-independent antibody production (Milanovic et al., 2017). Moreover, c-Rel promotes B cell differentiation and survival: in BCR-activated cells, c-Rel promotes the progression from G1 to S phase (Grumont et al., 1998).

Furthermore, c-Rel is crucial for T cell activation, proliferation and survival, and specifically for the development of follicular helper T cells as well as for the development and function of activated Tregs (Chen et al., 2010; Refaat et al., 2011). c-Rel was also shown to be involved in liver regeneration (Gieling et al., 2010) and memory (Ahn et al., 2008; Levenson et al., 2004).

Importantly, genome-wide analysis of gene expression in T-cells of c-Rel knockout mice revealed that very few genes are significantly affected by c-Rel deletion. The relatively subtle effects of c-Rel deletion could be explained by redundancy with other NF-κB members, i.e. functional compensation (Bunting et al., 2007).

Studies in double knockout mice lacking both c-Rel and p100/p50 proteins have suggested that the overlapping roles for these subunits seem to be restricted to the activation and function of mature cells (Pohl et al., 2002).

In addition to NF-κB/IKB proteins, c-Rel interacts with several partners, illustrating its pleiotropy in health and disease. Namely, c-Rel can interact with proteins involved in transcription (Foxp3, Cdk2/cyclinE), nuclear import/shuttling (importin alpha) (Fagerlund et al., 2008), signaling (BAFF-R, CD40, Calmodulin), as reviewed in (Gilmore and Gerondakis, 2011). Functional partners of c-Rel predicted or known from curated databases and textmining, mostly involve NF-κB family proteins (**Figure 27**).

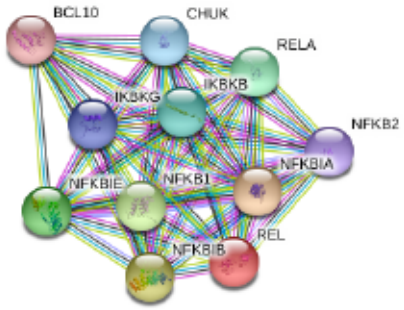

Figure 27: c-Rel interactome. Predicted and known functional partners of c-Rel are depicted, results exported from the STRING database of protein-protein interaction networks (string-db.org).

3.3. Functions of c-Rel in oncogenesis

Sustaining proliferative signaling and resisting cell death are the hallmarks of cancer (Hanahan and Weinberg, 2011), and, given its aforementioned target genes, the idea that deregulated c-Rel expression could contribute to oncogenesis seems readily predictable.

Several alterations affecting the *REL* gene have been associated with lymphoid and nonlymphoid human cancers: the *REL* gene was reported to be the target of amplifications and point mutations in several neoplasms, which could result in overexpression. Increased *REL* expression was often linked to adverse clinical features.

Interestingly, SNPs within or near the ***REL*** locus were reportedly associated with an increased susceptibility to Hodgkin lymphoma (Enciso-Mora et al., 2010).

3.3.1. Transforming abilities

REL, but not other NF-κB members, has a unique ability to transform avian lymphoid cells *in vitro* (Gilmore and Gerondakis, 2011) and was associated with increased lymphoma risk *in vivo* (Burkitt et al., 2013).

Even though deletion of both TAD subdomains obliterates the ability of ***REL*** to transform chicken spleen cells *in vitro*, deletion of either TAD subdomain alone, which reduces the transactivating ability of ***REL***, enhances its transforming activity (Starczynowski et al., 2003). Indeed, overexpression of a human ***REL*** mutant (***RELΔTAD1***) missing one transactivation domain enhanced the oncogenic properties of the human Burkitt lymphoma cell line BJAB by increasing the expression of target genes such as ***BCL2***, ***IRF4*** and ***MIR155*** (Chin et al., 2009).

Overexpression of mouse c-Rel in the mammary gland led to 31,6% of mice developing one or more mammary tumors. Steady overexpression of c-Rel led to increased cyclin D1 and p52 and p50 protein levels (Romieu-Mourez et al., 2003).

Studies on the roles of Xrel3, the c-Rel homologue of *Xenopus laevis*, revealed that overexpression of Xrel3 results in formation of tumors in early embryos (Yang et al., 1998). In HeLa human cervical cancer cells, expression of Xrel3 slowed cell growth and was proposed to play a dual role in apoptosis, displaying anti-apoptotic effects with low cisplatin treatment dosage (1 μM), but apoptotic effects with high dosage (5 μM) (Shehata et al., 2004).

3.3.2. REL gains/amplifications

REL gene amplifications occur mainly in tumors with a mature B cell phenotype, which is consistent with the stage of development where c-Rel plays a crucial role in normal B cell function: indeed, gain or amplification of REL was detected in approximately 46% of HL, 63% of primary cutaneous large B-cell lymphoma (PCLBCL), 15% of DLBCL and 5% of CLL cases, as reviewed in (Gilmore and Gerondakis, 2011).

Importantly, since c-Rel complexes are normally found in the nucleus of mature B cells, nuclear c-Rel staining by immunolocalization is not considered sufficient to establish a driver role for ***REL*** in oncogenesis (Gilmore and Gerondakis, 2011). Moreover, owing to its complex regulation, ***REL*** amplification or gain is not always correlated to increased mRNA or protein expression, with sometimes conflicting results for a given malignancy.

Gain of 2p including the ***REL*** locus in classical HL correlated with nuclear c-Rel staining, protein accumulation and constitutive NF-κB activity (Barth et al., 2003; Enciso-Mora et al., 2010; Joos et al., 2002; Martín-Subero et al., 2002). However,

another study found no correlation between ***REL*** amplification and high-level ***REL*** mRNA expression in classical HL (Kluiver et al., 2007).

In primary mediastinal B cell lymphoma (PMBL), amplification of the ***REL*** locus correlates with increased ***REL*** mRNA, nuclear c-Rel and NF-κB activity (Weniger et al., 2007).

And conversely, in DLBCL, amplification of the ***REL*** locus was not associated with nuclear accumulation of c-Rel nor with clinical parameters (Houldsworth, 2004). In a study with both PMBL and DLBCL cells, NF-κB activation was not necessarily associated with amplification of the ***REL*** locus, and increased abundance of c-Rel *per se* did not translate into increased NF-κB activity (Feuerhake et al., 2005).

In DLBCL, ***REL*** was found to be more frequently amplified than ***BCL11A*** and even appeared to be the only gene in the minimally amplified region. Gain of ***REL*** correlated with mRNA expression in one study (Fukuhara et al., 2006). ***REL*** mRNA is highly expressed in *de novo* DLBCLs and this elevated expression resulted in increased expression of many ***REL*** target genes (Rhodes et al., 2005). DLBCL cases with nuclear ***REL*** expression had a worse overall survival (Curry et al., 2009).

In a cohort of *de novo* DLBCL patients, nuclear c-Rel expression, used as surrogate of c-Rel activation observed in 26,3% of patients did not show significantly prognostic impact in the overall cohort, but was associated to significantly poorer OS in patients with mutant p53 or in activated B cell like DLBCL patients with low levels of BCL-2. ***REL*** amplifications did not correlate with c-Rel nuclear expression and patient survival, likely due to co-amplification of negative regulators of NF-κB (Li et al., 2015).

In FL tumors, ***REL*** amplification was frequent but resulted in weak transcript expression (Hu et al., 2017).

Increased ***REL*** mRNA expression has been correlated with a poorer prognosis in splenic marginal B cell lymphoma (Ruiz-Ballesteros et al., 2005) as well as in marginal zone B-cell lymphoma (Barth et al., 2001).

3.3.3. REL mutations

In addition to amplifications, mutations in ***REL*** could activate is oncogenicity in human lymphomas.

The point mutation S525P within the ***REL*** transactivation domain exhibited enhanced in vitro transforming activity in chicken spleen cells, and was identified in two human B cell lymphomas (FL and PMBL) (Starczynowski et al., 2007).

Targeted deep sequencing of 18 NF-κB core complex genes revealed several mutations in the ***REL*** gene in CLL (4/301 cases), associated with different cytogenetic aberrations but all with *IGHV*-UM (Mansouri et al., 2015).

3.3.4. Interactions with oncogenic REL

The p53 homologue DeltaNp63alpha is overexpressed and inhibits apoptosis in a subset of human squamous cell carcinomas (SCC). Both in normal keratinocytes overexpressing DeltaNp63alpha and in human SCC cells, DeltaNp63alpha physically associates with phosphorylated, transcriptionally active nuclear c-Rel, resulting in increased c-Rel nuclear accumulation, thereby promoting uncontrolled proliferation (King et al., 2008).

In large B-cell lymphoma cell lines, nuclear CD40 interacts with c-Rel, but not p65, to form complexes on the promoters of NF-κB target genes (CD154, BLyS/BAFF, and Bfl-1/A1), and support proliferation and survival (Zhou et al., 2007).

3.3.5. Reports of c-Rel implication in drug resistance

c-Rel is a critical regulator of NF-κB dependent TRAIL resistance of pancreatic cancer cells pancreatic ductal adenocarcinoma NF-κB signaling critical resistance against chemotherapy and death receptor induced apoptosis. Transfection with siRNA against c-Rel sensitized the TRAIL resistant cells, albeit in a similar manner to siRNA-mediated p65 downregulation (Geismann et al., 2014).

In adult T-cell leukemia/lymphoma (ATLL) the increased c-Rel expression was associated with resistance to therapy (Ramos et al., 2007).

Members of the Bcl-2 family are often deregulated in cancer (Ichim and Tait, 2016), and expression of many of them has been shown to be of prognostic significance for response to chemotherapy in various malignancies. This deregulated expression can stem from deregulation of c-Rel. In particular, antiapoptotic Bcl-2-family proteins are able to suppress cell death induced by cytotoxic anticancer drugs, thus constituting a form of intrinsic chemoresistance (Yip and Reed, 2008) (see **Section VI. 1**). However, in Bcl-2- DLBCL, c-Rel positivity correlated with significantly poorer survival (Li et al., 2015), supporting the idea that c-Rel exerted its oncogenic function via Bcl2-independent pathways (Heise et al., 2014).

4. Targeting NF-κB

4.1. Pan- NF-κB inhibitors

NF-κB has been implicated in almost all chronic diseases. Although more than 700 different inhibitors (aspirin to IκBα super repressor) of this transcription factor, acting at different blocking distinct steps of NF-κB pathway, have been reported, no NF-κB blocker has been approved yet for human use (Gilmore and Herscovitch, 2006; Gupta et al., 2010; Lim et al., 2012).

Several pharmacological inhibitors of NF-κB activity have been experimented in a variety of tumor types:

i. IKK inhibitors: the IKKbeta inhibitor BMS-345541 has been shown to selectively induce apoptosis in CLL cells (Lopez-Guerra et al., 2009), and so

did the IMD-0354 compound (Kanduri et al., 2011). MLN120B blocks multiple myeloma cell growth *in vitro* and *in vivo* (Hideshima et al., 2006). However, none is currently tested in a clinical trial due to their toxicities (Mansouri et al., 2016).

ii. Inhibition of NF-κB activation by blocking the activity of proteasomes: Bortezomib is a reversible 26S proteasome inhibitor, which showed no objective response in a single agent phase II study of 19 fludarabine-refractory CLL patients (Faderl et al., 2006).

iii. Non-steroidal anti-inflammatory drugs: aspirin (Bellosillo et al., 1998), the benzylamide analogue CP461 (Moon and Lerner, 2002) and curcumin (Everett et al., 2007) have all been found to induce apoptosis in CLL.

Indeed, targeting NF-κB leads to apoptosis of CLL cells, corroborating its role in the survival and clonal expansion of tumoral cells. In particular, inhibition of NF-κB can overcome the microenvironmental protection of CLL cells (Lopez-Guerra and Colomer, 2010; Vaisitti et al., 2017).

Interestingly, the D-tripeptide DTP3 targets the interaction between the NF-κB-regulated antiapoptotic factor GADD45β and the JNK kinase MKK7 and kills multiple myeloma cells effectively, and, selectively, since it did not affect normal cells. DTP3 has similar anticancer potency to bortezomib, but more than 100-fold higher cancer cell specificity *in vitro* (Tornatore et al., 2014).

PIKfyve inhibitors inhibit c-Rel DNA binding on IL-12p40 and IL-1β promoter, and prevented aberrant B cell activation and production of inflammatory cytokines (Terajima et al., 2016).

The NF-κB inhibitor 6-Amino-4-(4-phenoxyphenethylamino)quinazoline, which inverted the anti-apoptotic effect of IL-4 (see **Section III. 4**), preferentially blocked the response of genes positively correlated with ZAP-70 (e.g. CCR2, SUSD2), but enhanced the response of genes negatively correlated with ZAP-70 (e.g. AUH, BCL6, LY75, NFIL3) (Ruiz-Lafuente et al., 2014).

Since a healthy cellular steady state is not associated with NF-κB activity, a truly NF-κB specific drug would therefore not be expected to disturb normal cell functions (Shono et al., 2016). However, precisely, the molecules that block NF-κB activation generally lack specificity and thus interfere with NF-κB's physiological roles in immunity, inflammation, and cellular homeostasis. In addition to off-target effects, the concentrations of compounds used to inhibit NF-κB *in vitro* studies may be substantially different (often much higher) than could ever be used *in vivo* (Gilmore and Herscovitch, 2006; Gupta et al., 2010).

4.2. Targeting c-Rel

Because the activity of c-Rel is restricted to a small number hematopoietic lineages and linked to oncogenesis, a c-Rel specific inhibitor should likely have a better safety profile than a pan-NF-κB inhibitor (Shono et al., 2014).

Indeed, c-Rel has been proposed to be an appealing therapeutic target whose down-regulation by siRNA or chemical inhibitors can impair tumor growth without causing systemic tissue toxicity (Tian and Liou, 2009). Given the similarity within the RHD between ***REL*** and other NF-κB family members it is unlikely that sequences within the RHD could provide a specific therapeutic target, however the c-Rel transactivation domain might provide a specific target for inhibition (Gilmore and Gerondakis, 2011).

Importantly, RNAi-mediated c-Rel silencing leads to apoptosis of tumor B cells and suppresses antigenic immune response *in vivo* (Tian and Liou, 2009).

The siRNA-mediated knockdown of c-Rel in choriocarcinoma cells decreased their proliferative abilities however c-Rel overexpression using a CRISPR activation system did not affect cell proliferation c-Rel knockdown decreased proliferation and induced apoptosis in Jar and Bewo cells, the expression levels of Bcl-XL and Bcl-2 were not changed by c-Rel knockdown (Sekiya et al., 2017).

In acute lymphoblastic leukemia (ALL), inhibition using siRNA in c-Rel overexpressing pre-B blasts led to upregulation of Bcl-2 and down-regulation of Bax, which increased apoptosis and decreased proliferation (Mohammadi et al., 2017).

Selective inhibitors of c-Rel act through various mechanisms: for instance, STA-5326 suppresses c-Rel nuclear accumulation (Keino et al., 2008), FK506 (Sen et al., 1995) and Pin1 inhibitor (Fan et al., 2009) block c-Rel nuclear translocation, while epoxyquinoids inhibit c-Rel DNA binding (Liang et al., 2006).

Inhibition of c-Rel by PTXF reduced melanoma growth and potentiated anti-PD1 therapy without compromising systemic tolerance or causing autoimmunity. The specific implication of c-Rel was confirmed *in vivo*, as melanoma growth was drastically reduced in mice lacking c-Rel, but not p65, in Tregs (Grinberg-Bleyer et al., 2017).

A study group showed that c-Rel inhibition using a small-molecule inhibitor, named IT-603, was able to impair graft-versus-host-disease (GVHD) by reducing alloactivation of T cells without compromising their antigen-specific cytotoxicity (Shono et al., 2014). Moreover, IT-603 displayed anti-proliferative effects in DLBCL cell lines (Shono et al., 2014). In vitro treatment of T cells with thiohydanthoin IT-603 induces c-Rel deficiency resulting in suppression of T cell alloactivation without compromising antitumor activity of T cells/T cell activation triggered by recognition of tumor associated or viral antigens (Shono et al., 2014).

The small molecule c-Rel inhibitor IT-901 suppressed GVHD while preserving graft-versus-lymphoma activity during allogenic transplantation, and revealed antitumor properties in DLBCL, both *in vitro* and *in vivo*. This anti-lymphoma effect was attributed to induction of oxidative stress and was cancer selective, since IT-901 did not elicit increased levels of ROS in normal leucocytes. Both IT-603 and IT-901 act as direct NF-κB inhibitors by preventing DNA binding of c-Rel. IT-901, was found to be a more potent c-Rel inhibitor than IT-603: the estimated half maximal inhibitory concentration IC50 regarding global NF-κB activity was about 6 times lower for IT-901 (3 μM) compared with IT-603 (18,8 μM). However, incubation of T cells for 24

hours showed that IT-603/DMSO was much less toxic than IT-901/DMSO. Moreover, IT-901 concentrations above 10 µM become increasingly toxic and could thus lead to apoptosis of healthy cells. IT-901 displayed cross-reactivity regarding other NF-κB members, which is not surprising given that they are structurally related (see **Section V. 1**) (Shono et al., 2016).

In CLL, treatment with IT-901 displayed dual effects that resulted in successful disruption of NF-κB transcriptional activity: CLL cells exhibited elevated mitochondrial ROS, which damaged mitochondria and activated intrinsic apoptosis, while accessory cells such as stromal and myeloid cells failed to protect CLL cells from IT-901 induced apoptosis. IT-901 rapidly induced apoptosis in primary CLL cells, but not in normal B and T lymphocytes, independently of the mutational status of *IGHV* genes and presence of genetic lesions in *TP53*. Interestingly, IT-901 was also effective in RS primary cells. IT-901 showed synergistic activity with ibrutinib, arguing in favor of combination strategies (see **Section III. 7**). IT-901 potently inhibited DNA binding of c-Rel, p65 and p50. Silencing of p65 by shRNA recapitulated IT-901 functional effects (Vaisitti et al., 2017) (see **Section V. 2**).

The efficacy of anti-cancer drugs is usually assessed by measuring the rate of tumor cell death. In order to better understand the consequences of inhibiting *REL*/NF-κB subunits at the molecular and cellular levels, and more broadly to devise the most precise therapeutic strategy, the next chapter will focus on programmed cell death (**Chapter VI**).

While programmed cell death can be achieved by targeting proteins using pharmacological inhibitors, off-target effects can occur and must be accounted for and reduced to a minimum if possible. A much more specific targeting of a given protein of interest can be obtained using CRISPR-Cas9 technologies, which will be discussed in **Chapter VII**.

Chapter VI: Programmed cell death

Cell death is a crucial process during development, homeostasis and immunity of multicellular organisms, and its deregulation is associated with various diseases.

Different types of cell death can be defined by morphological and biochemical hallmarks, the main types being apoptosis (type I cell death), autophagic cell death (type II) and necrosis (type III) (Duprez et al., 2009; Green and Llambi, 2015).

1. Apoptosis

Apoptosis, also called programmed cell death, is a cell-intrinsic suicide program that, upon cell shrinkage, membrane blebbing and chromatin condensation, leads to the controlled breakdown of the cell into apoptotic bodies (Duprez et al., 2009).

Importantly, removal of apoptotic cells is immunologically silent, which is required for the restoration of normal tissue structure and function. Indeed, apoptotic bodies are ultimately recognized and engulfed by surrounding phagocytes such as macrophages and fibroblasts, which prevents apoptosis from provoking inflammation (Krysko et al., 2008). Loss of phospholipid asymmetry and surface exposure of phosphatidylserine (PS) is required for phagocyte engulfment of apoptotic cells (Fadok et al., 2001a).

Apoptosis plays a crucial role during development and is required for organ and tissue remodeling, for instance in cardiac morphogenesis and removal of interdigital webs (Penaloza et al., 2006). Moreover, formation of both the nervous and the immune systems are characterized by initial overproduction of cells followed by elimination of extra cells by apoptosis (Elmore, 2007).

Apoptosis engages two major evolutionary conserved protein families, namely:

i. the Bcl-2 family of proteins, which regulate mitochondrial integrity (Youle and Strasser, 2008) (see **Section VI. 1.1**),
ii. and caspases, which orchestrate the effector phase of apoptosis (Fuentes-Prior and Salvesen, 2004) (see **Section VI. 1.2**).

1.1. Bcl-2 family of proteins

BCL-2 family proteins, which exert either pro- or anti-apoptotic functions, control the point of no return for apoptosis induction and thus affect tumorigenesis and cellular responses to pathogens or anti-cancer therapy (Youle and Strasser, 2008).

There are three subfamilies of BCL-2 proteins (**Figure 28**):

1. Anti-apoptotic BCL-2 proteins: BCL-2, BCL-XL (BCL2L1), MCL1
2. Pro-apoptotic BH3-only proteins: PUMA, BID, BIM (BCL2L11)
3. Pro-apoptotic multi-domain proteins: BAX, BAK.

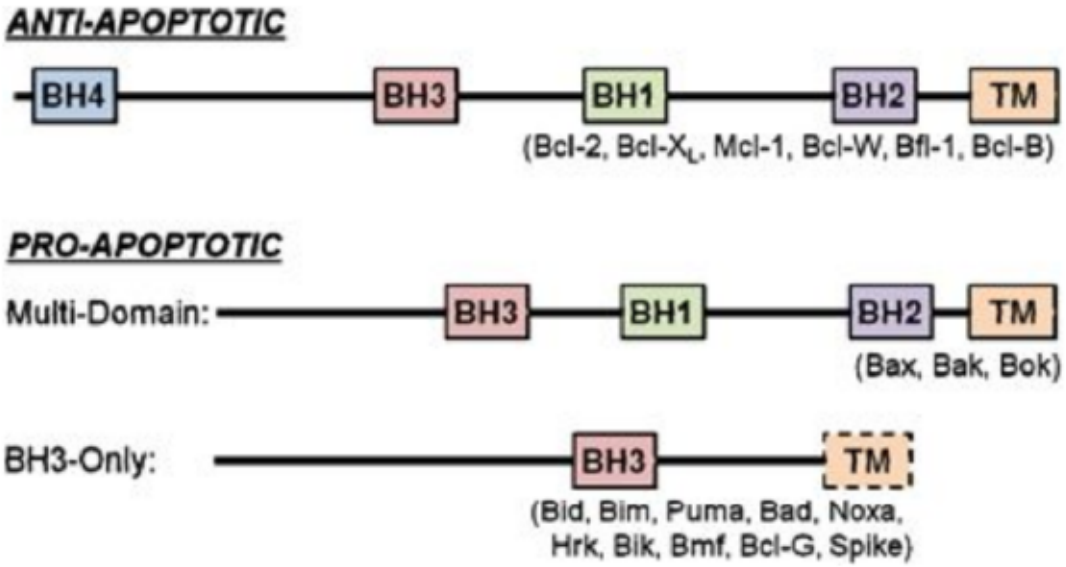

Figure 28: Comparisons of domain structures of Bcl-2-family proteins (Yip and Reed, 2008). Bcl-2-family proteins have at least one of four Bcl-2 homology (BH) domains (BH1, BH2, BH3 or BH4), and typically also possess a transmembrane domain (TM). Antiapoptotic Bcl-2-family members contain all four BH domains. Proapoptotic Bcl-2-family members can be separated into 'multi-domain' or 'BH3-only' proteins. Some BH3-only proteins do not have a TM (dotted line). Note that some BH3-only proteins have a limited set of BH domains (for example, Bcl-G has BH2 and BH3).

1.2. Caspases

Caspases (cysteine aspartic acid-specific proteases) are highly specific proteases that cleave their substrates after specific tetrapeptide motifs (P4-P3-P2-P1) where P1 is an Asp residue. Structurally, they are constituted of a pro-peptide (containing a caspase recruitment domain (CARD) or the death effector domain (DED)) followed by a large and a small subunit (**Figure 29**). CARD and DED domains typically enable interaction with proteins that contain the same domains (Green and Llambi, 2015; Taylor et al., 2008).

All caspases are expressed as inactive proenzymes in most nucleated animal cells. Apoptotic stimuli induce the activation of initiator caspases (caspases -2, -8, -9, -10) by dimerization upon recruitment into activation platforms. Once activated, the initiator caspases mediate the proteolytic cleavage of the effector caspases (caspases -3, -6, -7), resulting in their enzymatic activation (Salvesen and Riedl, 2008). Activation of caspases occurs through proteolytic processing between the large and small subunits to form a heterodimer, which rearranges the caspase active site into the active conformation.

Caspases characteristically function as heterotetramers, which are formed through dimerization of two caspase heterodimers. Initiator caspases exist as monomers in healthy cells, whereas effector caspases are present as pre-formed dimers. Catalytically active effector caspases orchestrate the destruction of key

cellular structures and organelles: for instance, ER and Golgi fragmentation, translational shutdown (Green and Llambi, 2015; Taylor et al., 2008) (**Figure 29**).

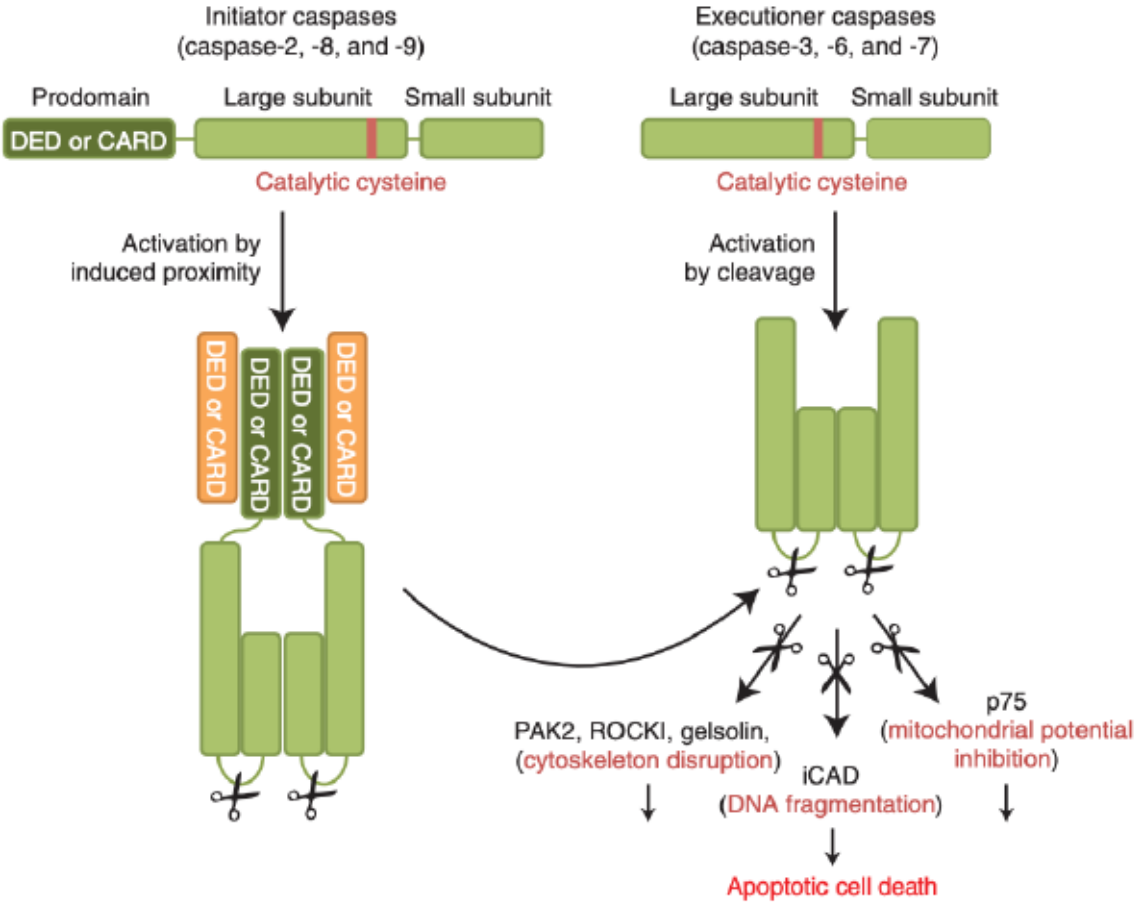

Figure 29: The caspase protein family (Green and Llambi, 2015).

Noteworthily, not all mammalian caspases participate in apoptosis. For example, caspase-1, -4, -5 and -12 are involved in the regulation of inflammatory cytokine processing (Taylor et al., 2008).

In mammalian cells, caspases can be activated by the intrinsic or the extrinsic apoptotic pathways (**Figure 30**).

1.3. Extrinsic apoptotic pathway

The extrinsic/death receptor apoptotic pathway is engaged upon stimulation of death receptors belonging to the TNFR family, such as TNFR1, FAS and TRAIL-R1/2 (Duprez et al., 2009; Ichim and Tait, 2016). Upon binding to their cognate ligand, death receptors can activate initiator caspases (8 and 10) through dimerization mediated by adaptor proteins such as FAS-associated death domain protein (FADD). Active caspase 8 and 10 then cleave and activate the effector caspases 3 and 7, leading to cleavage of caspase substrates and rapid cell death (Ichim and Tait, 2016; Taylor et al., 2008) (**Figure 30**).

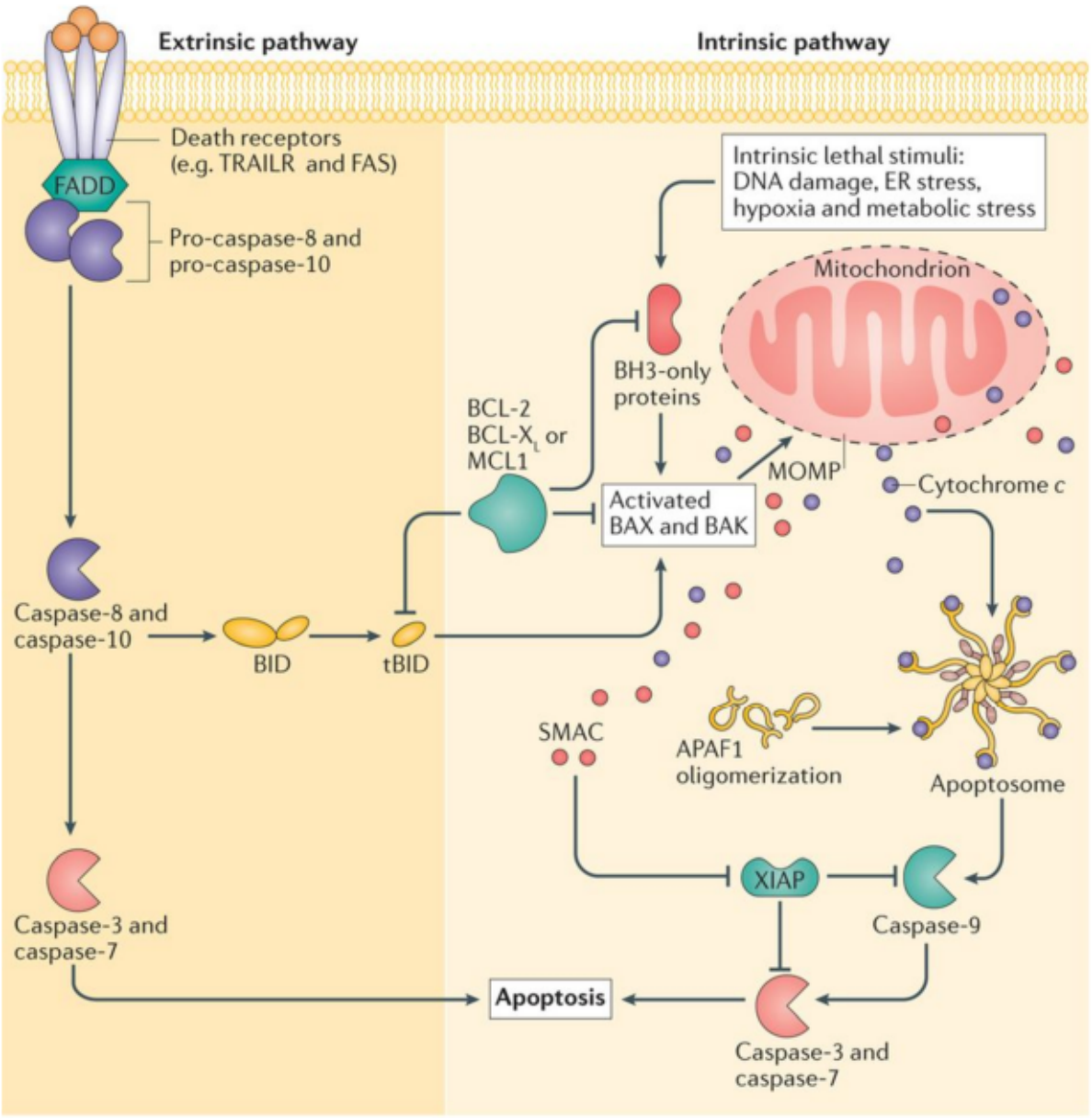

Figure 30: Extrinsic and intrinsic apoptotic signaling pathways (Ichim and Tait, 2016).

1.4. Intrinsic apoptotic pathway

The intrinsic (or mitochondrial) pathway of apoptosis is activated by a wide array of stimuli that are sensed intracellularly, including cytokine deprivation, DNA damage and ER stress (Czabotar et al., 2014); and acts through mitochondria, which are controlled by the Bcl-2 family of proteins (Duprez et al., 2009; Youle and Strasser, 2008).

These various apoptotic stresses engage BH3-only protein activation, leading to BAX and BAK activity, which converge to trigger one critical event: mitochondrial outer membrane permeabilization (MOMP).

MOMP results in release of cytochrome c and second mitochondria-derived activator of caspases (SMAC) from the mitochondrial intermembrane space into the cytosol. While SMAC blocks the caspase inhibitor XIAP, cytochrome c interacts with apoptotic protease activating factor 1 (APAF1), leading to the assembly of a cytoplasmic complex termed the apoptosome, which activates caspase 9. Active caspase 9 in turn activates caspases 3 and 7, leading to apoptosis (Ichim and Tait, 2016; Tait and Green, 2010) (**Figure 30**).

Caspase-8 cleavage of BID allows crosstalk between extrinsic and intrinsic apoptotic pathways by producing active truncated form of BID (tBID) that triggers MOMP (Li et al., 1998; Luo et al., 1998).

Because of this decisive role in cell death, MOMP is strongly regulated through interactions between BCL-2 family members (Czabotar et al., 2014). For instance, anti-apoptotic BCL-2 family proteins counteract BAX and BAK activity.

1.5. Tumour resistance to apoptosis

Resistance to apoptosis is a hallmark of cancer cells, which acquire it through various mechanisms that impede at different steps of apoptotic signaling (summarized in **Table 5**) (Igney and Krammer, 2002).

In addition to this intrinsic chemoresistance conveyed by Bcl-2, other mechanisms of drug resistance can implicate drug efflux, drug metabolism, drug inactivation (Yip and Reed, 2008).

2. Autophagic cell death

Autophagy is an evolutionary conserved catabolic pathway that allows eukaryotes to degrade and recycle cellular components. It is usually a survival process, engaged under metabolic stress. Proteins and organelles are sequestered in double membrane vesicles called autophagosomes. This envelops intracellular material and ultimately fuses with lysosomes allowing degradation of the enveloped material (Duprez et al., 2009; Green and Llambi, 2015).

The occurrence of autophagy during type II cell death, also designated as caspase-independent cell death accompanied by autophagy, typically characterizes a failed attempt to overcome lethal stress (Duprez et al., 2009; Green and Llambi, 2015).

3. Necrosis

Necrosis is mostly seen as an accidental, uncontrolled cell death, usually associated with severe physical or chemical tissue damage. Nevertheless, necrosis can also be induced in tightly controlled physiological conditions, as a caspase-independent pathway (sometimes called necroptosis) that can serve as a back-up mechanism for apoptosis if caspase activation is impeded. DNA damage, ligands of death receptors and Toll-like receptors (TLRs) 3 and 4, and detection of viral DNA in the cytosol can induce signaling pathways that all converge on the activation of

receptor interacting protein kinase 3 (RIP3). This leads to cytoplasmic and organelle swelling, followed by the rapid loss of cell membrane integrity and release of the cellular contents into the surrounding extracellular space (Duprez et al., 2009; Green and Llambi, 2015).

Table 5: Mechanisms of tumour resistance to apoptosis, as reviewed in (Igney and Krammer, 2002).

Expression of anti-apoptotic molecules	
BCL2 family members:	BCL2 BCL-X_L MCL1
FLIP	
Soluble receptors for death ligands:	Soluble CD95 DcR3
IAPs:	Survivin cIAP2 ML-IAP
PI-9/SPI-6	
Downregulation and mutation of pro-apoptotic genes	
BAX	
APAF1	
Caspase-8	
Death receptors:	CD95 TRAIL-R1 TRAIL-R2
XAF1	
Alterations of the p53 pathway	
p53	
INK4A/ARF	
ASPP	
Alterations of the PI3K/AKT pathway	
PI3K	
PTEN	
AKT	
Further mechanisms	
Expression of transporters:	MDR1/P-glycoprotein MRP
Alterations of NF-κB activity	
Extracellular matrix	

As a result, necrotic cells initiate a proinflammatory response by releasing DAMPs (Fadok et al., 2001b) and inflammatory cytokines (Vanden Berghe et al., 2006). Moreover, contrary to apoptosis, the uptake of disrupted necrotic cells by micropinocytosis is slower and less efficient (Krysko et al., 2003).

4. Pyroptosis

Pyroptosis designates a cellular suicide program that is uniquely dependent on the activation of the inflammatory caspase-1. Initiation of proinflammatory response leads to apoptosis, but accompanied by cell lysis and release of its cytoplasmic content, which further amplifies the inflammation (D'Arcy, 2019; Duprez et al., 2009).

Pyroptosis has been described in monocytes, macrophages and dendritic cells infected with a range of microbial pathogens, such as *Shigella* or *Salmonella*, and is hence considered to be a part of the host defense system (Bergsbaken et al., 2009).

5. Oncosis

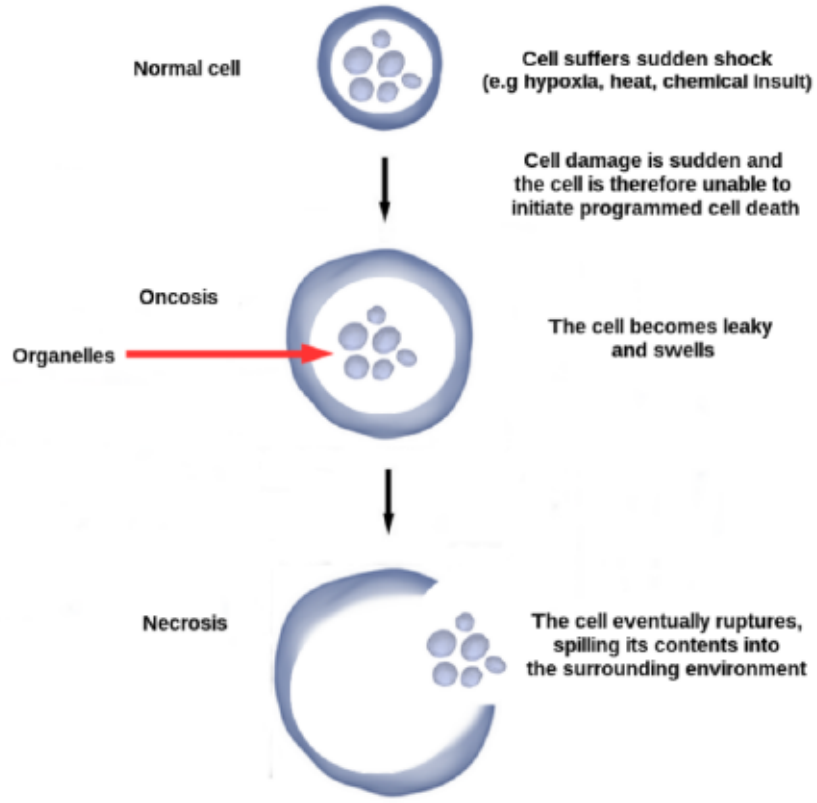

Figure 31: Progression of a normal cell, to an oncotic and necrotic cell. Following a sudden shock to the cell, and up-regulation of pro-inflammatory cytokines, the cell loses permeability, swells (oncosis) and then ruptures (necrosis), spilling its contents into the surrounding tissue (D'Arcy, 2019).

Oncosis designates a prelethal pathway triggered by sudden shock to the cell, such as ischemic injury, or some infections. It results in swelling of the cell as well as an increase in membrane permeability, and ultimately leads to cell death. Similarly to necrosis, oncosis is pro-inflammatory since it is associated with leakage of cellular debris and consequently damage in surrounding tissues (D'Arcy, 2019; Levin, 1998) (**Figure 31**).

Chapter VII: CRISPR-Cas gene editing

CRISPR-Cas systems were originally discovered as an adaptive immune system for bacteria and archaea. In the past few years, CRISPR-Cas technologies have revolutionized biology and sparked novel hopes for medicine, highlighting, *inter alia*, the tremendous importance of fundamental research.

1. CRISPR-Cas defense systems

Adaptive immunity had been long thought of as an exclusive feature of animals. However, the discovery of a plethora of diverse CRISPR/Cas immune systems, present in genomes of most archaea and almost half of the bacteria, proved otherwise. These systems can be categorized in two classes that are each subdivided into three types (Mohanraju et al., 2016) **(Figure 32)**.

CRISPRs, which stand for clustered regularly interspaced short palindromic repeats, designate well-organized repeated motifs (Jansen et al., 2002; Mojica and Garrett, 2013), that are interspaced with foreign short DNA sequences (< 50 bp) (Mojica et al., 2005). Their presence conferred resistance to viral infections, which revealed that CRISPR served in a form of adaptive immune system (Barrangou et al., 2007).

CRISPR-associated genes (Cas) encode endonuclease enzymes that use the information in CRISPR spacers as coordinates for silencing invading nucleic acids in a sequence-specific manner. This cleavage always happened within the sequence complementary to the spacer, at a specific distance from a recognized short (2-7 nt) sequence named the protospacer adjacent motif (PAM). Specifically, in type II CRISPR-Cas systems, two RNA fragments are needed for Cas9-mediated cleavage of foreign DNA: the CRISPR spacer (crRNA) and the trans-activating crRNA (tracrRNA), a trans-encoded small RNA with nucleotide complementarity to the repeat regions of crRNA (Deltcheva et al., 2011; Garneau et al., 2010).

Briefly, CRISPR/Cas-mediated adaptive immunity follows three stages (Bhaya et al., 2011; Brouns et al., 2008; Carte et al., 2008; Deltcheva et al., 2011; Gesner et al., 2011; Hatoum-Aslan et al., 2011; Haurwitz et al., 2010; Sashital et al., 2011; Terns and Terns, 2011; Wang et al., 2011; Wiedenheft et al., 2012):

i. in the adaptive phase, prokaryotes harboring one or more CRISPR loci respond to viral or plasmid challenge by incorporating short fragments of the invading sequence (termed protospacers) into the host chromosome at the leader end of the CRISPR array.
ii. during the expression phase, the CRISPR locus is transcribed as a precursor CRISPR RNA (pre-crRNA), which is processed to yield mature crRNA guides that can base pair with protospacer foreign sequences.

iii. in the interference phase, the Cas-crRNA complex scans invading viral or plasmid DNA for a complementary nucleic acid target, after which the target is degraded by a Cas nuclease.

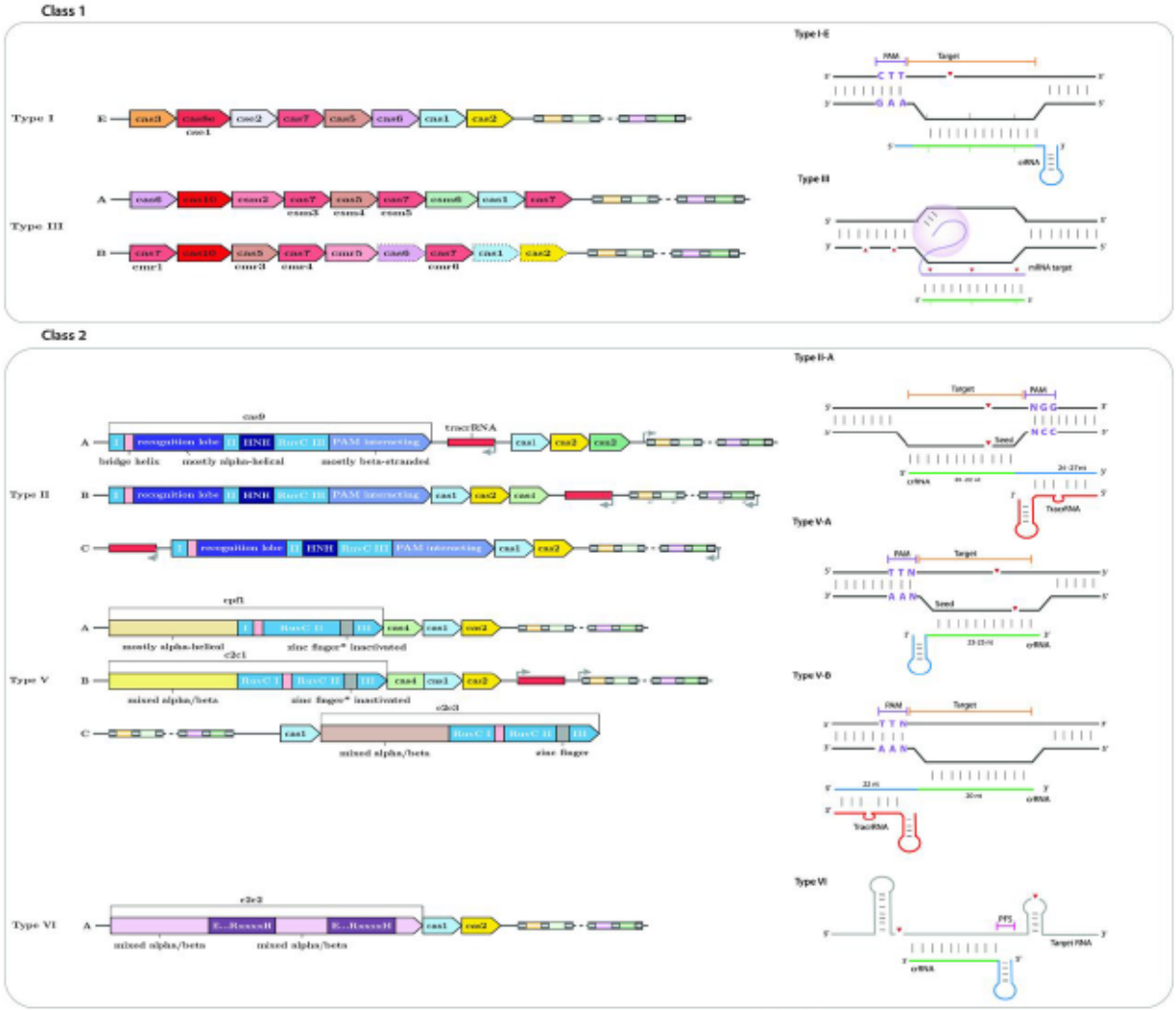

Figure 32: Genomic loci architecture of the components of class 1 and class 2 CRISPR-Cas systems and schematic representation of target interference for the different subtypes. The double-stranded DNA (target) is shown in black, the target RNA in gray, the CRISPR RNA (crRNA) repeat in blue, the spacer region of the crRNA in green, and the transactivating CRISPR RNA (tracrRNA) in red (Mohanraju et al., 2016).

Interestingly, not all sequenced bacteria possessed CRISPR/Cas systems, despite their ability to be horizontally transferred. Indeed, acquisition of foreign DNA can sometimes be beneficial, rendering CRISPR/Cas non adaptative in that case. The balance between fitness advantages and detrimental effects depend on species (Bondy-Denomy and Davidson, 2014).

2. CRISPR/Cas9-mediated targeted genome editing

Since crRNA and tracrRNA are complimentary sequences, they can bind into a double-strand that, in type II CRISPR/Cas systems, directs the CRISPR-associated protein Cas9 to generate double-stranded breaks (DSBs) in target DNA. Recognition of cleavage site requires crRNA-DNA base pairing and a three nucleotide PAM sequence (NGG) juxtaposed to the DNA complementary region (Jinek et al., 2012).

Importantly, since PAM sequences can be found anywhere in the human genome, any DNA sequence that contains the N20-NGG motif is a potential target site. And any RNA chimera sequence mimicking the tracrRNA-crRNA complex, henceforth referred to as single guide RNA (sgRNA), could be synthetized to recruit Cas9 to targeted genomic sites (Jinek et al., 2012), which allowed the adaptation of the type II CRISPR/Cas9 system to achieve targeted genome editing in diverse cell types and model organisms (Zheng et al., 2014).

Crystallography studies revealed that Cas9 contains two lobes: a target recognition lobe responsible for binding sgRNA and target DNA by recognizing the PAM sequence, and a nuclease lobe that performs cleavage of the target DNA (Gasiunas et al., 2012; Nishimasu et al., 2014).

The Cas9 contains two different DNA cutting domains: at sites complementary to the crRNA-guide sequence, the Cas9 HNH nuclease domain cleaves the complementary strand, whereas the Cas9 RuvC-like domain cleaves the noncomplementary strand **(Figure 33C)**. The Cas9 unwinds the DNA into two strands and then creates a blunt ended double strand break (Jinek et al., 2012).

DSBs pose threats to genome integrity, since they can result in mutations, chromosomal rearrangements or cell death if not precisely repaired (Heyer et al., 2010). To cope with these hazards, cells evolved two major repair mechanisms for DSBs: non-homologous end-joining (NHEJ) and homology-directed repair (HDR) (Meers et al., 2016).

CRISPR-mediated genome editing is initiated with the introduction of a DSB at a targeted genomic locus (Zheng et al., 2014) **(Figure 33A)**:

i. in the presence of a homology repair (HR) donor, i.e. a donor template with homology to the targeted locus, the HDR process can insert precise modifications in the target sequence.
ii. without HR donor, which is the default setting in most experiments discussed in this section, DSBs are repaired through the error prone NHEJ process, resulting in insertion or deletion (indel) mutations.

Indel mutations in the coding sequence may ultimately introduce premature stop codons or frame-shift mutations, thereby knocking out the function of the gene due to the production of truncated polypeptides and/or nonsense-mediated mRNA decay (Perez et al., 2008; Ramlee et al., 2015; Santiago et al., 2008; Sung et al., 2013).

Four potential outcomes can arise if we consider the targeting of a single diploid cell: no mutation, a heterozygous mutation (only one allele is mutated), a biallelic mutation (both alleles are mutated but the sequence of each allele is distinct) or a

homozygous mutation (both alleles carry the same mutation), which can also occur if one allele is used as a template to repair the break in the other allele. Expectedly, experiments performed in polyploid cells and animals, in chimera organisms, or screenings pools of samples generally yield more complex outcomes. Off-target mutations can further complicate the analysis (see **Section VII. 3**).

Some sgRNAs can alter splicing and induce exon skipping or large genomic deletions that encompass exons, adding to the unexpected outcomes that must be accounted for and taken advantage of in CRISPR experiments (Mou et al., 2017). For instance, CRISPR/Cas9 editing can result in chromosome elimination (Zuo et al., 2017).

Illegitimate translation, i.e. translation that is initiated from an in-frame ATG translation initiation codon other than the authentic ATG, can cause unexpected gene expression from on-target out-of-frame alleles created by CRISPR-Cas9 (Makino et al., 2016). Indeed, targeting CRISPR-Cas9 induced mutations to the 5'exons of candidate genes often yields in-frame variants that maintain functionality, whereas targeting mutagenesis to exons encoding functional protein domains can produce a higher proportion of null mutations (Shi et al., 2015).

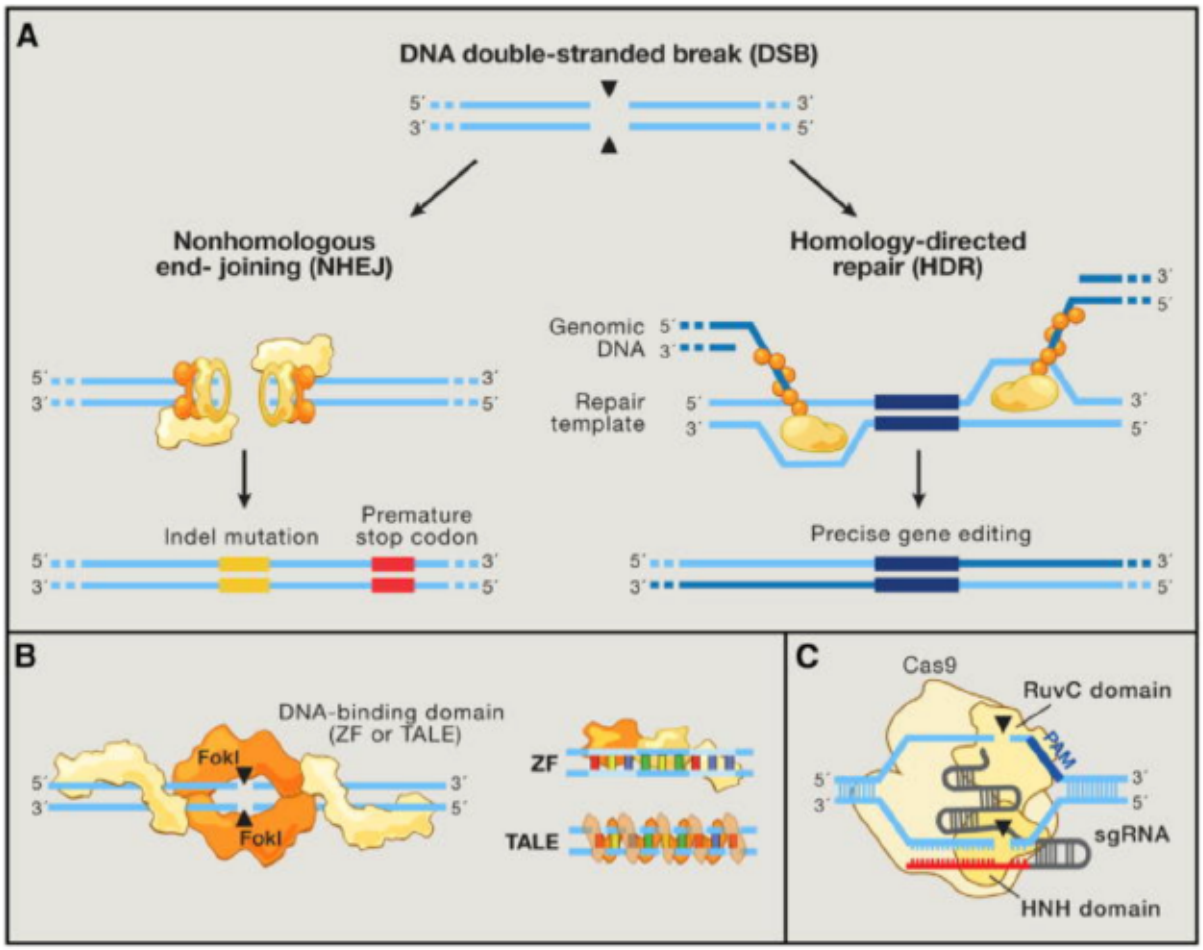

Figure 33: Genome editing technologies exploit endogenous DNA repair machinery. A: DNA double-strand breaks (DSBs) are typically repaired by nonhomologous end-joining (NHEJ) or homology-directed repair (HDR). In the error-

prone NHEJ pathway, indels are introduced when the complementary strands undergo end resection and misaligned repair due to micro-homology, eventually leading to frameshift mutations and gene knockout. Alternatively, HDR directs genomic recombination with homology arms on an exogenous repair template, resulting in the introduction of precise gene modifications. B: Zinc finger (ZF) proteins and transcription activator-like effectors (TALEs) are naturally occurring DNA-binding domains that can be modularly assembled to target specific sequences. ZF and TALE domains each recognize 3 and 1 bp of DNA, respectively. Such DNA-binding proteins can be fused to the FokI endonuclease to generate programmable site-specific nucleases. C: The Cas9 nuclease from the microbial CRISPR adaptive immune system is localized to specific DNA sequences via the guide sequence on its guide RNA (red), directly base-pairing with the DNA target. Binding of a protospacer-adjacent motif (PAM, blue) downstream of the target locus helps to direct Cas9-mediated DSBs (Hsu et al., 2014).

3. Designing CRISPR/Cas-based genome editing experiments with their specific caveats in mind

3.1. Targeting specificity

Since sgRNAs can tolerate certain mismatches and have rather short sequences (20 nt), CRISPR/Cas9 endonucleases can produce off-target cleavage due to unspecific recognition of non-target sequences and the off-target effects have hence been extensively examined (Pattanayak et al., 2013; Yee, 2016).

Mathematical analysis predicted that for a given sgRNA sequence, potential off-target homologies in the human genome are almost inevitable (Zhou et al., 2017). However, reported sequencing results were quite variable.

For instance, in human cells, the identified off-target sites harbored up to five mismatches, and many of them were mutagenized with frequencies comparable to (or higher than) those observed at the intended on-target site, suggesting that RNA-guided nucleases can be highly active even with imperfectly matched RNA-DNA interfaces in human cells (Fu et al., 2013).

Conversely, a whole genomic sequencing study revealed that CRISPR/Cas9 system was actually highly specific, with little to zero off-targets effects (García-Tuñón et al., 2017). In a research setting, the extensive identification of off-targets mutations seems relatively superfluous (Fellmann et al., 2017).

The 8-12 PAM proximal bases, termed the seed sequence, determine target specificity (Nishimasu et al., 2014). The specificity of RNA-guided endonucleases is rather complex and target-site dependent, with one or two mismatches often well tolerated. Mismatches at the 5'end of gRNAs better tolerated than those at the 3'end (Fu et al., 2013).

High-fidelity CRISPR-Cas9 variant nucleases, named SpCas9-HF1, was designed to diminish non-specific DNA contacts, and displayed no detectable genome-wide off-target cleavage activities (Kleinstiver et al., 2016).

A chemical modification (2 -O-methyl-3 -phosphonoacetate) incorporated at select sites in the ribosephosphate backbone of gRNAs can considerably decrease off-target effects while retaining high on-target efficacy (Ryan et al., 2017).

3.2. Cas9 integration and expression

Moreover, unwanted integration of DNA segments derived from plasmids encoding Cas9 and guide RNA at both on-target and off-target sites in the genome, potentially resulting in constant Cas9 production, represents a key limit, which could be circumvented by the use of inducible or integrase-deficient lentivirus vectors, as well as by direct delivery of Cas9 gRNA ribonucleoprotein (RNP) complexes.

For instance, delivery of purified recombinant Cas9 protein and guide RNA into cultured human cells, including typically hard-to-transfect cells such as fibroblasts and pluripotent stem cells, resulted in site-specific mutations at frequencies of up to 79%. Cleavage of chromosomal DNA occurs almost immediately after delivery and RNPs are promptly degraded in cells, reducing off-target mutations. Additionally, RNP delivery is less stressful to human embryonic stem cells, generating at least twofold more colonies than does plasmid transfection (Kim et al., 2014).

Inducible CRISPR/Cas9 system considerably reduced off-target effects with a pulse exposure of the genome to the Cas9/sgRNA complex (Cao et al., 2016). Similarly, tunable CRISPR-Cas system (tCRISPRi) provided a tunable and reversible control of gene expression (Li et al., 2016).

Cas9 activity can also be potently switched off by naturally occurring inhibitors of CRISPR-Cas9. For instance, three distinct families of small phage-encoded anti-CRISPR proteins (Acrs) that specifically block the CRISPR-Cas9 activity of *Neisseria meningitidis* were discovered and shown to block Cas9-mediated genome editing in cultured human cells (Pawluk et al., 2016), acting through various mechanisms (Harrington et al., 2017) (**Figure 34**).

3.3. Genome editing efficacy

Cleavage efficiency critically depend on several factors, namely genomic context of target DNA, GC percentage and secondary structure of sgRNA. Nucleotides at both PAM distal and PAM proximal regions of the sgRNA are significantly correlated with on-target efficacy (Liu et al., 2016b).

The chimeric structure of gRNA with original full length of crRNA and tracrRNA showed higher genome editing efficiency than the conventional sgRNA chimeric structure, probably owing of the formation of extra loop structure, which might enhance the stability of the guide RNA structure and subsequently the genome editing efficiency (Xu et al., 2017).

Efficacy of CRISPR-Cas9 genome editing experiments by HDR is improved through inhibition of 53BP1, which is a key regulator of DSB repair pathway choices in eukaryotic cells, and normally functions to favor NHEJ over HDR by suppressing end resection (Canny et al., 2018).

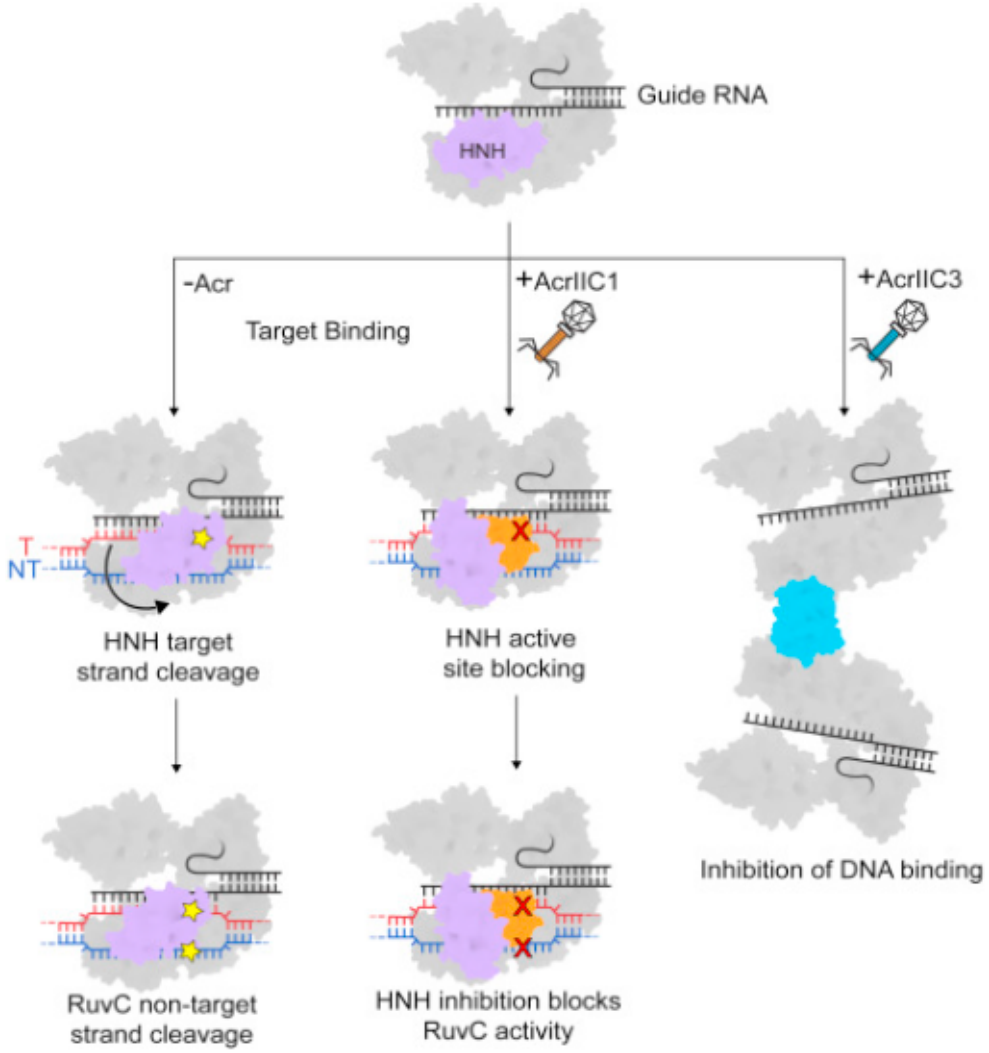

Figure 34: Model of AcrIIC1 and AcrIIC3 Inhibition of Cas9. Cas9 assembles with its guide RNA to form the search complex. Phage-encoded AcrIIC1 (orange) binds to Cas9, still allowing target dsDNA binding but occluding the HNH (purple) active site and stopping cleavage of the target strand. AcrIIC1 also conformationally restricts HNH docking, stopping cleavage on the non-target strand. For AcrIIC3 (blue), Cas9's target DNA binding is inhibited and Cas9 is caused to dimerize (Harrington et al., 2017).

3.4. Detection of on-target mutations

Upon DSB initiation, resulting mutations need to be confirmed and characterized. Several methods for the detection of targeted mutations can be used (**Table 6**), with the selection of the ideal method in any situation depending among other factors on the type of sample, the anticipated size and frequency of the mutations, and the cost of the method. The mismatch cleavage assay is a simple and cost-effective method for the detection of indels and is consequently the most commonly used technique to detect mutations induced by genome editing. This kind of assay uses enzymes, like the T7 endonuclease I for instance, that cleave heteroduplex DNA at mismatches and extrahelical loops formed by multiple

nucleotides, yielding two or more smaller fragments. A PCR product of ~300–1000 bp is generated with the predicted nuclease cleavage site off-center so that the resulting fragments are different in size and can easily be resolved by conventional gel electrophoresis (Zischewski et al., 2017).

In some cases, on-target efficacy can be assessed by disruption assays. For the instance, the activity of Cas9 targeted to a single integrated human ***EGFP*** reporter gene can also be quantified by assessing loss of fluorescence signal (Fu et al., 2013).

Table 6: PCR-based methods for the detection of on-target mutations induced by sequence specific nucleases (Zischewski et al., 2017).

Methods	Type of mutations preferentially detected	Reported sensitivity	Determination of mutation type?	Cost[a]	Throughput	Limitations
Mismatch cleavage assay	Small indels	0.5–3%	No	$	Moderate	T7E1 can overlook single nucleotide changes; Surveyor less sensitive than T7E1
HRMA	Small indels	2%	If insertion or deletion	$ (+ equipment)	High	Misses large indels
Heteroduplex mobility assay by PAGE	Small indels	0.5%	No	$	Moderate	Misses large indels
CAPS	All		No	$	Moderate	Availability of restriction site
Loss of primer binding site	Indels	10%	Yes	$	High	Misses substitutions
Sanger sequencing	All	1–2%	Yes	$$/$$$[b]	Low	Costly, labor intensive
NGS	All	0.01%	If insertion or deletion	$$$$	High	Misses large indels
AFLP	Large indels, also Mb		If insertion or deletion	$	Moderate	Misses small indels
Fluorescent PCR-capillary gel electrophoresis	Small indels	1%	Number of bp	$$	High	Misses substitutions

[a] Estimated cost per assay. $: <1 US$; $$: <5 US$, $$$: >100 US$; $$$$: >500 US$.
[b] Sequencing of bulk/cloned PCR products.

In addition to CRISPR-induced alterations at the mRNA level should also be checked CRISPR/Cas9-mediated alterations in the target exon may also result in altered splicing of the corresponding pre-mRNA, most likely due to mutations of splice-regulatory sequences, which give rise to aberrant protein products. These may potentially act as dominant-negative proteins and therefore interfere with the interpretation of results. (Kapahnke et al., 2016).

4. CRISPR/Cas9-mediated transcriptional regulation

Development of the catalytically dead Cas9 mutant (dCas9), which can be directed by the sgRNA to a chosen genomic location, but is defective in DNA cleavage, enabled its use for transcriptional regulation. Indeed, dCas9 fusions have been used to synthetically repress (CRISPRi) or activate (CRISPRa) expression in various ways (**Figure 35**) (Shalem et al., 2015).

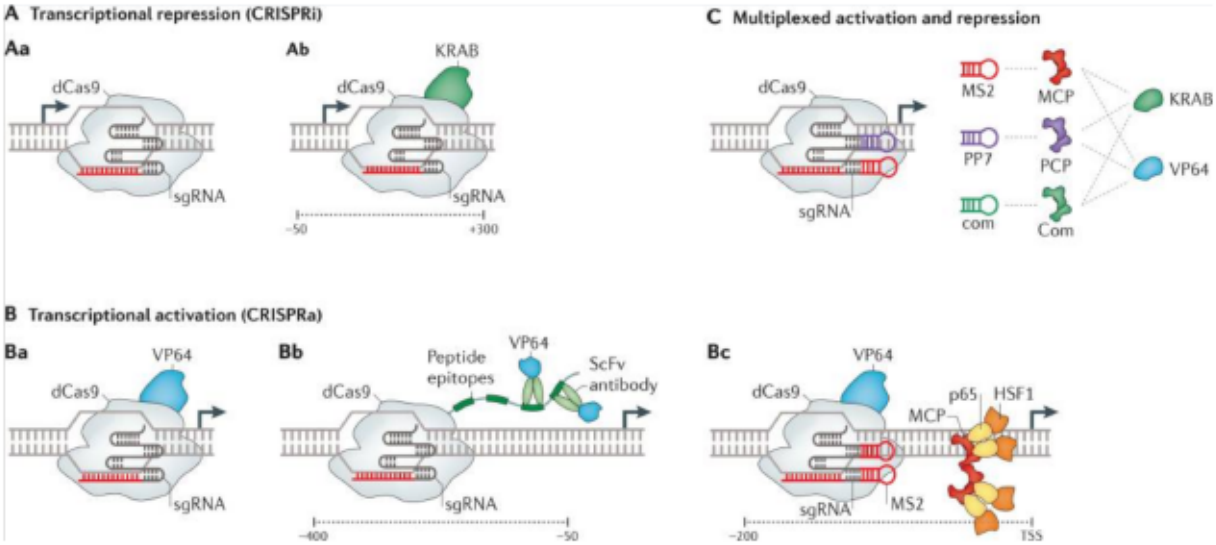

Figure 35: dCas9-mediated transcriptional modulation. A. Transcription repression. B. Transcription activation. C. Multiplexed activation and repression was implemented using an array of modified sgRNAs with different RNA recognition motifs (MS2, PP7 or com) and corresponding RNA-binding domains (MCP, PCP or Com) fused to different transcriptional effector domains (KRAB or VP64) (Shalem et al., 2015).

4.1. CRISPRi: transcriptional repression

To achieve transcription inhibition **(Figure 35A)**, dCas9 protein targeted to specific DNA sequences by sgRNA can be used by itself (whereby it directly blocks the RNA polymerase and thus represses transcription through steric hindrance) (**Figure 35Aa**) or can be used as part of a dCas9–KRAB transcriptional repressor fusion protein (**Figure 35Ab**) (Shalem et al., 2015).

Repressive chromatin modifier domains like Kruppel-associated box (KRAB) fused to the dCas9 protein improve transcriptional silencing compared to the dCas9 protein alone. Moreover, such silencing was shown to be highly specific, as seen with RNA-seq analysis (Gilbert et al., 2013).

The level of transcriptional repression varies depending on many factors such as sgRNA and target DNA sequence.

4.2. CRISPRa: transcriptional activation

For transcriptional activation, various approaches have been implemented that involve the transcriptional activation domain VP64 **(Figure 35B)**. Indeed, fusing the dCas9 protein to known activation domain proteins targeted to the promoter region results in increased gene expression levels at endogenous loci (Maeder et al., 2013; Perez-Pinera et al., 2013).

Several methods have been developed, namely:

i. dCas9–VP64 fusion protein (**Figure 35Ba**).
ii. fusion protein based on the supernova tag (SunTag) system: dCas9 is fused to a repeating array of peptide epitopes, which modularly recruit multiple copies of single-chain variable fragment (ScFv) antibodies fused to transcriptional activation VP64 domain (**Figure 35Bb**). This results in an

amplification of transcriptional induction at the targeted gene (Gilbert et al., 2014; Tanenbaum et al., 2014).

iii. dCas9–VP64 fusion protein combined with a modified sgRNA scaffold with an MS2 RNA motif loop. This MS2 RNA loop recruits MS2 coat protein (MCP) fused to additional transcriptional activators such as NF-κB p65 and heat shock factor 1 (HSF1) (**Figure 35Bc**), forming the synergistic activation mediator (SAM). The modified sgRNA sequence contains two RNA hairpin aptamers recognized by the bacteriophage coat protein MS2. The combination of VP64, p65 and HSF1 activation domains synergistically increases gene expression of the target sequence (Konermann et al., 2015).

Both these systems can increase gene expression up to 40-fold above baseline levels but the transcriptional activation will vary depending on the target sequence (Gilbert et al., 2014; Konermann et al., 2015).

5. Applications of CRISPR/Cas9 systems

The CRISPR/Cas9 system was modified and adapted in numerous ways to establish causal linkages between genetic variations and biological phenotypes (**Figure 36**).

For instance, CD34+ cells can be edited by CRISPR with multiple lesions with > 70% efficiency and expand *in vivo* after transplantation into immunodeficient mice to model clonal dynamics (Tothova et al., 2017).

Gene disruption can even be tailored to specifically target an allele by using a SNP-derived PAM, paving the way for potential treatment of autosomal dominant diseases (Christie et al., 2017).

Coupling CRISPR pooled screens with single cell RNA sequencing, referred to as CRISP-seq, enabled profiling perturbation and transcriptome in the same cell, which could be useful to dissect immune circuits, notably (Jaitin et al., 2016).

Oncogenic chromosomal rearrangements can be engineered in vivo with CRISPR-Cas9: for instance, the ***EML4-ALK*** rearrangement (see **Section IV. 4**) was induced in murine cells (Maddalo et al., 2014).

CRISPR/Cas9 technology was also used to efficiently generate genetically modified NSG mice to specifically interrogate the role of the niche-derived matricellular protein SPARC (Secreted Protein Acidic Rich in Cysteine), *in vivo*, in different human leukemic contexts (Tirado-Gonzalez et al., 2017).

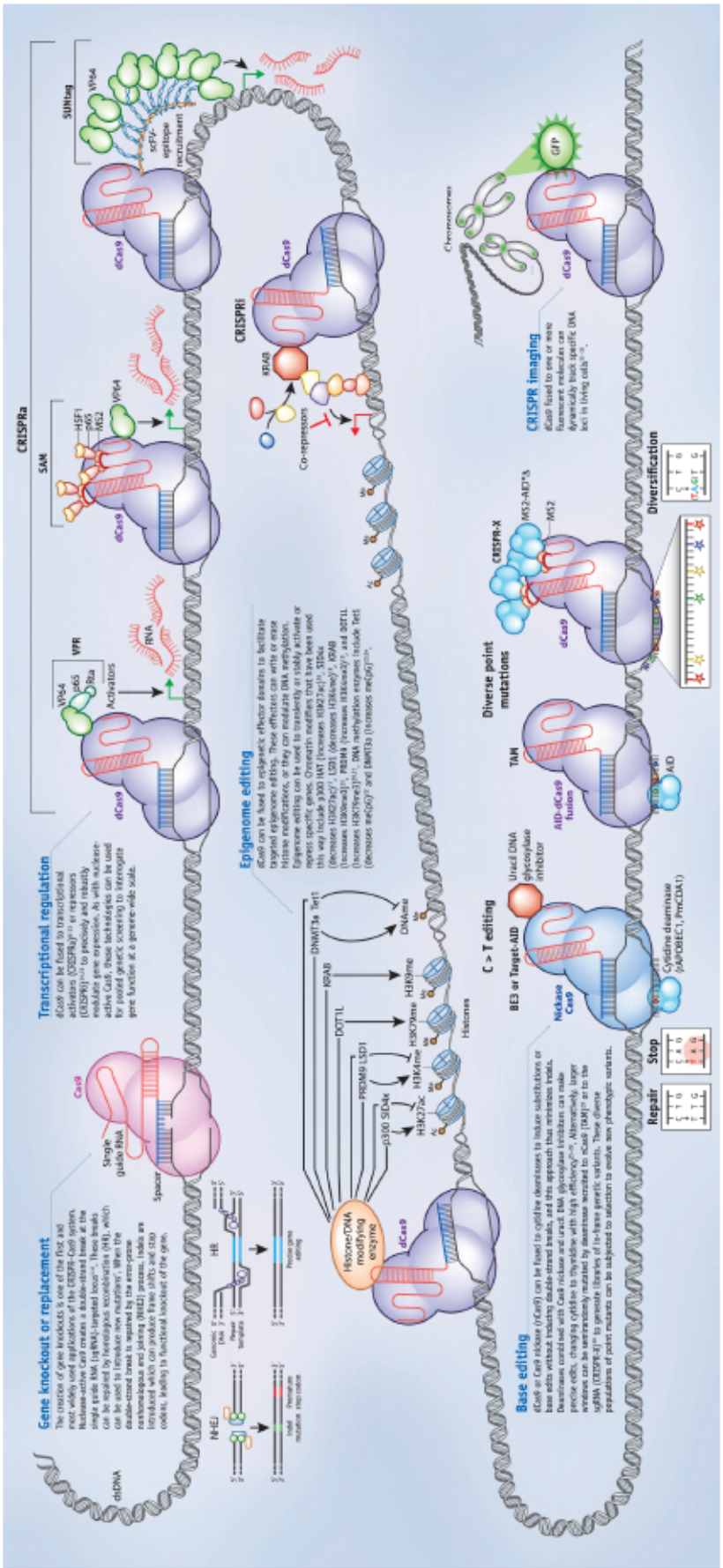

Figure 36: the expanding CRISPR toolbox (Tycko et al., 2017).

Thesis objectives

The overall aim of my thesis consisted of expanding the current understanding of the genetic basis and physiopathology of aggressive B-cell leukemias. More specifically, the aims were to:

I - Gain in the short arm of chromosome 2 (2p+) induces gene overexpression and drug resistance in chronic lymphocytic leukemia: analysis of the central role of *XPO1*

We report herein the identification of a minimal region of 2p gain, which encompasses among others *XPO1* and *REL*. Focusing on the *XPO1* gene, we report the cytogenetic and molecular features of 21 2p gain CLL patients, as well as their *in vitro* response to classical and novel inhibitors (XPO1 inhibitor and venetoclax). I am the second co-author of this article, where I conceived and performed experimental work, as well as analyzed the data.

II – Functional analysis of the role of REL in chronic lymphocytic leukemia (CLL) cell survival and in 2p gain-associated drug resistance

Amplification and/or activation of *REL* was proposed by many authors to be a potential central player in CLL disease progression and resistance to treatments, although the underlying mechanism remain elusive.

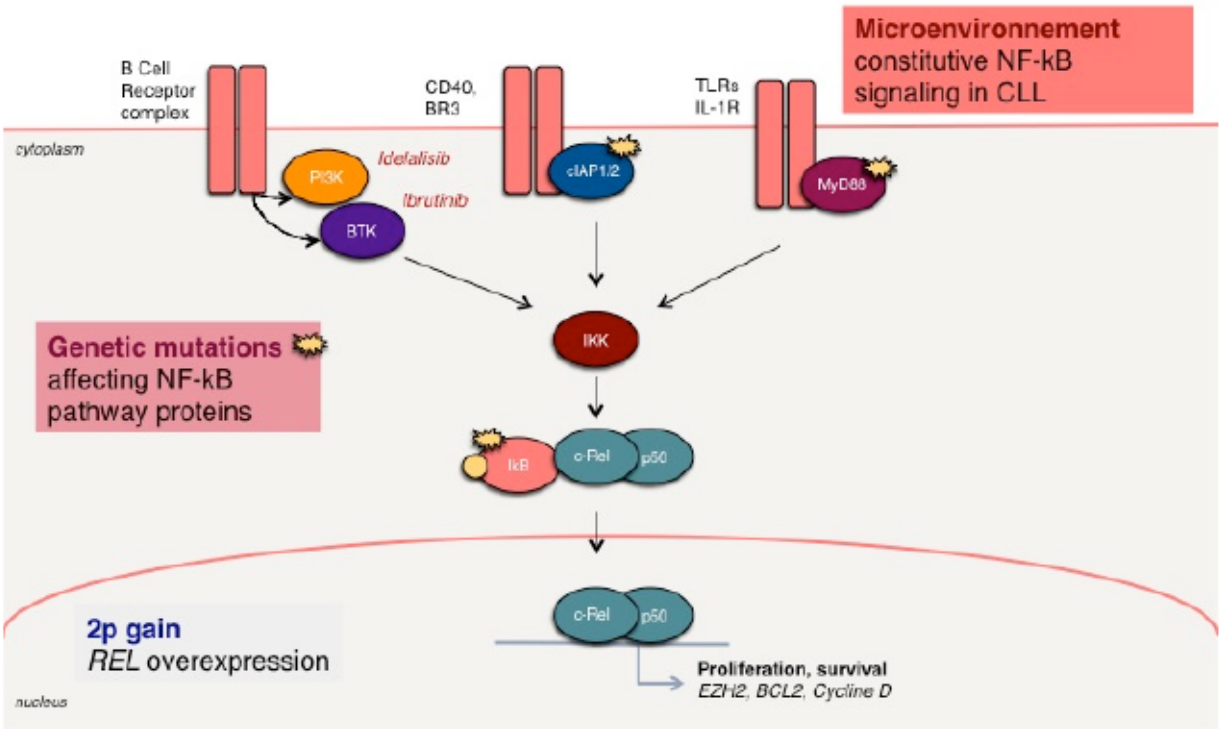

Figure 37: *REL* could be a central piece of the CLL drug resistance puzzle. 2p gain is a recurrent chromosomal abnormality in CLL, resulting in *REL* overexpression. Moreover, the microenvironment triggers a constitutive NF-κB signaling in CLL cells. Finally, numerous genetic mutations affecting NF-κB pathway proteins have been reported, for instance *MYD88* (MyD88), *BIRC3* (cIAP1/2) and *NFKBIE* (IκBε).

The present study, which was the main project of my thesis, aimed to shed some light on the functions of ***REL*** in CLL drug refractoriness **(Figure 37)**, by deploying various strategies: CRISPR-Cas9-mediated genetic deletion in 2p gain+ CLL cells, CRISPRa-mediated transcriptional activation in 2p gain- CLL cells, as well as pharmacological inhibition of c-Rel in primary patient cells. This project was realized in collaboration with the team of O. Bernard (IGR, Villejuif). I conceived and performed all experiments, analyzed the data and wrote the manuscript presented in this dissertation.

III - The Gain of the Short Arm of Chromosome 2 (2p gain) Plays an Important Role in CLL Drug Resistance, and Has to be Systematically Considered before Deciding an Adapted Therapy

The aim of this project was to analyze the hierarchy and the clonal evolution of the chromosomal abnormalities in 64 2p gain+ CLL patients. Conventional karyotype and fluorescence in situ hybridization (FISH) analyses were performed on each sample, and the samples are analyzed before and after treatment, and during the relapse. I am the second author of this project, where I was tasked with conceiving the method to analyze the data.

Review: Identifying the drivers of drug resistance in 2p gain CLL

Additionally, I wrote a comprehensive review on 2p gain and its impact on pathogenesis and drug resistance: see **Chapter IV + Future perspectives**.

IV - "Double-hit" chronic lymphocytic leukemia: An aggressive subgroup with 17p deletion and 8q24 gain.

CLL with del(17p) is associated with a lack of response to standard treatment and thus the worst clinical outcome. The objective of this study was to determine whether the type of chromosomal abnormality leading to del(17p) and the additional abnormalities influenced the prognosis in a series of 195 patients with del(17p) CLL. I am the eighth author of this article, where I conceived and performed experimental work.

V – Genetic Characterization of B-Cell Prolymphocytic Leukemia (B-PLL): A Hierarchical Prognostic Model Involving *MYC* and *TP53* Abnormalities. on Behalf of the *Groupe Francophone De Cytogenetique Hematologique* (GFCH) and the *French Innovative Leukemia Organization* (FILO) Group

B-PLL is an aggressive leukemia, usually resistant to standard chemo-immuno therapy, defined by the presence of prolymphocytes in peripheral blood exceeding 55% of lymphoid cells. The definition of B-PLL as a distinct neoplasm and its differentiation from classical CLL or other hemopathies was originally proposed by

Galton and colleagues (Galton et al., 1974). Here we report the cytogenetic and molecular features of a large cohort of 34 B-PLL cases, as well as their *in vitro* response to novel targeted drugs. This project was realized in collaboration with the team of O. Bernard (IGR, Villejuif). I am the third author of this project, where I conceived and performed experimental work, as well as analyzed the data.

Results and discussion

I - Gain in the short arm of chromosome 2 (2p+) induces gene overexpression and drug resistance in chronic lymphocytic leukemia: analysis of the central role of XPO1

Overall, our data suggest the existence in T-ALL of a disrupted RNA decapping pathway, mediated by the DNA methylation-associated loss of NUDT16, which contributes to the natural history of the disease by stabilizing transforming factors, such as is the case of the leukemogenic protein C-MYC.

CONFLICT OF INTEREST

The authors declare no conflict of interest.

ACKNOWLEDGEMENTS

This work was supported by the European Research Council under the European Community's Seventh Framework Programme (FP7/2007-2013) / ERC grant agreement no. 268626–EPINORC project, the Spanish Ministry of Economy and Competitiveness (MINECO Projects no. PI13-01339 and SAF2014-55000-R), the Instituto de Salud Carlos III (ISCIII), co-financed by the ERDF Fund, 'A way to achieve Europe', under the Integrated Project of Excellence no. PIE13/00022 (ONCOPROFILE), and the Spanish Cancer Research Network (RTICC) no. RD12/0036/0039, La Marató de TV3 Foundation #20131610, the Cellex Foundation, Obra Social 'La Caixa', Celgene Spain and the Health and Science Departments of the Catalan Government (Generalitat de Catalunya) AGAUR–project no. 2009SGR1315, 2014SGR633 and 2014SGR225. We thank the staff of the Animal Core Facility of IDIBELL for mouse care and maintenance. ME is an ICREA Research Professor.

C Anadón[1,8], G van Tetering[1,8], HJ Ferreira[1], C Moutinho[1], A Martínez-Cardús[1], A Villanueva[2], M Soler[1], H Heyn[1], S Moran[1], M Castro de Moura[1], F Setien[1], A Vidal[3], E Genescà[4], JM Ribera[4], JF Nomdedeu[5], S Guil[1] and M Esteller[1,6,7]

[1]*Cancer Epigenetics and Biology Program, Bellvitge Biomedical Research Institute (IDIBELL), L'Hospitalet, Barcelona, Spain;*
[2]*Translational Research Laboratory, Catalan Institute of Oncology, Bellvitge Biomedical Research Institute (IDIBELL), L'Hospitalet, Barcelona, Spain;*
[3]*Department of Pathological Anatomy, Bellvitge University Hospital, Bellvitge Biomedical Research Institute (IDIBELL), L'Hospitalet, Barcelona, Spain;*
[4]*Hematology Department, Catalan Institute of Oncology, Hospital Germans Trias i Pujol, Josep Carreras Leukaemia Research Institute (IJC), Universitat Autònoma de Barcelona, Barcelona, Spain;*
[5]*Department of Haematology, Hospital de la Santa Creu i Sant Pau, Barcelona, Spain;*
[6]*Physiological Sciences Department, School of Medicine and Health Sciences, University of Barcelona (UB), Barcelona, Spain and*
[7]*Institucio Catalana de Recerca i Estudis Avançats (ICREA), Barcelona, Spain*
E-mail: sguil@idibell.cat or mesteller@idibell.cat
[8]*These authors contributed equally to this work.*

REFERENCES

1 Franks TM, Lykke-Andersen J. The control of mRNA decapping and P-body formation. *Mol Cell* 2008; **32**: 605–615.
2 Arribas-Layton M, Wu D, Lykke-Andersen J, Song H. Structural and functional control of the eukaryotic mRNA decapping machinery. *Biochim Biophys Acta* 2013; **1829**: 580–589.
3 Jonas S, Izaurralde E. The role of disordered protein regions in the assembly of decapping complexes and RNP granules. *Genes Dev* 2013; **27**: 2628–2641.
4 Wang Z, Jiao X, Carr-Schmid A, Kiledjian M. The hDcp2 protein is a mammalian mRNA decapping enzyme. *Proc Natl Acad Sci USA* 2002; **99**: 12663–12668.
5 Bessman MJ, Frick DN, O'Handley SF. The MutT proteins or 'Nudix' hydrolases, a family of versatile, widely distributed, 'housecleaning' enzymes. *J Biol Chem* 1996; **271**: 25059–25062.
6 Song MG, Li Y, Kiledjian M. Multiple mRNA decapping enzymes in mammalian cells. *Mol Cell* 2010; **40**: 423–342.
7 Li Y, Song M, Kiledjian M. Differential utilization of decapping enzymes in mammalian mRNA decay pathways. *RNA* 2011; **17**: 419–428.
8 Hopkins KC, Tartell MA, Herrmann C, Hackett BA, Taschuk F, Panda D *et al.* Virus-induced translational arrest through 4EBP1/2-dependent decay of 5'-TOP mRNAs restricts viral infection. *Proc Natl Acad Sci USA* 2015; **112**: E2920–E2929.
9 Esteller M. Epigenetics in cancer. *N Engl J Med* 2008; **358**: 1148–1159.
10 Iorio F, Knijnenburg TA, Vis DJ, Bignell GR, Menden MP, Schubert M *et al.* A landscape of pharmacogenomic interactions in cancer. *Cell* 2016; **166**: 740–754.
11 Fustin JM, Doi M, Yamaguchi Y, Hida H, Nishimura S, Yoshida M *et al.* RNA-methylation-dependent RNA processing controls the speed of the circadian clock. *Cell* 2013; **155**: 793–806.
12 Cepeda D, Ng HF, Sharifi HR, Mahmoudi S, Cerrato VS, Fredlund E *et al.* CDK-mediated activation of the SCF(FBXO) (28) ubiquitin ligase promotes MYC-driven transcription and tumourigenesis and predicts poor survival in breast cancer. *EMBO Mol Med* 2013; **5**: 999–1018.
13 Pan J, Deng Q, Jiang C, Wang X, Niu T, Li H *et al.* USP37 directly deubiquitinates and stabilizes c-Myc in lung cancer. *Oncogene* 2015; **34**: 3957–3967.
14 Weng AP, Millholland JM, Yashiro-Ohtani Y, Arcangeli ML, Lau A, Wai C *et al.* c-Myc is an important direct target of Notch1 in T-cell acute lymphoblastic leukemia/lymphoma. *Genes Dev* 2006; **20**: 2096–2109.
15 Palomero T, Lim WK, Odom DT, Sulis ML, Real PJ, Margolin A *et al.* NOTCH1 directly regulates c-MYC and activates a feed-forward-loop transcriptional network promoting leukemic cell growth. *Proc Natl Acad Sci USA* 2006; **103**: 18261–18266.

Supplementary Information accompanies this paper on the Leukemia website (http://www.nature.com/leu)

Gain in the short arm of chromosome 2 (2p+) induces gene overexpression and drug resistance in chronic lymphocytic leukemia: analysis of the central role of XPO1

Leukemia (2017) **31,** 1625–1629; doi:10.1038/leu.2017.100

Chronic lymphocytic leukemia (CLL), the most common adulthood leukemia, is characterized by an accumulation of abnormal $CD5^+$ B lymphocytes in the peripheral blood, bone marrow and secondary lymphoid organs. Acquired genetic mutations play an important role in CLL pathogenesis, and massive parallel sequencing identified new recurrently mutated genes such as *NOTCH1, SF3B1, XPO1, MYD88, EGR2* and *NFKBIE*.[1–4] In addition, frequent

Accepted article preview online 27 March 2017; advance online publication, 18 April 2017

chromosomal abnormalities, such as 11q, 13q and 17p deletions, or trisomy 12 could explain both the clinical heterogeneity of CLL and the drug resistance of this disease.[5] Therefore, identifying deregulated genes in CLL are important to improving our understanding about the development and evolution of CLL, and to propose new targeted strategies.

We and others have previously reported that the gain of the short arm of chromosome 2 (2p+) is a frequent chromosomal abnormality in CLL. *MYCN*, *REL*, *BCL11A* and *MSH2* have been proposed as candidate disease genes associated with a 2p gain, although the underlying mechanisms have not been elucidated.[6–11] In this study, we identified chromosome region maintenance/exportin-1 (*CRM1/XPO1*) as a critical gene in CLL patients by unveiling a minimal 2p gained region. Thus we assessed the response of 2p+/CLL cells to commonly used anti-CLL drugs, including the tri-therapy fludarabine, cyclophosphamide, rituximab (FCR), ibrutinib, rituximab-idelalisib (R-Idelalisib) and the XPO1 inhibitor selinexor.[12]

In our study, we have initially identified 36 CLL patients with 2p+ by a cytogenetic approach. Their characteristics are reported in Supplementary Table S1 and Supplementary Figure S1. To investigate the prognostic value of the 2p+, we scrutinized the clinical parameters of the 2p+/CLL patients ($n=21$) included in a clinical trial.[13] The 2p+ was observed in 16% (21/132) of the patients included in this trial and was significantly associated with two of the most relevant factors of poor prognosis in CLL: del(11q) and unmutated *IGHV* status (Supplementary Table S2). These findings point toward an oncogenic cooperation between a 11q deletion and a 2p gain.

We next narrowed down the gained chromosome 2 regions using a SNP array on the 23/36 2p+/CLL samples with the available material (Figure 1a). Although most patients showed large 2p gains, we identified the following two minimally gained regions: a 674 kb region containing one single gene (*TTC27*) and a 1.28 Mb region harboring nine genes (*BCL11A, PAPOLG, REL, PUS10, PEX13, KIAA1841, AHSA2, USP34* and *XPO1*). Because

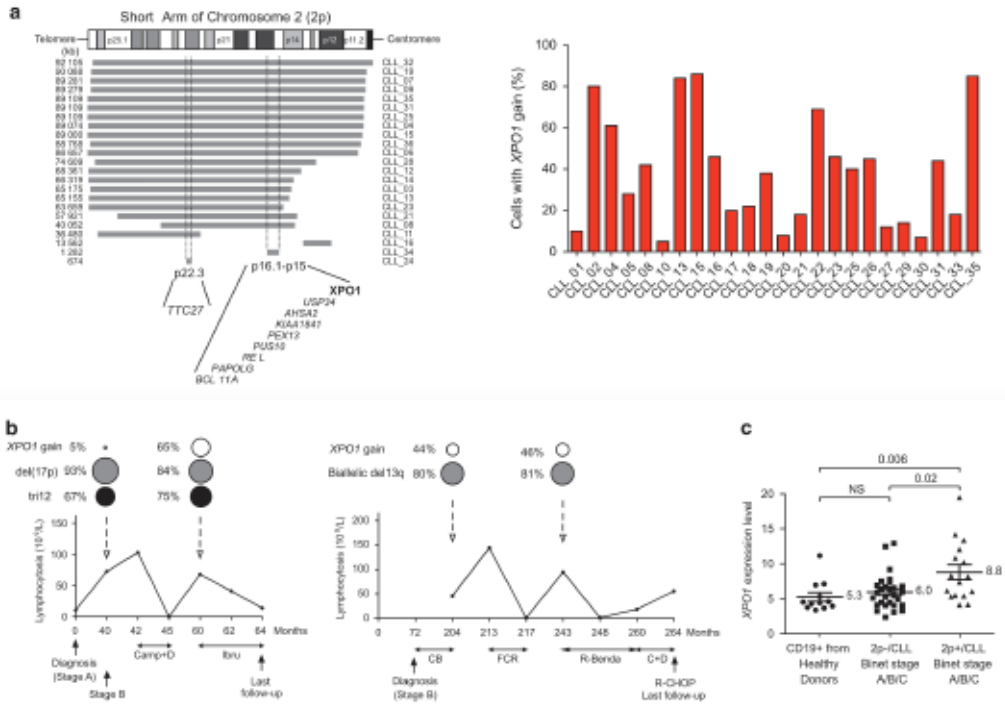

Figure 1. *XPO1*: SNP array and FISH analysis, and overexpression in 2p+/CLL cells. (**a**) Left: Schematic representation of the minimal gained region in the short arm of the chromosome 2 (2p) identified in 23 2p+/CLL by SNP array. Full lines represent the gained regions in individual 2p+ patient. This approach yields the gain of two minimal regions. One region of 674 kb in 2p22.3 included *TTC27*. The second region of 1.28 Mb placed in p16.1-p15 encompassed the indicated nine genes. Right: The percentage of cells carrying a *XPO1* gain was determined by FISH in 24 2p+/CLL patients and plotted as a histogram. (**b**) Monitoring of lymphocytosis and cytogenetic abnormalities in two 2p+/CLL patients upon treatment. The vertical axis shows lymphocytosis and follow-up is reported on the horizontal axis. Color-coded circles show the percentage of cells carrying the indicated cytogenetic abnormality. Arrows represent clinically relevant time points. Left (Patient CLL_10): before treatment, the major clones unveiled by FISH are del(17p) and tri12 (93% and 67% of cells; respectively). At this stage, *XPO1* gain was only present in a sub-clone representing 5% of cells. At relapse, del(17p) and tri12 were still present (84% and 75%, respectively), and the *XPO1* gain had expanded to 65% of the malignant cells. Right (Patient CLL_31): at diagnosis, *XPO1* gain surrogate of 2p+ is present in 44% of cells, and del(13q) in 80% of cells. At relapse, both abnormalities were still present in the same percentages. (**c**) *XPO1* mRNA levels were determined by real-time RT-PCR in CD19$^+$ cells purified from healthy donors ($n=12$), CLL patients without 2p gain (2p−) ($n=28$), or with CLL individuals with 2p gain (2p+) ($n=16$). The *ABL1* mRNA expression was used to normalize the data. The plot depicts the mean ± s.e.m. The statistical analysis was performed with the Mann–Whitney *U*-test. FISH, fluorescence *in situ* hybridization; mRNA, messenger RNA; NS, non significant.

XPO1 is recurrently mutated in CLL[1] and its overexpression is associated with poor prognosis and resistance to therapy in various cancers,[14] we focused our analyses on this particular gene. First, using a fluorescence *in situ* hybridization approach, we fully confirmed the gain of *XPO1* in all tested 2p+/CLL samples (Supplementary Table S1). Second, in comparing the gain of *XPO1* with other cytogenetic abnormalities present in the same sample, we found that the *XPO1* gain was often a later event (13/22 cases). Particularly when associated with the 11q deletion, the *XPO1* gain occurred as a second event in 6/7 evaluable cases (Figure 1a; Supplementary Table S1). These results are consistent with the evolution of the events in the progression model of the CLL proposed by Landau *et al.*[15] Third, longitudinal fluorescence *in situ* hybridization analyses performed on eight 2p+/CLL-treated patients showed a similar or increasing percentage of cells carrying a *XPO1* gain at relapse compared with at the time of diagnosis (Figure 1b; Supplementary Table S3). This result indicates that the clone carrying a *XPO1* gain does not disappear after the treatments, underlining the potential relevance of XPO1 in CLL drug resistance. Finally, we investigated whether the 2p+ induced *XPO1* overexpression. A comparison between B lymphocytes from healthy donors with 2p−/CLL (without 2p gain) and 2p+/CLL fully confirmed that the 2p gain is associated with significant *XPO1* overexpression (Figure 1c; Supplementary Figure S2). Of note, among the other genes including in the two minimally gained regions, the 2p+ was also significantly associated with *TTC27, BCL11A, REL, AHSA2, USP34* overexpression (Supplementary Figure S2).

To investigate the potential role of XPO1 on drug resistance in CLL patients with 2p+, we initially assessed the consequences of XPO1 inhibition by selinexor, a selective inhibitor of nuclear export compound currently in Phase I/II clinical trials. This inhibitor has been shown to exhibit antitumor activity in several hemopathies, including CLL.[13,16] As depicted in Supplementary Figure S3, our findings confirm that selinexor induced programmed cell death (PCD) in the B tumor cells from CLL patients, including B cells with del(17p) or unmutated *IGHV* status. In contrast, selinexor had no effect on the B cells from healthy donors or on the non-leukemic cells of CLL patients. Altogether, these results corroborated that XPO1 represents a potential therapeutic target in CLL.[12,16] From a mechanistic point of view, selinexor induced PCD in CLL through a caspase-dependent mechanism. Indeed, selinexor-induced PCD in CLL was blocked by caspase inhibitors, induced the cleavage and activation of the caspase-3, and promoted a mitochondrial dysfunction associated with the upregulation/activation of the pro-apopototic BCL-2 member BAX (Supplementary Figure S4).

Using *in vitro* assays, we next tested the PCD response of the 2p+ CLL samples to commonly used anti-CLL drugs and selinexor. Notably, to visualize the differences, we used a drug concentration that induced ~40% of PCD in the CLL samples (Supplementary Figure S5). Using this approach, we observed that the PCD induced by FCR, ibrutinib, R-idelalisib or selinexor was significantly lower in the 2p+/CLL cells compared with the 2p−/CLL control cells (Figure 2a), independently of adverse prognostic factors in these patients. This was illustrated in individual cases in which the percentage of cells with 2p+ influenced the response against anti-CLL drugs (Supplementary Figure S6). Therefore, the drug resistance associated with 2p+/CLL appeared directly linked to the gain in the short arm of chromosome 2 and not to the other prognostic CLL markers, such as 11q or 17p deletions, or overexpression of key antiapoptotic BCL-2 family members overexpressed in CLL cells (for example, MCL-1 or BCL-2; Supplementary Figure S3 and S7). Surprisingly, our findings also indicated that the *XPO1* overexpression associated with 2p+ was sufficient to significantly downmodulate selinexor-induced PCD in CLL.

To substantiate our results in a complementary cellular system, we analyzed the relevance of 2p+ in two well-described B CLL-like cell lines: OSU-CLL (2p− CLL cells) and JVM-3 (B-prolymphocytic leukemia cells with 2p+; Supplementary Table S4). As depicted in the Figure 2b, the rate of PCD induced by FCR, ibrutinib, R-idelalisib and selinexor was lower in JVM-3, the cell line presenting a 2p+. Thus, the data obtained in primary CLL cells and in established B-cell lines (Figures 2a and b) seem to confirm that the gain in the short arm of chromosome 2 influences the response to anti-CLL drugs.

To substantiate the role of XPO1 in the resistance associated to drugs implicating a nuclear access to provoke PCD (as such described in Figure 2), we tested whether the effect of Venetoclax, a Bcl-2-specific inhibitor that induced PCD via a direct mitochondrial damage, was also modulated by 2p+. As depicted in Supplementary Figure S8, contrary to that observed in Figure 2, there were no significant differences in the PCD induced by Venetoclax in primary B cells from 2p− and 2p+ CLL patients and in the cell lines OSU-CLL (2p−) and JVM-3 (2p+). It seems therefore that both 2p+ and the overexpression of XPO1 specifically modulate the PCD response to drugs requiring a nuclear/cytosolic signaling transfer.

As *XPO1* is commonly mutated in CLL,[1] we searched for a potential relationship between 2p+ and the *XPO1* mutation (for example, if the percentage of CLL with *XPO1* mutations was higher in 2p+/CLL than in 2p−/CLL). Therefore, we sequenced the *XPO1* gene in the following situations: (i) 308 previously untreated patients (Binet stages B/C) included in two prospective trials;[13,17] (ii) 97 untreated CLLs from the biobank of Pitié-Salpêtrière Hospital and (iii) 31/36 2p+/CLLs with available material. Using this approach, we identified *XPO1* mutations in 25/436 patients with CLL, including 2/31 CLL patients with 2p+ (Supplementary Table S1, CLL_17 and CLL_33). These findings first indicated that the frequency of *XPO1* mutations was not significantly higher in 2p+/CLL compared with 2p−/CLL (Supplementary Table S2). Remarkably, all identified *XPO1* mutations targeted the amino-acidic residue E571, which was localized in the binding domain of the protein (a highly conserved region of the molecule), indicating that the mutation affects XPO1 activity.[1] More precisely, we observed 14/25 E571K (including the two 2p+/CLL), 4 E571G, 3 E571V, 2 E571A and 2 E571Q mutations, all of which changed a glutamic acid to a basic residue.[18]

To evaluate the therapeutic potential of selinexor in CLL more broadly, we compared its PCD effect in *XPO1*-wild type and *XPO1*-mutated CLL cells. As represented in Figure 2c, selinexor was significantly less efficient at inducing death in *XPO1*-mutated cells. In contrast, the treatment of *XPO1*-wild type and *XPO1*-mutated CLL with FCR or ibrutinib did not show any significant PCD difference. Altogether, these data indicated that the mutations in *XPO1* characterizing CLL modulated the cytotoxic effect of selinexor; however, they did not affect the response of the malignant B cells to FCR or ibrutinib treatments. Interestingly, in an illustrative case (CLL_17) with both 2p+ and *XPO1 E571K*-mutated form, we showed that the cells were sensitive to FCR and ibrutinib. Concerning the response to selinexor, we observed that the *XPO1* mutation partially reversed PCD drug resistance. Indeed, the 2p+ *XPO1 E571K* CLL-mutated cells presented exactly the PCD behavior of the 2p− *XPO1 E571K* CLL-mutated cells. Thus, the *XPO1* mutation seemed sufficient enough to switch off the drug resistance associated to 2p+, corroborating the specific and central role of *XPO1* in the 2p gain (Supplementary Figure S9).

Altogether, our findings confirm the high frequency of the 2p gain in CLL and its association with poor prognosis factors such as del(11q) and unmutated *IGHV*. Additionally, for the first time, we demonstrated that a 2p gain promotes FCR, ibrutinib, R-idelalisib drug resistance in CLL. Finally, our results showed that selinexor inefficiently induces PCD in CLL B cells with mutations in *XPO1*. Relevant genes are localized on the short arm of the chromosome 2,

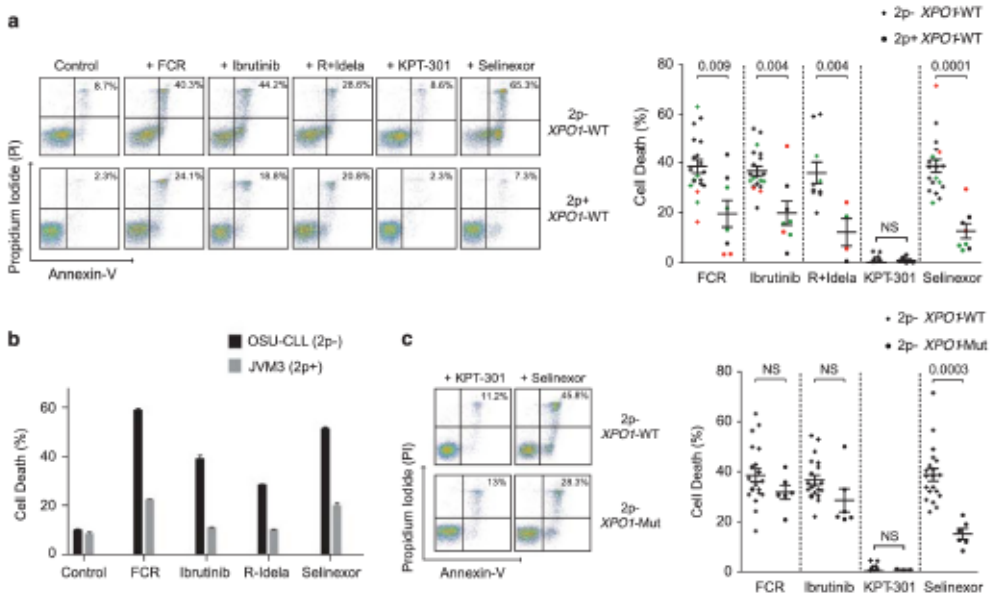

Figure 2. 2p+ confers resistance to FCR, ibrutinib, R-idelalisib and selinexor. The mutations in *XPO1* in CLL block the effect of selinexor. (**a**) Cell death was measured by double Annexin-V and propidium iodide (PI) staining in 2p−/XPO1-WT ($n=20$) and 2p+/XPO1-WT ($n=8$) CLL cells untreated (Control) or treated for 24 h with FCR (35 μM; 5 nM; 10 μg/ml), ibrutinib (15 μM), selinexor (250 nM) or the negative control KPT-301 (250 nM). Alternatively, 2p−/*XPO1*-WT ($n=10$) and 2p+/*XPO1*-WT ($n=4$) CLL cells were treated with R-idelalisib (10 μg/ml; 50 μM). Drug concentration and time treatment have been adapted to *in vitro* assays in which the spontaneous apoptosis associated to primary CLL cell culture is about 15%. Representative flow cytometry plots are shown. The percentages refer to Annexin-V positive and Annexin-V/PI co-positive staining. In the right histogram, CLL cells were similarly treated, after accounting for spontaneous apoptosis, the percentages of Annexin-V positive and Annexin-V/PI co-positive cells were quantified and plotted. Crosses and dots represent individual samples. Bars are the mean ± s.e.m. Green and red symbols represent samples with del(11q) and del(17p), respectively. (**b**) Apoptosis was measured as in **a** in two B-cell lines: OSU-CLL (2p− cell line) and JVM-3 (B-prolymphocytic leukemia 2p+ cell line). The PCD induced by FCR, ibrutinib, R-idelalisib and selinexor was lower in JVM-3, the 2p+ cell line ($n=2$). (**c**) Apoptosis was induced and measured as in **a** in 2p−/*XPO1*-WT ($n=20$) and 2p−/*XPO1*-mutated ($n=6$) CLL samples. Representative flow cytometry plots are shown. The percentages refer to Annexin-V positive and Annexin-V/PI co-positive staining. In the right histogram, after accounting for spontaneous apoptosis, the percentages of Annexin-V positive and Annexin-V/PI co-positive cells were quantified and plotted. Crosses and dots represent individual samples. Bars are the mean ± s.e.m. Statistical analyses were performed using Mann–Whitney *U*-test. WT, wild type.

including *REL*, *BCL11A* or *XPO1*. Even if further investigations are needed to evaluate whether a cooperation exists between *XPO1* and other 2p genes, our results indicated that *XPO1* plays a central role in the CLL drug resistance associated to 2p+. Additionally, we revealed that a simple point mutation in the binding domain of the protein switches off the PCD resistance associated to 2p+. Overall, our work advocates for assessing 2p+ and *XPO1* mutations before choosing a CLL therapy. Because 2p+ is observed in a wide range of B-cell malignancies, it could be proposed to extend these recommendations to all selinexor treatments.

CONFLICT OF INTEREST

YL is an employee of Karyopharm Therapeutics Inc. and receives compensation, and holds equity in the company. The remaining authors declare no conflict of interest.

ACKNOWLEDGEMENTS

We thank the Centre de Ressource Biologique de Caen for Lepretre's trial samples. We are also grateful to O Bernard for critical comments, X Troussard, R Guieze, S Struski, E Fontenay, R Delepine, O Kosmider, D Bouscary, C Delacroix and L Ceboli for invaluable help, and LY Jebaeli for the gift of the JVM-3 cell line. OSU-CLL cells were provided by The Ohio State University's Human Genetics Sample Bank. This work was supported by Roche Diagnostics, the Association Laurette Fugain (ALF10/09, ALF14/08 and ALF 15/09), Ligue Contre le Cancer (RS15/75-63 and RS16/75-50) and Fondation ARC (Association pour la Recherche sur le Cancer) (SFI20111203530 and PJA20151203407). AC holds PhD fellowships from Fondation pour la Recherche Medicale (FDT20140931078) and Société Française d'Hématologie.

AUTHOR CONTRIBUTIONS

AC conceived and performed experimental work, analyzed the data, and helped to write the manuscript. EC, NB, H-AC, CA, CG, LH and M-NB-N conceived, and performed experimental work and analyzed the data. FD, HM-B, SC, MU, VM, VL, KM, SL, PF, LS, MLG-T enrolled patients and managed CLL samples. JL, CL, JLe performed statistical analysis. YL provided selinexor and KPT-301. SAS and FN-K conceived and supervised the project, designed experiments, interpreted the data and wrote the manuscript.

A Cosson[1,2,3], E Chapiro[1,2,4,12], N Bougacha[1,2,3,12], J Lambert[5], L Herbi[1,2,3], H-A Cung[4], C Algrin[4], B Keren[6], F Damm[7], C Gabillaud[4], M-N Brunelle-Navas[1,2,3], F Davi[1,2,4], H Merle-Béral[1,2,4], M Le Garff-Tavernier[1,2,4], D Roos-Weil[7], S Choquet[4], M Uzunov[4], V Morel[6], V Leblond[4], K Maloum[4], S Lepretre[8], P Feugier[9], C Lesty[4], J Lejeune[5], L Sutton[10], Y Landesman[11], SA Susin[1,2,3,13] and F Nguyen-Khac[1,2,4,13]

[1]INSERM UMR_S 1138, Cell Death and Drug Resistance in Lymphoproliferative Disorders Team, Centre de Recherche des Cordeliers, Paris, France;
[2]Sorbonne Universités, UPMC Univ Paris 06, UMR_S 1138, Centre de Recherche des Cordeliers, Paris, France;
[3]Université Paris Descartes, Sorbonne Paris Cité, UMR_S 1138, Centre de Recherche des Cordeliers, Paris, France;
[4]Service d'Hématologie Biologique, GH Pitié-Salpêtrière, Paris, France;
[5]Service de Biostatistique et Informatique Médicale, Hôpital Saint Louis, Paris, France.;
[6]Département de génétique, GH Pitié-Salpêtrière, Paris, France;
[7]INSERM U1170, Institut Gustave Roussy, Villejuif, France;
[8]Département d'Hématologie, Hôpital Becquerel, Rouen, France;
[9]Pôle d'Hématologie, Hôpital Brabois, Vandoeuvre-les-Nancy, France;
[10]Service d'Hématologie Clinique, Hôpital d'Argenteuil, Argenteuil, France and
[11]Karyopharm Therapeutics, Newton, MA, USA
E-mail: santos.susin@crc.jussieu.fr or florence.nguyen-khac@psl.aphp.fr
[12]These authors contributed equally to this work.
[13]Senior coauthorship.

REFERENCES

1 Puente XS, Pinyol M, Quesada V, Conde L, Ordonez GR, Villamor N *et al.* Whole-genome sequencing identifies recurrent mutations in chronic lymphocytic leukaemia. *Nature* 2011; **475**: 101–105.
2 Quesada V, Conde L, Villamor N, Ordonez GR, Jares P, Bassaganyas L *et al.* Exome sequencing identifies recurrent mutations of the splicing factor *SF3B1* gene in chronic lymphocytic leukemia. *Nat Genet* 2012; **44**: 47–52.
3 Wang L, Lawrence MS, Wan Y, Stojanov P, Sougnez C, Stevenson K *et al.* SF3B1 and other novel cancer genes in chronic lymphocytic leukemia. *N Engl J Med* 2011; **365**: 2497–2506.
4 Damm F, Mylonas E, Cosson A, Yoshida K, Della Valle V, Mouly E *et al.* Acquired initiating mutations in early hematopoietic cells of CLL patients. *Cancer Discov* 2014; **4**: 1088–1101.
5 Dohner H, Stilgenbauer S, Benner A, Leupolt E, Krober A, Bullinger L *et al.* Genomic aberrations and survival in chronic lymphocytic leukemia. *N Engl J Med* 2000; **343**: 1910–1916.
6 Bea S, Lopez-Guillermo A, Ribas M, Puig X, Pinyol M, Carrio A *et al.* Genetic imbalances in progressed B-cell chronic lymphocytic leukemia and transformed large-cell lymphoma (Richter's syndrome). *Am J Pathol* 2002; **161**: 957–968.
7 Schwaenen C, Nessling M, Wessendorf S, Salvi T, Wrobel G, Radlwimmer B *et al.* Automated array-based genomic profiling in chronic lymphocytic leukemia: development of a clinical tool and discovery of recurrent genomic alterations. *Proc Natl Acad Sci USA* 2004; **101**: 1039–1044.
8 Pfeifer D, Pantic M, Skatulla I, Rawluk J, Kreutz C, Martens UM *et al.* Genome-wide analysis of DNA copy number changes and LOH in CLL using high-density SNP arrays. *Blood* 2007; **109**: 1202–1210.
9 Chapiro E, Leporrier N, Radford-Weiss I, Bastard C, Mossafa H, Leroux D *et al.* Gain of the short arm of chromosome 2 (2p) is a frequent recurring chromosome aberration in untreated chronic lymphocytic leukemia (CLL) at advanced stages. *Leuk Res* 2010; **34**: 63–68.
10 Rinaldi A, Mian M, Kwee I, Rossi D, Deambrogi C, Mensah AA *et al.* Genome-wide DNA profiling better defines the prognosis of chronic lymphocytic leukaemia. *Br J Haematol* 2011; **154**: 590–599.
11 Edelmann J, Holzmann K, Miller F, Winkler D, Buhler A, Zenz T *et al.* High-resolution genomic profiling of chronic lymphocytic leukemia reveals new recurrent genomic alterations. *Blood* 2012; **120**: 4783–4794.
12 Lapalombella R, Sun Q, Williams K, Tangeman L, Jha S, Zhong Y *et al.* Selective inhibitors of nuclear export show that CRM1/XPO1 is a target in chronic lymphocytic leukemia. *Blood* 2012; **120**: 4621–4634.
13 Sutton L, Chevret S, Tournilhac O, Divine M, Leblond V, Corront B *et al.* Autologous stem cell transplantation as a first-line treatment strategy for chronic lymphocytic leukemia: a multicenter, randomized, controlled trial from the SFGM-TC and GFLLC. *Blood* 2011; **117**: 6109–6119.
14 Turner JG, Dawson J, Sullivan DM. Nuclear export of proteins and drug resistance in cancer. *Biochem Pharmacol* 2012; **83**: 1021–1032.
15 Landau DA, Tausch E, Taylor-Weiner AN, Stewart C, Reiter JG, Bahlo J *et al.* Mutations driving CLL and their evolution in progression and relapse. *Nature* 2015; **526**: 525–530.
16 Zhong Y, El-Gamal D, Dubovsky JA, Beckwith KA, Harrington BK, Williams KE *et al.* Selinexor suppresses downstream effectors of B-cell activation, proliferation and migration in chronic lymphocytic leukemia cells. *Leukemia* 2014; **28**: 1158–1163.
17 Lepretre S, Aurran T, Malhe B, Cazin B, Tournilhac O, Maisonneuve H *et al.* Excess mortality after treatment with fludarabine and cyclophosphamide in combination with alemtuzumab in previously untreated patients with chronic lymphocytic leukemia in a randomized phase 3 trial. *Blood* 2012; **119**: 5104–5110.
18 Jeromin S, Weissmann S, Haferlach C, Dicker F, Bayer K, Grossmann V *et al.* SF3B1 mutations correlated to cytogenetics and mutations in NOTCH1, FBXW7, MYD88, XPO1 and TP53 in 1160 untreated CLL patients. *Leukemia* 2014; **28**: 108–117.

Supplementary Information accompanies this paper on the Leukemia website (http://www.nature.com/leu)

Supplementary Figure S1. Relationship of 2p+ with other cytogenetic and genetic aberrations characterizing CLL. Columns represent patients and lines represent genetic aberrations (grey: absence, black: presence of the abnormality, white: not done)

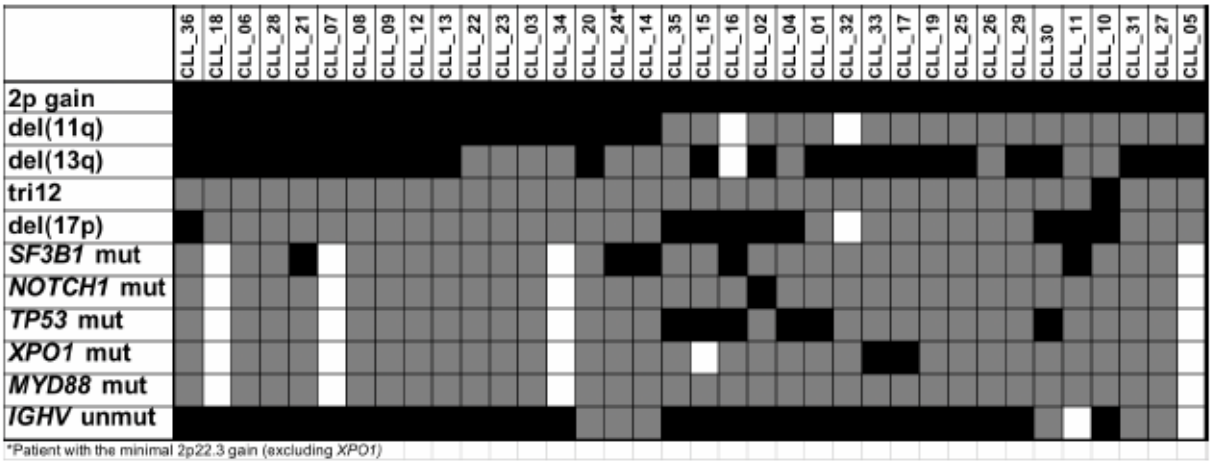

Supplementary Table S1. Clinical and biological characteristics of 36 2p+/CLL.

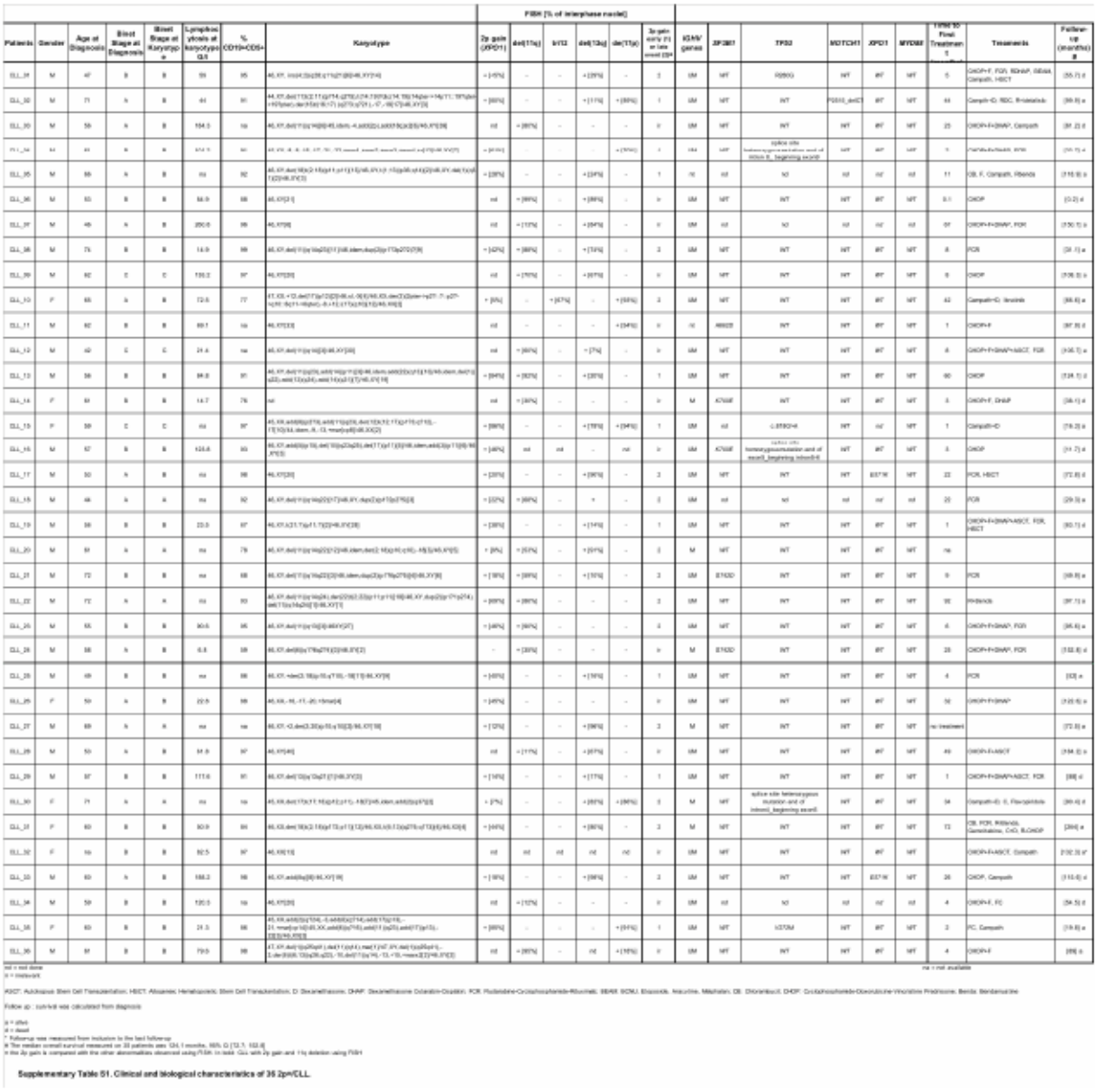

Supplementary Table S2: Characteristics of 2p+ CLL and 2p- CLL included in the clinical trial by Sutton et al.

		2p- CLL		2p+ CLL		p-value
		n=111		n=21		
Gender	Male	83/111	75%	18/21	86%	ns
	Female	28/111	25%	3/21	14%	
Age at inclusion years		111	55 [51; 58]	21	58 [55;61]	ns
Binet stage at diagnosis	B	88/111	79%	18/21	86%	ns
	C	23/111	21%	3/21	14%	
Lymphocytosis at inclusion (10^9/L)		110	48.6 [20.5; 11.6]	21	82.6 [59.2; 12.4]	ns
Complex Karyotype		16/96	16%	6/18	33%	ns
Cytogenetic abnormalities (FISH)	del(11q)	23/101	23%	12/19	63%	**0,0008**
	tri12	11/104	11%	0/19	0%	ns
	del(13q)	54/99	55%	10/18	56%	ns
	del(17p)	6/101	6%	3/19	16%	ns
IGHV unmutated		67/105	64%	18/20	90%	**0,02**
SF3B1 mutated		16/105	15%	4/18	22%	ns
TP53 mutated		9/105	9%	2/18	11%	ns
NOTCH1 mutated		11/105	10%	0/18	0%	ns
XPO1 mutated		9/105	9%	1/18	6%	ns
MYD88 mutated		1/105	1%	0/18	0%	ns
TFS		106	13,9 [21; 35,1]	20	7,2 [2,4; 25,4]	ns
OS			144,9 [112.2; NA]		127,4 [62,3; NA]	ns

Complex karyotype: ≥ 3 abnormalities
OS: Overall Survival
TFS: Time from Diagnosis to First Treatment
ns: not significant
NA: not available
qualitative data are presented with count and percentage among non missing values range on compared using Fisher exact test
quantitative data are presented with number of non missing values, median and interquartile range on compared using Mann-Whitney test
OS is presented with median and its 95% confidence interval on compared using log-rank test

Supplementary Table S2 : Characteristics of 2p+ CLL and 2p- CLL included in the clinical trial by Sutton et *al.*

						FISH [% of interphase nuclei]				
Patients	Follow-up from diagnosis (months)	Status	Treatment	Lymphocytosis (10^9/L)	Karyotype	2p gain (*XPO1*)	del(11q)	tri12	del(13q)	del(17p)
CLL_31	0	diagnosis (Binet stage A)								
	72	Binet stage B	splenectomy, CB							
	206			45.8	46,XX,der(18q2;18p)?2;p11[12]/46,XX,t(6;13)(p21;q13)[4]	+ [48%]	-	-	+ [86%]	-
	213		FCR	14.6						
	217			1.2						
	243	relapse	R+Benda	94.8	46,XX,der(18q2;18p)?2;p11[2]/46,XX[8]	+ [46%]	-	-	+ [81%]	-
	248			1.6						
	260	relapse	C+D	18.4						
	264		R-CHOP	55.5						
CLL_29	0	diagnosis (Binet stage B)	FCR	15.1	46,XY,+der(2;18)p10;q11)[1]/46,XY[9]	+ [40%]	-	-	+ [76%]	-
	40	relapse		12.2	46,XY,+der(2;18)p10;q11)[1]/46,XY[17]	+ [34%]	-	-	-	-
	52			14.7		+ [56%]	-	-	-	-
CLL_02	0	diagnosis (Binet stage A)		8.8						
	29			17.8		nd	-	-	-	+ [51%]
	40	Binet stage B	Campath+D	44	44,XY,der(11;82;11)(p?14;q?15),t(14;19)(?dic(14;19)(14pter->14p11::19?pter->19?)plet),der(18)(18;17)(p?15;q?21)-17,-19[17]/46,XY[3]	+ [80%]	-	-	+ [11%]	+ [89%]
	79		R+DHC	85.5	43,XY,add(11)(p23),add(12)(p13),-13,t(14;19)(dic(14;19)(14pter->14p11::19?pter->19?)plet),der(18)(18;17)(p?23;q?21),-17,-19[9]/46,XY[3]	+ [90%]	-	-	+ [81%]	+ [88%]
	92		R+Ibrela	57	44,XY,del(9)(p21),der(11;82;11)(p?14;q?15),add(12)(p?13,?dic(14;19),der(18)(18;17)(p?23;q?21)-17,-19[2]/46,XY[2]	+ [62%]	-	-	+ [88%]	+ [94%]
	93			7.4	44,XY,del(9)(p21),der(11;82;11)(p?14;q?15),add(12)(p?13,?dic(14;19),der(18)(18;17)(p?23;q?21)-17,-19[11]/46,XY[9]	+ [45%]	-	-	+ [88%]	+ [48%]
CLL_19	0	diagnosis (Binet stage A)		16.4						
	40	Binet stage B		72.6	47,XX,+12,del(17)(p12)[2]/46,sl,-9,t(4;7)(46,XX,der(2)(2pter->p21::?::p27->q10::8q11->8qter),-8,+12,add(17)(p12)[12]/46,XX[2]	+ [6%]	-	+ [67%]	-	+ [99%]
	42		Campath+D	10.0						
	60	relapse		67.1	46,XX,der(2)(2pter->p21::?::p27->q10::8q11->8qter),-8,+12,-17[cp10]/10]	+ [65%]	-	+ [75%]	-	+ [84%]
	64		Ibru	1.1						
CLL_38	0	diagnosis (Binet stage A)		18.5	46,XX,t(17;18)(p12;p11)[2]/46,XX,idem,add(2)(p37)[2]/46,XX[11]	-	-	-	+ [46%]	+ [37%]
	34	Binet stage B	Campath, F+Campath	87.7						
	42			5.4						
	47		Campath+D	18.8	45,XX,der(17;18)(p12;p11),-18[7]/45,idem,add(2)(p37)[2]	+ [7%]	-	-	+ [82%]	+ [88%]
	60	relapse		14.4	45,XX,der(17;18)(p12;p11),-18[10]/46,idem,add(2)(p37)[4]/46,XX,der(17)(17;18)(p12;p11)-18[6]/46,XX[1]	+ [20%]	-	-	+ [91%]	+ [87%]
	74		Flavopiridol	42.7	46,XX,der(17;18)(p12;p11),-18[10]/46,sl,add(2)(p37)[3]/46,sl2,+18[7]	+ [20%]	-	-	+ [86%]	+ [73%]
	90	dead								
CLL_01	0	diagnosis (Binet stage B)	CHOP+F	56	46,XY, ins(4;2)(q35;q11q21)[6]/46,XY[14]	+ [<5%]	-	-	+ [29%]	-
	0	relapse	FCR, RDHAP, BEAM							
	39		Campath	52.8	46,XY,ins(4;2)(q27?;q?12q14)[7]/46,XY,?dic(2;12)(q27?;q27?)[2]/46,XY[3]	+ [10%]	-	-	+ [80%]	-
	44		HSCT							
	50	dead								
CLL_17	0	diagnosis (Binet stage A)								
	24	Binet stage B	FCR	65.8		+ [20%]	-	-	+ [90%]	-
	61	relapse	HSCT	6	46,XY,der(8)(2;8)p11.p11)[16]/46,XY[4]	+ [73%]	-	-	+ [98%]	-
	73	dead								

						FISH [% of interphase nuclei]				
Patients	Follow-up from diagnosis [months]	Status	Treatment	Lymphocytosis (10^9/L)	Karyotype	2p gain (XPO1)	del(11q)	tri12	del(13q)	del(17p)
CLL_18		(Diagnosis: Binet stage A)		27	46,XY,del(11)(q21q22)[8]/46,XY[2]	+ [72%]	+ [66%]	-	+ [9%]	-
	22	Binet stage B	PCR	48	46,XY,del(11)(q14q22)[17]/48,XY,dup(2)(p11?2p25)[3]	+ [28%]	+ [66%]	-	+ [9%]	-

nd: not done

HSCT: Allogeneic Hematopoietic Stem Cell Transplantation; Gemci: Gemcitabine; Ibru: Ibrutinib; D: Dexamethasone; DHAP: Dexamethasone Cytarabin-Cisplatin; FCR: Fludarabine-Cyclophosphamide-Rituximab; BEAM: BCNU, Etoposide, Aracytine, Melphalan; CB: Chlorambucil; CHOP: Cyclophosphamide-Doxorubicine-Vincristine Prednisone; Benda: Bendamustine

Supplementary Table S3. Longitudinal analysis of eight 2p+/CLL.

	OSU-CLL*	JVM-3#
	CLL	**B-PLL**
	15% tetraploïd cells	tetraploid cells
FISH		
tri12	+ [94%]	+ [94%]
del13q	-	+ [8%]
del11q	-	-
del17p	-	+ [26%]
***XPO1* gain**	-	+ [83%]
***XPO1* status**	*WT*	*WT*

Supplementary Table S4. OSU-CLL and JVM-3 cell lines

*Hertlein et *al.*, *PLoS One* 2013

#Melo et al., *Int Jour of Cancer* 1986

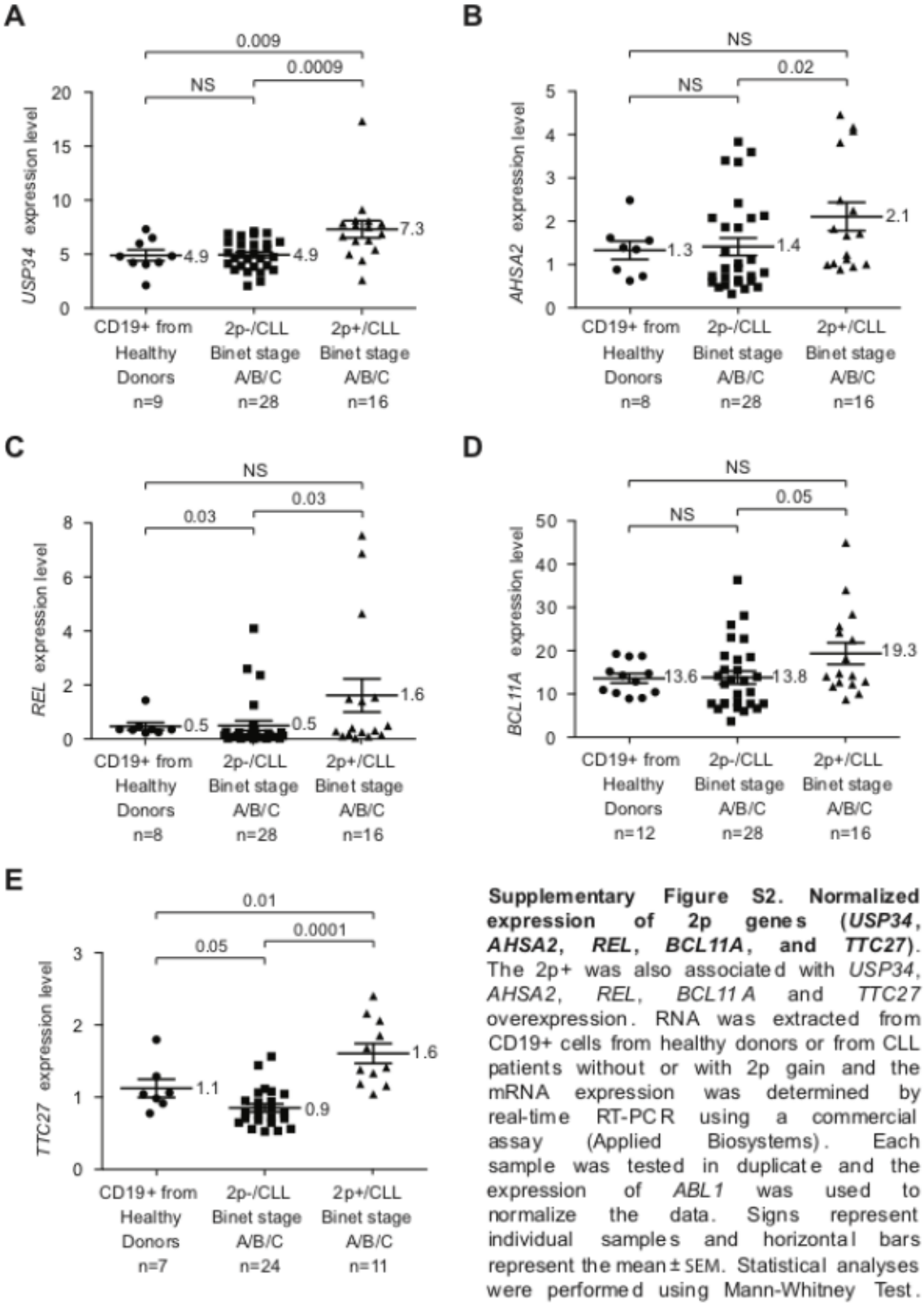

Supplementary Figure S2. Normalized expression of 2p genes (*USP34*, *AHSA2*, *REL*, *BCL11A*, and *TTC27*). The 2p+ was also associated with *USP34*, *AHSA2*, *REL*, *BCL11A* and *TTC27* overexpression. RNA was extracted from CD19+ cells from healthy donors or from CLL patients without or with 2p gain and the mRNA expression was determined by real-time RT-PCR using a commercial assay (Applied Biosystems). Each sample was tested in duplicate and the expression of *ABL1* was used to normalize the data. Signs represent individual samples and horizontal bars represent the mean ± SEM. Statistical analyses were performed using Mann-Whitney Test.

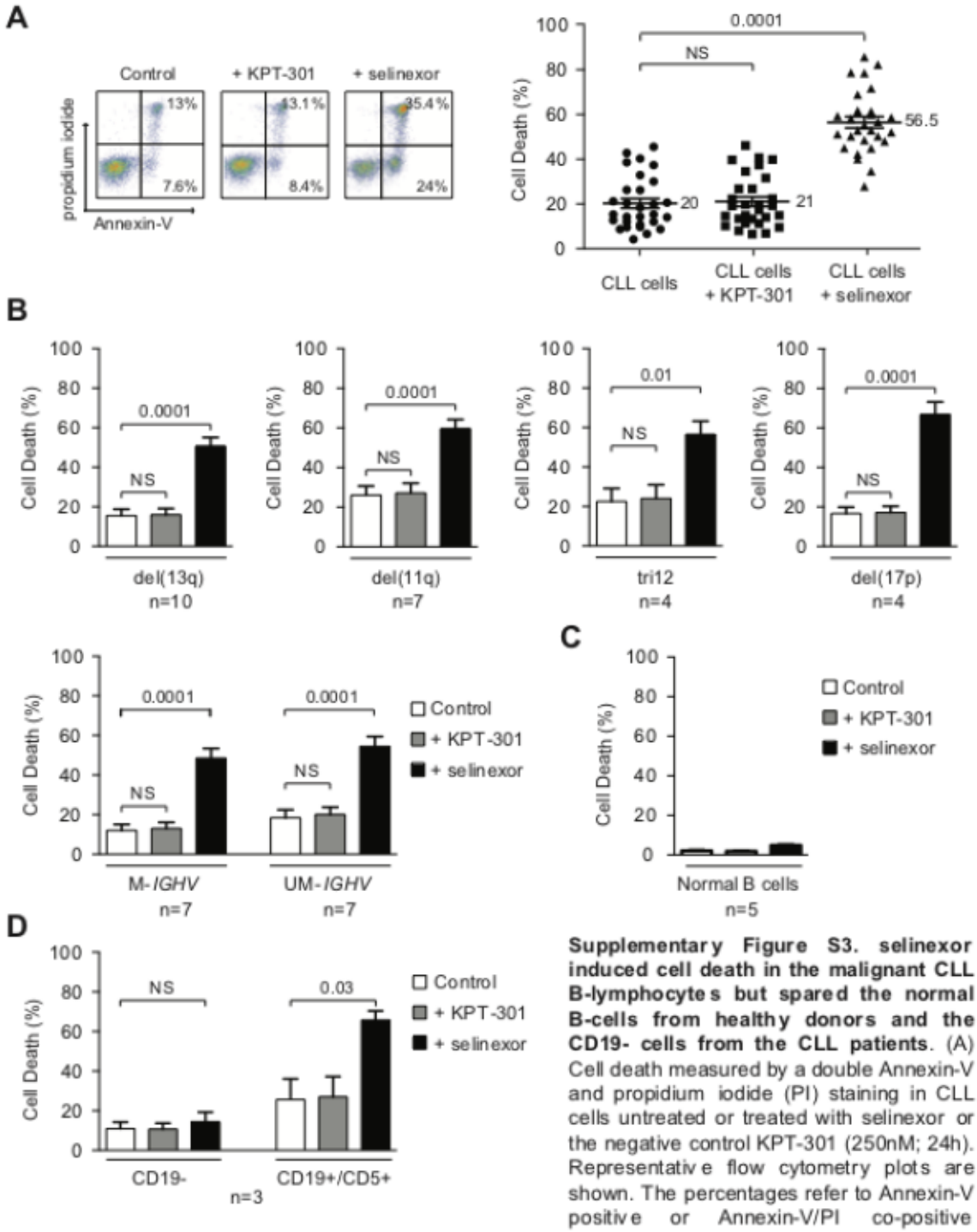

Supplementary Figure S3. selinexor induced cell death in the malignant CLL B-lymphocytes but spared the normal B-cells from healthy donors and the CD19- cells from the CLL patients. (A) Cell death measured by a double Annexin-V and propidium iodide (PI) staining in CLL cells untreated or treated with selinexor or the negative control KPT-301 (250nM; 24h). Representative flow cytometry plots are shown. The percentages refer to Annexin-V positive or Annexin-V/PI co-positive staining. In the right panel, CLL cells were treated as above and graphed. The percentages refer to the mean of the Annexin-V positive staining ± SEM (n=29). (B) B-cells from CLL patients with positive or adverse prognostic features were treated as in (A) and plotted as the mean ± SEM. M: mutated; UM: unmutated; del: deletion; tri: trisomy. (C-D) B-cells (CD19+) from healthy donors (n=5), CD19- and CD19+/CD5+ cells from CLL patients (n=3) were treated as in (A) and graphed. The percentages refer to the mean of the Annexin-V positive staining ± SEM. The p value, assessed by an Anova approach, is indicated. NS : non significant.

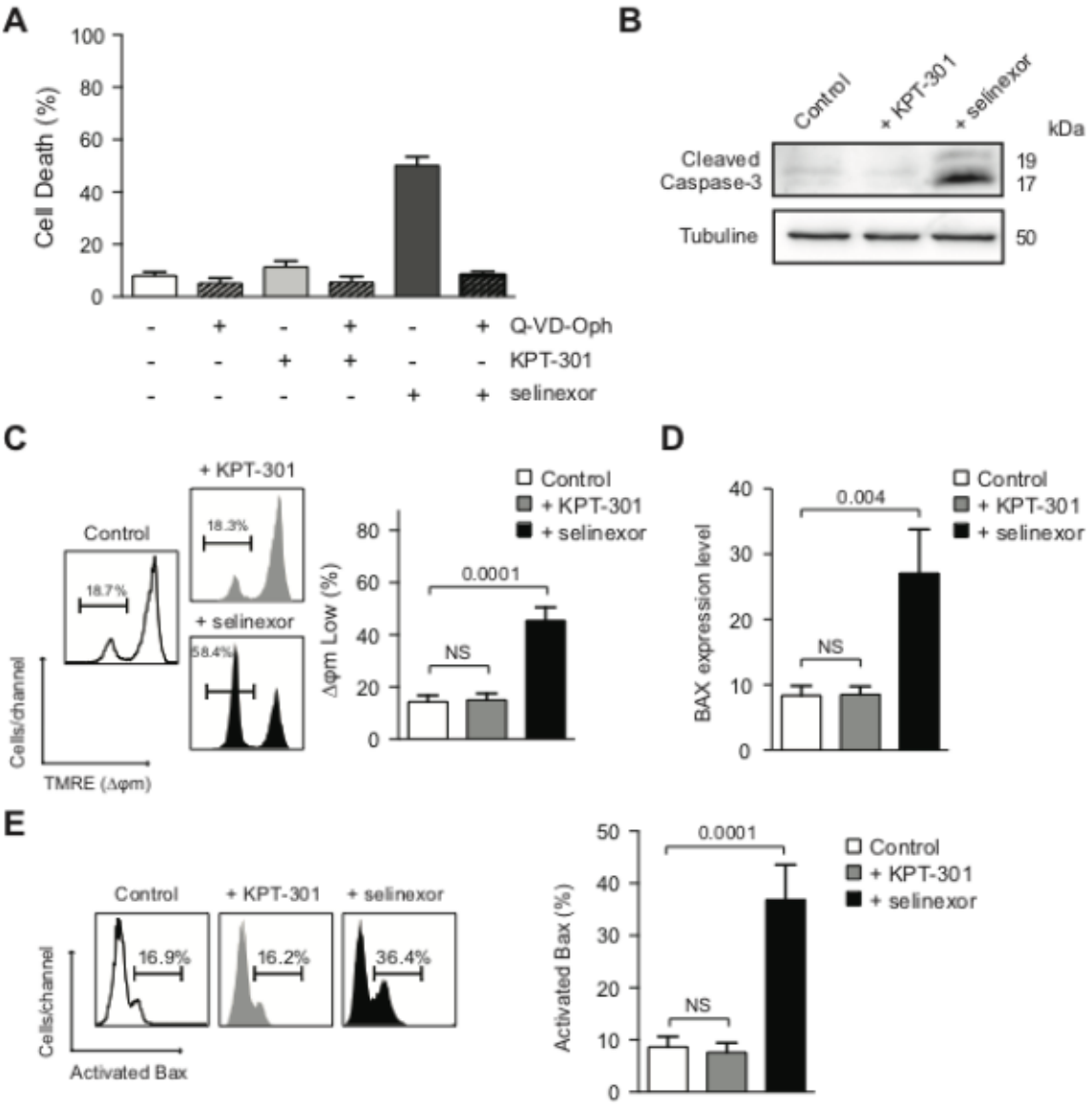

Supplementary Figure S4. Treatment with selinexor promotes cell death through a caspase-dependent mechanism implicating the mitochondria and the proapoptotic protein Bax. (A) CLL patients cells (n=3) were treated (+) or not (-) with selinexor or the negative control KPT-301 (250 nM; 24 h) in the presence or the absence of the pan-caspase inhibitor Q-VD-Oph (10 μM) and the percentage of cell death was evaluated by Annexin-V staining. The data are graphed as the mean ± SEM. (B) A representative immunoblot of activated caspase-3 is shown for the untreated CLL cells (Control), KPT-301, or selinexor-treated CLL cells. Equal loading was confirmed by α-tubulin probing. (C) Cells were untreated or treated with the negative control KPT-301 or selinexor (250 nM; 24 h), then labeled with TMRE and assessed for ΔΨm (mitochondrial transmembrane potential) by flow cytometry. Results are the means of seven independent experiments ± SEM. In cytometry panels, percentages refer to cells with ΔΨm loss. (D) BAX mRNA levels were determined in CLL B-cells (n=8) untreated or treated with KPT-301 or selinexor (250 nM; 12 h). The numbers refer to the mean BAX transcript expression ± SEM. The ABL1 mRNA expression was used to normalize the data. Statistical analyses were performed using Anova. (E) CLL cells were untreated or treated with KPT-301 or selinexor as in (A), and Bax activation was measured by flow cytometry and illustrated as a bar chart. Data are the means ± SEM (n=8). In cytometry panels, percentages refer to cells with activated Bax.

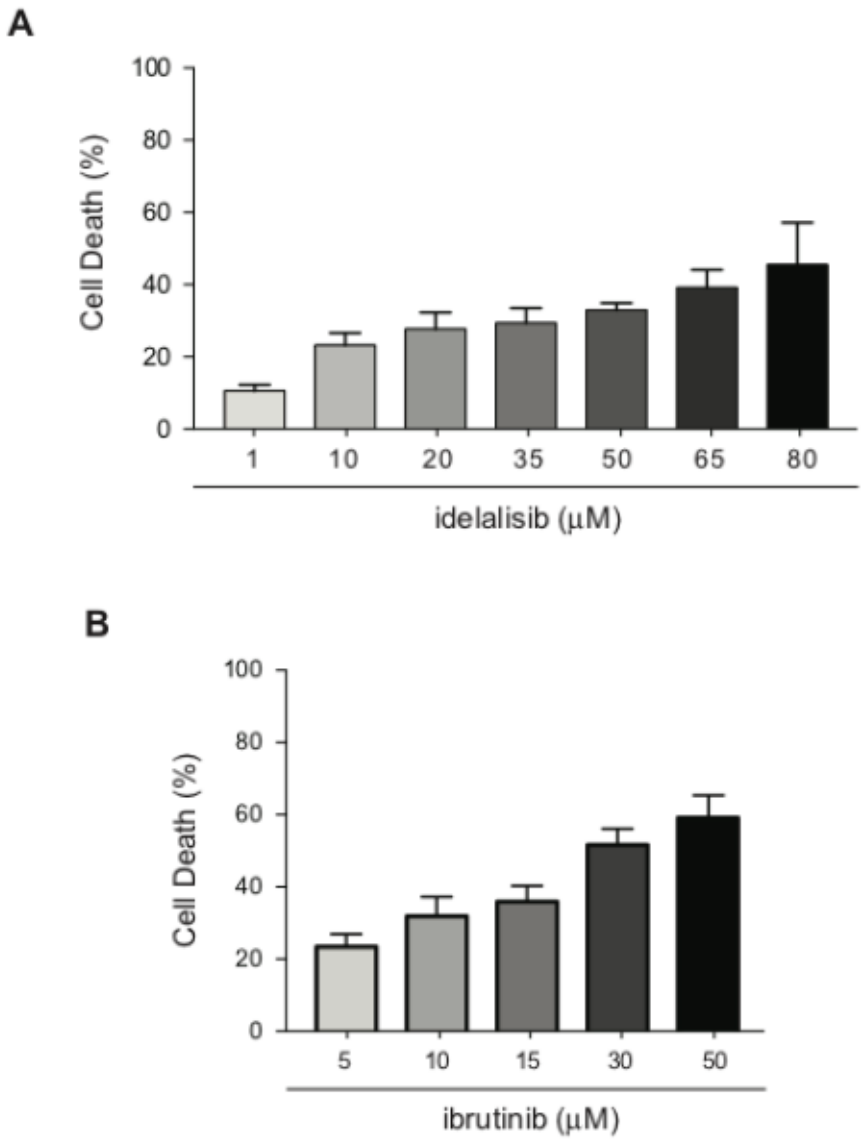

Supplementary Figure S5. Cytotoxicity of idelalisib and ibrutinib in CLL cells. Cell death measured by a double Annexin-V and propidium iodide (PI) staining in CLL cells untreated or treated with (A) idelalisib at different doses (1 to 80 μM) plus rituximab (10 μg/mL), or (B) different doses of ibrutinib (5 to 50 μM). CLL cells were treated as above and, after accounting for spontaneous apoptosis, the percentage of Annexin-V positive and Annexin-V/PI co-positive cells was quantified and plotted. Bars represent mean ± SEM (n=4).

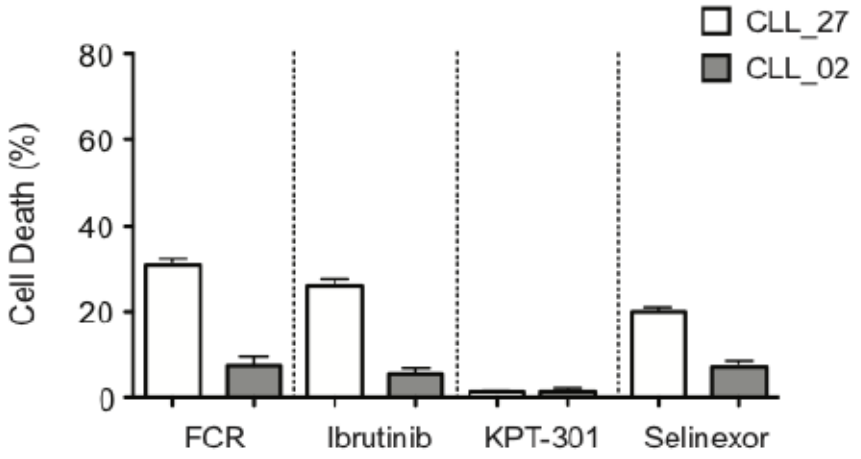

Supplementary Figure S6. Relationship between CLL drug resistance and percentage of B-cells with 2p+. Cell death was measured by double Annexin-V and propidium iodide (PI) staining in B-cells from CLL patients presenting differents percentages of 2p+ cells: CLL_27 (12%) and CLL_02 (90%). CLL cells were treated for 24 h with FCR (35 µM; 5 mM; 10 µg/mL), ibrutinib (15 µM), the negative control KPT-301 (250 nM), or selinexor (250 nM). After accounting for spontaneous apoptosis, the % of Annexin-V positive and Annexin-V/PI co-positive cells were quantified and plotted. Bars represent mean ± SEM (n=2).

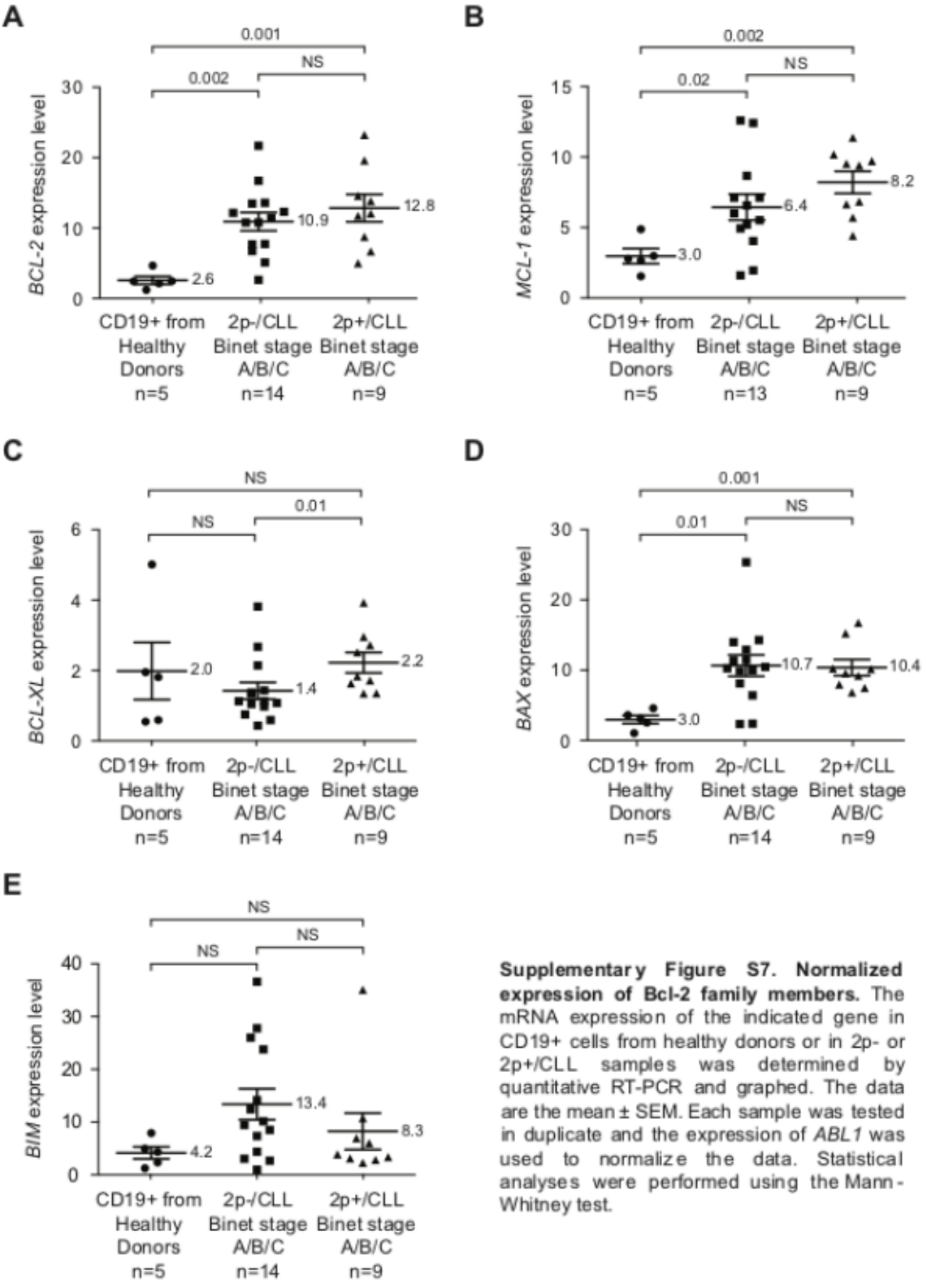

Supplementary Figure S7. Normalized expression of Bcl-2 family members. The mRNA expression of the indicated gene in CD19+ cells from healthy donors or in 2p- or 2p+/CLL samples was determined by quantitative RT-PCR and graphed. The data are the mean ± SEM. Each sample was tested in duplicate and the expression of *ABL1* was used to normalize the data. Statistical analyses were performed using the Mann-Whitney test.

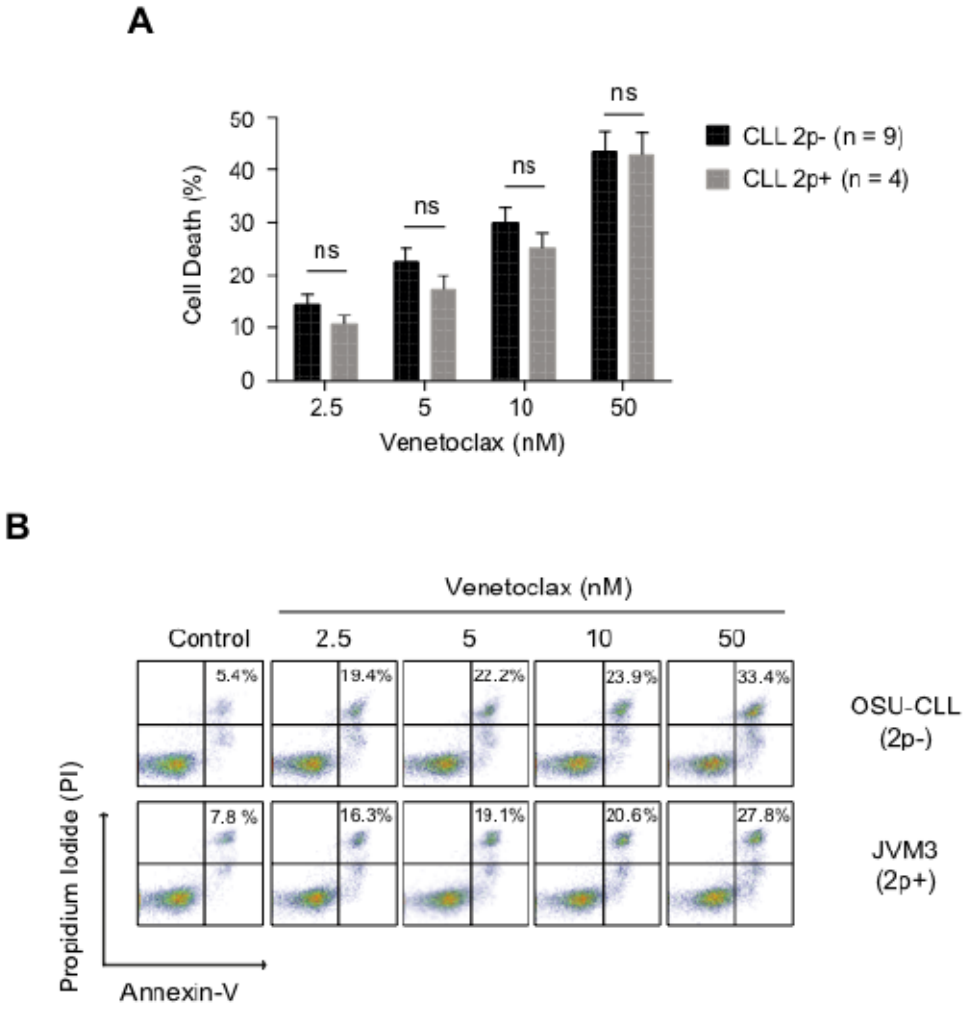

Supplementary Figure S8. Venetoclax induces cell death in 2p- and 2p+ CLL cells. (A) Cell death was measured by double Annexin-V and propidium iodide (PI) staining in B-cells from 2p- or 2p+ CLL patients treated during 24 h with Venetoclax at different doses. After accounting for spontaneous apoptosis, the percentages of Annexin-V positive and Annexin-V/PI co-positive cells were quantified and plotted. The panel of patients used here were also tested for drug resistance in Figure 2A. Statistical significance was calculated by Mann-Whitney test (ns = not significant). Bars represent mean ± SEM. (B) OSU-CLL and JVM-3 cell lines were left untreated (Control), or were incubated during 24 h with Venetoclax at different doses, before assessment of cell death in a flow cytometer by a double Annexin-V and PI staining. Representative flow cytometry plots are shown. The percentages refer to the Annexin-V or the Annexin-V/PI-positive staining.

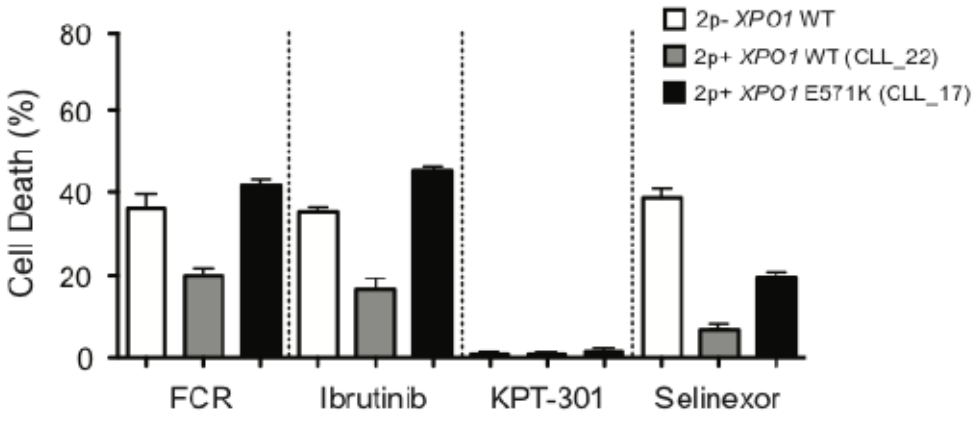

Supplementary Figure S9. XPO1 mutation is sufficient enough to switch off 2p+ drug resistance. Cell death was measured by double Annexin-V and propidium iodide (PI) staining in B-cells from representative 2p- *XPO1*-WT, 2p+ *XPO1*-WT (CLL_22), or 2p+ *XPO1* E571K (CLL_17) CLL patients treated for 24 h with FCR (35 µM; 5 mM; 10 µg/mL), ibrutinib (15 µM), the negative control KPT-301 (250 nM), or selinexor (250 nM). After accounting for spontaneous apoptosis, the percentages of Annexin-V positive and Annexin-V/PI co-positive cells were quantified and plotted. Bars represent mean ± SEM (n=2).

II – Functional Analysis of the role of *REL* in Chronic Lymphocytic Leukemia (CLL) cell survival and in 2p gain-associated drug resistance

Manuscript proposal

Abstract

Chronic lymphocytic leukemia (CLL), the most common form of adult leukemia in the West, is a highly heterogeneous disease, with a large panel of genetic alterations leading to variable clinical outcomes. Gain of the short arm of chromosome 2 (2p gain) is a frequent chromosomal abnormality in CLL and in other malignancies. Our group has reported that 2p gain was associated with drug refractoriness and poor prognosis factors such as unmutated *IGHV* and 11q deletion. We previously identified a minimally gained region that encompasses several genes, including ***REL***, a NF-κB family gene coding for a pro-survival transcription factor (c-Rel). RT-qPCR analyses confirmed that ***REL*** was overexpressed in 2p gain CLL patients. The objective of this study was to characterize the role of ***REL*** in CLL drug refractoriness using three complementary strategies: 1) Pharmacological inhibition of c-Rel induced CD specifically in 2p gain- primary CLL cells, while sparing the non-leukemic cells from patients or B cells from healthy donors. IT-603 induced CLL CD through a caspase-dependent apoptotic pathway, as evidenced by inhibition of CD by Q-VD-Oph. Primary 2p gain+ CLL cells were resistant to IT-603- and IT-901-induced CD. 2) Inactivation of ***REL*** in JVM-3 cells by CRISPR-Cas9 induced a significant increase in drug response as well as a decrease in proliferation both in a polyclonal as well as in 6 monoclonal cell lines, as compared to the controls. Targeting and inactivation of ***REL*** was fully confirmed by Sanger sequencing, RT-qPCR and Western Blotting analyses. 3) Transcriptional activation of ***REL*** by CRISPRa in OSU-CLL cells did not significantly decrease spontaneous or drug-induced CD, and did not affect proliferation, as compared to controls, in agreement with data from cells of 2p gain+ CLL patients. Altogether, our data provide substantial progress in the understanding of the role of ***REL*** in CLL cell survival and 2p gain-associated drug resistance. Indeed, results from knockout, transcriptional activation and pharmacological inhibition experiments strongly suggest that ***REL*** is a major element in the cell survival characterizing CLL, and probably acts in cooperation with other putative 2p oncogenes, namely ***XPO1, BCL11A*** and/or ***MYCN***, to drive drug resistance in 2p gain CLL. To verify this hypothesis, I have developed various cellular models of transcriptional activation (CRISPRa) and inactivation (CRISPR-Cas9) for each one of these candidate genes.

Key words: chronic lymphocytic leukemia, ***REL***, NF-κB, 2p gain, drug resistance.

Introduction

Chronic lymphocytic leukemia (CLL), the most common adult leukemia in Western countries, is a human malignancy caused by an imbalance between proliferation and programmed cell death (PCD). Despite remarkable progress in treatments, CLL remains incurable.

Our group and others have recently reported that the gain of the short arm of chromosome 2 (2p) is a frequent chromosomal abnormality in CLL: the 2p gain was

identified in 16% (21/132) of patients in a CLL clinical trial (Sutton et al., 2011) and was found to be significantly associated with poor prognosis factors, namely del11q (involving *ATM*) and unmutated *IGHV* (Chapiro et al., 2010; Cosson et al., 2017). Gain of 2p was also described in other types of cancers, for instance in lymphomas and solid tumors. The 2p contains several known oncogenes such as *REL*, *ALK*, *BCL11A*, *MYCN* and *XPO1*, which could be of critical importance in CLL disease development and evolution. By comparing 2p gain- (without 2p gain) CLL to 2p gain+ CLL B lymphocytes, we have recently shown that the 2p gain was significantly associated with *XPO1*, *TTC27*, *BCL11A*, *REL*, *AHSA2* and *USP34* overexpression (Cosson et al., 2017).

The Nuclear Factor (NF)-κB/Rel family of transcription factors is comprised of five structurally related members: *RELA* (coding for p65 protein), *RELB* (RelB), *REL* (c-Rel), *NFKB1* (p105/p50) and *NFKB2* (p100/p52). NF-κB subunits form either homo- or heterodimers, and in most unstimulated cells, remain inactive in the cytosol through their interaction with IκB proteins (such as IκBα or IκBε). Upon stimulation by various ligands, these IκB inhibitors are phosphorylated by the IκB kinase (IKK) complex and degraded, which leads to nuclear translocation of NF-κB and target genes transcription. Activation of NF-κB signaling pathways is known to be of tremendous importance in a myriad of oncogenic and immunological processes, such as lymphoid development. Although inducible in most cells, NF-κB can also be found as a constitutively active, nuclear protein in some cell types, including mature B cells and macrophages, as well as in a variety of tumor cells (reviewed in (Oeckinghaus and Ghosh, 2009). NF-κB ubiquity in physiological cellular responses renders strategies to selectively inhibit protumoral activity arduous.

REL (c-Rel) is quite a peculiar NF-κB member, notably owing to its central and specific role in B and T cell differentiation and function, as well as in human pathology. The c-Rel subunit regulates lymphocyte survival and proliferation following antigen receptor triggering. c-Rel is expressed in a restricted number of hematopoietic lineages (T and B lymphocytes, monocytes/macrophages and dendritic cells) and p50/c-Rel dimers are the major component of the constitutively active NF-κB detected in mature B cells (Grumont and Gerondakis, 1994; Miyamoto et al., 1994). Importantly, the *REL* locus is frequently altered (amplified, mutated or rearranged), and expression of *REL* is increased in numerous B and T cell malignancies. Indeed, *REL* gene amplifications have been found in Hodgkin lymphoma (46%), diffuse large B-cell lymphomas (15%), Burkitt's lymphoma (7%), follicular (17%) and mediastinal (21%) lymphomas, as well as several T cell lymphomas (Gilmore and Gerondakis, 2011). Specifically inhibiting c-Rel could thus have therapeutic benefits and represent a safer strategy than using a pan-NF-κB inhibitor (Shono et al., 2014).

Furthermore, CLL cells extracted from the tissue microenvironment, and specifically from the lymph nodes, were shown to display up-regulation of gene signatures related to B-cell receptor (BCR) signaling and NF-κB activation. The latter pathways are thus thought to play a key role in disease progression (Herishanu et al., 2011).

Finally, recurrent somatic mutations in *MYD88*, *BIRC3* and *NFKBIE* genes have been recently described in CLL (Rossi et al., 2013). Deregulated expression of the corresponding proteins, which act upstream of c-Rel, could affect c-Rel activation and the resulting target genes transcription.

Studies evaluating the functional consequence and the clinical impact of *REL* gain are lacking. In the present study, we sought to evaluate whether c-Rel activation could contribute to CLL tumor cell growth and survival through the induction of target genes including regulators of cell cycle, proliferation and survival.
Because our work also indicated that *XPO1* plays an important role in CLL drug resistance associated to 2p gain + (Cosson et al., 2017), and since other genes are overexpressed in 2p gain + CLL, we hypothesized that they could play a role and perhaps cooperate in drug resistance.

Results

1. Gain of 2p is linked with *REL* overexpression and conferred drug resistance

To verify the relevance of 2p gain to drug refractoriness in a cellular system, we initially analyzed the response to classical drugs in two well-described CLL-like cell lines: OSU-CLL (2p gain- CLL cells) (Hertlein et al., 2013) and JVM-3 (2p gain+ B prolymphocytic leukemia cells) (Melo et al., 1988). As depicted in **Figure 1C-D**, the rate of PCD induced by FC and ibrutinib was significantly lower in 2p gain+ JVM-3 cells, as compared to 2p gain- OSU-CLL cells. Using FISH analyses, we fully confirmed the gain of *REL* in 2p gain+ JVM-3 cells (**Table 1**). As shown in **Figure 1B**, these cells displayed a 1,4-fold overexpression of *REL*, as compared to OSU-CLL cells.

Table 1: Cytogenetic analyses of OSU-CLL and JVM-3 cell lines

Cell line	OSU-CLL	JVM-3
Caryotype	48,XY,inv(2)(p12q14)c,+12,+19[10]	96,XXYY,der(2),+der(2),+3,?del(7)(q)x2,+12,+add(12)(q?24)[cp4]/94,sl,-17,-21[cp7]
FISH: *REL* probe	2 copies	5 copies

2. Pharmacological inhibition of c-Rel induced cell death in primary CLL cells

In order to evaluate the role of *REL* in CLL drug resistance, our initial approach featured a selective inhibitor of c-Rel, IT-603. IT-603 acts by blocking c-Rel DNA binding and further transcriptional activity, and has been shown to display anti-lymphoma activity (Shono et al., 2014). As shown in **Figure 2**, c-Rel inhibition induced programmed cell death (PCD) in CLL cells. PCD was specifically observed in the B leukemic cells from CLL patients, sparing non-leukemic cells of CLL patients as well as B lymphocytes from healthy donors. Cells from 2p gain+ CLL patients were resistant to IT-603-induced cell death compared to cells from 2p gain- CLL patients, which suggests that *REL* overexpression associated with 2p gain was sufficient to significantly downmodulate IT-603-mediated CLL cytotoxicity. Caspase inhibitors blocked IT-603-induced PCD, which indicates a caspase-dependent mechanism.

The anti-leukemic effects of c-Rel inhibition were then confirmed with a more potent molecule, IT-901. Shono and colleagues described another potent c-Rel inhibitor exhibiting *in vitro* and *in vivo* antitumor properties. IT-901 displayed selective activity in human diffuse large B-cell lymphoma (DLBCL) cells, and its estimated half maximal inhibitory concentration (IC_{50}) regarding global NF-κB activity was about six times lower (3 µmol/L) compared with IT-603 (18.8 µmol/L) (Shono et al., 2016).

Assessment of cell death induced by IT-603 and IT-901 in ***REL***-deleted JVM-3 cell lines for 24h showed that these two molecules are not specific of c-Rel, suggesting a perhaps wider inhibitory activity towards NF-κB subunits.

3. CRISPR-Cas9 mediated knockout of *REL* in 2p gain+ JVM-3 cells increased spontaneous and drug-induced cell death, while decreasing proliferation

To further substantiate the role of ***REL*** in CLL drug refractoriness, we wondered if deleting ***REL*** gene in a 2p gain+ CLL-like model (JVM-3) would impact the response to common anti-CLL drugs. Briefly, single guide RNAs (sgRNAs) sequences were designed and selected *in silico* according to their scores of predicted efficacy and selectivity toward human ***REL*** exon 2. The selected sgRNAs were then inserted in vectors containing the *S. pyogenes* Cas9 fused by a T2A peptide to the fluorescent tracer Cherry (lentiCRISPRv2). In order to determine the most efficient sgRNA using an *in vitro* assay, the CRISPR/Cas9 constructs were first electroporated in OCI-LY1 cells, a human B cell lymphoma cell line that allowed transfection with high efficiency and viability. Genomic cleavage efficiency was estimated by a T7 endonuclease I assay performed on the PCR-amplified DNA of Cherry+ cells **(Figure 3)**.

We next sought to verify that the lentiviral CRISPR-Cas9-RELsg1 construct effectively induces target gene deletion in the OCI-LY1 B cell line. As depicted in **Figure 4**, transfection of OCI-LY1 cells with the CRISPR-Cas9-RELsg1 vector and FACS sorting of Cherry+ single cell into individual vials yielded 11 clones, which were characterized for ***REL*** deletion by PCR and T7 endonuclease I assay, Western blotting and Sanger sequencing. Functional analysis revealed that although ***REL*** deletion did not affect cell viability or sensitivity to drugs, as compared to the parental cell line (WT), proliferation was significantly decreased in ***REL***-deleted cell clones, in comparison with WT cells.

After validation of the sgRNA1 efficiency, we then proceeded to transduce the 2p gain+ CLL-like cellular model. As shown in **Figure 5**, transduction of JVM-3 cells with the CRISPR-Cas9-RELsg1 vector yielded a pool of edited cells (Bulk) and single edited cells-derived clones (RELsg1 #N), which were similarly characterized for ***REL*** deletion by PCR and T7 endonuclease I assay, Western blotting and Sanger sequencing. Freshly transduced cells as well as cells from the cherry + Bulk cell line were sorted by FACS into single cells, which were amplified, producing 17 single cell-derived cell lines. Sanger sequencing showed that all of them had an edited ***REL*** genetic sequence, probably owing to the genomic integration of the CRISPR-Cas9 construct in cells that were amplified and maintained in culture for several weeks. Indeed, RT-qPCR analysis showed little to no ***REL*** mRNA expression in the modified cell lines, as compared to the control. Moreover, to confirm that the CRISPR/Cas9 system efficiently truncated the ***REL*** gene, the presence of the protein was tested by Western blot analysis, and protein expression was undetectable in edited cells. Six of

the *REL*-deleted JVM-3 cell lines were randomly selected for functional analysis, which indicated that *REL* deletion significantly increased sensitivity to anti-CLL drugs, as compared with empty-Cas9 control **(Figure 5B)**. Proliferation was decreased in the cherry+ bulk as well as in the clonal cell lines, in comparison with WT cells or the empty-Cas9 control **(Figure 5C)**.

In order to gain a mechanistic insight, expression of target genes (*COX2* and *EZH2* for instance) as well as expression of other NF-κB genes (namely *NFKB1, NFKB2, RELA, RELB, NFKBIA* and *NFKBIE*) was determined by real-time RT-PCR analyses but did not reveal clear compensatory effects of other NF-κB subunits regarding drug response (data not shown).

4. Transcriptional activation of *REL* in 2p gain- OSU-CLL cells

In order to substantiate the relevance of *REL* in 2p gain-associated drug resistance, we overexpressed this gene in the 2p gain- OSU-CLL cell line using a dCas9-VP64 construct and sgRNAs specifically designed to enhance gene transcription of the endogenous *REL* sequence. To this end, OSU-CLL cells were initially transduced with a lentivirus expressing a constitutive dCas9, thereby establishing the OSU-dCas9-GFP cell line, which enables the generation of any CLL overexpression model by selecting sgRNAs targeted to the promoter regions of the genes of interest. Three sgRNAs were selected *in silico* using programs (CRISPOR, Zhang MIT, Broad Institute) that rank candidate sgRNAs targeting the *REL* promoter according to predictive specificity and efficacy scores. Vectors containing each sgRNA were constructed and packaged in lentiviruses.

OSU-dCas9 cells were then transduced with lentiviruses expressing sgRNAs specific for the *REL* gene, in order to obtain 3 polyclonal cell lines, namely RELsgA1, 2 and 3. As shown in **Figure 6**, successful transcriptional activation was achieved in the RELsgA2 cell line. *REL* overexpression decreased both spontaneous and drug-induced apoptosis in *REL* activated cell lines in comparison with the control, albeit without reaching significance. Moreover, although protein expression was similar between sgRNAs, mRNA expression levels were different between dCas9-RELsgA2 on one hand and -RELsgA1/-RELsgA3 cell lines on the other hand. Hence, *REL* overexpression by CRISPRa did not lead to a significant decrease in spontaneous or drug-induced apoptosis.

5. CRISPR-dCas9-mediated transcriptional activation of *XPO1, BCL11A* and *MYCN* genes in OSU-CLL cells

Since most 2p gain+ CLL patients show large 2p gains, including important genes for oncogenesis, we hypothesized that there could be oncogenic cooperation between *REL* and other 2p genes such as *XPO1, MYCN, ALK* and *BCL11A*. To answer to this question, we activated the transcription of these 2p genes using the same CRISPRa approach as previously in JVM-3 cells, then examined their phenotypic consequences. sgRNAs were designed and lentiviral CRISPR-dCas9 vectors were constructed. *In vitro* selection and validation of the most efficient guides for each 2p gene was performed (**Figure 7**).

6. CRISPR-Cas9-mediated editing of *XPO1, BCL11A, MYCN* and *ALK* genes in JVM-3 cells

We then deleted 2p genes using the same CRISPR-Cas9 approach as previously in JVM-3 cells, then examined the phenotypic consequences of these genetic deletions. sgRNAs were designed and lentiviral CRISPR-Cas9 vectors were constructed. *In vitro* selection and validation of the most efficient guides for each 2p gene was performed (**Figure 8**).

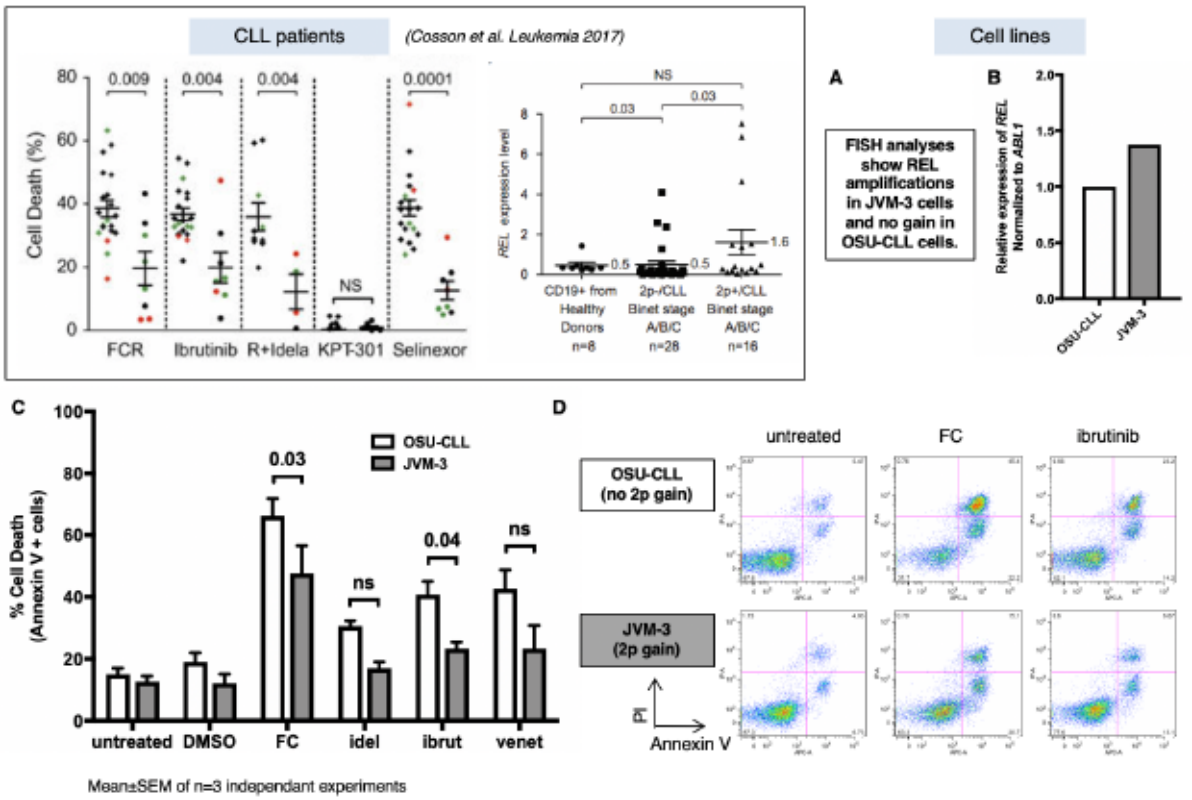

Figure 1: Amplification of *REL* in 2p gain+ cell line JVM-3 is associated with gene overexpression and drug refractoriness.
Top panel: Left: the rate of PCD induced by CLL drugs was significantly lower in 2p gain+ patients, as compared to 2p gain- patients. Right: ***REL*** mRNA levels were determined by RT-qPCR in CD19⁺ cells isolated from healthy donors and from 2p gain- or 2p gain+ CLL patients (*Cosson et al., 2017*). A: FISH analyses were performed and showed the gain of ***REL*** in 2p gain+ JVM-3 cells. B: ***REL*** mRNA levels were determined by RT-qPCR in two B-cell lines: OSU-CLL (2p gain-) and JVM-3 (2p gain+). JVM-3 cells displayed a 1,4-fold overexpression of ***REL***, as compared to OSU-CLL cells. The ***ABL1*** mRNA expression was used to normalize the data. C and D: Apoptosis was measured in JVM-3 and OSU-CLL cells after 24h with or without treatment. PCD induced by FC and ibrutinib was significantly lower in 2p+ JVM-3 cells. C: the percentages of Annexin-V positive and Annexin-V/PI co-positive cells were quantified and plotted. Mean + SEM of n=3 independent experiments). The statistical analysis was performed using two-way ANOVA test. Statistically significant differences (p-value < 0.05) are indicated, ns: not significant. D: Representative flow cytometry plots are shown.

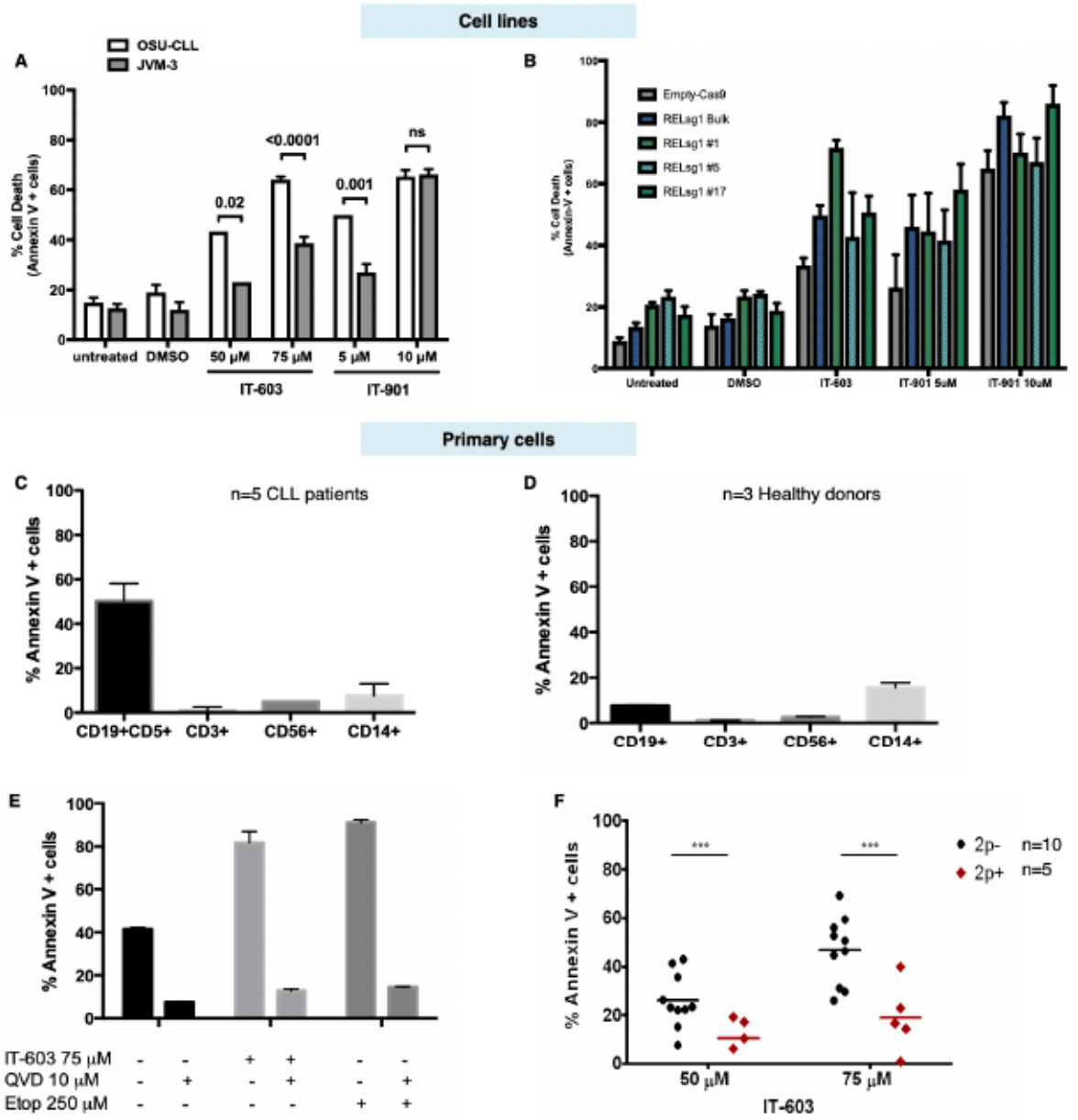

Figure 2: Pharmacological inhibition of c-Rel/NF-κB induced cell death in CLL cell lines and patient primary cells. A: OSU-CLL and JVM-3 cells were treated with c-Rel inhibitors IT-603 (50 and 75 µM) and IT-901 (5 and 10 µM) for 24h, or left untreated. DMSO represent the vehicle control (final concentration of 1% DMSO). Cell death was assessed by Annexin V and Propidium Iodide staining and analyzed by flow cytometry: the percentages refer to Annexin-V+/PI- and Annexin-V/PI co-positive staining. B: specificity of IT-603 and IT-901 for c-Rel was assessed by treating *REL*-deleted JVM-3 cell lines for 24h and measuring cell death. C: Cells from CLL patients (n=5) were magnetically sorted and were treated for 24h with c-Rel inhibitor (IT-603). IT-603 induced cell death specifically in the CD19+/CD5+ fraction (= tumoral cells), sparing the non-leukemic cells. D: CD19+ B lymphocytes from Healthy Donors (n=3), as well as the other major blood cell types (CD3+ T lymphocytes, CD56+ NK lymphocytes, CD14+ monocytes) are not sensitive to IT-603-induced cell death. E: QVD, a pan-caspase inhibitor, blocks the induction of CLL cells death mediated by IT-603 (n=1). Etop (etoposide): induces apoptosis of tumor cells (positive control). F: Cells from 2p gain+ patients (n=5) are resistant to IT-603

induced cell death compared to cells from 2p gain- CLL patients (n=10). Dots represent individual samples. The statistical analysis was performed using Mann-Whitney *U*-test. Asterisks represent statistically significant differences (p-value < 0.05), *** summarizes p-values ≤ 0.001).

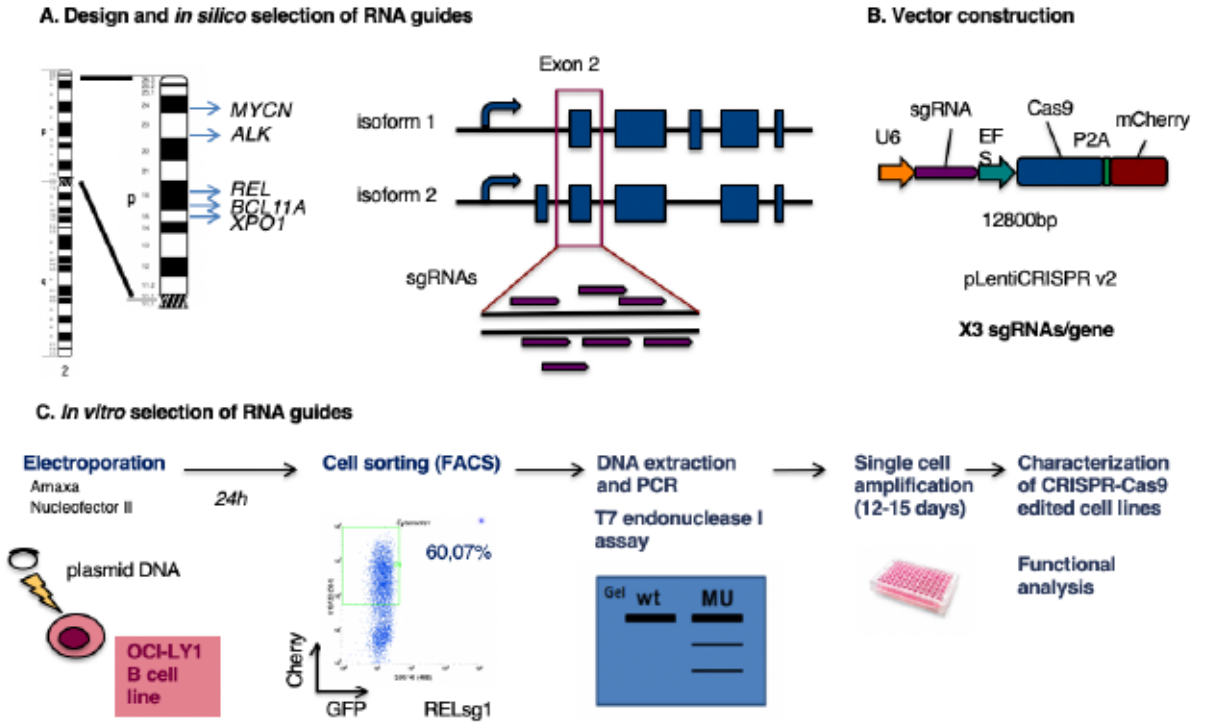

Figure 3: Overview of the single guide RNA design and selection. A: Three sgRNAs were selected *in silico* using programs (CRISPOR, Zhang MIT, Broad Institute) that rank candidate sgRNAs according to predictive specificity and efficacy scores. B: The selected sgRNAs were inserted in lentiviral Cas9-cherry vectors. Correct insertion was confirmed by Sanger sequencing. C: OCI-LY1 cells were electroporated with the three sgRNA constructs, sorted by FACS and DNA was extracted and amplified by PCR for the targeted ***REL*** region. A mismatch cleavage assay using the T7 endonuclease I allowed the determination of the construct containing the sgRNA1 as the most efficient for genomic cleavage of ***REL in vitro***. Subsequently, cells were transfected with the selected RNA guide, sorted by FACS and characterized prior to functional analysis.

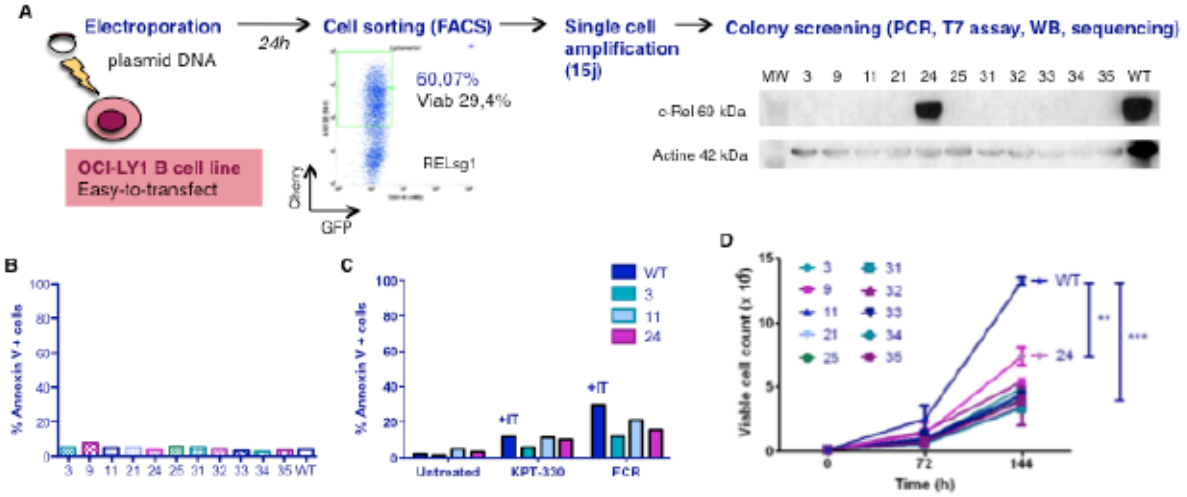

Figure 4: Characterization and functional analysis of *REL*-deleted OCI-LY1 clones. A: Characterization of OCI-LY1 cells electroporated with the lentiviral CRISPR-Cas9-RELsg1 vector. Cells were sorted by FACS as single cells in 96-well plates, and amplified for approximately 2 weeks. Viable clones were further amplified. The Western Blot analysis shows 10 deleted clones and a "WT-like" clone (24), which harbored a heterozygous deletion as determined by Sanger sequencing. B: Assessment of spontaneous cell death by AnnexinV/PI co-staining after 24h of incubation (n=2). C: First, wild-type (WT) cells were treated with IT-603 (75 µM) ± FCR (35 µm; 5 mm; 10 µg/ml), ibrutinib (15 µM), idelalisib (50 µM) or KPT-330 (250nM). The only IT-603 + antiCLL drug combination that induced PCD in WT cells was the combination of IT-603 and FCR (28% of PCD) (data not shown). Next, we subjected three ***REL***-deleted clones to FCR treatment and assessed PCD as previously described. KPT-330 was used as a negative control. D: The number of viable cells was determined at different culture time points and plotted for the different ***REL***-deleted cell clones (numbers) as compared with the wild-type OCI-LY1 cell line (WT) (mean + SEM of n=3 independent experiments). The statistical analysis was performed using two-way ANOVA test. Asterisks represent statistically significant differences (p-value < 0.05), ** $p \leq 0.01$, *** $p \leq 0.001$).

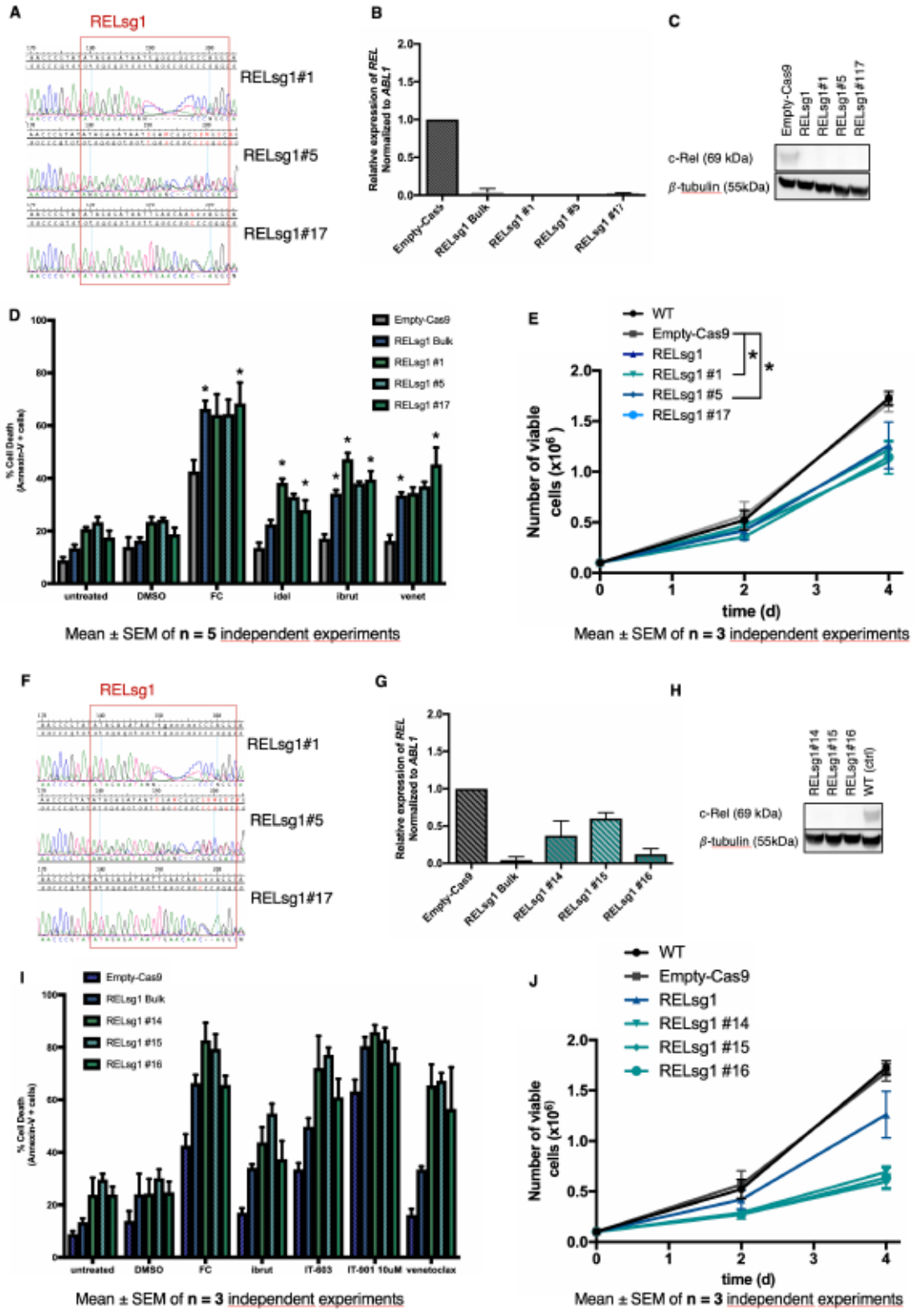

Figure 5: CRISPR-Cas9 mediated knockout of *REL* increased spontaneous and drug-induced cell death, while decreasing proliferation. Characterization and functional analysis of *REL*-deleted JVM-3 cell lines. JVM-3 cells were transduced with the lentiviral CRISPR-Cas9-*REL*sg1 vector, sorted by FACS and amplified to establish one polyclonal Cherry+ cell line (RELsg1 bulk) as well as 17 single-cell derived cell lines (RELsg1#N). Six cell lines were randomly selected for further

analysis. A,F: Efficient genetic editing of ***REL*** was confirmed in all cell lines by Sanger sequencing. For instance, the RELsg1 cell line displayed a 7bp deletion in ***REL*** as determined by alignment to a WT reference sequence using the DNAstar Seqman software. B,G: ***REL*** mRNA levels were determined by RT-qPCR. Transcript levels were strongly decreased in ***REL***-edited cell lines, in comparison with the controls (WT or EmptyCas9 cell lines). The ***ABL1*** mRNA expression was used to normalize the data. C,H: The Western Blot analysis shows that the polyclonal and all monoclonal RELsg1(#N) cell lines were deleted for ***REL***. D,I: Assessment of CLL drugs-induced cell death by AnnexinV/PI double staining after 24h of incubation. E,J: The number of viable cells was determined at different culture time points and plotted for the different ***REL***-deleted cell lines (numbers) as compared with the wild-type JVM-3 cell line (WT) (n=1).

A Overview of the experimental design

sgRNA design

GRCh37/hg19: REL chr2				Benchling (Doench 2016)		(Gilbert 2014)
Position	**Strand**	**Protospacer sequence**	**PAM**	**Specificity Score**	**Efficiency Score**	**sgRNA ID**
61108627	-1	ACGCAGCAACCCTCACCCGG	AGG	78.5459432	71.733227526 38072	REL-4
61108405	-1	TGACGGCTAGCAGCGTGAGA	AGG	89.3755837	57.900104484 99915	REL-1
61108664	-1	GGCGGGAGGGGAATTTCCCG	CGG	77.4251797	57.671136842 78048	REL-10
61108654	-1	GAATTTCCCGCGGCTGACGT	AGG	92.8407165	56.287110602 8084	REL-5
61108658	1	CGTCGGGCCTACGTCAGCCG	CGG	95.1141507	54.037387060 26494	REL-9

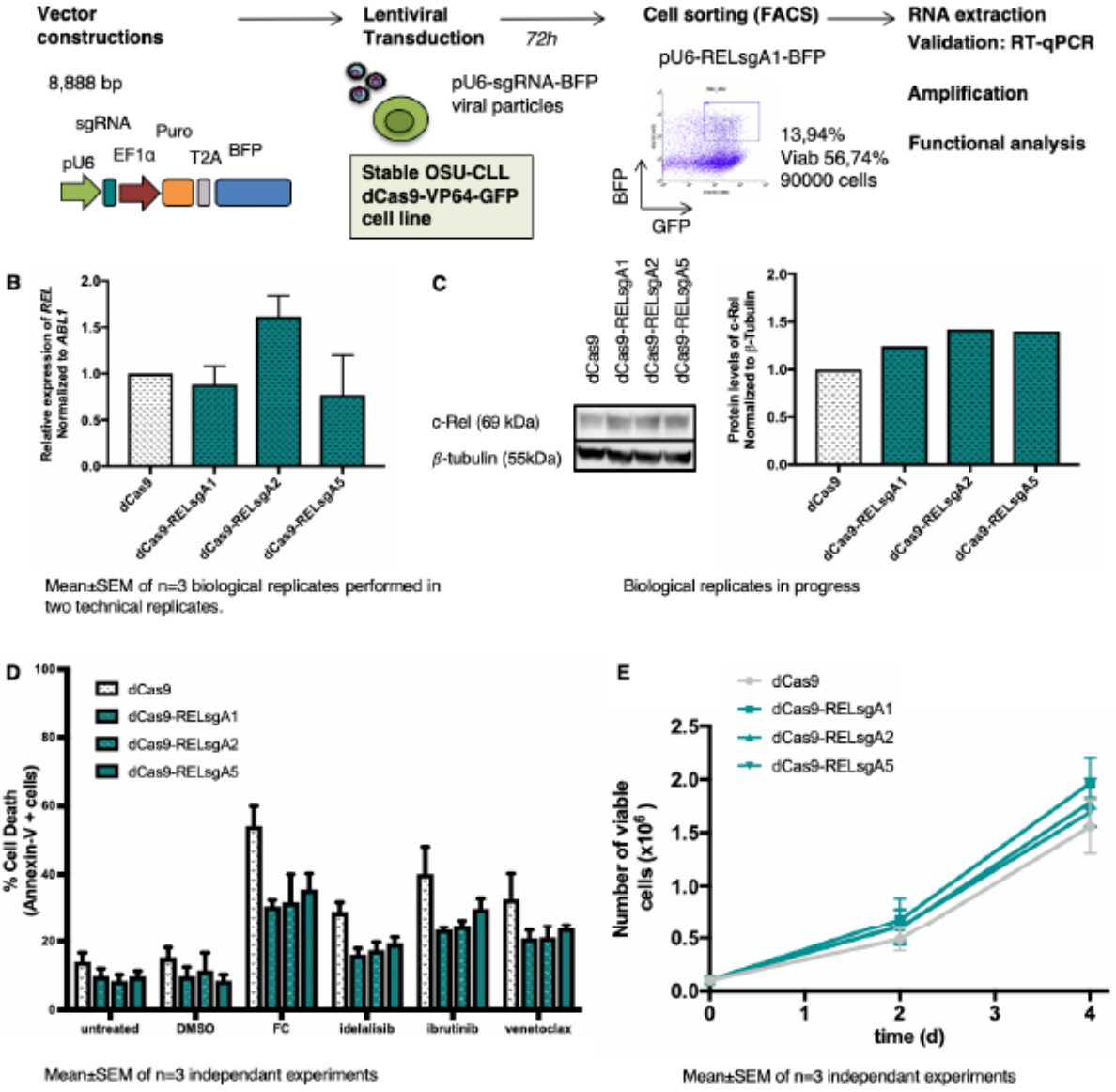

Figure 6: CRISPRa-mediated transcriptional activation of *REL* decreases spontaneous and drug-induced cell death, without affecting proliferation

A: Overview of the single guide RNA design and selection. Three sgRNAs were selected *in silico* using programs (CRISPOR, Zhang MIT, Broad Institute) that rank candidate sgRNAs according to predictive specificity and efficacy scores.

Establishment of the stable OSU-dCas9-GFP cell line enables a selective transcriptional activation of any gene of interest in OSU-CLL cells. OSU-dCas9-GFP cells were transduced with each selected lentiviral RELsgA#N vector, sorted by FACS and amplified to generate stable OSU-dCas9-RELsgA#N cell lines.
B-C: Characterization of the OSU-dCas9-RELsgA cell lines. B. ***REL*** mRNA levels were determined by RT-qPCR. The ***ABL1*** mRNA expression was used to normalize the data. C. The Western Blot analysis showed a subtle overexpression in all three RELsgA cell lines. B: Assessment of spontaneous and drug-induced cell death by AnnexinV/PI co-staining after 24h of incubation (mean + SEM of n=3 independent experiments). C: The number of viable cells was determined at different culture time points and plotted for the different dCas9-RELsgA cell lines as compared with the control cell line (dCas9) (mean + SEM of n=3 independent experiments). The statistical analysis was performed using two-way ANOVA test and showed there no statistically significant differences.

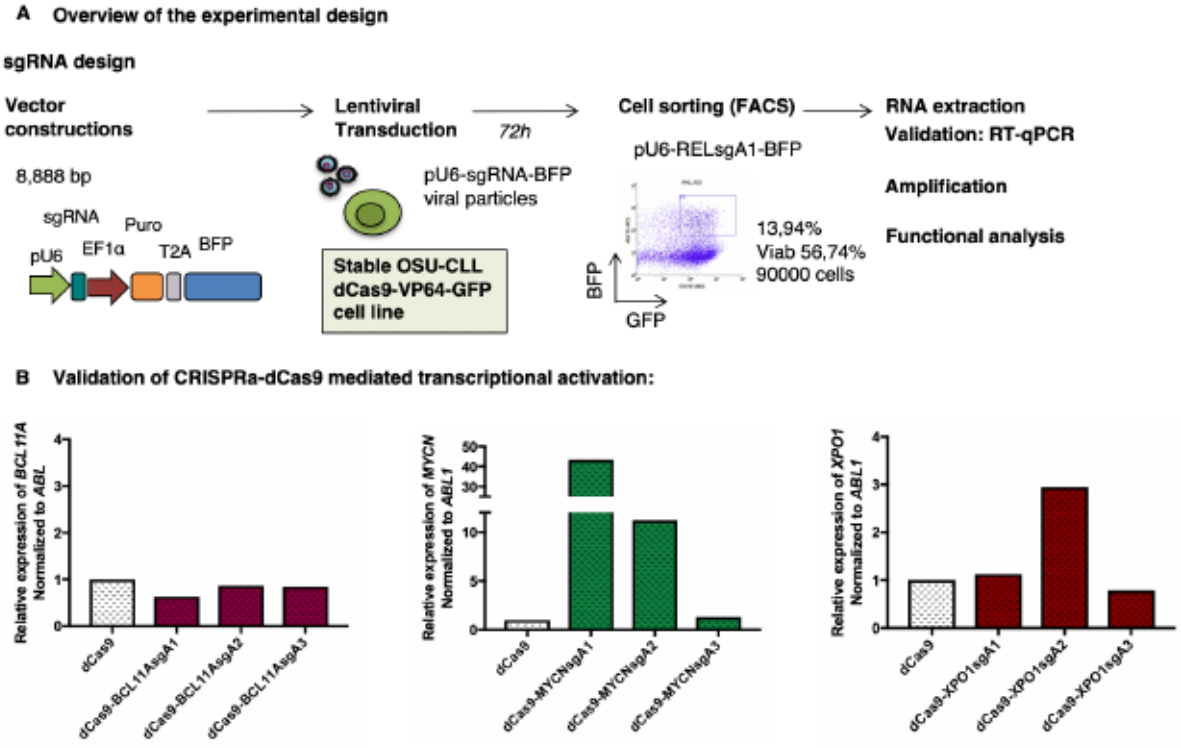

Figure 7: CRISPRa-mediated transcriptional activation of other putative 2p oncogenes. A: For each gene, namely ***BCL11A***, ***MYCN*** and ***XPO1***, single guide RNAs were designed and selected as previously described. Three sgRNAs were selected *in silico* using programs (CRISPOR, Zhang MIT, Broad Institute) that rank candidate sgRNAs according to predictive specificity and efficacy scores. OSU-dCas9-GFP cells were transduced with each selected lentiviral sgRNA vector, sorted by FACS and amplified to generate stable OSU-dCas9-GENEsgA#N cell lines. B: Characterization of the OSU-dCas9-GENEsgA#N cell lines. ***REL*** mRNA levels were determined by RT-qPCR. The ***ABL1*** mRNA expression was used to normalize the data.

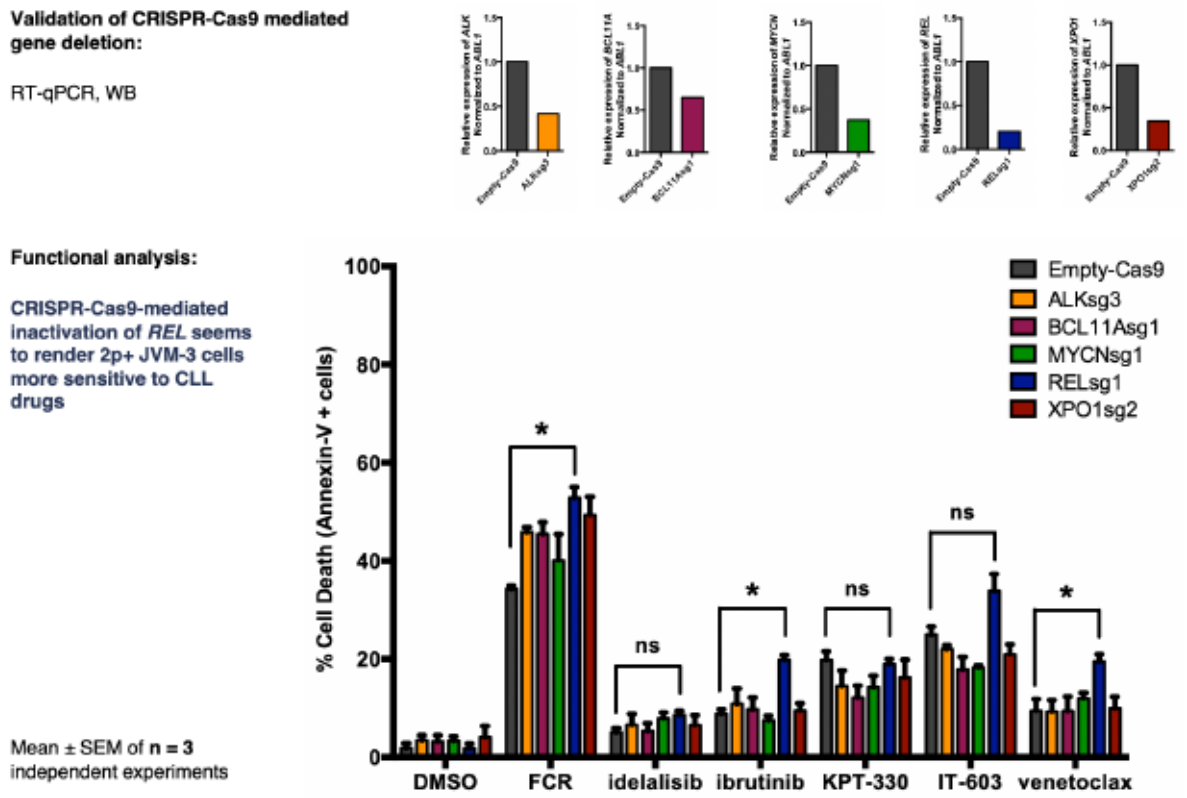

Figure 8: CRISPR-Cas9-mediated deletion of other putative 2p oncogenes. For each gene, namely *BCL11A*, *MYCN* and *XPO1*, single guide RNAs were designed and selected as previously described. Three sgRNAs were selected *in silico* using programs (CRISPOR, Zhang MIT, Broad Institute) that rank candidate sgRNAs according to predictive specificity and efficacy scores. JVM-3 cells were transduced with each selected lentiviral sgRNA vector, sorted by FACS and amplified to generate stable edited cell lines. Top: mRNA levels of each studied gene were determined by RT-qPCR. Transcript levels were strongly decreased in edited cell lines, in comparison with the controls (WT or EmptyCas9 cell lines). The ***ABL1*** mRNA expression was used to normalize the data. Bottom: Assessment of CLL drugs-induced cell death by AnnexinV/PI double staining after 24h of incubation.

Materials and methods

Cell lines
HEK 293T cells were used for lentivirus production. They were maintained in DMEM supplemented with 10% FBS and 1% penicillin/streptomycin (p/s). OSU-CLL and JVM-3 cells were maintained in RPMI supplemented with 10% FBS and 1% p/s. OCI-LY1 cells were maintained in IMDM supplemented with 20% FBS and 1% p/s.

Patients and healthy donors
The clinicopathological features of the study cohort are shown in Table 1.
Data patients Pitié/CRC.

Isolation of PBMC/B lymphocytes
Blood samples were separation by Ficoll density gradient, distinct cell types were isolated by magnetic bead separation (MACS, Miltenyi).

T7 endonuclease assay (mismatch cleavage)
After PCR amplification the PCR fragments were hybridized and digested with a T7 endonuclease (NEB, cat M0302) for 15 minutes at 37°C. Afterwards, the digested product was analyzed on a 1.5% agarose gel alongside the undigested PCR product as control.

Lentiviral constructs sgRNA design and sgRNA cloning
The sgRNA sequences were designed by combining the best ranking sgRNAs in three CRISPR software: CRISPOR (crispor.tefor.net/), Broad Institute (https://portals.broadinstitute.org/gpp/public/analysis-tools/sgrna-design) and the late crispr.mit.edu. The two complementary oligos were denatured at 95°C for 5 min and ramp cooled to 25 over a period of 2-3h to allow annealing, and finally ligated with the linearized plasmid. Competent cells were transformed with the ligated plasmid and single colonies were grown before proceeding to plasmid extraction using the Qiagen maxiprep kit. The correct insertion of the sgRNA sequence in the plasmid was confirmed using Sanger sequencing.

Lentiviral production and cell transduction
Briefly, CRISPR constructs were co-transfected with Gag/Pol (viral packing plasmid) and VSV-G (envelope plasmid) in HEK-293T cells using Jetprime reagent, lentiviral particles were collected 48h after transfection and were concentrated by ultra-centrifugation. Lentiviral particles were frozen at -80°C. OSU-CLL and JVM-3 cells were infected in 24 well plates with $1x10^6$ cells/well cultured in enriched medium.

Establishment of stable CRISPR-modified cell lines
To obtain a stable OSU-CLL cell line expressing dCas9-GFP, lentiviral particles containing the dCas9-empty plasmid were transduced into OSU-CLL cells. 72h after infection, GFP positive cells were sorted using FACS Influx cytometer and amplified.
To establish (d)Cas9-edited cell lines, lentiviral particles containing the indicated (d)Cas9-sgRNAs plasmids were transduced into JVM-3 or OSU-CLL cells. 72h after infection, GFP or Cherry positive cells were sorted using FACS Influx cytometer and

single cells were seeded in 96-well plates. Amplification of these single cells yielded 17 clonal cell lines with *REL* inactivation.

Sanger sequencing

Genomic DNA was extracted using the Norgen kit following the manufacturer's instructions. To amplify the region of *REL*, PCR was performed. PCR products were purified and were sequenced by Sanger method using forward PCR primer (Eurofins).

Apoptosis assay

Cells were treated with c-Rel/NF-κB inhibitors, classical anti-CLL drugs, 1% DMSO (vehicle control) or left untreated for 24h. Drugs were prepared extemporaneously by diluting stock solutions, and added to cell cultures to reach final concentrations indicated in **Table 2**.

Table 2: c-Rel inhibitors and classical anti-CLL drugs used in this study

Drug	Mode of action	Manufacturer	Final concentration
fludarabine	DNA synthesis inhibitor	Selleckchem	35 µM
cyclophosphamide (endoxan)	Alkylating agent	Sigma-Aldrich	5 mM
rituximab	Anti-CD20 antibody	Roche	10 µg/mL
ibrutinib	BTK inhibitor	Selleckchem	15 µM
idelalisib	PI3K inhibitor	Selleckchem	50 µM
KPT-330 (selinexor)	XPO1 inhibitor	Karyopharm Therapeutics	250 nM
IT-603	c-Rel/NF-κB inhibitor	Merck	50-100 µM
IT-901	c-Rel/NF-κB inhibitor	Bio-techne	5-10 µM
venetoclax	BCL2 inhibitor	Selleckchem	50-100 nM

After 24h, $1x10^5$ cells/condition were collected and washed twice in PBS, then labeled with an Annexin V(AnV)-APC and propidium iodide (PI) co-staining, allowing the discrimination of living intact cells (AnV-PI-), early apoptotic cells (AnV+PI-), late apoptotic and necrotic cells (AnV+PI+). Cells were analyzed on a FACS Canto II flow cytometer using FACS-DIVA (BD Biosciences) and FlowJo (TreeStar) softwares.

Cell electroporation

Cells were electroporated using the Amaxa system (Lonza) and resuspended in medium with 20% serum. Addition of serum to electroporated cells, to reach 20% final serum concentration, was proven to improve survival and transfection efficiency, by effectively sealing cells in less than 10 minutes after electroporation (Bahnson and Boggs, 1990).

RT-qPCR analyses

RNA was extracted using the Norgen kit following the manufacturer's instructions). The *ABL1* mRNA expression was used to normalize the data.

Western blotting

Whole cell lysates were prepared in 1x final Laemmli buffer prior to sonication. The lysate samples were denaturated at 95 for 5 minutes before loading onto a 10% SDS-PAGE (Mini Protean TGX Precast protein gels, Biorad) 5 µL of prestained protein standards or 20 µL of samples were loaded onto the gel. The gel was electrophorized for 1h30 at 100 mV in 1x running buffer. Proteins were transferred onto a nitrocellulose membrane at 100 V for 1h30 at 4°C in 1x transfer buffer, and subsequently immunoblotted using the indicated antibodies and horseradish peroxidase-labeled secondary antibodies.

Primary antibodies were diluted in 5% skim milk in PBS/Tween and incubated overnight at 4°C with shaking. Antibodies to c-Rel (Cell Signaling technology), actin (Sigma) were used for immunoblotting. After incubation, membranes were washed with PBS Tween 0.1% for three times 10 min. after washing membranes were incubated with secondary antibody diluted in 5% skim milk in PBS/tween for 1h at RT with shaking and then washed again as above. Membrane was visualized under chemiluminescence with HRP substrate (Thermo Fischer Scientific) at various exposure times, and image blots were recorded on a Imager and quantified using ImageJ software.

Statistical analysis

To compare treatment effect across cells, an unpaired t-test was applied. Using ImageJ software, western blot membranes were analyzed for the mean band intensity for c-Rel el as well as for the loading control Actin. The relative abundance of c-Rel was determined as a ratio of the loading control. These ratios were then normalized to the negative control with no c-Rel. A two-way ANOVA test using Tukeys was performed to compare between samples. All analyses were conducted using GraphPad software Prism 7.

Discussion

Despite major improvements in therapeutic strategies in patients with CLL, eradication of the disease remains a challenge because of the emergence of drug resistance. In particular, the 2p gain is frequent in CLL, and is associated with the progression of the disease and the drug resistance. Potentially significant genes are localized in 2p, including ***REL***. Although the transcription factor NF-κB is known as a key player in tumor formation, the relevance of its particular subunits is still underestimated. Because of the peculiar roles of ***REL*** in health and disease compared to other members of the NF-κB family, targeting c-Rel could impair tumor growth while maintaining NF-κB physiological functions and thus prevent unwanted side-effects. Hence, it has been suggested that ***REL*** could be one of the critical target genes of 2p12-16 amplification in CLL, however little experimental evidence to date actually supports this notion. For the first time, the present study sought to precisely assess the functional relevance of ***REL*** in 2p gain pathophysiology.

We used RNA-guided transcriptional activation of ***REL*** via CRISPR/dCas9 in order to mimic an overexpression phenotype in CLL cells. To our knowledge, this is the first report of a c-Rel overexpression experiment in CLL or 2p gain-harboring lymphomas/leukemias.
Efficient yet subtle overexpression of ***REL*** was achieved in the CRISPRa-edited B cellular models presented here. This is consistent with previous reports, where the magnitude of transcriptional upregulation attained by individual sgRNAs is usually low: CRISPRa, by activating transcription at the endogenous locus, generally induce low to moderate expression levels as compared to classical cDNA overexpression studies (Joung et al., 2017a; Konermann et al., 2013; Maeder et al., 2013; Mali et al., 2013; Perez-Pinera et al., 2013). Tiling a promoter region with several sgRNAs can generate a more robust transcriptional activation (Maeder et al., 2013; Mali et al., 2013; Perez-Pinera et al., 2013). However, a subtle overexpression conveniently results in a viable and more pathophysiological phenotype. Indeed, our group has previously shown that gain of 2p was associated with a relatively modest (3,2-fold) overexpression of ***REL*** in CLL patients (Cosson et al., 2017), and strong gene upregulation can lead to aberrant cell functions. in some situations, high-level expression of c-Rel can even induce cell-cycle arrest (Bash et al., 1997). For instance, generation of transgenic mice with c-Rel under the control of a B-cell specific promoter was reportedly impossible, suggesting that overexpression of c-Rel may be toxic at some stages of B cell development (Gerondakis et al., 2006).

Moreover, edited cells were selected and amplified as mixed pools in order to circumvent sgRNA-related off-target effects, and to control for clonal effects such as *de novo* mutations, epigenetic or metabolic variation between monoclonal cell lines populations, as well as biases due to lentivirus integration. Indeed, due to difficulty in transiently transfecting hematopoietic cells, we have adopted a lentiviral system to deliver the CRISPR/(d)Cas9 components into the poorly transfectable CLL cell lines, but this can result in integration of lentivirus components in unwanted loci. This method also avoids delays due to the slow proliferation rate and poor survival of leukemic cells when cultured from single cells.

Very few relevant CLL models or human B cell lymphoma/leukemia cell lines with a highly amplified ***REL*** locus/2p gain are available. Moreover, the ones that do exist are usually obtained by EBV immortalization, which is known to alter host transcription programs and result in a proliferative advantage (Drexler and Matsuo, 2000; Wang et al., 2019). For instance, OSU-CLL is a cell line established by EBV transformation of a CD5+ CLL with trisomy 12 and 19 (Hertlein et al., 2013). JVM-3 was induced by EBV and polyclonal B cell activator TPA is derived from prolymphocytic leukemia carrying a trisomy 12 (Melo et al., 1988). When possible and relevant, different cell lines should be subjected to the alteration of interest to account for this potential bias.

Furthermore, additional control experiments using non-targeting sgRNAs should be performed in parallel in order to confirm that transcription level changes are due to dCas9-dependant gene activation (Miles et al., 2016).

We have shown that transcriptional activation of ***REL*** by three different sgRNAs in dCas9-VP64 OSU-CLL cells did not affect proliferation nor significantly diminish spontaneous or drug-induced cell death, suggesting that ***REL*** might not be the driver gene accounting for the poor clinical features associated with 2p gain in CLL. This notion is also supported by the observation that 2p gain+ CLL primary cells were resistant to cell death induced by NF-κB-inhibitors, similarly to any other anti-CLL drugs, as compared with 2p gain- CLL samples.

Pharmacological inhibitors IT-603 and IT-901 induced cell death specifically in primary CLL tumoral cells but not in healthy donor lymphocytes, in line with the consistently observed high levels of nuclear NF-κB-binding activity in unstimulated CLL B cells relative to that detected in nonmalignant human B cells (Furman et al., 2000). Cell lines were more sensitive to IT-603 and IT-901 than patient cells, in keeping with a higher constitutive activation NF-κB, independently from microenvironmental conditions.

Vaisitti and colleagues reported that addition of IT-901 to CLL cells *in vitro* significantly decreased DNA binding p50, p65 and c-Rel, with p65 being most sensitive, suggesting that the main effects of the drug are through p65 (Vaisitti et al., 2017). Consistently, assessment of cell death induced by IT-603 and IT-901 in ***REL***-deleted JVM-3 cell lines for 24h showed that both of these molecules are not specific of c-Rel, suggesting a perhaps wider inhibitory activity towards NF-κB subunits.

Moreover, we have also found that IT-603 induced cell death through a caspase-dependent mechanism. The latter observations should be completed by assessing caspase-3 and PARP cleavage, as well as down-regulation of XIAP or upregulation of BIM proteins. IT-901 was reported to act by activating intrinsic apoptosis upon increase in mitochondrial reactive oxygen species, which damage mitochondria, limit oxidative phosphorylation and ATP production (Vaisitti et al., 2017).

The CRISPR/Cas9 genomic editing technology allows the ablation of gene causing an absence of oncoprotein expression and blocking its effects *in vitro*. Here, we report the successful establishment of a polyclonal cell line as well as 17 single cell derived monoclonal cell lines, all carrying CRISPR/Cas9-mediated mutations in the ***REL*** gene. Efficient gene editing and complete lack of c-Rel protein expression

were confirmed in all cell lines. Importantly, our data regarding the *in vitro* ablation of ***REL*** by CRISPR/Cas9 in 2p gain+ B cells showed a significantly increased drug-induced and spontaneous apoptosis, as well as decreased cell proliferation. The results obtained in the pool of edited cells (Bulk) were confirmed in six edited cell lines each derived from a single cell, endorsing the notion that the loss of ability to grow was solely due to the disruption of the ***REL*** gene.

Further, edited cells should be precisely characterized using indel tracking algorithms such as Tide https://tide-calculator.nki.nl. However, because of the polyploid nature of JVM-3 cells, precise characterization of ***REL*** gene disruption was difficult in most CRISPR-edited cell lines. Moreover, since most methods of detection of on-target mutations are based on the PCR, they usually tend to underestimate the frequency of on-target activity because large deletions that extend beyond the boundaries of the PCR amplicon are not detected, and large insertions are amplified less efficiently than small mutations (if at all) and are therefore less likely to be identified. This is however less critical when a single gRNA is used because small indels are much more frequent than large deletions or insertions (Zischewski et al., 2017).

In agreement with our results, CRISPR/Cas9-mediated knockout of ***c-REL*** in HeLa Kyoto cells, a model system for cervical cancers, resulted in a significantly decreased cell proliferation in comparison to wildtype (Slotta et al., 2017). However, surprisingly, the same study reported that ***c-REL*** knockout did not affect apoptosis, and further led to significantly increased resistance against the chemotherapeutic agents 5-Fluoro-2'-deoxyuridine (5-FUDR) and cisplatin (Slotta et al., 2017). This discrepancy might be due to the differences in cellular models and pathologies. Nevertheless, further investigations are warranted to shed light on the intricate consequences of c-Rel expression on survival and drug response.

Reproducibility of the results was confirmed by repeating the experiments, each performed independently, in order to obtain at least three biological replicates, allowing the determination of accurate p-values for individual sgRNAs as well as individual genes.

Our results suggest that the functional consequence of 2p amplification may not be ***REL*** activation and that therefore other genes mapped within 2p might be the target(s) of the amplification event. Indeed, most 2p gain+ CLL patients display large 2p gains, including important genes for oncogenesis, namely ***XPO1***, ***MYCN***, ***ALK*** and ***BCL11A***. We therefore postulated that there could be oncogenic cooperation between ***REL*** and other 2p genes. To verify this hypothesis, using the stable OSU-dCas9 cell line, we designed and constructed lentiviral sgRNA vectors and transduced OSU-CLL cells in order to activate the transcription of these 2p genes using the same CRISPRa approach as previously described. Successful transcriptional activation was attained in numerous transduced polyclonal cell lines.

Moreover, we then deleted 2p genes using the same CRISPR-Cas9 approach as previously described, then examined the phenotypic consequences of these genetic deletions. sgRNAs were designed and lentiviral CRISPR-Cas9 vectors were constructed. *In vitro* selection and validation of the most efficient guides for each 2p gene was performed. Successful decrease in gene expression was achieved in numerous transduced polyclonal cell lines.

Phenotypic consequences of CRISPRa- and CRISPR-Cas9-mediated modifications need to be carefully examined, in terms of apoptosis, proliferation, cell cycle, and NF-κB activation. Numerous readouts of NF-κB ought to be evaluated, by assessing changes in activation or gene expression downstream of c-Rel/NF-κB signaling, for instance in expression of antiapoptotic proteins as well as EZH2.

Conclusion

We have shown that transcriptional activation of ***REL*** by CRISPRa in OSU-CLL cells decreases spontaneous and drug-induced cell death, without affecting proliferation. Inactivation of ***REL*** by CRISPR/Cas9 in 2p gain JVM-3 cells decreases proliferation and enhances sensitivity to CLL drugs. Pharmacological inhibition of NF-κB specifically induces cell death in leukemic cells of CLL patients. Altogether, these findings indicate that ***REL*** could play a major role in CLL cell survival, but does not seem to be the sole player accounting for 2p gain-associated drug resistance. Since most 2p gain+ CLL patients display large 2p gains, including important genes for oncogenesis, namely ***XPO1***, ***MYCN***, ***ALK*** and ***BCL11A***, we developed several cellular models of gene knockout and transcriptional activation for each one of these genes in order to identify actors and potential oncogenic cooperation driving 2p gain resistance in 2p gain CLL.

Acknowledgements

We thank LY Sebaert for the gift of the JVM-3 cell line, Nadine Varin Blank and her team for HG-3 cell line. OSU-CLL cells were provided by The Ohio State University's Human Genetics Sample Bank. CRISPR base vectors were kindly provided by Camille Lobry and his team. This work was supported by Roche Diagnostics, the Association Laurette Fugain (ALF10/09, ALF14/08 and ALF 15/09), Ligue Contre le Cancer (RS15/75-63 and RS16/75-50) and Fondation ARC (Association pour la Recherche sur le Cancer) (SFI20111203530 and PJA20151203407).

III - The Gain of the Short Arm of Chromosome 2 (2p gain) Plays an Important Role in CLL Drug Resistance, and Has to be Systematically Considered before Deciding an Adapted Therapy

Fotini Kostopoulou, Nadia Bougacha, Clementine Gabillaud, Elise Chapiro, Simon Bouzy, Magali Le Garff-Tavernier, Karim Maloum, Choquet Sylvain, Veronique Leblond, Jean Gabarre, Anne Lavaud, Veronique Morel, Damien Roos-Weil, Madalina Uzunov, Romain Guieze, Olivier Tournilhac, Santos Susin, Olivier Bernard and Florence Nguyen-Khac

Abstract published in Blood 2017 130:1729; Article published in Cancer Med 2019: https://www.ncbi.nlm.nih.gov/pubmed/31066214

Chronic lymphocytic leukemia (CLL) is characterized by a variety of genomic aberrations including the chromosomal abnormalities del11q, del13q and del17p, tri12, as well as the 2p gain. The 2p gain is frequent in symptomatic CLL (16%), and is associated with poor prognostic factors (del11q, unmutated *IGHV*) and drug resistance. At least two minimal regions of gain 2p15-16 and 2p24 have been identified. The aim of the present study is to describe the relationship between 2p gain and other key CLL chromosomal abnormalities and to investigate the evolution of the 2p gain under therapeutic pressure.

We have collected data for 64 CLL patients (pts) with 2p gain detected by karyotype (K) and/or extensive fluorescence in situ hybridization (FISH). In all pts K and extensive FISH have been performed, including the 4 classical CLL probes and probes encompassing *MYCN* (2p24), *REL* (2p16) *XPO1* (2p15), and *BIRC3* (11q22) genes. The *IGHV* status was also determined. Longitudinal cytogenetic analyses were available for 22/64 patients.

Eighty three percent (53/64) of patients with 2p gain were male, with a median age at diagnosis of 60 years (range: 42-80). Out of 52 successful K, 21 (40.4%) were complex (C) (≥3 abnormalities) (9/52, 17.3%) or high C (≥5 abnormalities) (12/52, 27.1%). The 2p gain was clearly identified in 13/52 (25%) K, and was due to a duplication in the short arm of chromosome 2 in 5 cases, while in the remaining cases it was fused to chromosomes 4, 8, 13, 20, 22 and most frequently to chromosome 18 (5/15, 38.4%). In the majority of cases 2p gain was accompanied by other aberrations, including 56.2% del13q, 45.3% del11q, 21.8% del17p and 1.5% tri12. The *IGHV* status was unmutated in 51/56 (91%) patients.

Regarding the 22 patients with longitudinal samples, the median number of samples was 3 (range 2-5), and the median follow up (FU) was 8.6 years (range 4-26). Among them, 20 patients required treatment, with a median time from diagnosis to treatment of 26.3 months (1-72). Seven patients died, with a median OS of 9.3 years (range 4-26). Investigating the 2p gain in more detail, we found that the three oncogenes *XPO1*, *REL* and *MYCN* were gained in the same proportion of cells in the large majority (68.2%) of cases. However, in 7/22 (31.8%) CLL, we observed a divergence in the gain of 2p15-16 (*XPO1/REL*) and 2p24 (*MYCN*) regions. In 6/7

cases, the 2p15-16 region was gained in more tumor cells than 2p24, including 3 CLL without any detectable gain of *MYCN*; conversely in one patient, 2p24 was gained in a higher percentage of cells than 2p15-16. Regarding the 11q deletion, *ATM* and *BIRC3* were both deleted in 10/12 (83%) cases. Only 2 cases had a deletion involving *ATM* only; no case of simple *BIRC3* deletion was observed.

During the evolution, the 2 untreated patients had a stable % of 2p gain, with a FU of 6 and 24 months. A median of 3 lines of therapies was used in the 20 patients requiring treatment. Thus, in our study, we have compared cytogenetic data for each line before treatment and at relapse (Tab 1). Among the 20 patients: i. Seven were treated with fludarabine/cyclophosphamide/rituximab in front line. Time to relapse was within 3 years in 5 patients, and the 2p gain remained stable (3/7) or increased (4/7) (Fig 1A); ii. Nine pts were treated with bendamustine/ofatumumab/methylprednisolone (BOMP), after 1 to 3 lines of previous therapies; the 9 cases relapsed (including 1 death) within 3 years. At relapse, the 2p gain decreased (4/9) or disappeared (1/9) (Fig 1B), remained stable in 3 cases, and increased in one patient. Of note, 4/9 patients had a del17p, which remained stable or increased; and iii. Three patients were treated with ibrutinib: the 2p gain decreased in one patient after 11 months, and remained stable in two patients, despite a normal lymphocyte count at 13 and 17 months. Finally, only one patient received R/idelalisib after 2 previous lines, and died at 25 months, with a stable 2p gain.

Conclusion: In the era of precision medicine, our results suggest that in addition of the other classical prognostic factors, 2p gain has to be specifically evaluated in CLL before deciding the treatment strategy. As 2p gain could be overlooked by conventional karyotype, we suggest searching systematically this abnormality by FISH with at least two sets of probes (*XPO1/REL* and *MYCN*). The majority of the drugs seem not to be effective on the elimination of the 2p gain clone, but the BOMP regimen could be an option. No data are available regarding BCL-2 inhibitors in this setting.

n=22	del17p	Disease statut at sampling	2pgain decrease	2pgain stable	2pgain increase
Untreated patients (n=2)	0	Stable (6m, 24 m)	0	2	0
FCR (Front line) (n=7)	0	Relapse≤36m (n=5), 48m, 60m	0	3	4
BOMP (R/R after 1-3 lines) (n=9)	4	Relapse≤36m (n=9)	5*	3	1
ibrutinib (R/R after 1 line) (n=3)	2	Normal lymphocytosis (10m, 13m, 17m)	1	2	0
idelasisib-rituximab (R/R after 2 lines) (n=1)	1	Relapse ≤36m	0	1	0

Table 1. Follow up of twenty-two CLL with 2pgain. R/R: relapse refractory; m=months;
*: 1 disappeared

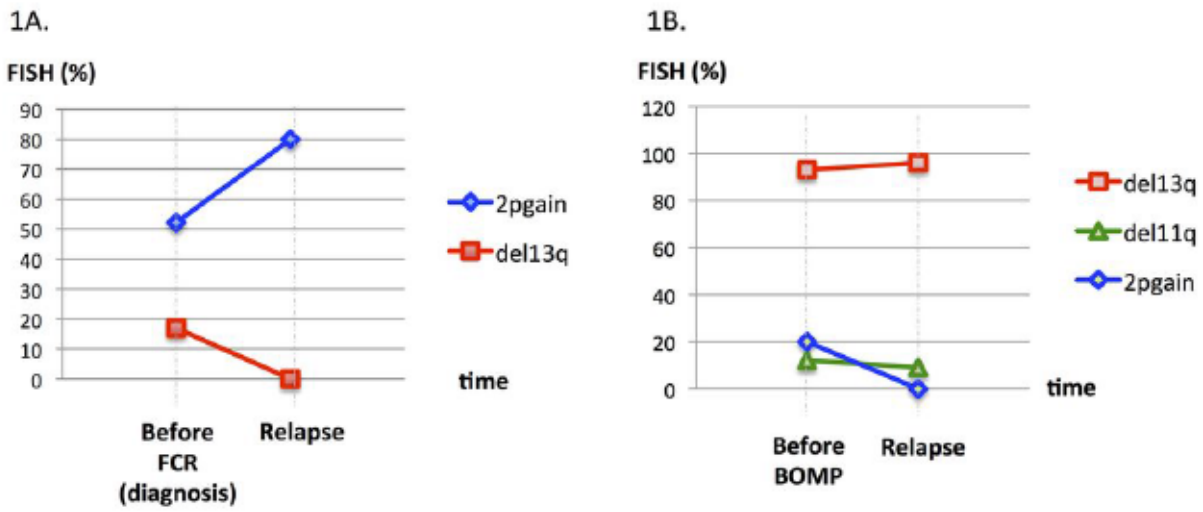

Figure 1. A: CLL(L) patient: FISH: % of cells with 2pgain and del13q at diagnosis and at relapse after FCR (32 months). 2pgain increased, whereas del13q disappeared. **B: CLL(LJ) patient: FISH: % of cells with 2pgain, del11q and del13q before treatment (BOMP) and at relapse (17 months):** 2pgain disappeared, whereas del13q and del11q remained stable.

IV - "Double-hit" chronic lymphocytic leukemia: An aggressive subgroup with 17p deletion and 8q24 gain

Received: 14 November 2017 | Revised: 21 November 2017 | Accepted: 27 November 2017

DOI: 10.1002/ajh.24990

RESEARCH ARTICLE

WILEY AJH

"Double-hit" chronic lymphocytic leukemia: An aggressive subgroup with 17p deletion and 8q24 gain

Elise Chapiro[1,2,3] | Claude Lesty[2,3] | Clémentine Gabillaud[3] | Eric Durot[4] | Simon Bouzy[3] | Marine Armand[1,2,3] | Magali Le Garff-Tavernier[1,3] | Nadia Bougacha[1,2] | Stéphanie Struski[5] | Audrey Bidet[6] | Elodie Laharanne[6] | Carole Barin[7] | Lauren Veronese[8] | Nolwen Prié[8] | Virginie Eclache[9] | Baptiste Gaillard[10] | Lucienne Michaux[11] | Christine Lefebvre[12] | Jean-Baptiste Gaillard[13] | Christine Terré[14] | Dominique Penther[15] | Christian Bastard[15] | Nathalie Nadal[16] | Sandra Fert-Ferrer[17] | Nathalie Auger[18] | Catherine Godon[19] | Laurent Sutton[20] | Olivier Tournilhac[21] | Santos A. Susin[1,2] | Florence Nguyen-Khac[1,2,3] | On behalf of the GroupeFrancophone de Cytogénétique Hématologique(GFCH) and the French Innovative Leukemia Organization (FILO) group

[1]INSERM UMR_S 1138, Centre de Recherche des Cordeliers, Paris, France; [2]Sorbonne Universités, UPMC Paris 6, Paris, France; [3]Service d'Hématologie Biologique, Hôpital Pitié-Salpêtrière, AP-HP, Paris, France; [4]Service d'Hématologie Clinique, CHU Reims, Reims, France; [5]Laboratoire de Cytogénétique, Institut Universitaire du Cancer de Toulouse, Toulouse, France; [6]CHU Bordeaux, Service d'Hématologie biologique, F-33000, Bordeaux, France; [7]Unité de Génétique, CHU Bretonneau, Tours, France; [8]Laboratoire de Cytogénétique, CHU Estaing, Clermont-Ferrand, France; [9]Laboratoire d'Hématologie, Hôpital Avicenne, AP-HP, Bobigny, France; [10]Laboratoire d'Hématologie, Hôpital Robert Debré, Reims, France; [11]Center for Human genetics, Leuven, Belgium; [12]Laboratoire de Cytogénétique Onco-hématologique, CHU Grenoble, Grenoble, France; [13]Laboratoire de Cytogénétique, CHU Caremeau, Nimes, France; [14]Centre Hospitalier de Versailles, Laboratoire de Cytogénétique, Versailles, France; [15]Laboratoire de Génétique Oncologique, centre de lutte contre le cancer Henri Becquerel, Rouen, France; [16]Service de génétique chromosomique et moléculaire, CHU Dijon, Dijon, France; [17]Centre Hospitalier Métropole Savoie, Laboratoire de Génétique Chromosomique, France, Chambéry; [18]Laboratoire de Cytogénétique, Institut Gustave Roussy, Villejuif, France; [19]Laboratoire de Cytogénétique Hématologique, CHU Nantes, Nantes, France; [20]Centre Hospitalier Métropole Savoie, Service d'Hématologie Clinique, Chambéry, France; [21]Service d'Hématologie Clinique, CHU Estaing, Clermont-Ferrand, France

Correspondence
Florence Nguyen-Khac, Service d'Hématologie Biologique, Bâtiment Pharmacie, 5e étage, University Hospital Pitié-Salpêtrière/Charles Foix, 83 Bd de l'Hôpital, F-75013 Paris, France.
Email: florence.nguyen-khac@psl.aphp.fr

Funding information
Fondation ARC pour la Recherche sur le Cancer, SFI20111203530

Abstract

Chronic lymphocytic leukemia (CLL) with 17p deletion (17p-) is associated with a lack of response to standard treatment and thus the worst possible clinical outcome. Various chromosomal abnormalities (including unbalanced translocations, deletions, ring chromosomes and isochromosomes) result in the loss of 17p and one copy of the *TP53* gene. The objective of the present study was to determine whether the type of chromosomal abnormality leading to 17p- and the additional aberrations influenced the prognosis in a series of 195 patients with 17p-CLL. Loss of 17p resulted primarily from an unbalanced translocation (70%) with several chromosome partners (the most frequent being chromosome 18q), followed by deletion 17p (23%), monosomy 17 (8%), isochromosome 17q [i(17q)] (5%) and a ring chromosome 17 (2%). In a univariate analysis, monosomy 17, a highly complex karyotype (≥5 abnormalities), and 8q24 gain were associated with poor treatment-free survival, and i(17q) ($P = .04$), unbalanced translocations ($P = .03$) and 8q24 gain ($P = .001$) were significantly associated with poor overall survival. In a multivariate analysis, 8q24 gain remained a significant predictor of poor overall survival. We conclude that 17p deletion and

8q24 gain have a synergistic impact on outcome, and so patients with this "double-hit" CLL have a particularly poor prognosis. Systematic, targeting screening for 8q24 gain should therefore be considered in cases of 17p- CLL.

1 | INTRODUCTION

Chronic lymphocytic leukemia (CLL), the most common leukemia in adults, has a highly variable course, reflecting its biological heterogeneity. Many patients do not require treatment for years, whereas others exhibit aggressive disease, do not respond to treatment, and thus have a poor prognosis. Chromosomal abnormalities (including deletions of 11q, 13q or 17p (17p-), and trisomy 12) are present in about 80% of cases of CLL. Fluorescence *in situ* hybridization (FISH) is used to routinely screen for these chromosomal abnormalities.[1] Patients with 17p- CLL have the worst clinical outcomes, and the shortest progression-free and overall survival (OS) times.[2] The 17p deletion is found in 10% or less of patients with CLL but in up to 40% of relapsed or treatment-refractory patients. Loss of the short arm of the chromosome 17 results from various chromosomal abnormalities, including unbalanced translocations, deletions, ring chromosomes and isochromosomes.[3] All these aberrations lead to the loss of one copy of the *TP53* gene, and the remaining allele is mutated in most instances. Furthermore, 17p- is often associated with genomic complexity as detected with conventional karyotyping or genomic microarrays.[4,5]

The dismal prognosis for patients with 17p- CLL is mainly due to a lack of response to conventional treatments. In keeping with the role of *TP53* as a pivotal regulator of the DNA response pathway, loss of this gene is associated with resistance to DNA-damaging agents (e.g., fludarabine and cyclophosphamide). Recently, new drugs targeting the B-cell receptor signaling pathway or the apoptosis machinery have shown efficacy in 17p- CLL, with a better treatment response and longer progression-free survival.[6–8] Despite good initial responses to these new targeted therapies, relapse can still occur - particularly in patients bearing a complex karyotype (K).[9] In contrast, some patients with *de novo* 17p- CLL have stable disease and remain asymptomatic for prolonged periods of time.[10,11] All these observations underline the clinical heterogeneity of 17p- CLL. It has been shown that a number of clinical and biological markers (such as *IGHV* mutational status, the size of the 17p- clone, and genomic complexity) are significantly linked to the clinical outcome in the subgroup of patients with 17p- CLL.[12,13]

The objectives of the present study of a series of 195 patients with 17p- CLL were to determine whether (i) the type of chromosomal abnormality leading to 17p loss (i.e., translocations, deletions, rings and isochromosomes, as identified by K analysis) was associated with the prognosis, and (ii) additional aberrations had an impact on the clinical outcome.

2 | METHODS

2.1 | Patient selection

Databases from 20 French and Belgian institutions were retrospectively screened for cases with a morphological and immunological diagnosis of CLL according to the iwCLL criteria,[14] in which informative K analysis showed a loss of 17p and FISH confirmed the loss of the *TP53* gene. A total of 195 patients were identified. The patients' clinical and biological characteristics were extracted retrospectively from medical records. The study was performed in accordance with the Declaration of Helsinki, and was approved by the local investigational review board (CPP-Ile-de-France VI, Paris, France; date: 09/15/2011).

2.2 | Karyotype and FISH analyses

All the K results were reviewed by the members of the Groupe *Francophone de Cytogénétique Hématologique* and then classified according to the International System for Human Cytogenetic Nomenclature (ISCN 2016). Complex Ks were defined as the presence of three or more numerical or structural chromosomal abnormalities (CK $\geq$ 3), and highly complex Ks were defined as the presence of five or more abnormalities (CK $\geq$ 5). Monosomal Ks were defined as the presence of 2 autosomal monosomies or 1 monosomy with at least 1 structural abnormality. Data from routine FISH analyses were available for some of patients: 11q22 (*ATM*) (n = 158), 13q14 (n = 118), centromere of chromosome 12 (n = 102), and 8q24 (*MYC*) (n = 12).

2.3 | TP53 mutations and functional assays

TP53 mutations were analyzed by (i) Sanger sequencing of exons 2 to 11 (n = 17), exons 4 to 10 (n = 29) or exons 4 to 9 (n = 12), or (ii) next-generation sequencing (NGS) on a MiSeq® platform (Illumina, San Diego, CA) using the CLL MASTR PLUS kit (Multiplicom, Niel, Belgium) (n = 9) or on a Ion Torrent platform (Life Technologies, Carlsbad, CA) using the Ion AmpliSeq™ TP53 Panel (Life Technologies) (n = 8). A negative result with Sanger sequencing was not considered to be informative because this technique does not cover all the exons and is not sensitive (10%). A functional assay of p53 was carried out as described previously.[15]

2.4 | Statistical analysis

Treatment-free survival (TFS) and OS were defined as the time interval between diagnosis and first-line treatment or death, respectively, or (in the absence of these events) last follow-up.

Categorical variables were compared using the chi-squared test or Fisher's exact test, while continuous variables were compared using the Mann-Whitney test. Survival analyses were performed using the Kaplan-Meier method. The log-rank test was used for intergroup comparisons of OS or TFS curves. The variables analyzed were age (<65 vs. ≥65), Binet stage (A vs. B/C), *IGHV* mutation status, the percentage of cells bearing the *TP53* deletion (≤20% vs. >20%, ≤35% vs. >35%, ≤80% vs. >80%), occurrence of 17p- after treatment, the number of 17p abnormalities (1 vs ≥2), a 17p abnormality alone (according

to the K), an unbalanced translocation involving 17p (U-translocation-17p), a deletion 17p, a monosomy 17, an isochromosome 17q [i(17q)], a der/dic(17;18)(q10;q10), a CK with ≥3 or ≥5 abnormalities, a monosomal K, U-translocations (all: 17p and not 17p), the presence of additional U-translocations (U-translocation-not 17p), 8q24 gain, 8p deletion, trisomy 12, and 11q deletion. Multivariate analysis (with Cox proportional hazards regression models) was subsequently performed to assess the independent prognostic value of covariates that were significant in the univariate analysis. There were too few data on *IGHV* mutations for inclusion in the multivariate analysis. The quality of the multivariate models for TFS and OS was confirmed in a log-likelihood-ratio test ($P < .0001$). The prognostic significance of each variable was assessed with the Wald test.

To compare survival in patients in whom 17p- occurred before vs. after treatment, the time interval between the first documentation of 17p- and death or last follow-up was also evaluated.

All tests were two-sided, and the threshold for statistical significance was set to $p \leq 0.05$. All statistical analyses were performed using MedCalc software (version 17.8.6, MedCalc Software bvba, Ostend, Belgium; http://www.medcalc.org; 2017).

3 | RESULTS

3.1 | Characteristics of the study population

The characteristics of the 195 included patients (median [range] age at diagnosis: 63 [33–88] years; males: 66%) are summarized in Table 1. The Binet stage at diagnosis was A in 100 patients (59%), B in 48 (29%), and C in 21 (12%). Data on *IGHV* mutational status was available for 47 patients, of whom 38 (81%) did not bear mutations. The median [range] follow-up time from diagnosis was 70 months [0–401]. Most of the patients with informative data had been treated (158 out of 182, 87%), and the median number of lines of treatments was 2.5 [0–10]. In 71 patients, the time of occurrence of the 17p- could not be determined because (i) cytogenetic analyses were not performed before treatment ($n = 58$), or (ii) data on treatment were missing ($n = 13$). When considering the remaining 124 patients, 28 (23%) did not present with 17p- at diagnosis; hence, the deletion had occurred after treatment (a median of 77.5 months [22–291] after diagnosis). In 96 of the 124 patients (77%, including 24 patients not having been treated at last follow-up), the 17p- was present before treatment; the median time interval between diagnosis and first detection of 17p- was 1 month [0–291]. The *TP53* gene was mutated in 55 of the 60 (92%) patients with informative data. The protein p53 was dysfunctional in all 42 cases tested, including 2 patients in whom a *TP53* mutation was not detected by NGS.

3.2 | Karyotyping and FISH data

Karyotyping and FISH results are summarized in Table 2. According to K, the median [range] number of chromosomal abnormalities (including 17p-) was 4 [1-26]; a CK ≥ 3 was found in 141 of the 195 (72%) patients, including 89 (46%) with a highly CK ≥ 5. The K was monosomal in 52 of the 195 patients (27%). A large majority of patients (181 out of 195, 93%) displayed one or more U-translocation (s); some involved 17p, and others did not. The presence of U-translocations was strongly associated with CK ≥ 3 (78% vs. 0% in patients with and without U-translocations, respectively; $P < .0001$) and CK ≥ 5 (49% vs. 0%, respectively; $P = .0001$). A total of 240 17p abnormalities were found in the 195 patients: 162 (83%) of these patients had one 17p abnormality, 25 (13%) had two independent 17p abnormalities, and 8 (4%) had three or more 17p abnormalities. The 17p- was the sole abnormality detected by K in 28 of the 195 (14%) cases. When other abnormalities were also present, the 17p- was in the primary clone in 43 of the 195 (26%) patients, in a sub-clone in 42 (25%), in the same clone as the other aberrations in 64 (38%), or in an independent clone in 18 (11%). In the majority of cases, loss of 17p resulted from a U-translocation involving 17p (-17p) and various chromosome partners (Supporting Information Figure S1). A total of 167 U-translocations(-17p) were found in 158 of the 195 patients (81%). The partner was not identified in 35 cases [add(17p)]. Of the 132 translocations with an identified partner, 68 were arm-to-arm translocations; 32 of the latter involving the long arm of the chromosome 18. In 7 of these 32 cases, the dicentric nature of the derivative chromosome dic (17;18)(p11;p11) was proven by FISH with centromere probes. According to the ISCN nomenclature, the other cases were der(17;18)(q10;

TABLE 1 Characteristics of the study population ($n = 195$)

Characteristics	Study Population
Sex (M/F)	128/67 (66% 34%)
Age at diagnosis, median [range] ($n = 185^a$)	63 y [33–88]
Binet stage at diagnosis ($n = 169^a$)	
A	100 (59%)
B	48 (29%)
C	21 (12%)
IGHV unmutated ($n = 47^a$)	38 (81%)
TP53 mutated ($n = 60^a$)	55 (92%)
Treated patients ($n = 182^a$)	158 (87%)
TP53 deletion acquired after treatment ($n = 124^a$)	28 (23%)
Number of treatment lines, median [range] ($n = 179^a$)	2,5 [0–10]
Treatment-free survival, median (95% CI) ($n = 93^{a,b}$)	18 mo (11–29)
Deaths ($n = 179^a$)	63 (35%)
Overall survival, median (95% CI) ($n = 183^a$)	179 mo (135–242)
Follow-up from diagnosis, median [range] ($n = 183^a$)	70 mo [0–401]

[a]Available data; y: years; mo: months.
[b]Analyzed on the 96 patients with 17p deletion before treatment.
IGHV unmutated: homology ≥ 98%.

TABLE 2 Karyotyping and FISH data ($n = 195$)

Parameter	Median [range]	n (%)
Number of abnormalities, 17p included	4 [1–26]	
Complex karyotype (≥3 abnormalities)		141 (72%)
Highly complex karyotype (≥5 abnormalities)		89 (46%)
Monosomal karyotype		52 (27%)
Unbalanced translocations (all: involving 17p or not)		181 (93%)
Number of 17p abnormalities		
1		162 (83%)
2		25 (13%)
3 or more		8 (4%)
17p- alone by karyotype		28 (14%)
Clonal hierarchy for 17p abnormalities when not alone, $n = 167$		
Primary		43 (26%)
Secondary		42 (25%)
Same clone		64 (38%)
Independant clone		18 (11%)
Types of 17p abnormalities[a]		
Unbalanced translocation		158 (81%)
Unbalanced translocation with identified partner		*123 (63%)*
arm-to-arm translocation		*62 (32%)*
der/dic(17;18)		*32 (16%)*
Other unbalanced translocation		*61 (31%)*
Unbalanced translocation, add(17)(p)		*35 (18%)*
17p deletion		45 (23%)
Monosomy 17		15 (8%)
Isochromosome 17q		9 (5%)
Ring 17		4 (2%)
% of cells with TP53 deletion (FISH)	70 [3–100]	
Additional abnormalities		
Unbalanced translocations (not 17p)		121 (63%)
8p deletion, $n = 189$[b]		40 (21%)
8q24 gain, $n = 112$[c]		14 (12.5%)
Trisomy 12, $n = 195$		30 (15%)
13q14 deletion, $n = 118$[d]		71 (60%)
11q deletion (*ATM* gene), $n = 161$[d]		20 (12%)

[a]The number of patients with the corresponding abnormality is given. The frequencies are related to the total cohort ($n = 195$). The total is higher than 100% because 33 patients have more than one 17p abnormality.
[b]The presence of a 8p deletion could not be determined in 6 patients with a complex karyotype including a monosomy 8 and addition(s) of chromosomal material of undermined origin.
[c]The presence of a 8q24 gain could not be determined in 83 patients having a complex karyotype with addition(s) of chromosomal material of undermined origin, without FISH analysis with MYC probe.
[d]Detected by FISH.

q10). Overall, der/dic(17;18) was the most frequent U-translocation (-17p) because it was present in 32 of the 195 patients (16%). The other frequent arm-to-arm translocations involved chromosomes 8q ($n = 11$, resulting in 8p deletion), 14q ($n = 6$), 4q ($n = 4$), 13q ($n = 4$), and 21q ($n = 4$). The remaining 64 U-translocations(-17p) (not arm-to-arm) involved a wider variety of partners - most frequently chromosome 8 ($n = 15$); this led to del8p ($n = 6$), gain8q ($n = 6$), or del8q ($n = 3$) (Supporting Information Figure S1B). The other 17p abnormalities were 17p deletion ($n = 45$ out of 195, 23%), monosomy 17 ($n = 15$, 8%), i(17q) ($n = 9$, 5%) and ring chromosome 17 ($n = 4$, 2%) (Table 2 and Supporting Information Figure S1A). Lastly, FISH showed that the percentage of cells with a *TP53* deletion ranged from 3% to 100% (median: 70%).

When considering the additional abnormalities associated with 17p-, U-translocations(-not 17p) were found in 121 of the 195 patients (63%). The presence of U-translocations(-not 17p) was associated with CK ≥ 3 (95% vs. 35% in patients with and without U-translocations (-not 17p), respectively; $P < .0001$) and CK ≥ 5 (68% vs. 9%, respectively; $P < .0001$). After combination of the K and available FISH findings, 13q14 deletion was detected in 71 of the 118 documented cases (60%), 8p deletion in 40 out of 189 cases (21%), trisomy 12 in 30 out of 195 cases (15%), 8q24 gain in 14 out of 112 cases (12.5%), and 11q deletion (*ATM* gene) in 20 out of 161 cases (12%).

3.3 | Treatment-free and overall survival

Treatment-free survival was studied for the 96 patients in whom 17p was present before treatment. The median TFS time was 18 months. In a univariate analysis, the parameters associated with significantly shorter TFS were Binet stage B/C (hazard ratio (HR)=6.24, $P < .0001$), monosomy 17 (HR = 2.07, $P = .04$), a high CK (HR = 1.81, $P = .009$) and 8q24 gain (HR = 6.46, $P < .0001$). In a multivariate analysis, stage B/C and 8q24 gain remained significantly associated with shorter TFS (Table 3).

For the study population as a whole, the median OS time from diagnosis was 179 months. In a univariate analysis, we found that age ≥65, Binet stage B/C, and unmutated *IGHV* status were associated with a significantly shorter median OS time (Table 3, Supporting Information Figure S2). There were no significant statistical differences in the impact on OS between the different abnormalities leading to loss of 17p, i.e., U-translocations(-17p), der/dic(17;18), monosomy 17 or deletion 17p. Likewise, the number of 17p- abnormalities and the percentage of cells harboring the del*TP53* (whether dichotomized or not) were not significant factors. The presence of an i(17q) was correlated with trisomy 12 (44% vs. 14% in patients with or without i(17q), respectively; $P = .03$), a higher percentage of tumor cells with del*TP53* (a median of 88% vs. 60% in patients with or without i(17q), respectively; $P = .003$), and a shorter OS (69 vs. 179 months in patients with or without i(17q), respectively; $P = .04$) (Figure 1). Analysis of the impact of the other cytogenetic aberrations revealed that the presence of U-translocations(-not 17p) was associated with a shorter OS time (153 vs. 223 months in patients with or without U-translocations(-not 17p), respectively; $P = .03$). When taking account of all the U-

TABLE 3 Univariate and multivariate analyses of variables with a significant impact on TFS and OS

Variable		n	Univariate HR (95%CI)	P-value	Multivariate HR (95%CI)	P-value
TFS						
Binet stage B/C at diagnosis	Yes/no	31/60	6.24 (2.89.13.47)	<.0001	119.75 (14.53–986.65)	<.0001
Monosomy 17	Yes/no	8/85	2.07 (0.76-5.61)	.04	2.83 (0.63-12.71)	.17
Highly CK ≥5 abnormalities	Yes/no	41/52	1.81 (1.10-2.97)	.009	1.62 (0.77-3.38)	.19
8q24 gain (involving *MYC*)	Yes/no	4/49	6.46 (0.59–71.23)	<.0001	5.76 (1.18 – 28.05)	.03
OS						
Age at diagnosis	≥65y/<65y	80/97	1.85 (1.06-3.21)	.01	2.65 (1.12-6.27)	.03
Binet stage B/C at diagnosis	Yes/no	68/96	3.10 (1.78-6.40)	<.001	10.01 (3.60-27.78)	<.0001
IGHV unmutated	Yes/no	32/8	2.89(1.04–8.07)	.04	-	
Isochromosome 17q	Yes/no	8/169	2.77 (0.55-14.01)	.04	4.07 (0.59-27.97)	.15
Unbalanced translocations (all: including 17p or not)	Yes/no	165/12	5.96 (2.49-14.29)	.04	4.80 (0.61-37.50)	.13
Unbalanced translocations (not 17p)	Yes/no	109/68	1.79 (1.09-2.96)	.03	0.84 (0.39-1.80)	.66
8q24 gain (involving *MYC*)	Yes/no	13/89	3.48 (0.93-13.07)	.001	3.73 (1.32-10.54)	.01

HR: hazard ratio, CI: confidence interval. There were too few data on *IGHV* mutational status for inclusion in the multivariate analysis.

translocations (i.e., 17p and not 17p), a shorter OS was also observed in the group with U-translocations (171 months vs. median not reached, $P = .04$). Lastly, the presence of an 8q24 gain strongly impacted the OS (HR = 3.48, $P = .001$) (Figure 1). In a multivariate analysis, age ≥ 65 (HR = 2.65, $P = .03$), Binet stage B/C (HR = 10.01, $P < .0001$) and 8q24 gain (HR = 3.73, $P = .01$) were independently and significantly associated with poor OS (Table 3).

When comparing the survival time after the first documentation of 17p-, the patients who acquired this abnormality after treatment had a shorter OS time than those presenting with 17p- prior to treatment (HR = 2.02, $P = .03$) (Supporting Information Figure S3).

4 | DISCUSSION

To the best of our knowledge, the present study of 195 CLL patients with 17p- is the largest cohort in which the clinical significance of chromosome 17p abnormalities has been assessed in detail. In line with the literature data, we found that loss of the short arm of chromosome 17 is mainly due to unbalanced translocations (in 70% of cases), rather than 17p deletion, an isochromosome 17q or monosomy 17.[3,16] Most of the U-translocations(-17p) (52%) were arm-to-arm events. In the remaining U-translocations(-17p), the breakpoints were mainly located in 17p11 or p12. In general (and regardless of the type of 17p abnormality), all or almost all of the 17p arm was lost. This supports the recent hypothesis whereby the effects of 17p deletion on tumor progression and treatment resistance might involve several genes and might not be solely due to *TP53* loss.[17]

The most frequent U-translocation(-17p) was dic/der(17;18), since it accounted for 16% of the study population. Woyach et al. suggested that dic(17;18) may correspond to the most aggressive subset of 17p-CLL cases.[18] We could not confirm this hypothesis; when compared with the other chromosomal abnormalities involving 17p in our large series, dic(17;18) did not have a significant impact on outcome.

In a univariate analysis, we found that monosomy 17 was significantly associated with a shorter TFS (relative to the other 17p abnormalities), and that isochromosome 17q was significantly associated with a shorter OS. Isochromosome 17q has been described as a frequent aberration (up to 33%) in small series of CLL cases with a *TP53* deletion.[3,19] A much lower incidence (4%) was observed in the present study. Moreover, i(17q) was significantly associated with trisomy 12 (44%, $P = .03$) and a larger clone 17p- size. In a recent study, CLL patients with i(17q) tended to have poorer OS than patients with other abnormalities affecting 17p13 – even though all the tested individuals were *IGHV* mutated.[20] In the present series, the *IGHV* genes were sequenced in only 2 of the 9 patients with i(17q); neither carried *IGHV* mutations. This finding shows that mutated *IGHV* status is not a constant feature in cases of i(17q). The present results corroborated the association between i(17q) status and a poor outcome because this defect was significantly correlated with shorter OS ($P = .04$). However, further studies are needed to establish whether i(17q) is an independent prognostic marker in 17p- CLL.

In accordance with previous reports,[12,21,22] we observed a shorter OS (calculated following the first documentation of 17p-) in patients having acquired the 17p- after treatment than in those with 17p- present before treatment. This finding might simply reflect the fact that patients with acquired 17p- have a more advanced disease but may also suggest that treatment selected a more aggressive clone with a growth advantage.

In contrast to other series, we did not observe a significant association between the percentage of cells with *TP53* deletion and the

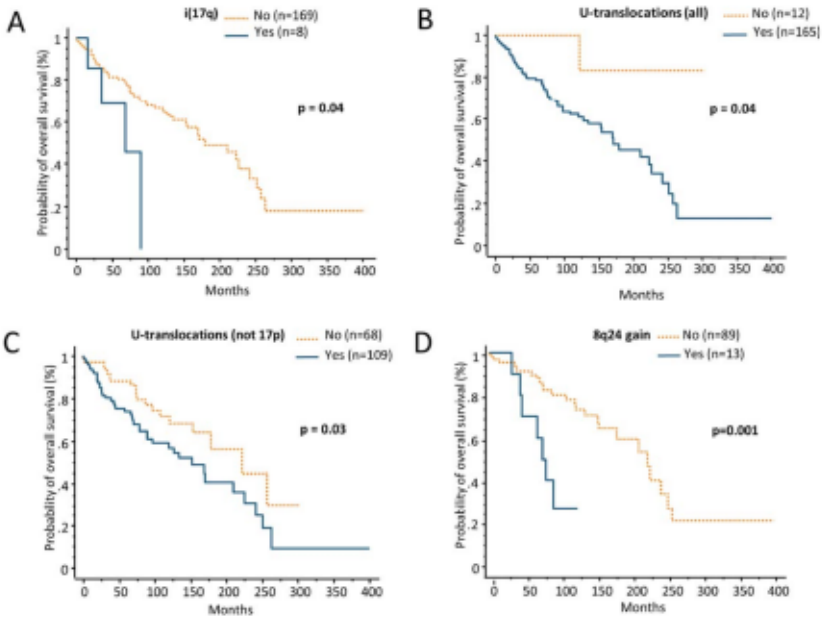

FIGURE 1 Overall survival in the whole study population, according to the presence or absence of isochromosome 17q [i(17q)] (A), unbalanced translocations (U-translocations) (all, including 17p) (B), additional U-translocations to 17p- (C), and 8q24 gain (D) [Color figure can be viewed at wileyonlinelibrary.com]

clinical outcomes. In the literature, it has been reported that a low percentage of 17p- cells is associated with a more favorable outcome. However, the optimal cut-off varied markedly from one study to another (from 10% to 80%)[10,12,23,24] - indicating that this parameter is cohort-dependent and should not be taken into account when evaluating the prognosis of patients with CLL. Furthermore, several reports have documented the impact of small clones with disrupted *TP53* genes on disease progression.[25,26]

Although only a small proportion of 17p- patients were analyzed, we found that all the tested individuals had a dysfunctional p53 protein (including 2 cases without a *TP53* mutation). These results highlight the importance of continuing to screen for 17p loss on a routine basis. FISH is still the best technique for detecting *TP53* deletion; its sensitivity threshold of about 5% is much lower than those obtained with innovative tools such as single nucleotide polymorphism arrays, multiplex ligation-dependent probe amplification and massively parallel sequencing.

We also looked at whether additional chromosomal abnormalities could influence the outcome. We confirm that a complex K is very frequent in 17p- CLL, since it was detected in 72% of our patients.[12,24,27] Karyotype complexity is a recently discovered factor for a poor prognosis in CLL in general[4,28,29] and in the 17p- subset.[24,30] In the literature, the cut-off used to define a complex K varies from 3 to 5 abnormalities.[4,31] In our series, a highly CK (≥5 abnormalities) was associated with worse TFS, whereas a CK (≥3 abnormalities) had no clinical impact. This finding suggests that a cut-off of 5 abnormalities is more suitable for identifying 17p- CLL patients with the most aggressive disease. Previous studies of unselected CLL patients have described the poor prognosis of unbalanced translocations.[4,27,30,32,33] Our present results showed that U-translocations are also associated with shorter OS in the 17p- CLL subset. Regarding the classical abnormalities detected by FISH in CLL (such as tri12, del13q and del11q), we were surprised to find the same frequency of these aberrations in the 17p- subset as in the whole population of patients with CLL.[1] This suggests that 17p- appears independently, and that none of the other abnormalities promotes its occurrence. However, i(17q) - correlated with trisomy 12 - appears to be an exception.

The 8q24 gain (encompassing the *MYC* gene) is detected with microarrays in 3–4% of the overall population of patients with CLL, and is independently associated with shorter OS and/or shorter time to first treatment.[34–36] In the literature, the frequency of 8q24 gain is higher in the 17p- CLL subset and ranges from 9% to 44%.[13,24,35–37] In the present large series, we found an 8q24 gain in 12.5% of patients. Furthermore, we demonstrated that 8q24 gain is a strong, predictive marker of poor outcome within the 17p- CLL subgroup, and has independent prognostic value for OS. This observation suggests that *TP53* deletion and *MYC* gain act in synergy; the outcome is particularly dismal when both are present. Indeed, the occurrence of both alterations may represent a "double-hit" CLL that is reminiscent of the aggressive,

"double-hit," high-grade B-cell lymphomas harboring rearrangements of *MYC* and *BCL2* or *BCL6*.[38] It is noteworthy that we did not observe any translocation involving *MYC* in the present series. Given the high frequency of genomic complexity in these patients, 8q24 gain can be missed by karyotyping. In order to validate the clinical significance of this aberration, 17p- CLL patients enrolled in prospective clinical trials should be systematically screened by FISH analysis using a *MYC* probe.

In conclusion, our data show that patients with 17p- CLL often present CK (≥3 abnormalities) and highly CK (≥5 abnormalities), unbalanced translocations, 8q24 gain, and unmutated *IGHV*. The various abnormalities leading to loss of 17p do not have all the same clinical significance: i(17q) is associated with a shorter OS than the other 17p aberrations. Furthermore, the presence of additional unbalanced translocations aggravates the outcome. Our results highlight the value of conventional karyotyping for identifying alterations that modulate the prognosis in this aggressive subset of patients. Lastly, 8q24 gain is a strong, independent factor for poor survival; systematic, targeted screening for this abnormality should be considered with a view to better defining the prognosis of patients with 17p- CLL and identifying the very high-risk "double-hit" subgroup.

ACKNOWLEDGMENTS

We thank Philippe Solal-Céligny and Stéphane Leprêtre for their helpful comments. This work was supported by Roche Diagnostics, Association Laurette Fugain (ALF14/08), Fondation ARC (SFI20111203530), and GEFLUC.

ORCID

Elise Chapiro http://orcid.org/0000-0003-3427-7596
Eric Durot http://orcid.org/0000-0003-3463-0089
Florence Nguyen-Khac http://orcid.org/0000-0003-3107-6668

REFERENCES

[1] Dohner H, Stilgenbauer S, Benner A, et al. Genomic aberrations and survival in chronic lymphocytic leukemia. *N Engl J Med*. 2000;343(26):1910–1916.

[2] Hallek M, Fischer K, Fingerle-Rowson G, et al. Addition of rituximab to fludarabine and cyclophosphamide in patients with chronic lymphocytic leukaemia: a randomised, open-label, phase 3 trial. *Lancet*. 2010;376(9747):1164–1174.

[3] Fink SR, Smoley SA, Stockero KJ, et al. Loss of TP53 is due to rearrangements involving chromosome region 17p10 approximately p12 in chronic lymphocytic leukemia. *Cancer Genet Cytogenet*. 2006;167(2):177–181.

[4] Baliakas P, Iskas M, Gardiner A, et al. Chromosomal translocations and karyotype complexity in chronic lymphocytic leukemia: a systematic reappraisal of classic cytogenetic data. *Am J Hematol*. 2014;89(3):249–255.

[5] Ouillette P, Collins R, Shakhan S, et al. Acquired genomic copy number aberrations and survival in chronic lymphocytic leukemia. *Blood*. 2011;118(11):3051–3061.

[6] Furman RR, Sharman JP, Coutre SE, et al. Idelalisib and rituximab in relapsed chronic lymphocytic leukemia. *N Engl J Med*. 2014;370(11):997–1007.

[7] Farooqui MZ, Valdez J, Martyr S, et al. Ibrutinib for previously untreated and relapsed or refractory chronic lymphocytic leukaemia with TP53 aberrations: a phase 2, single-arm trial. *Lancet Oncol*. 2015;16(2):169–176.

[8] Stilgenbauer S, Eichhorst B, Schetelig J, et al. Venetoclax in relapsed or refractory chronic lymphocytic leukaemia with 17p deletion: a multicentre, open-label, phase 2 study. *Lancet Oncol*. 2016;17(6):768–778.

[9] Thompson PA, O'brien SM, Wierda WG, et al. Complex karyotype is a stronger predictor than del(17p) for an inferior outcome in relapsed or refractory chronic lymphocytic leukemia patients treated with ibrutinib-based regimens. *Cancer*. 2015;121(20):3612–3621.

[10] Tam CS, Shanafelt TD, Wierda WG, et al. De novo deletion 17p13.1 chronic lymphocytic leukemia shows significant clinical heterogeneity: the M. D. Anderson and Mayo Clinic experience. *Blood*. 2009;114(5):957–964.

[11] Best OG, Gardiner AC, Davis ZA, et al. A subset of Binet stage A CLL patients with TP53 abnormalities and mutated IGHV genes have stable disease. *Leukemia*. 2009;23(1):212–214.

[12] Delgado J, Espinet B, Oliveira AC, et al. Chronic lymphocytic leukaemia with 17p deletion: a retrospective analysis of prognostic factors and therapy results. *Br J Haematol*. 2012;157(1):67–74.

[13] Delgado J, Salaverria I, Baumann T, et al. Genomic complexity and IGHV mutational status are key predictors of outcome of chronic lymphocytic leukemia patients with TP53 disruption. *Haematologica*. 2014;99(11):e231–e234.

[14] Hallek M, Cheson BD, Catovsky D, et al. Guidelines for the diagnosis and treatment of chronic lymphocytic leukemia: a report from the International Workshop on Chronic Lymphocytic Leukemia updating the National Cancer Institute-Working Group 1996 guidelines. *Blood*. 2008;111(12):5446–5456.

[15] Le Garff-Tavernier M, Blons H, Nguyen-Khac F, et al. Functional assessment of p53 in chronic lymphocytic leukemia. *Blood Cancer J*. 2011;1(2):e5.

[16] Callet-Bauchu E, Salles G, Gazzo S, et al. Translocations involving the short arm of chromosome 17 in chronic B-lymphoid disorders: frequent occurrence of dicentric rearrangements and possible association with adverse outcome. *Leukemia*. 1999;13(3):460–468.

[17] Liu Y, Chen C, Xu Z, et al. Deletions linked to TP53 loss drive cancer through p53-independent mechanisms. *Nature*. 2016;531(7595):471–475.

[18] Woyach JA, Heerema NA, Zhao J, et al. Dic(17;18)(p11.2;p11.2) is a recurring abnormality in chronic lymphocytic leukaemia associated with aggressive disease. *Br J Haematol*. 2010;148(5):754–759.

[19] Alhourani E, Rincic M, Melo JB, et al. Isochromosome 17q in chronic lymphocytic leukemia. *Leuk Res Treatment*. 2015;2015:489592.

[20] Collado R, Puiggros A, Lopez-Guerrero JA, et al. Chronic lymphocytic leukemia with isochromosome 17q: An aggressive subgroup associated with TP53 mutations and complex karyotypes. *Cancer Letters*. 2017;409:42–48.

[21] Shanafelt TD, Witzig TE, Fink SR, et al. Prospective evaluation of clonal evolution during long-term follow-up of patients with untreated early-stage chronic lymphocytic leukemia. *J Clin Oncol*. 2006;24:4634–4641.

[22] Stilgenbauer S, Sander S, Bullinger L, et al. Clonal evolution in chronic lymphocytic leukemia: acquisition of high-risk genomic aberrations associated with unmutated VH, resistance to therapy, and short survival. *Haematologica*. 2007;92(9):1242–1245.

[23] Oscier D, Wade R, Davis Z, et al. Prognostic factors identified three risk groups in the LRF CLL4 trial, independent of treatment allocation. *Haematologica*. 2010;95(10):1705–1712.

[24] Blanco G, Puiggros A, Ballakas P, et al. Karyotypic complexity rather than chromosome 8 abnormalities aggravates the outcome of chronic lymphocytic leukemia patients with TP53 aberrations. *Oncotarget*. 2016;7:80916–80924.

[25] Landau DA, Carter SL, Getz G, et al. Clonal evolution in hematological malignancies and therapeutic implications. *Leukemia*. 2014;28(1):34–43.

[26] Nadeu F, Delgado J, Royo C, et al. Clinical impact of clonal and subclonal TP53, SF3B1, BIRC3, NOTCH1, and ATM mutations in chronic lymphocytic leukemia. *Blood*. 2016;127(17):2122–2130.

[27] Haferlach C, Dicker F, Schnittger S, et al. Comprehensive genetic characterization of CLL: a study on 506 cases analysed with chromosome banding analysis, interphase FISH, IgV(H) status and immunophenotyping. *Leukemia*. 2007;21(12):2442–2451.

[28] Le Bris Y, Struski S, Guieze R, et al. Major prognostic value of complex karyotype in addition to TP53 and IGHV mutational status in first-line chronic lymphocytic leukemia. *Hematol Oncol*. 2016.

[29] Rigolin GM, Cavallari M, Quaglia FM, et al. In CLL, comorbidities and the complex karyotype are associated with an inferior outcome independently of CLL-IPI. *Blood*. 2017;129(26):3495–3498.

[30] Herling CD, Klaumunzer M, Rocha CK, et al. Complex karyotypes and KRAS and POT1 mutations impact outcome in CLL after chlorambucil-based chemotherapy or chemoimmunotherapy. *Blood*. 2016;128(3):395–404.

[31] Jaglowski SM, Ruppert AS, Heerema NA, et al. Complex karyotype predicts for inferior outcomes following reduced-intensity conditioning allogeneic transplant for chronic lymphocytic leukaemia. *Br J Haematol*. 2012;159(1):82–87.

[32] Mayr C, Speicher MR, Kofler DM, et al. Chromosomal translocations are associated with poor prognosis in chronic lymphocytic leukemia. *Blood*. 2006;107(2):742–751.

[33] Van Den Neste E, Robin V, Francart J, et al. Chromosomal translocations independently predict treatment failure, treatment-free survival and overall survival in B-cell chronic lymphocytic leukemia patients treated with cladribine. *Leukemia*. 2007;21(8):1715–1722.

[34] Brown JR, Hanna M, Tesar B, et al. Integrative genomic analysis implicates gain of PIK3CA at 3q26 and MYC at 8q24 in chronic lymphocytic leukemia. *Clin Cancer Res*. 2012;18(14):3791–3802.

[35] Rinaldi A, Mian M, Kwee I, et al. Genome-wide DNA profiling better defines the prognosis of chronic lymphocytic leukaemia. *Brit J Haematol*. 2011;154(5):590–599.

[36] Houldsworth J, Guttapalli A, Thodima V, et al. Genomic imbalance defines three prognostic groups for risk stratification of patients with chronic lymphocytic leukemia. *Leuk Lymphoma*. 2014;55(4):920–928.

[37] Forconi F, Rinaldi A, Kwee I, et al. Genome-wide DNA analysis identifies recurrent imbalances predicting outcome in chronic lymphocytic leukaemia with 17p deletion. *Br J Haematol*. 2008;143(4):532–536.

[38] Aukema SM, Siebert R, Schuuring E, et al. Double-hit B-cell lymphomas. *Blood*. 2011;117(8):2319–2331.

SUPPORTING INFORMATION

Additional Supporting Information may be found online in the supporting information tab for this article.

How to cite this article: Chapiro E, Lesty C, Gabillaud C, et al. "Double-hit" chronic lymphocytic leukemia: An aggressive subgroup with 17p deletion and 8q24 gain. *Am J Hematol*. 2018;93:375–382. https://doi.org/10.1002/ajh.24990

Supplemental Figures

Legends to figures

Supplemental Figure 1. 17p- abnormalities

A. Distribution of the different abnormalities leading to 17p loss (n=240)
B. Chromosomes involved in unbalanced translocations with an identified partner, including 68 arm-to-arm translocations (dark blue histograms) and 64 other translocations (light blue histograms).

Supplemental Figure 2. Overall survival in the whole cohort, according to age (A), Binet stage (B), and *IGHV* mutation status (C).

Supplemental Figure 3. Overall survival time after the first documentation of 17p- according to occurrence before or after treatment (n=124). Hazard Ratio= 2.02 (Confidence Interval 95%: 0.92-4.42)

Supplemental Figure 1.

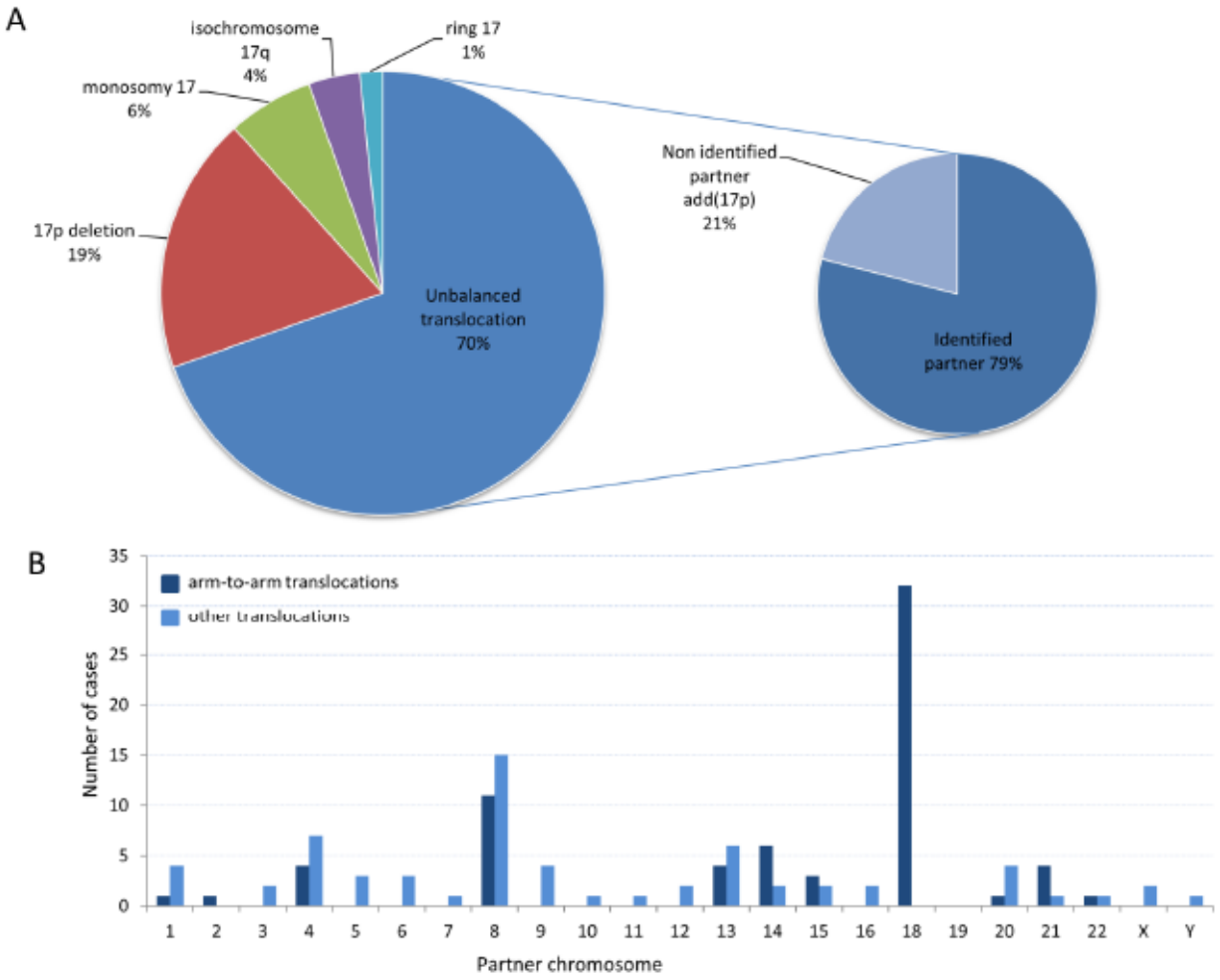

Supplemental Figure 2.

A

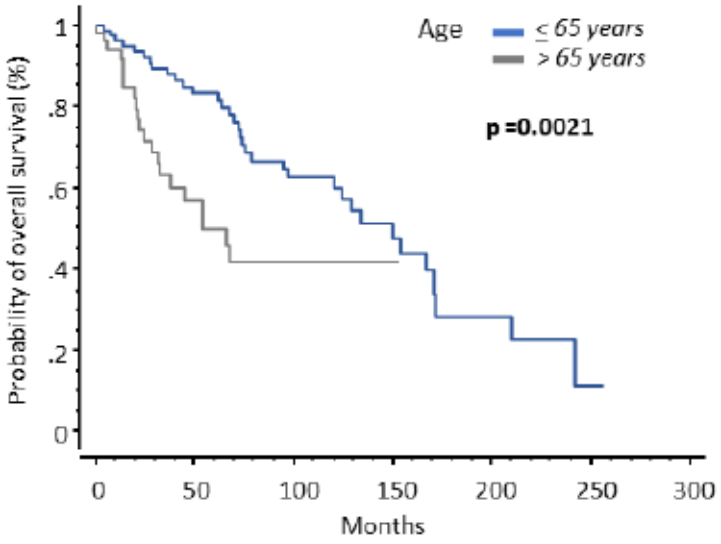

B

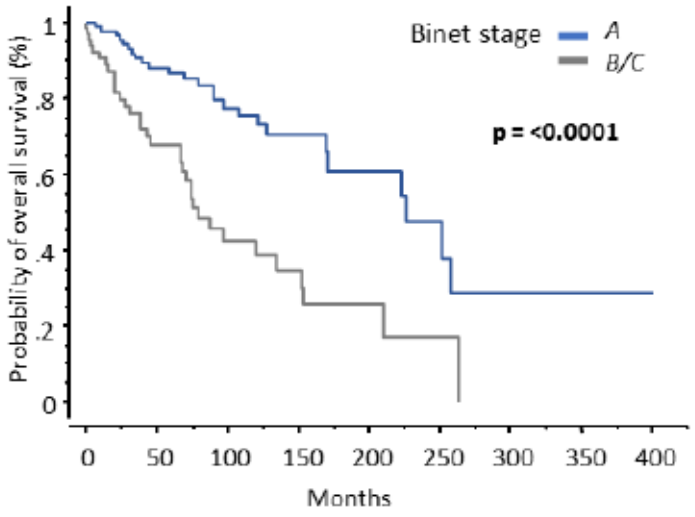

C

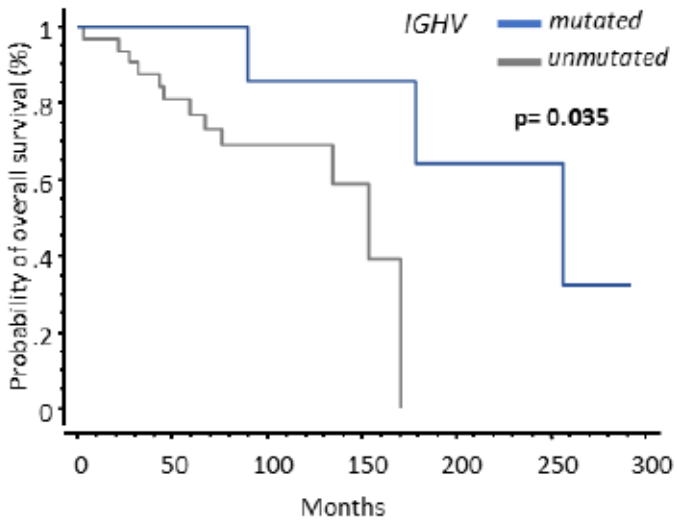

Supplemental Figure 3.

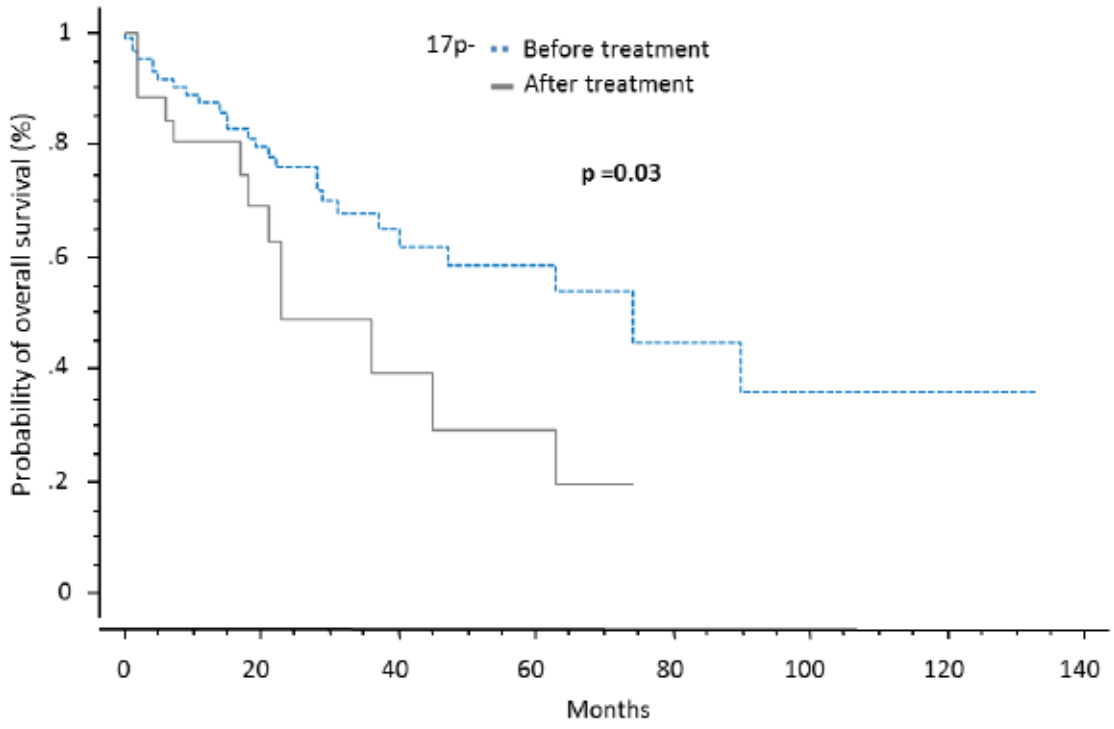

V – Genetic Characterization of B-Cell Prolymphocytic Leukemia (B-PLL): A Hierarchical Prognostic Model Involving *MYC* and *TP53* Abnormalities. on Behalf of the *Groupe Francophone De Cytogenetique Hematologique* (GFCH) and the *French Innovative Leukemia Organization* (FILO) Group

Abstract published in Blood 2018 132:943; doi: https://doi.org/10.1182/blood-2018-99-115085
Article published in Blood 2019 https://www.ncbi.nlm.nih.gov/pubmed/31527074

Elise Chapiro, Damien Roos-
Weil, Nadia Bougacha, Clementine Gabillaud, Clémentine Dillard, Elodie Pramil, Mel anie Yon, Karim Maloum, Catherine Settegrana, Lucile Baseggio, Claude Lesty, Fred eric Davi, Magali Le Garff-Tavernier, M'boyba Khadija Diop, Nathalie M Droin, Philippe Dessen, Veronique Leblond, Caroline Algrin, Simon Bouzy, Virginie Eclache, Baptiste Gaillard, Evelyne Callet-
Bauchu, Marc Muller, Christine Lefebvre, Nathalie Nadal, Antoine Ittel, Stéphanie Str uski, Marie-Agnes Collonge-Rame, Benoit Quilichini, Sandra Fert-
Ferrer, Nathalie Auger, Isabelle Radford-
Weiss, Lena Wagner, Sebastian Scheinost, Thorsten Zenz, Santos Susin, Olivier Ber nard and Florence Nguyen-Khac

B-PLL is defined by the presence of prolymphocytes in peripheral blood exceeding 55% of lymphoid cells. The diagnosis, mainly based on clinical and morphological data, can be difficult because of overlap with other B-cell malignancies. Because of the rarity of the disease, only case reports and small series describe its cytogenetic features. Few prognostic markers have been identified in this aggressive leukemia usually resistant to standard chemo-immuno therapy. We report here the cytogenetic and molecular findings in a large series of B-PLL. We also studied the *in vitro* response to novel targeted drugs on primary B-PLL cells.

The study included 34 cases with a diagnosis of B-PLL validated by morphological review performed by three independent expert cytologists. The diagnosis of mantle cell lymphoma was excluded by karyotype (K) and FISH using *CCND1*, *CCND2* and *CCND3* probes. Median age at diagnosis was 72 years [46-88]. K was complex (≥3 abnormalities) in 73%, and highly complex (HCK≥5) in 45%. Combining K and FISH data, the most frequent chromosomal aberrations were: translocation targeting the *MYC* gene [t(*MYC*)] (21/34, 62%), 17p deletion including *TP53* gene (13/34, 38%), trisomy 18/18q (10/33, 30%), 13q14 deletion (10/34, 29%), trisomy 3 (8/33, 24%), trisomy 12 (8/34, 24%) and 8p deletion (7/31, 23%). Whole-Exome Sequencing analysis of paired tumor-control DNA was performed in 16 patients. The most frequently mutated genes were *TP53* (6/16, 38%), associated with del17p in all, *MYD88* (n=4), *BCOR* (n=4), *MYC* (n=3), *SF3B1* (n=3), *FAT1* (n=3), *SETD2* (n=2), *CHD2* (n=2), *CXCR4* (n=2), *BCLAF1* (n=2) and *NFASC* (n=2). Distribution of the chromosomal aberrations is shown in Fig 1. The main group of patients (21/34, 62%) had a t*(MYC)* that was associated with a higher % of prolymphocytes (86 vs 76, p=0.03), CD38 expression (90% vs 15%, p<0.001), and a lower K complexity

(HCK≥5: 20% vs 85%, p=0.0004). Mutations in *MYC* and in genes involved in RNA metabolism and chromatin remodeling were almost exclusively observed with t(*MYC*). Principal component analysis of gene expression data in 12 cases analyzed by RNA-Seq showed that the 7 patients with t(*MYC*) clustered together. These results suggest that t(*MYC*) form a homogeneous subgroup of B-PLL. A second group with *MYC* gain (5/34, 15%), was associated with HCK≥5 (100% vs 36%, p=0,01) and trisomy 3 (80% vs 14%, p=0,008). Altogether, 26/34 patients (76%) had a *MYC* activation, translocation or gain, that were mutually exclusive.

The median overall survival (OS) for the entire cohort was 126 months with a median follow-up time of 47 months [0.2-141]. We found *MYC* activation (translocation or gain) to be associated with a shorter OS (p=0.03). Regarding *MYC* and del17p, we identified 3 distinct cytogenetic prognostic groups, with significant differences in OS (p=0.0006) (Fig 2). The patients without *MYC* activation had the lower risk (n=8, median not reached). Patients with a *MYC* activation without del17p had an intermediate risk (n=18, 125 months). The highest risk group corresponded to patients with both *MYC* and *TP53* aberrations (n=7, 11 months).
We performed drug response profiling on primary B-PLL cells using the ATP-based CellTiter Glo kit (Promega) (n=5). We observed that after 48h of exposure to increased doses, response was heterogeneous, with a majority of samples resistant to fludarabine (n=3), ibrutinib (n=3), idelalisib (n=4), venetoclax (n=3) and OTX015 (n=4). Annexin/PI assays using flow cytometry showed that the induced cell death could be increased by combination of ibrutinib or venetoclax with OTX015 or JQ1, two BET protein inhibitors that target *MYC* signaling (n=1/2).

In summary, B-PLL have complex and highly complex K, a high frequency of *MYC* activation by translocation or gain, frequent 17p deletion, and frequent mutations in *MYC*, *TP53*, *BCOR*, and *MYD88* genes. We identified 3 prognostic subgroups according to *MYC* and 17p status. Patients with *MYC* activation + 17p deletion have the shorter OS, and should be considered as a high-risk "double-hit" subgroup. Our results show that cytogenetic analysis is a useful diagnostic tool in B-PLL that improves prognostic stratification. We recommend to perform K and FISH (*MYC* and *TP53*) analyses systematically when a B-PLL is suspected. Our *in vitro* data suggest that drugs targeting the BCR and BCL2 in combination with MYC inhibition may be a therapeutic option in some patients.

Figure 1: Distribution of the chromosomal aberrations in 34 B-PLL

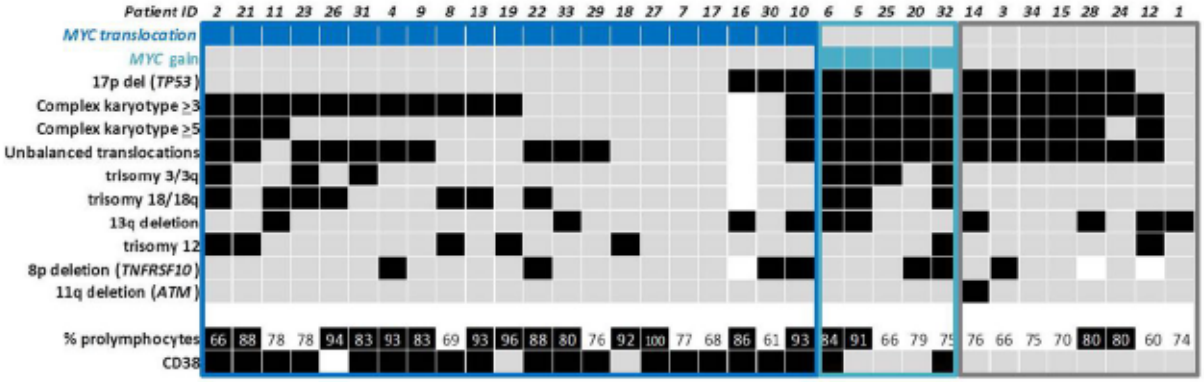

Figure 2. Overall survival in B-PLL patients according to 17p deletion and *MYC* status

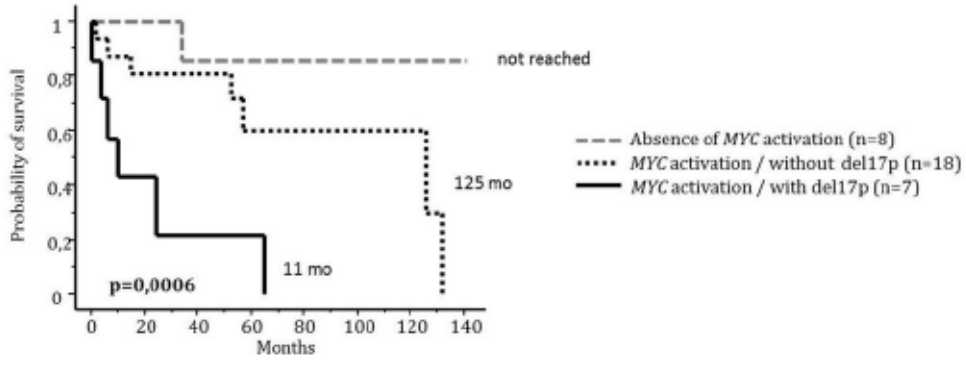

Conclusions and future perspectives

Altogether, our work has expanded the current knowledge regarding poor prognosis CLL and B-PLL, and yielded several recommendations for clinical practice:

i. We have shown that 2p gain is associated with drug resistance and poor prognostic features, and therefore recommend specific and systematic assessment of 2p gain in CLL prior to treatment, preferably by FISH with at least two sets of probes (*XPO1/REL* and *MYCN*).
ii. Our findings showed that 17p deletion and 8q24 gain have a synergistic impact on outcome, therefore patients with this "double-hit" CLL have a particularly poor prognosis. Systematic, targeted screening for 8q24 gain should thus be considered in cases of CLL with del(17p).
iii. We have characterized the molecular features of B-PLL: complex and highly complex karyotype, a high frequency of *MYC* activation by translocation or gain, frequent del(17p), and frequent mutations in *MYC*, *TP53*, *BCOR*, and *MYD88* genes. We identified a prognostic hierarchy according to *MYC* and 17p status, where patients with *MYC* activation + 17p deletion have the shorter OS. Systematic, targeted screening for *MYC* and *TP53* abnormalities by FISH and karyotype should thus be performed when a B-PLL is suspected. Moreover, our *in vitro* results indicate that drugs targeting the BCR and BCL2 in combination with MYC inhibition may be a therapeutic option in some patients.

Gain of 2p gain was described in various lymphomas and leukemias where the recurrence of highly amplified *REL* amplicon suggested its selection for functional importance. In CLL, the minimal region of 2p gain included *REL*. However, its particular role in pathogenesis was never investigated in functional analyses. Here, we report, for the first time, precise molecular studies examining the role of *REL* and the impact of its overexpression in CLL, carried out on patient-derived CLL cells as well as specific cellular models.

We have shown that transcriptional activation of *REL* by CRISPRa in OSU-CLL cells did not significantly decrease spontaneous and drug-induced cell death, nor did it affect proliferation, in agreement with the observation that primary cells of 2p gain+ CLL patients were resistant to pharmacological inhibition of REL/NF-κB. Inactivation of *REL* by CRISPR/Cas9 in 2p gain+ JVM-3 cells decreased proliferation and enhanced sensitivity to anti-CLL drugs and targeted agents. Pharmacological inhibition of NF-κB selectively induced cell death in leukemic cells of CLL patients. Altogether, these findings indicate that *REL* could play a major role in CLL cell survival, but does not seem to be the main or sole player accounting for 2p gain-associated drug resistance. Further studies will be required to identify the genetic drivers of drug resistance in 2p gain.

Characterizing 2p gain in the era of precision medicine

The fundamental ambition of precision medicine is to use population-based molecular, clinical and other data to make individually tailored clinical decisions for patients (Biankin, 2017). The comprehensive characterization of the set of genetic lesions in cancer is critical for the development of personalized medicine, because driver genes may inform prognosis and identify lesions that may be targeted

therapeutically (Landau et al., 2015). Conversely, therapeutic strategies might also apply selective pressure and thus shape the landscape of cancer lesions.

Extracting valuable information and recognizing patterns in a patient cohort that includes samples collected at variable times, from subjects exposed to a variety of therapies, is rather arduous. A systematic and more accurate assessment of 2p gain, together with a careful analysis of clinical and biological features, would directly and indirectly improve the clinical management of patients, by providing both a more complete picture of the CLL phenotypes as well as statistical power by enabling larger cohort sizes.

Elucidating the genetic basis of the aggressive phenotype associated with 2p gain might also pave the way for novel treatment strategies in malignancies that are equally plagued with this abnormality, notably NB and HL.

We have found most drugs to be rather ineffective to eliminate the 2p gain clone, and although further studies are required, it seems that FCR was linked to 2p gain increase and conversely, the BOMP regimen to 2p gain decrease, which could make the latter an option. As previously mentioned we have therefore proposed the systematic assessment of 2p gain in CLL patients before deciding a CLL therapy, ideally by FISH with at least two sets of probes (***XPO1/REL*** and ***MYCN***).

The gold standard for detecting cytogenetic abnormalities in CLL is interphase FISH performed on cell smears or tissue sections on glass slides. Fluorescently labelled DNA probes bind to specific chromosomal regions and the signal detected by fluorescent microscopy. Usually, only 200 cells are assessed and the limit of sensitivity is 3% positive cells. The recent development of imaging flow cytometry, or "immuno-flowFISH", to assess chromosomes by FISH in thousands of phenotyped CLL cells in suspension using an automated, high throughput imaging flow cytometer, could improve the detection of early or minor subclones (Hui et al., 2018).

Additionally, it would be valuable to confirm whether the % of 2p gain positive cells is proportional to the severity of the clinical phenotype (Cosson et al., 2017), which could be readily modeled *in vitro* by designing overexpression systems with two or three different transcript levels.

Here, 2p gain was exclusively present as a secondary anomaly. Importantly, drug response should also be assessed in early stage and previously untreated 2p gain CLL cases, in order to determine if the observed drug refractoriness is solely inherent to 2p gain or acquired as a result of an interplay with concomitant lesions.

Furthermore, the impact of the epigenome on tumor progression should not be ignored.

Multidrug resistance phenotype

ATP-binding cassette (ABC) proteins form a family of transmembrane transporters, which control the passage of several substrates across cell membranes, including drugs. Several members of this family significantly modulate the absorption, metabolism, cellular effectivity and toxicity of pharmacological agents,

and are thus involved in the occurrence of multidrug resistance (MDR) phenotype, including the classical P-glycoprotein (PGP, MDR1, ABCB1), ABCC1 (MRP1) and ABCG2 (BCRP) (Arrigoni et al., 2016; Glavinas et al., 2004).

The multidrug resistance gene ABCC1 mapping to cytoband 16p13.11 was overexpressed and gained in the therapy-resistant HL cell line KMH2 (Steidl et al., 2010). Interestingly, simultaneous targeting of MCL1 and ABCB1 was able to overcome drug resistance in human acute leukemia. Specifically, RNAi-mediated downregulation of MCL1 sensitized multidrug resistant leukemia cells towards chemotherapy and induced cell death (Ji et al., 2009).

Investigating the MDR genes and corresponding proteins in 2p gain CLL might shed some light on the observed drug refractoriness.

Developing relevant 2p gain CLL models

Very few human B cell lymphoma or leukemia cell lines with a highly amplified ***REL*** locus or 2p gain are available. The cell systems that we describe here provide elegant *in vitro* model systems to further unravel the complex roles and interactions of c-Rel/NF-κB pathways in blood malignancies. Indeed, the data obtained in our CRISPRa-established B cell lines, by activating transcription at the endogenous gene locus, and in moderate levels, seem to accurately substantiate the relevance of ***REL*** gain in CLL drug refractoriness.

Establishing one or several cell lines derived from 2p gain+ CLL patients (O. Bernard, personal communication) could provide useful models for the functional exploration of this abnormality. Cell lines with different concomitant genetic lesions, with different percentages of 2p gain, or with distinct loci of high amplification could further refine the analysis and provide novel insights in pathogenesis and oncogenic cooperation.

Given the preponderance of the microenvironment on CLL cells, the *in vitro* culture setting should be carefully devised using cells and molecules that mimic the CLL environment with the highest possible fidelity. For instance, co-culture with stromal and myeloid nurse-like cells at least partially recreate the pro-leukemic niche (Vaisitti et al., 2017). Recently, it was demonstrated that some culture conditions could make CLL cells proliferate *ex vivo*: namely, BCR engagement by anti-IgM ligation, together with CD40 ligand, IL-4 and IL-21 stimulation. This proliferative response was higher in ZAP70 positive CLL cells, and could be further augmented by the use of a tri-dimensional matrix of methylcellulose and the addition of TLR9 agonists (Schleiss et al., 2019).

Genome-scale screens

Candidate gene approaches, which are rather costly and time-consuming, and *in silico* interrogation of genes and pathways databases, like Panther, DAVID or Msig, can be both easily riddled with confirmation bias. In my opinion, the most comprehensive and unbiased methods to identify the drivers of 2p gain drug resistance would therefore be:

i. RNAseq studies performed in 2p gain+ compared to 2p gain- CLL patients, in order to confirm and perhaps extend the data obtained by micro-array studies (Fabris et al., 2013).
ii. Proteomic analyses, featuring mass spectrometry, of 2p gain+ and 2p gain- CLL samples
iii. A genome-scale CRISPRa transcriptional activation screening in several 2p gain- mature B cell lines, followed by drug treatment and sequencing of the newly resistant cells.

The latter method will be further discussed in this last section, and a general protocol is proposed in the **Annex**.

Pooled genetic screens, i.e. the simultaneous testing of thousands of individual perturbations in a single batch, can be executed with existing infrastructure by most laboratories that are already performing cell culture (albeit at a larger scale than typical experiments) and at a reasonable cost (Doench, 2017; Shalem et al., 2015).

Before the advent of CRISPR-based technologies, gain-of-functions screens were mainly limited to cDNA overexpression libraries, which exhibited several caveats, namely incomplete representation, overexpression beyond physiological levels, endogenous regulation, lack of isoform diversity and high cost of construction. CRISPRa overcomes these shortcomings because it produces gene transcription at the endogenous locus and only requires the synthesis and cloning of RNA guides, rendering it much more affordable (Joung et al., 2017a).

Non-coding loci exert diverse roles in gene regulation and cellular function. Indeed, non-coding genetic sequences, such as enhancers, shape cell type specific transcriptional programs and response to extracellular cues, therefore alterations in these elements can contribute to disease (Ernst et al., 2011; Farh et al., 2015; Maurano et al., 2012). By enabling the targeting of virtually any region of interest, the CRISPRa method could identify non-coding loci that influence a phenotype of interest. For instance, a genome scale activation screen identified a long non-coding (lncRNA) locus regulating a gene neighborhood (Joung et al., 2017b).

Loss-of-functions screens present several advantages; however, they might not be the ideal method for studying amplified regions.

Lentivirus-delivered sgRNA/Cas9 genome editing was also proven to be useful to engineer a wide array of *in vivo* cancer models that better reflect the complexity of human disease. Indeed, delivering combinations of sgRNAs and Cas9 with a lentiviral vector led to modification of up to five genes in a single mouse HSC, generating models of AML with cooperating mutations in genes encoding epigenetic modifiers, transcription factors and mediators of cytokine signaling, recapitulating the combinations of mutations observed in patients (Heckl et al., 2014).

Interestingly, since many gene families in eukaryotic genomes exhibit partially overlapping functions, the knockout of one gene might be compensated by the function of the other. In order to knockout simultaneously multiple homologous genes, CRISPys was recently developed: it stands for an algorithm devised for the

optimal design of sgRNAs that would simultaneously target multiple members of a given gene family (Hyams et al., 2018).

A systematic comparison between shRNA and CRISPR/Cas9 screens, performed to identify essential genes in human leukemic cells, showed little correlation in terms of results (Morgens et al., 2016). CRISPR screens identified more lethal genes than RNAi, implying that the identification of many cellular dependencies may require full gene inactivation, however they generated false-positive hits in highly amplified genomic regions (Munoz et al., 2016). Indeed, genome-scale loss of function screens showed a robust correlation between increased gene copy number and decreased cell viability after genome editing, in other words editing of amplified loci resulted in gene-independent antiproliferative cell responses (Aguirre et al., 2016). Conversely, CRISPRi reportedly yielded no detectable off target effects (Qi et al., 2013), and does not induce non-specific toxicity at amplified genomic loci (Horlbeck et al., 2016), but should rationally display the same caveats as RNA interference screens.

Annex

Protocol for a genome-scale CRISPRa transcriptional activation screening to identify drivers of drug refractoriness in 2p gain CLL

1. Introduction of a library of sgRNAs into populations of 2p gain- CLL cells

Lentiviruses or other retroviruses are used for this step because they integrate into the genome of the target cells, and thus a cell's genome is permanently marked by the perturbation it received. Lentiviral transduction of sgRNA libraries is typically performed at MOIs between 0.4 and 0.6 transduction units/cell to ensure that each cell contains a single sgRNA (Shalem et al., 2014; Wang et al., 2014).

Conveniently, many libraries are commercially available as pooled plasmid libraries, as reviewed in (Miles et al., 2016). Alternatively, they can be synthetized. Either way, they must contain an adequate proportion of scramble sgRNAs for control.

Performing the screen in multiple cell lines might avoid specific limitations such as the genetic background of the cell line or transduction efficiency. Indeed, a cell line with low transduction efficiency will result in increased struggles in generating a pool of cells with acceptable representation of the sgRNA library (Miles et al., 2016).

2. Treatment of all infected cells with anti-CLL drugs

This step will select and physically separate cells displaying a drug resistance phenotype from those that do not. The precise protocol that includes dose and duration of treatment should be carefully developed and adapted to the selected cell lines beforehand.

3. Extraction of genomic DNA and PCR

4. Massively parallel sequencing to quantify the abundance of each sgRNA

The level of sequencing depth will vary depending on the type of screen and size of library, for example, 10-20x10^6 reads allows to adequately sequence a complex library of 1x10^5 elements (Joung et al., 2017a; Miles et al., 2016).

Bibliography

Abate, F., Todaro, M., van der Krogt, J.-A., Boi, M., Landra, I., Machiorlatti, R., Tabbò, F., Messana, K., Abele, C., Barreca, A., et al. (2015). A novel patient-derived tumorgraft model with TRAF1-ALK anaplastic large-cell lymphoma translocation. Leukemia *29*, 1390–1401.

Abraham, M., Klein, S., Bulvik, B., Wald, H., Weiss, I.D., Olam, D., Weiss, L., Beider, K., Eizenberg, O., Wald, O., et al. (2017). The CXCR4 inhibitor BL-8040 induces the apoptosis of AML blasts by downregulating ERK, BCL-2, MCL-1 and cyclin-D1 via altered miR-15a/16-1 expression. Leukemia *31*, 2336–2346.

Aguirre, A.J., Meyers, R.M., Weir, B.A., Vazquez, F., Zhang, C.-Z., Ben-David, U., Cook, A., Ha, G., Harrington, W.F., Doshi, M.B., et al. (2016). Genomic Copy Number Dictates a Gene-Independent Cell Response to CRISPR/Cas9 Targeting. Cancer Discov. *6*, 914–929.

Ahn, H.J., Hernandez, C.M., Levenson, J.M., Lubin, F.D., Liou, H.-C., and Sweatt, J.D. (2008). c-Rel, an NF-kappaB family transcription factor, is required for hippocampal long-term synaptic plasticity and memory formation. Learn. Mem. *15*, 539–549.

Ahn, I.E., Underbayev, C., Albitar, A., Herman, S.E.M., Tian, X., Maric, I., Arthur, D.C., Wake, L., Pittaluga, S., Yuan, C.M., et al. (2017). Clonal evolution leading to ibrutinib resistance in chronic lymphocytic leukemia. Blood *129*, 1469–1479.

Alberti, C., Pinciroli, P., Valeri, B., Ferri, R., Ditto, A., Umezawa, K., Sensi, M., Canevari, S., and Tomassetti, A. (2012). Ligand-dependent EGFR activation induces the co-expression of IL-6 and PAI-1 via the NFkB pathway in advanced-stage epithelial ovarian cancer. Oncogene *31*, 4139–4149.

Allan, J.N., and Furman, R.R. (2018). Current trends in the management of Richter's syndrome. Int. J. Hematol. Oncol. *7*, IJH09.

Alshareef, A., Irwin, M.S., Gupta, N., Zhang, H.-F., Haque, M., Findlay, S.D., Seong, B.K.A., Lai, J., Rayis, M., Al-Dandan, S., et al. (2018). The absence of a novel intron 19-retaining ALK transcript (ALK-I19) and MYCN amplification correlates with an excellent clinical outcome in neuroblastoma patients. Oncotarget *9*, 10698–10713.

Alves, B.N., Tsui, R., Almaden, J., Shokhirev, M.N., Davis-Turak, J., Fujimoto, J., Birnbaum, H., Ponomarenko, J., and Hoffmann, A. (2014). IκBε is a key regulator of B cell expansion by providing negative feedback on cRel and RelA in a stimulus-specific manner. J. Immunol. *192*, 3121–3132.

Argyropoulos, K. V, Vogel, R., Ziegler, C., Altan-Bonnet, G., Velardi, E., Calafiore, M., Dogan, A., Arcila, M., Patel, M., Knapp, K., et al. (2016). Clonal B cells in Waldenström's macroglobulinemia exhibit functional features of chronic active B-cell receptor signaling. Leukemia *30*, 1116–1125.

Arrigoni, E., Galimberti, S., Petrini, M., Danesi, R., and Di Paolo, A. (2016). ATP-binding cassette transmembrane transporters and their epigenetic control in cancer: an overview. Expert Opin. Drug Metab. Toxicol. *12*, 1419–1432.

Backhaus, O. (2018). Generation of Antibody Diversity. In Antibody Engineering,

(InTech).

Bahnson, A.B., and Boggs, S.S. (1990). Addition of serum to electroporated cells enhances survival and transfection efficiency. Biochem. Biophys. Res. Commun. *171*, 752–757.

Bai, R.Y., Dieter, P., Peschel, C., Morris, S.W., and Duyster, J. (1998). Nucleophosmin-anaplastic lymphoma kinase of large-cell anaplastic lymphoma is a constitutively active tyrosine kinase that utilizes phospholipase C-gamma to mediate its mitogenicity. Mol. Cell. Biol. *18*, 6951–6961.

Baliakas, P., Iskas, M., Gardiner, A., Davis, Z., Plevova, K., Nguyen-Khac, F., Malcikova, J., Anagnostopoulos, A., Glide, S., Mould, S., et al. (2014). Chromosomal translocations and karyotype complexity in chronic lymphocytic leukemia: a systematic reappraisal of classic cytogenetic data. Am. J. Hematol. *89*, 249–255.

Baliakas, P., Hadzidimitriou, A., Sutton, L.-A., Rossi, D., Minga, E., Villamor, N., Larrayoz, M., Kminkova, J., Agathangelidis, A., Davis, Z., et al. (2015). Recurrent mutations refine prognosis in chronic lymphocytic leukemia. *29*, 329–336.

Baliakas, P., Jeromin, S., Iskas, M., Puiggros, A., Plevova, K., Nguyen-Khac, F., Davis, Z., Rigolin, G.M., Visentin, A., Xochelli, A., et al. (2019). Cytogenetic complexity in chronic lymphocytic leukemia: definitions, associations, and clinical impact. Blood *133*, 1205–1216.

Banerjee, A., Grumont, R., Gugasyan, R., White, C., Strasser, A., and Gerondakis, S. (2008). NF-kappaB1 and c-Rel cooperate to promote the survival of TLR4-activated B cells by neutralizing Bim via distinct mechanisms. Blood *112*, 5063–5073.

Bao, E.L., Cheng, A.N., Sankaran, V.G. (2019). The genetics of human hematopoiesis and its disruption in disease. EMBO Molecular Medicine. 11 (8).

Barrangou, R., Fremaux, C., Deveau, H., Richards, M., Boyaval, P., Moineau, S., Romero, D.A., and Horvath, P. (2007). CRISPR Provides Acquired Resistance Against Viruses in Prokaryotes. Science (80-.). *315*, 1709–1712.

Barth, T.F., Bentz, M., Leithäuser, F., Stilgenbauer, S., Siebert, R., Schlotter, M., Schlenk, R.F., Döhner, H., and Möller, P. (2001). Molecular-cytogenetic comparison of mucosa-associated marginal zone B-cell lymphoma and large B-cell lymphoma arising in the gastro-intestinal tract. Genes. Chromosomes Cancer *31*, 316–325.

Barth, T.F.E., Martin-Subero, J.I., Joos, S., Menz, C.K., Hasel, C., Mechtersheimer, G., Parwaresch, R.M., Lichter, P., Siebert, R., and Möoller, P. (2003). Gains of 2p involving the REL locus correlate with nuclear c-Rel protein accumulation in neoplastic cells of classical Hodgkin lymphoma. Blood *101*, 3681–3686.

Bash, J., Zong, W.-X., Line, C.É., and Linas, G.É. (1997). c-Rel Arrests the Proliferation of HeLa Cells and Affects Critical Regulators of the G 1 /S-Phase Transition.

Baylin, S.B., and Jones, P.A. (2011). A decade of exploring the cancer epigenome — biological and translational implications. Nat. Rev. Cancer *11*, 726–734.

Bea, S., Zettl, A., Wright, G., Salaverria, I., Jehn, P., Moreno, V., Burek, C., Ott, G., Puig, X., Yang, L., et al. (2005). Diffuse large B-cell lymphoma subgroups have distinct genetic profiles that influence tumor biology and improve gene-expression-based survival prediction. Blood *106*, 3183–3190.

Bellosillo, B., Piqué, M., Barragán, M., Castaño, E., Villamor, N., Colomer, D., Montserrat, E., Pons, G., and Gil, J. (1998). Aspirin and salicylate induce apoptosis and activation of caspases in B-cell chronic lymphocytic leukemia cells. Blood *92*, 1406–1414.

Beltran, H. (2014). The N-myc Oncogene: Maximizing its Targets, Regulation, and Therapeutic Potential. Mol. Cancer Res. *12*, 815–822.

Ben-Neriah, Y., and Karin, M. (2011). Inflammation meets cancer, with NF-κB as the matchmaker. Nat. Immunol. *12*, 715–723.

Vanden Berghe, T., Kalai, M., Denecker, G., Meeus, A., Saelens, X., and Vandenabeele, P. (2006). Necrosis is associated with IL-6 production but apoptosis is not. Cell. Signal. *18*, 328–335.

Bergsbaken, T., Fink, S.L., and Cookson, B.T. (2009). Pyroptosis: host cell death and inflammation. Nat. Rev. Microbiol. *7*, 99–109.

Berry, T., Luther, W., Bhatnagar, N., Jamin, Y., Poon, E., Sanda, T., Pei, D., Sharma, B., Vetharoy, W.R., Hallsworth, A., et al. (2012). The ALKF1174L Mutation Potentiates the Oncogenic Activity of MYCN in Neuroblastoma. Cancer Cell *22*, 117–130.

Bertrand, J.Y., Kim, A.D., Violette, E.P., Stachura, D.L., Cisson, J.L., and Traver, D. (2007). Definitive hematopoiesis initiates through a committed erythromyeloid progenitor in the zebrafish embryo. Development *134*, 4147–4156.

Bhaya, D., Davison, M., and Barrangou, R. (2011). CRISPR-Cas systems in bacteria and archaea: versatile small RNAs for adaptive defense and regulation. Annu. Rev. Genet. *45*, 273–297.

Biankin, A. V (2017). The road to precision oncology. Nat. Genet. *49*, 320–321.

Binet, J.L., Auquier, A., Dighiero, G., Chastang, C., Piguet, H., Goasguen, J., Vaugier, G., Potron, G., Colona, P., Oberling, F., et al. (1981). A new prognostic classification of chronic lymphocytic leukemia derived from a multivariate survival analysis. Cancer *48*, 198–206.

Bischof, D., Pulford, K., Mason, D.Y., and Morris, S.W. (1997). Role of the nucleophosmin (NPM) portion of the non-Hodgkin's lymphoma-associated NPM-anaplastic lymphoma kinase fusion protein in oncogenesis. Mol. Cell. Biol. *17*, 2312–2325.

Blombery, P., Anderson, M.A., Gong, J.-N., Thijssen, R., Birkinshaw, R.W., Thompson, E.R., Teh, C.E., Nguyen, T., Xu, Z., Flensburg, C., et al. (2019). Acquisition of the Recurrent Gly101Val Mutation in BCL2 Confers Resistance to Venetoclax in Patients with Progressive Chronic Lymphocytic Leukemia. Cancer Discov. *9*, 342–353.

Bondy-Denomy, J., and Davidson, A.R. (2014). To acquire or resist: the complex biological effects of CRISPR–Cas systems. Trends Microbiol. *22*, 218–225.

Bone, K.M., Wang, P., Wu, F., Wu, C., Li, L., Bacani, J.T., Andrew, S.E., and Lai, R. (2015). NPM-ALK mediates phosphorylation of MSH2 at tyrosine 238, creating a functional deficiency in MSH2 and the loss of mismatch repair. Blood Cancer J. *5*, e311–e311.

Borer, R.A., Lehner, C.F., Eppenberger, H.M., and Nigg, E.A. (1989). Major nucleolar proteins shuttle between nucleus and cytoplasm. Cell *56*, 379–390.

De Bortoli, M., Castellino, R.C., Lu, X.-Y., Deyo, J., Sturla, L.M., Adesina, A.M., Perlaky, L., Pomeroy, S.L., Lau, C.C., Man, T.-K., et al. (2006). Medulloblastoma outcome is adversely associated with overexpression of EEF1D, RPL30, and RPS20 on the long arm of chromosome 8. BMC Cancer *6*, 223.

Bradford, J.W., and Baldwin, A.S. (2014). IKK/Nuclear Factor-kappaB and Oncogenesis. In Advances in Cancer Research, pp. 125–145.

DE Braekeleer, M., Tous, C., Guéganic, N., LE Bris, M.-J., Basinko, A., Morel, F., and Douet-Guilbert, N. (2016). Immunoglobulin gene translocations in chronic lymphocytic leukemia: A report of 35 patients and review of the literature. Mol. Clin. Oncol. *4*, 682–694.

Brander, D.M. (2017). Rationale for combinatory chronic lymphocytic leukaemia treatment paradigms in the era of the B-cell receptor pathway and anti-apoptotic inhibitors: how do we mix, match, and move forward? Br. J. Haematol. *176*, 337–340.

Brouns, S.J.J., Jore, M.M., Lundgren, M., Westra, E.R., Slijkhuis, R.J.H., Snijders, A.P.L., Dickman, M.J., Makarova, K.S., Koonin, E. V, and van der Oost, J. (2008). Small CRISPR RNAs guide antiviral defense in prokaryotes. Science *321*, 960–964.

De Brouwer, S., De Preter, K., Kumps, C., Zabrocki, P., Porcu, M., Westerhout, E.M., Lakeman, A., Vandesompele, J., Hoebeeck, J., Van Maerken, T., et al. (2010). Meta-analysis of neuroblastomas reveals a skewed ALK mutation spectrum in tumors with MYCN amplification. Clin. Cancer Res. *16*, 4353–4362.

Brown, A., Sciascia-Visani, I., Farrell, D., Smith, M., Felix, C., Mutharajah, V., Ruell, J., and Taylor, G. (2019). A patient with a diagnosis of nodal marginal zone B-cell lymphoma and a t(2;14)(p24;q32) involving MYCN and IGH. Mol. Cytogenet. *12*, 3.

Brown, J.R., Hallek, M.J., and Pagel, J.M. (2016). Chemoimmunotherapy Versus Targeted Treatment in Chronic Lymphocytic Leukemia: When, How Long, How Much, and in Which Combination? Am. Soc. Clin. Oncol. Educ. B. *36*, e387–e398.

Bunting, K., Rao, S., Hardy, K., Woltring, D., Denyer, G.S., Wang, J., Gerondakis, S., and Shannon, M.F. (2007). Genome-wide analysis of gene expression in T cells to identify targets of the NF-kappa B transcription factor c-Rel. J. Immunol. *178*, 7097–7109.

Bureau, F., Vanderplasschen, A., Jaspar, F., Minner, F., Pastoret, P.P., Merville, M.P., Bours, V., and Lekeux, P. (2002). Constitutive nuclear factor-κB activity preserves homeostasis of quiescent mature lymphocytes and granulocytes by controlling the expression of distinct Bcl-2 family proteins. Blood *99*, 3683–3691.

Burger, J.A. (2011). Nurture versus Nature: The Microenvironment in Chronic Lymphocytic Leukemia. Hematology *2011*, 96–103.

Burger, J.A., and Chiorazzi, N. (2013). B cell receptor signaling in chronic lymphocytic leukemia. Trends Immunol. *34*, 592–601.

Burger, J.A., Landau, D.A., Taylor-Weiner, A., Bozic, I., Zhang, H., Sarosiek, K., Wang, L., Stewart, C., Fan, J., Hoellenriegel, J., et al. (2016). Clonal evolution in patients with chronic lymphocytic leukaemia developing resistance to BTK inhibition. Nat. Commun. *7*, 11589.

Burkitt, M.D., Williams, J.M., Duckworth, C.A., O'Hara, A., Hanedi, A., Varro, A., Caamaño, J.H., and Pritchard, D.M. (2013). Signaling mediated by the NF-κB subunits NF-κB1, NF-κB2 and c-Rel differentially regulate Helicobacter felis-induced gastric carcinogenesis in C57BL/6 mice. Oncogene *32*, 5563–5573.

Burns, A., Alsolami, R., Becq, J., Stamatopoulos, B., Timbs, A., Bruce, D., Robbe, P., Vavoulis, D., Clifford, R., Cabes, M., et al. (2018). Whole-genome sequencing of chronic lymphocytic leukaemia reveals distinct differences in the mutational landscape between IgHVmut and IgHVunmut subgroups. Leukemia *32*, 332–342.

Byrd, J.C., Furman, R.R., Coutre, S.E., Flinn, I.W., Burger, J.A., Blum, K.A., Grant, B., Sharman, J.P., Coleman, M., Wierda, W.G., et al. (2013). Targeting BTK with Ibrutinib in Relapsed Chronic Lymphocytic Leukemia. N. Engl. J. Med. *369*, 32–42.

Byrd, J.C., Jones, J.J., Woyach, J.A., Johnson, A.J., and Flynn, J.M. (2014). Entering the Era of Targeted Therapy for Chronic Lymphocytic Leukemia: Impact on the Practicing Clinician. J. Clin. Oncol. *32*, 3039–3047.

Byrd, J.C., Furman, R.R., Coutre, S.E., Burger, J.A., Blum, K.A., Coleman, M., Wierda, W.G., Jones, J.A., Zhao, W., Heerema, N.A., et al. (2015). Three-year follow-up of treatment-naive and previously treated patients with CLL and SLL receiving single-agent ibrutinib. Blood *125*, 2497–2506.

Byrd, J.C., Smith, S., Wagner-Johnston, N., Sharman, J., Chen, A.I., Advani, R., Augustson, B., Marlton, P., Commerford, S.R., Okrah, K., et al. (2018). First-in-human phase 1 study of the BTK inhibitor GDC-0853 in relapsed or refractory B-cell NHL and CLL. Oncotarget *9*, 13023–13035.

Cahill, N., Bergh, A.-C., Kanduri, M., Göransson-Kultima, H., Mansouri, L., Isaksson, A., Ryan, F., Smedby, K.E., Juliusson, G., Sundström, C., et al. (2013). 450K-array analysis of chronic lymphocytic leukemia cells reveals global DNA methylation to be relatively stable over time and similar in resting and proliferative compartments. Leukemia *27*, 150–158.

Calero, R., Morchon, E., Johnsen, J.I., and Serrano, R. (2014). Sunitinib Suppress Neuroblastoma Growth through Degradation of MYCN and Inhibition of Angiogenesis. PLoS One *9*, e95628.

Calin, G.A., Dumitru, C.D., Shimizu, M., Bichi, R., Zupo, S., Noch, E., Aldler, H., Rattan, S., Keating, M., Rai, K., et al. (2002). Frequent deletions and down-regulation of micro- RNA genes miR15 and miR16 at 13q14 in chronic lymphocytic leukemia. Proc. Natl. Acad. Sci. *99*, 15524–15529.

Calissano, C., Damle, R.N., Hayes, G., Murphy, E.J., Hellerstein, M.K., Moreno, C., Sison, C., Kaufman, M.S., Kolitz, J.E., Allen, S.L., et al. (2009). In vivo intraclonal and interclonal kinetic heterogeneity in B-cell chronic lymphocytic leukemia. Blood *114*, 4832–4842.

Camus, V., Stamatoullas, A., Mareschal, S., Viailly, P.-J., Sarafan-Vasseur, N., Bohers, E., Dubois, S., Picquenot, J.M., Ruminy, P., Maingonnat, C., et al. (2016). Detection and prognostic value of recurrent exportin 1 mutations in tumor and cell-free circulating DNA of patients with classical Hodgkin lymphoma. Haematologica *101*, 1094–1101.

Canny, M.D., Moatti, N., Wan, L.C.K., Fradet-Turcotte, A., Krasner, D., Mateos-

Gomez, P.A., Zimmermann, M., Orthwein, A., Juang, Y.-C., Zhang, W., et al. (2018). Inhibition of 53BP1 favors homology-dependent DNA repair and increases CRISPR-Cas9 genome-editing efficiency. Nat. Biotechnol. *36*, 95–102.

Cao, J., Wu, L., Zhang, S.-M., Lu, M., Cheung, W.K.C., Cai, W., Gale, M., Xu, Q., and Yan, Q. (2016). An easy and efficient inducible CRISPR/Cas9 platform with improved specificity for multiple gene targeting. Nucleic Acids Res. *44*, gkw660.

Cao, Q., Liu, Z., Huang, Y., Qi, C., and Yin, X. (2019). NCOA1–ALK: a novel ALK rearrangement in one lung adenocarcinoma patient responding to crizotinib treatment. Onco. Targets. Ther. *Volume 12*, 1071–1074.

Carte, J., Wang, R., Li, H., Terns, R.M., and Terns, M.P. (2008). Cas6 is an endoribonuclease that generates guide RNAs for invader defense in prokaryotes. Genes Dev. *22*, 3489–3496.

Cavallari, M., Cavazzini, F., Bardi, A., Volta, E., Melandri, A., Tammiso, E., Saccenti, E., Lista, E., Quaglia, F.M., Urso, A., et al. (2018). Biological significance and prognostic/predictive impact of complex karyotype in chronic lymphocytic leukemia. Oncotarget *9*, 34398–34412.

Cavazzini, F., Hernandez, J.A., Gozzetti, A., Russo Rossi, A., De Angeli, C., Tiseo, R., Bardi, A., Tammiso, E., Crupi, R., Lenoci, M.P., et al. (2008). Chromosome 14q32 translocations involving the immunoglobulin heavy chain locus in chronic lymphocytic leukaemia identify a disease subset with poor prognosis. Br. J. Haematol. *142*, 529–537.

Chapiro, E., Leporrier, N., Radford-Weiss, I., Bastard, C., Mossafa, H., Leroux, D., Tigaud, I., De Braekeleer, M., Terré, C., Brizard, F., et al. (2010). Gain of the short arm of chromosome 2 (2p) is a frequent recurring chromosome aberration in untreated chronic lymphocytic leukemia (CLL) at advanced stages. Leuk. Res. *34*, 63–68.

Chapiro, E., Lesty, C., Gabillaud, C., Durot, E., Bouzy, S., Armand, M., Le Garff-Tavernier, M., Bougacha, N., Struski, S., Bidet, A., et al. (2018). "Double-hit" chronic lymphocytic leukemia: An aggressive subgroup with 17p deletion and 8q24 gain. Am. J. Hematol. *93*, 375–382.

Chen, C., Edelstein, L.C., and Gélinas, C. (2000). The Rel/NF-kappaB family directly activates expression of the apoptosis inhibitor Bcl-x(L). Mol. Cell. Biol. *20*, 2687–2695.

Chen, F.E., Huang, D.B., Chen, Y.Q., and Ghosh, G. (1998). Crystal structure of p50/p65 heterodimer of transcription factor NF-kappaB bound to DNA. Nature *391*, 410–413.

Chen, G., Hardy, K., Bunting, K., Daley, S., Ma, L., and Shannon, M.F. (2010). Regulation of the IL-21 Gene by the NF- B Transcription Factor c-Rel. J. Immunol. *185*, 2350–2359.

Chen, L., Widhopf, G., Huynh, L., Rassenti, L., Rai, K.R., Weiss, A., and Kipps, T.J. (2002). Expression of ZAP-70 is associated with increased B-cell receptor signaling in chronic lymphocytic leukemia. Blood *100*, 4609–4614.

Chen, L., Alexe, G., Dharia, N. V, Ross, L., Iniguez, A.B., Conway, A.S., Wang, E.J., Veschi, V., Lam, N., Qi, J., et al. (2018). CRISPR-Cas9 screen reveals a MYCN-

amplified neuroblastoma dependency on EZH2. J. Clin. Invest. *128*, 446–462.

Cheng, S., Hsia, C.Y., Leone, G., and Liou, H.-C. (2003). Cyclin E and Bcl-xL cooperatively induce cell cycle progression in c-Rel–/– B cells. Oncogene *22*, 8472–8486.

Chiarle, R., Gong, J.Z., Guasparri, I., Pesci, A., Cai, J., Liu, J., Simmons, W.J., Dhall, G., Howes, J., Piva, R., et al. (2003). NPM-ALK transgenic mice spontaneously develop T-cell lymphomas and plasma cell tumors. Blood *101*, 1919–1927.

Chin, M., Herscovitch, M., Zhang, N., Waxman, D.J., and Gilmore, T.D. (2009). Overexpression of an activated REL mutant enhances the transformed state of the human B-lymphoma BJAB cell line and alters its gene expression profile. Oncogene *28*, 2100–2111.

Chiorazzi, N., Rai, K.R., and Ferrarini, M. (2005). Chronic Lymphocytic Leukemia. N. Engl. J. Med. *352*, 804–815.

Chitalia, A., Swoboda, D.M., McCutcheon, J.N., Ozdemirli, M., Khan, N., and Cheson, B.D. (2019). Descriptive analysis of genetic aberrations and cell of origin in Richter transformation. Leuk. Lymphoma 1–9.

Christie, K.A., Courtney, D.G., DeDionisio, L.A., Shern, C.C., De Majumdar, S., Mairs, L.C., Nesbit, M.A., and Moore, C.B.T. (2017). Towards personalised allele-specific CRISPR gene editing to treat autosomal dominant disorders. Sci. Rep. *7*, 16174.

Coscia, M., Pantaleoni, F., Riganti, C., Vitale, C., Rigoni, M., Peola, S., Castella, B., Foglietta, M., Griggio, V., Drandi, D., et al. (2011). IGHV unmutated CLL B cells are more prone to spontaneous apoptosis and subject to environmental prosurvival signals than mutated CLL B cells. Leukemia *25*, 828–837.

Cosson, A., Chapiro, E., Bougacha, N., Lambert, J., Herbi, L., Cung, H.-A., Algrin, C., Keren, B., Damm, F., Gabillaud, C., et al. (2017). Gain in the short arm of chromosome 2 (2p+) induces gene overexpression and drug resistance in chronic lymphocytic leukemia: Analysis of the central role of XPO1. Leukemia *31*.

Cumano, A., and Godin, I. (2007). Ontogeny of the Hematopoietic System. Annu. Rev. Immunol. *25*, 745–785.

Cuní, S., Pérez-Aciego, P., Pérez-Chacón, G., Vargas, J.A., Sánchez, A., Martín-Saavedra, F.M., Ballester, S., García-Marco, J., Jordá, J., and Durántez, A. (2004). A sustained activation of PI3K/NF-κB pathway is critical for the survival of chronic lymphocytic leukemia B cells. Leukemia *18*, 1391–1400.

Curry, C. V, Ewton, A.A., Olsen, R.J., Logan, B.R., Preti, H.A., Liu, Y.-C., Perkins, S.L., and Chang, C.-C. (2009). Prognostic impact of C-REL expression in diffuse large B-cell lymphoma. J. Hematop. *2*, 20–26.

Czabotar, P.E., Lessene, G., Strasser, A., and Adams, J.M. (2014). Control of apoptosis by the BCL-2 protein family: implications for physiology and therapy. Nat. Rev. Mol. Cell Biol. *15*, 49–63.

D'Arcy, M. (2019). Cell Death. A review of the major forms of Apoptosis, Necrosis and Autophagy. Cell Biol. Int. cbin.11137.

Damle, R.N., Wasil, T., Fais, F., Ghiotto, F., Valetto, A., Allen, S.L., Buchbinder, A.,

Budman, D., Dittmar, K., Kolitz, J., et al. (1999). Ig V gene mutation status and CD38 expression as novel prognostic indicators in chronic lymphocytic leukemia. Blood *94*, 1840–1847.

Damm, F., Mylonas, E., Cosson, A., Yoshida, K., Della Valle, V., Mouly, E., Diop, M., Scourzic, L., Shiraishi, Y., Chiba, K., et al. (2014). Acquired initiating mutations in early hematopoietic cells of CLL patients. Cancer Discov. *4*, 1088–1101.

Dancescu, M., Rubio-Trujillo, M., Biron, G., Bron, D., Delespesse, G., and Sarfati, M. (1992). Interleukin 4 protects chronic lymphocytic leukemic B cells from death by apoptosis and upregulates Bcl-2 expression. J. Exp. Med. *176*, 1319–1326.

Davis, R.E., Ngo, V.N., Lenz, G., Tolar, P., Young, R.M., Romesser, P.B., Kohlhammer, H., Lamy, L., Zhao, H., Yang, Y., et al. (2010). Chronic active B-cell-receptor signalling in diffuse large B-cell lymphoma. Nature *463*, 88–92.

Deambrogi, C., De Paoli, L., Fangazio, M., Cresta, S., Rasi, S., Spina, V., Gattei, V., Gaidano, G., and Rossi, D. (2010). Analysis of the REL, BCL11A, and MYCN proto-oncogenes belonging to the 2p amplicon in chronic lymphocytic leukemia. Am. J. Hematol. *85*, 541–544.

Decker, T., Pasca di Magliano, M., McManus, S., Sun, Q., Bonifer, C., Tagoh, H., and Busslinger, M. (2009). Stepwise Activation of Enhancer and Promoter Regions of the B Cell Commitment Gene Pax5 in Early Lymphopoiesis. Immunity *30*, 508–520.

DeFranco, A.L. (2016). The germinal center antibody response in health and disease. F1000Research *5*.

Deltcheva, E., Chylinski, K., Sharma, C.M., Gonzales, K., Chao, Y., Pirzada, Z.A., Eckert, M.R., Vogel, J., and Charpentier, E. (2011). CRISPR RNA maturation by trans-encoded small RNA and host factor RNase III. Nature *471*, 602–607.

Ding, J., Miao, Z.-H., Meng, L.-H., and Geng, M.-Y. (2006). Emerging cancer therapeutic opportunities target DNA-repair systems. Trends Pharmacol. Sci. *27*, 338–344.

Diouf, B., Cheng, Q., Krynetskaia, N.F., Yang, W., Cheok, M., Pei, D., Fan, Y., Cheng, C., Krynetskiy, E.Y., Geng, H., et al. (2011). Somatic deletions of genes regulating MSH2 protein stability cause DNA mismatch repair deficiency and drug resistance in human leukemia cells. Nat. Med. *17*, 1298–1303.

Doench, J.G. (2017). Am I ready for CRISPR? A user's guide to genetic screens. Nat. Rev. Genet.

Döhner, H., Stilgenbauer, S., James, M.R., Benner, A., Weilguni, T., Bentz, M., Fischer, K., Hunstein, W., and Lichter, P. (1997). 11q deletions identify a new subset of B-cell chronic lymphocytic leukemia characterized by extensive nodal involvement and inferior prognosis. Blood *89*, 2516–2522.

Döhner, H., Stilgenbauer, S., Benner, A., Leupolt, E., Kröber, A., Bullinger, L., Döhner, K., Bentz, M., and Lichter, P. (2000). Genomic Aberrations and Survival in Chronic Lymphocytic Leukemia. N. Engl. J. Med. *343*, 1910–1916.

Dong, H., Shi, P., Zhou, Y., Yu, Y., Guo, X., Yao, Y., Liu, P., and Xu, B. (2017). High BCL11A Expression in Adult Acute Myeloid Leukemia Patients Predicts a Worse Clinical Outcome. Clin. Lab. *63*.

Douglas, R.S., Capocasale, R.J., Lamb, R.J., Nowell, P.C., and Moore, J.S. (1997). Chronic Lymphocytic Leukemia B Cells Are Resistant to the Apoptotic Effects of Transforming Growth Factor-β. Blood *89*.

Dranoff, G. (2004). Cytokines in cancer pathogenesis and cancer therapy. Nat. Rev. Cancer *4*, 11–22.

Drexler, H.G., and Matsuo, Y. (2000). Malignant hematopoietic cell lines: in vitro models for the study of multiple myeloma and plasma cell leukemia. Leuk. Res. *24*, 681–703.

Dubois, S., Viailly, P.-J., Mareschal, S., Bohers, E., Bertrand, P., Ruminy, P., Maingonnat, C., Jais, J.-P., Peyrouze, P., Figeac, M., et al. (2016). Next-Generation Sequencing in Diffuse Large B-Cell Lymphoma Highlights Molecular Divergence and Therapeutic Opportunities: a LYSA Study. Clin. Cancer Res. *22*, 2919–2928.

Duprez, L., Wirawan, E., Berghe, T. Vanden, and Vandenabeele, P. (2009). Major cell death pathways at a glance. Microbes Infect. *11*, 1050–1062.

Dürig, J., Nückel, H., Hüttmann, A., Kruse, E., Hölter, T., Halfmeyer, K., Führer, A., Rudolph, R., Kalhori, N., Nusch, A., et al. (2003). Expression of ribosomal and translation-associated genes is correlated with a favorable clinical course in chronic lymphocytic leukemia. Blood *101*, 2748–2755.

Dyer, M.J.S. (2003). The pathogenetic role of oncogenes deregulated by chromosomal translocation in B-cell malignancies. Int. J. Hematol. *77*, 315–320.

Edelmann, J., Holzmann, K., Miller, F., Winkler, D., Bühler, A., Zenz, T., Bullinger, L., Kühn, M.W.M., Gerhardinger, A., Bloehdorn, J., et al. (2012). High-resolution genomic profiling of chronic lymphocytic leukemia reveals new recurrent genomic alterations. Blood *120*, 4783–4794.

Edwards, J.C.W., and Cambridge, G. (2006). B-cell targeting in rheumatoid arthritis and other autoimmune diseases. Nat. Rev. Immunol. *6*, 394–403.

Elmore, S. (2007). Apoptosis: A Review of Programmed Cell Death. Toxicol. Pathol. *35*, 495–516.

Enciso-Mora, V., Broderick, P., Ma, Y., Jarrett, R.F., Hjalgrim, H., Hemminki, K., van den Berg, A., Olver, B., Lloyd, A., Dobbins, S.E., et al. (2010). A genome-wide association study of Hodgkin's lymphoma identifies new susceptibility loci at 2p16.1 (REL), 8q24.21 and 10p14 (GATA3). Nat. Genet. *42*, 1126–1130.

Ernst, J., Kheradpour, P., Mikkelsen, T.S., Shoresh, N., Ward, L.D., Epstein, C.B., Zhang, X., Wang, L., Issner, R., Coyne, M., et al. (2011). Mapping and analysis of chromatin state dynamics in nine human cell types. Nature *473*, 43–49.

Etchin, J., Berezovskaya, A., Conway, A.S., Galinsky, I.A., Stone, R.M., Baloglu, E., Senapedis, W., Landesman, Y., Kauffman, M., Shacham, S., et al. (2017). KPT-8602, a second-generation inhibitor of XPO1-mediated nuclear export, is well tolerated and highly active against AML blasts and leukemia-initiating cells. Leukemia *31*, 143–150.

Everett, P.C., Meyers, J.A., Makkinje, A., Rabbi, M., and Lerner, A. (2007). Preclinical assessment of curcumin as a potential therapy for B-CLL. Am. J. Hematol. *82*, 23–30.

Fabbri, G., and Dalla-Favera, R. (2016). The molecular pathogenesis of chronic lymphocytic leukaemia. Nat. Rev. Cancer *16*.

Fabbri, G., Rasi, S., Rossi, D., Trifonov, V., Khiabanian, H., Ma, J., Grunn, A., Fangazio, M., Capello, D., Monti, S., et al. (2011). Analysis of the chronic lymphocytic leukemia coding genome: role of NOTCH1 mutational activation. J. Exp. Med. *208*, 1389–1401.

Fabbri, G., Khiabanian, H., Holmes, A.B., Wang, J., Messina, M., Mullighan, C.G., Pasqualucci, L., Rabadan, R., and Dalla-Favera, R. (2013). Genetic lesions associated with chronic lymphocytic leukemia transformation to Richter syndrome. J. Exp. Med. *210*, 2273–2288.

Fabris, S., Mosca, L., Cutrona, G., Lionetti, M., Agnelli, L., Ciceri, G., Barbieri, M., Maura, F., Matis, S., Colombo, M., et al. (2013). Chromosome 2p gain in monoclonal B-cell lymphocytosis and in early stage chronic lymphocytic leukemia. Am. J. Hematol. *88*, 24–31.

Faderl, S., Rai, K., Gribben, J., Byrd, J.C., Flinn, I.W., O'Brien, S., Sheng, S., Esseltine, D.-L., and Keating, M.J. (2006). Phase II study of single-agent bortezomib for the treatment of patients with fludarabine-refractory B-cell chronic lymphocytic leukemia. Cancer *107*, 916–924.

Fadok, V.A., de Cathelineau, A., Daleke, D.L., Henson, P.M., and Bratton, D.L. (2001a). Loss of Phospholipid Asymmetry and Surface Exposure of Phosphatidylserine Is Required for Phagocytosis of Apoptotic Cells by Macrophages and Fibroblasts. J. Biol. Chem. *276*, 1071–1077.

Fadok, V.A., Bratton, D.L., Guthrie, L., and Henson, P.M. (2001b). Differential effects of apoptotic versus lysed cells on macrophage production of cytokines: role of proteases. J. Immunol. *166*, 6847–6854.

Fagerlund, R., Melén, K., Cao, X., and Julkunen, I. (2008). NF-kappaB p52, RelB and c-Rel are transported into the nucleus via a subset of importin alpha molecules. Cell. Signal. *20*, 1442–1451.

Fama, R., Bomben, R., Rasi, S., Dal Bo, M., Ciardullo, C., Monti, S., Rossi, F., D'Agaro, T., Zucchetto, A., Gattei, V., et al. (2014). Ibrutinib-naive chronic lymphocytic leukemia lacks Bruton tyrosine kinase mutations associated with treatment resistance. Blood *124*, 3831–3833.

Fan, G., Fan, Y., Gupta, N., Matsuura, I., Liu, F., Zhou, X.Z., Lu, K.P., and Gelinas, C. (2009). Peptidyl-Prolyl Isomerase Pin1 Markedly Enhances the Oncogenic Activity of the Rel Proteins in the Nuclear Factor- B Family. Cancer Res. *69*, 4589–4597.

Farh, K.K.-H., Marson, A., Zhu, J., Kleinewietfeld, M., Housley, W.J., Beik, S., Shoresh, N., Whitton, H., Ryan, R.J.H., Shishkin, A.A., et al. (2015). Genetic and epigenetic fine mapping of causal autoimmune disease variants. Nature *518*, 337–343.

Faria, A.V.S., Tornatore, T.F., Milani, R., Queiroz, K.C.S., Sampaio, I.H., Fonseca, E.M.B., Rocha-Brito, K.J.P., Santos, T.O., Silveira, L.R., Peppelenbosch, M.P., et al. (2017). Oncophosphosignaling Favors a Glycolytic Phenotype in Human Drug Resistant Leukemia. J. Cell. Biochem. *118*, 3846–3854.

Farooqui, M.Z.H., Valdez, J., Martyr, S., Aue, G., Saba, N., Niemann, C.U., Herman,

S.E.M., Tian, X., Marti, G., Soto, S., et al. (2015). Ibrutinib for previously untreated and relapsed or refractory chronic lymphocytic leukaemia with TP53 aberrations: a phase 2, single-arm trial. Lancet Oncol. *16*, 169–176.

Fellmann, C., Gowen, B.G., Lin, P.-C., Doudna, J.A., and Corn, J.E. (2017). Cornerstones of CRISPR–Cas in drug discovery and therapy. Nat. Rev. Drug Discov. *16*, 89–100.

Ferreri, A.J.M., Govi, S., Pileri, S.A., and Savage, K.J. (2012). Anaplastic large cell lymphoma, ALK-positive. Crit. Rev. Oncol. / Hematol. *83*, 293–302.

Feuerhake, F., Kutok, J.L., Monti, S., Chen, W., LaCasce, A.S., Cattoretti, G., Kurtin, P., Pinkus, G.S., de Leval, L., Harris, N.L., et al. (2005). NFkappaB activity, function, and target-gene signatures in primary mediastinal large B-cell lymphoma and diffuse large B-cell lymphoma subtypes. Blood *106*, 1392–1399.

Fix, A., Lucchesi, C., Ribeiro, A., Lequin, D., Pierron, G., Schleiermacher, G., Delattre, O., and Janoueix-Lerosey, I. (2008). Characterization of amplicons in neuroblastoma: high-resolution mapping using DNA microarrays, relationship with outcome, and identification of overexpressed genes. Genes. Chromosomes Cancer *47*, 819–834.

Flinn, I.W., Hillmen, P., Montillo, M., Nagy, Z., Illés, Á., Etienne, G., Delgado, J., Kuss, B.J., Tam, C.S., Gasztonyi, Z., et al. (2018). The phase 3 DUO trial: duvelisib vs ofatumumab in relapsed and refractory CLL/SLL. Blood *132*, 2446–2455.

Fornerod, M., Ohno, M., Yoshida, M., and Mattaj, I.W. (1997). CRM1 is an export receptor for leucine-rich nuclear export signals. Cell *90*, 1051–1060.

Fu, L., Lin-Lee, Y.-C., Pham, L. V, Tamayo, A., Yoshimura, L., and Ford, R.J. (2006). Constitutive NF-kappaB and NFAT activation leads to stimulation of the BLyS survival pathway in aggressive B-cell lymphomas. Blood *107*, 4540–4548.

Fu, Y., Foden, J.A., Khayter, C., Maeder, M.L., Reyon, D., Joung, J.K., and Sander, J.D. (2013). High-frequency off-target mutagenesis induced by CRISPR-Cas nucleases in human cells. Nat. Biotechnol. *31*, 822–826.

Fuentes-Prior, P., and Salvesen, G.S. (2004). The protein structures that shape caspase activity, specificity, activation and inhibition. Biochem. J. *384*, 201–232.

Fukuhara, N., Tagawa, H., Kameoka, Y., Kasugai, Y., Karnan, S., Kameoka, J., Sasaki, T., Morishima, Y., Nakamura, S., and Seto, M. (2006). Characterization of target genes at the 2p15-16 amplicon in diffuse large B-cell lymphoma. Cancer Sci. *97*, 499–504.

Furman, R.R., Asgary, Z., Mascarenhas, J.O., Liou, H.C., and Schattner, E.J. (2000). Modulation of NF-kappa B activity and apoptosis in chronic lymphocytic leukemia B cells. J. Immunol. *164*, 2200–2206.

Furman, R.R., Sharman, J.P., Coutre, S.E., Cheson, B.D., Pagel, J.M., Hillmen, P., Barrientos, J.C., Zelenetz, A.D., Kipps, T.J., Flinn, I., et al. (2014). Idelalisib and Rituximab in Relapsed Chronic Lymphocytic Leukemia. N. Engl. J. Med. *370*, 997–1007.

Galloway, J.L., and Zon, L.I. (2003). 3 Ontogeny of hematopoiesis: Examining the emergence of hematopoietic cells in the vertebrate embryo. Curr. Top. Dev. Biol. *53*, 139–158.

Galton, D.A.G., Goldman, J.M., Wiltshaw, E., Catovsky, D., Henry, K., and Goldenberg, G.J. (1974). Prolymphocytic Leukaemia. Br. J. Haematol. *27*, 7–23.

Gao, Y., Wu, H., He, D., Hu, X., and Li, Y. (2013). Downregulation of BCL11A by siRNA induces apoptosis in B lymphoma cell lines. Biomed. Reports *1*, 47–52.

García-Tuñón, I., Hernández-Sánchez, M., Ordoñez, J.L., Alonso-Pérez, V., Álamo-Quijada, M., Benito, R., Guerrero, C., Hernández-Rivas, J.M., and Sánchez-Martín, M. (2017). The CRISPR/Cas9 system efficiently reverts the tumorigenic ability of <i>BCR/ABL in vitro</i> and in a xenograft model of chronic myeloid leukemia. Oncotarget *8*, 26027–26040.

Garneau, J.E., Dupuis, M.-È., Villion, M., Romero, D.A., Barrangou, R., Boyaval, P., Fremaux, C., Horvath, P., Magadán, A.H., and Moineau, S. (2010). The CRISPR/Cas bacterial immune system cleaves bacteriophage and plasmid DNA. Nature *468*, 67–71.

Gasiunas, G., Barrangou, R., Horvath, P., and Siksnys, V. (2012). Cas9-crRNA ribonucleoprotein complex mediates specific DNA cleavage for adaptive immunity in bacteria. Proc. Natl. Acad. Sci. *109*, E2579–E2586.

Geismann, C., Grohmann, F., Sebens, S., Wirths, G., Dreher, A., Häsler, R., Rosenstiel, P., Hauser, C., Egberts, J.-H., Trauzold, A., et al. (2014). c-Rel is a critical mediator of NF-κB-dependent TRAIL resistance of pancreatic cancer cells. Cell Death Dis. *5*, e1455.

Gellert, M. (2002). V(D)J Recombination: RAG Proteins, Repair Factors, and Regulation. Annu. Rev. Biochem. *71*, 101–132.

Gerondakis, S., Grumont, R., Gugasyan, R., Wong, L., Isomura, I., Ho, W., and Banerjee, A. (2006). Unravelling the complexities of the NF-kappaB signalling pathway using mouse knockout and transgenic models. Oncogene *25*, 6781–6799.

Gesner, E.M., Schellenberg, M.J., Garside, E.L., George, M.M., and MacMillan, A.M. (2011). Recognition and maturation of effector RNAs in a CRISPR interference pathway. Nat. Struct. Mol. Biol. *18*, 688–692.

Ghamlouch, H., Ouled-Haddou, H., Damaj, G., Royer, B., Gubler, B., and Marolleau, J.-P. (2013). A Combination of Cytokines Rescues Highly Purified Leukemic CLL B-Cells from Spontaneous Apoptosis In Vitro. PLoS One *8*, e60370.

Ghia, P., and Hallek, M. (2014). Management of chronic lymphocytic leukemia. Haematologica *99*, 965–972.

Gieling, R.G., Elsharkawy, A.M., Caamaño, J.H., Cowie, D.E., Wright, M.C., Ebrahimkhani, M.R., Burt, A.D., Mann, J., Raychaudhuri, P., Liou, H.-C., et al. (2010). The c-Rel subunit of nuclear factor-kappaB regulates murine liver inflammation, wound-healing, and hepatocyte proliferation. Hepatology *51*, 922–931.

Gilbert, L.A., Larson, M.H., Morsut, L., Liu, Z., Brar, G.A., Torres, S.E., Stern-Ginossar, N., Brandman, O., Whitehead, E.H., Doudna, J.A., et al. (2013). CRISPR-Mediated Modular RNA-Guided Regulation of Transcription in Eukaryotes. Cell *154*, 442–451.

Gilbert, L.A., Horlbeck, M.A., Adamson, B., Villalta, J.E., Chen, Y., Whitehead, E.H., Guimaraes, C., Panning, B., Ploegh, H.L., Bassik, M.C., et al. (2014). Genome-Scale CRISPR-Mediated Control of Gene Repression and Activation. Cell *159*, 647–661.

Gilling, C.E., Mittal, A.K., Chaturvedi, N.K., Iqbal, J., Aoun, P., Bierman, P.J., Bociek, R.G., Weisenburger, D.D., and Joshi, S.S. (2012). Lymph node-induced immune tolerance in chronic lymphocytic leukaemia: a role for caveolin-1. Br. J. Haematol. *158*, 216–231.

Gilmore, T.D. (2006). Introduction to NF-κB: players, pathways, perspectives. Oncogene *25*, 6680–6684.

Gilmore, T.D., and Gerondakis, S. (2011). The c-Rel Transcription Factor in Development and Disease. Genes Cancer *2*, 695–711.

Gilmore, T.D., and Herscovitch, M. (2006). Inhibitors of NF-kappaB signaling: 785 and counting. Oncogene *25*, 6887–6899.

Gilmore, T.D., Kalaitzidis, D., Liang, M.-C., and Starczynowski, D.T. (2004). The c-Rel transcription factor and B-cell proliferation: a deal with the devil. Oncogene *23*, 2275–2286.

Del Giudice, I., Rossi, D., Chiaretti, S., Marinelli, M., Tavolaro, S., Gabrielli, S., Laurenti, L., Marasca, R., Rasi, S., Fangazio, M., et al. (2012). NOTCH1 mutations in +12 chronic lymphocytic leukemia (CLL) confer an unfavorable prognosis, induce a distinctive transcriptional profiling and refine the intermediate prognosis of +12 CLL. Haematologica *97*, 437–441.

Glavinas, H., Krajcsi, P., Cserepes, J., and Sarkadi, B. (2004). The Role of ABC Transporters in Drug Resistance, Metabolism and Toxicity. Curr. Drug Deliv. *1*, 27–42.

Gogolin, S., Batra, R., Harder, N., Ehemann, V., Paffhausen, T., Diessl, N., Sagulenko, V., Benner, A., Gade, S., Nolte, I., et al. (2013). MYCN-mediated overexpression of mitotic spindle regulatory genes and loss of p53-p21 function jointly support the survival of tetraploid neuroblastoma cells. Cancer Lett. *331*, 35–45.

Goldin, L.R., Pfeiffer, R.M., Li, X., and Hemminki, K. (2004). Familial risk of lymphoproliferative tumors in families of patients with chronic lymphocytic leukemia: results from the Swedish Family-Cancer Database. Blood *104*, 1850–1854.

Göllner, S., Oellerich, T., Agrawal-Singh, S., Schenk, T., Klein, H.-U., Rohde, C., Pabst, C., Sauer, T., Lerdrup, M., Tavor, S., et al. (2017). Loss of the histone methyltransferase EZH2 induces resistance to multiple drugs in acute myeloid leukemia. Nat. Med. *23*, 69–78.

Green, D.R., and Llambi, F. (2015). Cell Death Signaling. Cold Spring Harb. Perspect. Biol. *7*, a006080.

Grinberg-Bleyer, Y., Oh, H., Desrichard, A., Bhatt, D.M., Caron, R., Chan, T.A., Schmid, R.M., Klein, U., Hayden, M.S., and Ghosh, S. (2017). NF-κB c-Rel Is Crucial for the Regulatory T Cell Immune Checkpoint in Cancer. Cell *170*, 1096–1108.e13.

Grossmann, M., O'Reilly, L.A., Gugasyan, R., Strasser, A., Adams, J.M., and Gerondakis, S. (2000). The anti-apoptotic activities of Rel and RelA required during B-cell maturation involve the regulation of Bcl-2 expression. EMBO J. *19*, 6351–6360.

Grumont, R.J., and Gerondakis, S. (1994). The subunit composition of NF-kappa B complexes changes during B-cell development. Cell Growth Differ. *5*, 1321–1331.

Grumont, R.J., and Gerondakis, S. (2000). Rel induces interferon regulatory factor 4 (IRF-4) expression in lymphocytes: modulation of interferon-regulated gene expression by rel/nuclear factor kappaB. J. Exp. Med. *191*, 1281–1292.

Grumont, R.J., Richardson, I.B., Gaff, C., and Gerondakis, S. (1993). rel/NF-kappa B nuclear complexes that bind kB sites in the murine c-rel promoter are required for constitutive c-rel transcription in B-cells. Cell Growth Differ. *4*, 731–743.

Grumont, R.J., Rourke, I.J., O'Reilly, L.A., Strasser, A., Miyake, K., Sha, W., and Gerondakis, S. (1998). B lymphocytes differentially use the Rel and nuclear factor kappaB1 (NF-kappaB1) transcription factors to regulate cell cycle progression and apoptosis in quiescent and mitogen-activated cells. J. Exp. Med. *187*, 663–674.

Grumont, R.J., Strasser, A., and Gerondakis, S. (2002). B cell growth is controlled by phosphatidylinosotol 3-kinase-dependent induction of Rel/NF-kappaB regulated c-myc transcription. Mol. Cell *10*, 1283–1294.

Guarini, A., Chiaretti, S., Tavolaro, S., Maggio, R., Peragine, N., Citarella, F., Ricciardi, M.R., Santangelo, S., Marinelli, M., De Propris, M.S., et al. (2008). BCR ligation induced by IgM stimulation results in gene expression and functional changes only in IgV H unmutated chronic lymphocytic leukemia (CLL) cells. Blood *112*, 782–792.

Guièze, R., and Wu, C.J. (2015). Genomic and epigenomic heterogeneity in chronic lymphocytic leukemia. Blood *126*, 445–453.

Gunnarsson, R., Mansouri, L., Isaksson, A., Göransson, H., Cahill, N., Jansson, M., Rasmussen, M., Lundin, J., Norin, S., Buhl, A.M., et al. (2011). Array-based genomic screening at diagnosis and during follow-up in chronic lymphocytic leukemia. Haematologica *96*, 1161–1169.

Gupta, S.C., Sundaram, C., Reuter, S., and Aggarwal, B.B. (2010). Inhibiting NF-κB activation by small molecules as a therapeutic strategy. BBA - Gene Regul. Mech. *1799*, 775–787.

Guruharsha, K.G., Kankel, M.W., and Artavanis-Tsakonas, S. (2012). The Notch signalling system: recent insights into the complexity of a conserved pathway. Nat. Rev. Genet. *13*, 654–666.

ten Hacken, E., and Burger, J.A. (2014). Molecular Pathways: Targeting the Microenvironment in Chronic Lymphocytic Leukemia—Focus on the B-Cell Receptor. Clin. Cancer Res. *20*, 548–556.

ten Hacken, E., Gounari, M., Ghia, P., and Burger, J.A. (2019). The importance of B cell receptor isotypes and stereotypes in chronic lymphocytic leukemia. Leukemia *33*, 287–298.

Hallek, M., Cheson, B.D., Catovsky, D., Caligaris-Cappio, F., Dighiero, G., Döhner, H., Hillmen, P., Keating, M., Montserrat, E., Chiorazzi, N., et al. (2018). Guidelines for diagnosis, indications for treatment, response assessment and supportive management of chronic lymphocytic leukemia. Blood *131*, blood-2017-09-806398.

Hallek, M. (2019). Chronic lymphocytic leukemia: 2020 update on diagnosis, risk stratification and treatment. Am J Hematol *94*, 1266–1287.

Hamblin, T.J., Davis, Z., Gardiner, A., Oscier, D.G., and Stevenson, F.K. (1999). Unmutated Ig V(H) genes are associated with a more aggressive form of chronic

lymphocytic leukemia. Blood *94*, 1848–1854.

Hanahan, D., and Weinberg, R.A. (2011). Hallmarks of Cancer: The Next Generation. Cell *144*, 646–674.

Hancarova, M., Simandlova, M., Drabova, J., Mannik, K., Kurg, A., and Sedlacek, Z. (2013). A patient with de novo 0.45 Mb deletion of 2p16.1: The role of ***BCL11A*** , ***PAPOLG*** , ***REL*** , and ***FLJ16341*** in the 2p15-p16.1 microdeletion syndrome. Am. J. Med. Genet. Part A *161*, 865–870.

Hansford, L.M., Thomas, W.D., Keating, J.M., Burkhart, C.A., Peaston, A.E., Norris, M.D., Haber, M., Armati, P.J., Weiss, W.A., and Marshall, G.M. (2004). Mechanisms of embryonal tumor initiation: distinct roles for MycN expression and MYCN amplification. Proc. Natl. Acad. Sci. U. S. A. *101*, 12664–12669.

Hardy, R.R., Kincade, P.W., and Dorshkind, K. (2007). The Protean Nature of Cells in the B Lymphocyte Lineage. Immunity *26*, 703–714.

Harrington, L.B., Doxzen, K.W., Ma, E., Liu, J.-J., Knott, G.J., Edraki, A., Garcia, B., Amrani, N., Chen, J.S., Cofsky, J.C., et al. (2017). A Broad-Spectrum Inhibitor of CRISPR-Cas9. Cell *170*, 1224–1233.e15.

Hasan, M.K., Nafady, A., Takatori, A., Kishida, S., Ohira, M., Suenaga, Y., Hossain, S., Akter, J., Ogura, A., Nakamura, Y., et al. (2013). ALK is a MYCN target gene and regulates cell migration and invasion in neuroblastoma. Sci. Rep. *3*, 3450.

Hatoum-Aslan, A., Maniv, I., and Marraffini, L.A. (2011). Mature clustered, regularly interspaced, short palindromic repeats RNA (crRNA) length is measured by a ruler mechanism anchored at the precursor processing site. Proc. Natl. Acad. Sci. U. S. A. *108*, 21218–21222.

Haurwitz, R.E., Jinek, M., Wiedenheft, B., Zhou, K., and Doudna, J.A. (2010). Sequence- and structure-specific RNA processing by a CRISPR endonuclease. Science *329*, 1355–1358.

Hayden, M.S., and Ghosh, S. (2012). NF- B, the first quarter-century: remarkable progress and outstanding questions. Genes Dev. *26*, 203–234.

Heckl, D., Kowalczyk, M.S., Yudovich, D., Belizaire, R., Puram, R. V, McConkey, M.E., Thielke, A., Aster, J.C., Regev, A., and Ebert, B.L. (2014). Generation of mouse models of myeloid malignancy with combinatorial genetic lesions using CRISPR-Cas9 genome editing. Nat. Biotechnol. *32*, 941–946.

Heise, N., De Silva, N.S., Silva, K., Carette, A., Simonetti, G., Pasparakis, M., and Klein, U. (2014). Germinal center B cell maintenance and differentiation are controlled by distinct NF-κB transcription factor subunits. J. Exp. Med. *211*, 2103–2118.

Henssen, A., Althoff, K., Odersky, A., Beckers, A., Koche, R., Speleman, F., Scha fers, S., Bell, E., Nortmeyer, M., Westermann, F., et al. (2016). Targeting MYCN-Driven Transcription By BET-Bromodomain Inhibition. Clin. Cancer Res. *22*, 2470–2481.

Herishanu, Y., Perez-Galan, P., Liu, D., Biancotto, a., Pittaluga, S., Vire, B., Gibellini, F., Njuguna, N., Lee, E., Stennett, L., et al. (2011). The lymph node microenvironment promotes B-cell receptor signaling, NF- B activation, and tumor proliferation in chronic lymphocytic leukemia. Blood *117*, 563–574.

Herling, C.D., Klaumunzer, M., Rocha, C.K., Altmuller, J., Thiele, H., Bahlo, J., Kluth, S., Crispatzu, G., Herling, M., Schiller, J., et al. (2016). Complex karyotypes and KRAS and POT1 mutations impact outcome in CLL after chlorambucil-based chemotherapy or chemoimmunotherapy. Blood *128*, 395–404.

Herling, C.D., Abedpour, N., Weiss, J., Schmitt, A., Jachimowicz, R.D., Merkel, O., Cartolano, M., Oberbeck, S., Mayer, P., Berg, V., et al. (2018). Clonal dynamics towards the development of venetoclax resistance in chronic lymphocytic leukemia. Nat. Commun. *9*, 727.

Herman, S.E.M., Mustafa, R.Z., Gyamfi, J.A., Pittaluga, S., Chang, S., Chang, B., Farooqui, M., and Wiestner, A. (2014). Ibrutinib inhibits BCR and NF- B signaling and reduces tumor proliferation in tissue-resident cells of patients with CLL. Blood *123*, 3286–3295.

Hernández, J.A., Land, K.J., and McKenna, R.W. (1995). Leukemias, myeloma, and other lymphoreticular neoplasms. Cancer *75*, 381–394.

Hernández, L., Pinyol, M., Hernández, S., Beà, S., Pulford, K., Rosenwald, A., Lamant, L., Falini, B., Ott, G., Mason, D.Y., et al. (1999). TRK-fused gene (TFG) is a new partner of ALK in anaplastic large cell lymphoma producing two structurally different TFG-ALK translocations. Blood *94*, 3265–3268.

Herndon, T.M., Chen, S.-S., Saba, N.S., Valdez, J., Emson, C., Gatmaitan, M., Tian, X., Hughes, T.E., Sun, C., Arthur, D.C., et al. (2017). Direct in vivo evidence for increased proliferation of CLL cells in lymph nodes compared to bone marrow and peripheral blood. Leukemia *31*, 1340–1347.

Hertlein, E., Beckwith, K.A., Lozanski, G., Chen, T.L., Towns, W.H., Johnson, A.J., Lehman, A., Ruppert, A.S., Bolon, B., Andritsos, L., et al. (2013). Characterization of a New Chronic Lymphocytic Leukemia Cell Line for Mechanistic In Vitro and In Vivo Studies Relevant to Disease. PLoS One *8*, 1–12.

Hewamana, S., Alghazal, S., Lin, T.T., Clement, M., Jenkins, C., Guzman, M.L., Jordan, C.T., Neelakantan, S., Crooks, P.A., Burnett, A.K., et al. (2008). The NF- B subunit Rel A is associated with in vitro survival and clinical disease progression in chronic lymphocytic leukemia and represents a promising therapeutic target. Blood *111*, 4681–4689.

Hewamana, S., Lin, T.T., Rowntree, C., Karunanithi, K., Pratt, G., Hills, R., Fegan, C., Brennan, P., and Pepper, C. (2009). Rel A Is an Independent Biomarker of Clinical Outcome in Chronic Lymphocytic Leukemia. J. Clin. Oncol. *27*, 763–769.

Heyer, W.-D., Ehmsen, K.T., and Liu, J. (2010). Regulation of homologous recombination in eukaryotes. Annu. Rev. Genet. *44*, 113–139.

Heyman, B., Volkheimer, A.D., and Weinberg, J.B. (2016). Double IGHV DNA gene rearrangements in CLL: influence of mixed-mutated and -unmutated rearrangements on outcomes in CLL. Blood Cancer J. *6*.

Hideshima, T., Neri, P., Tassone, P., Yasui, H., Ishitsuka, K., Raje, N., Chauhan, D., Podar, K., Mitsiades, C., Dang, L., et al. (2006). MLN120B, a Novel I B Kinase Inhibitor, Blocks Multiple Myeloma Cell Growth In vitro and In vivo. Clin. Cancer Res. *12*, 5887–5894.

Hing, Z.A., Mantel, R., Beckwith, K.A., Guinn, D., Williams, E., Smith, L.L., Williams,

K., Johnson, A.J., Lehman, A.M., Byrd, J.C., et al. (2015). Selinexor is effective in acquired resistance to ibrutinib and synergizes with ibrutinib in chronic lymphocytic leukemia. Blood *125*, 3128–3132.

Hing, Z.A., Fung, H.Y.J., Ranganathan, P., Mitchell, S., El-Gamal, D., Woyach, J.A., Williams, K., Goettl, V.M., Smith, J., Yu, X., et al. (2016). Next-generation XPO1 inhibitor shows improved efficacy and in vivo tolerability in hematological malignancies. Leukemia *30*, 2364–2372.

Hirvonen, H., Hukkanen, V., Salmi, T., Makela, T., Pelliniemi, T., Knuutila, S., and Alitalo, R. (1991). Expression of L-myc and N-myc proto-oncogenes in human leukemias and leukemia cell lines. Blood *78*.

Hoesel, B., and Schmid, J.A. (2013). The complexity of NF-κB signaling in inflammation and cancer. Mol. Cancer *12*, 86.

Höfer, T., and Rodewald, H.-R. (2018). Differentiation-based model of hematopoietic stem cell functions and lineage pathways. Blood *132*, 1106–1113.

Horie, R., Watanabe, M., Ishida, T., Koiwa, T., Aizawa, S., Itoh, K., Higashihara, M., Kadin, M.E., and Watanabe, T. (2004). The NPM-ALK oncoprotein abrogates CD30 signaling and constitutive NF-kappaB activation in anaplastic large cell lymphoma. Cancer Cell *5*, 353–364.

Horlbeck, M.A., Gilbert, L.A., Villalta, J.E., Adamson, B., Pak, R.A., Chen, Y., Fields, A.P., Park, C.Y., Corn, J.E., Kampmann, M., et al. (2016). Compact and highly active next-generation libraries for CRISPR-mediated gene repression and activation. Elife *5*.

Houldsworth, J. (2004). Relationship between REL amplification, REL function, and clinical and biologic features in diffuse large B-cell lymphomas. Blood *103*, 1862–1868.

Hsu, P.D., Lander, E.S., and Zhang, F. (2014). Development and Applications of CRISPR-Cas9 for Genome Engineering. Cell *157*, 1262–1278.

Hu, X., Baytak, E., Li, J., Akman, B., Okay, K., Hu, G., Scuto, A., Zhang, W., and Küçük, C. (2017). The relationship of REL proto-oncogene to pathobiology and chemoresistance in follicular and transformed follicular lymphoma. Leuk. Res. *54*, 30–38.

Huang, W., Yue, L., Qiu, W., Wang, L.-W., Zhou, X., and Sun, Y. (2009). Prognostic value of CRM1 in pancreas cancer. Clin. Invest. Med. *32*, E315.

Hui, H., Fuller, K.A., Chuah, H., Liang, J., Sidiqi, H., Radeski, D., and Erber, W.N. (2018). Imaging flow cytometry to assess chromosomal abnormalities in chronic lymphocytic leukaemia. Methods *134–135*, 32–40.

Hunter, J.E., Leslie, J., and Perkins, N.D. (2016). c-Rel and its many roles in cancer: an old story with new twists. Br. J. Cancer *114*, 1–6.

Hyams, G., Abadi, S., Lahav, S., Avni, A., Halperin, E., Shani, E., and Mayrose, I. (2018). CRISPys: Optimal sgRNA Design for Editing Multiple Members of a Gene Family Using the CRISPR System. J. Mol. Biol. *430*, 2184–2195.

Ichim, G., and Tait, S.W.G. (2016). A fate worse than death : apoptosis as an oncogenic process. Nat. Publ. Gr. *16*, 539–548.

Igney, F.H., and Krammer, P.H. (2002). Death and anti-death: tumour resistance to apoptosis. Nat. Rev. Cancer *2*, 277–288.

Ivanovs, A., Rybtsov, S., Welch, L., Anderson, R.A., Turner, M.L., and Medvinsky, A. (2011). Highly potent human hematopoietic stem cells first emerge in the intraembryonic aorta-gonad-mesonephros region. J. Exp. Med. *208*, 2417–2427.

Iwahara, T., Fujimoto, J., Wen, D., Cupples, R., Bucay, N., Arakawa, T., Mori, S., Ratzkin, B., and Yamamoto, T. (1997). Molecular characterization of ALK, a receptor tyrosine kinase expressed specifically in the nervous system. Oncogene *14*, 439–449.

Jagannathan-Bogdan, M., and Zon, L.I. (2013). Hematopoiesis. Development *140*, 2463–2467.

Jain, P., Kanagal-Shamanna, R., Wierda, W., Keating, M., Sarwari, N., Rozovski, U., Thompson, P., Burger, J., Kantarjian, H., Patel, K.P., et al. (2016). Clinical and molecular characteristics of XPO1 mutations in patients with chronic lymphocytic leukemia. Am. J. Hematol. *91*, E478–E479.

Jain, P., Nogueras González, G.M., Kanagal-Shamanna, R., Rozovski, U., Sarwari, N., Tam, C., Wierda, W.G., Thompson, P.A., Jain, N., Luthra, R., et al. (2018). The absolute percent deviation of IGHV mutation rather than a 98% cut-off predicts survival of chronic lymphocytic leukaemia patients treated with fludarabine, cyclophosphamide and rituximab. Br. J. Haematol. *180*, 33–40.

Jaitin, D.A., Weiner, A., Yofe, I., Lara-Astiaso, D., Keren-Shaul, H., David, E., Salame, T.M., Tanay, A., van Oudenaarden, A., and Amit, I. (2016). Dissecting Immune Circuits by Linking CRISPR-Pooled Screens with Single-Cell RNA-Seq. Cell *167*, 1883–1896.e15.

Jansen, R., Embden, J.D.A. van, Gaastra, W., and Schouls, L.M. (2002). Identification of genes that are associated with DNA repeats in prokaryotes. Mol. Microbiol. *43*, 1565–1575.

Jardin, F., Pujals, A., Pelletier, L., Bohers, E., Camus, V., Mareschal, S., Dubois, S., Sola, B., Ochmann, M., Lemonnier, F., et al. (2016). Recurrent mutations of the exportin 1 gene (XPO1) and their impact on selective inhibitor of nuclear export compounds sensitivity in primary mediastinal B-cell lymphoma. Am. J. Hematol. *91*, 923–930.

Jarosova, M., Urbankova, H., Plachy, R., Papajik, T., Holzerova, M., Balcarkova, J., Pikalova, Z., Divoky, V., and Indrak, K. (2010). Gain of chromosome 2p in chronic lymphocytic leukemia: significant heterogeneity and a new recurrent dicentric rearrangement. Leuk. Lymphoma *51*, 304–313.

Jarosova, M., Hruba, M., Oltova, A., Plevova, K., Kruzova, L., Kriegova, E., Fillerova, R., Koritakova, E., Doubek, M., Lysak, D., et al. (2017). Chromosome 6q deletion correlates with poor prognosis and low relative expression of *FOXO3* in chronic lymphocytic leukemia patients. Am. J. Hematol. *92*, E604–E607.

Jarošová, M., Plevová, K., Kotašková, J., Doubek, M., and Pospíšilová, Š. (2019). The importance of complex karyotype in prognostication and treatment of chronic lymphocytic leukemia (CLL): a comprehensive review of the literature. Leuk. Lymphoma 1–8.

Jayappa, K.D., Portell, C.A., Gordon, V.L., Capaldo, B.J., Bekiranov, S., Axelrod, M.J., Brett, L.K., Wulfkuhle, J.D., Gallagher, R.I., Petricoin, E.F., et al. (2017). Microenvironmental agonists generate de novo phenotypic resistance to combined ibrutinib plus venetoclax in CLL and MCL. Blood Adv. *1*, 933–946.

Jeison, M., Ash, S., Halevy-Berko, G., Mardoukh, J., Luria, D., Avigad, S., Feinberg-Gorenshtein, G., Goshen, Y., Hertzel, G., Kapelushnik, J., et al. (2010). 2p24 Gain region harboring MYCN gene compared with MYCN amplified and nonamplified neuroblastoma: biological and clinical characteristics. Am. J. Pathol. *176*, 2616–2625.

Jelinek, D.F., Tschumper, R.C., Stolovitzky, G.A., Iturria, S.J., Tu, Y., Lepre, J., Shah, N., and Kay, N.E. (2003). Identification of a global gene expression signature of B-chronic lymphocytic leukemia. Mol. Cancer Res. *1*, 346–361.

Jeromin, S., Weissmann, S., Haferlach, C., Dicker, F., Bayer, K., Grossmann, V., Alpermann, T., Roller, A., Kohlmann, A., Haferlach, T., et al. (2014). SF3B1 mutations correlated to cytogenetics and mutations in NOTCH1, FBXW7, MYD88, XPO1 and TP53 in 1160 untreated CLL patients. Leukemia *28*, 108–117.

Ji, M., Li, J., Yu, H., Ma, D., Ye, J., Sun, X., and Ji, C. (2009). Simultaneous targeting of MCL1 and ABCB1 as a novel strategy to overcome drug resistance in human leukaemia. Br. J. Haematol. *145*, 648–656.

Jiang, B., Zhang, X., Su, J., Meng, W., Yang, X., Yang, J., Zhou, Q., Chen, Z., Chen, Z., Xie, Z., et al. (2013). BCL11A overexpression predicts survival and relapse in non-small cell lung cancer and is modulated by microRNA-30a and gene amplification. Mol. Cancer *12*, 61.

Jin, J., Hu, H., Li, H.S., Yu, J., Xiao, Y., Brittain, G.C., Zou, Q., Cheng, X., Mallette, F.A., Watowich, S.S., et al. (2014). Noncanonical NF-κB Pathway Controls the Production of Type I Interferons in Antiviral Innate Immunity. Immunity *40*, 342–354.

Jinek, M., Chylinski, K., Fonfara, I., Hauer, M., Doudna, J.A., and Charpentier, E. (2012). A Programmable Dual-RNA-Guided DNA Endonuclease in Adaptive Bacterial Immunity. Science (80-.). *337*, 816–821.

Joos, S., Menz, C.K., Wrobel, G., Siebert, R., Gesk, S., Ohl, S., Mechtersheimer, G., Trümper, L., Möller, P., Lichter, P., et al. (2002). Classical Hodgkin lymphoma is characterized by recurrent copy number gains of the short arm of chromosome 2. Blood *99*, 1381–1387.

Joos, S., Granzow, M., Holtgreve-Grez, H., Siebert, R., Harder, L., Martín-Subero, J.I., Wolf, J., Adamowicz, M., Barth, T.F.E., Lichter, P., et al. (2003). Hodgkin's lymphoma cell lines are characterized by frequent aberrations on chromosomes 2p and 9p including REL and JAK2. Int. J. Cancer *103*, 489–495.

Joung, J., Konermann, S., Gootenberg, J.S., Abudayyeh, O.O., Platt, R.J., Brigham, M.D., Sanjana, N.E., and Zhang, F. (2017a). Genome-scale CRISPR-Cas9 knockout and transcriptional activation screening. Nat. Protoc. *12*, 828–863.

Joung, J., Engreitz, J.M., Konermann, S., Abudayyeh, O.O., Verdine, V.K., Aguet, F., Gootenberg, J.S., Sanjana, N.E., Wright, J.B., Fulco, C.P., et al. (2017b). Genome-scale activation screen identifies a lncRNA locus regulating a gene neighbourhood. Nature *548*, 343–346.

Kaileh, M., and Sen, R. (2012). NF-κB function in B lymphocytes. Immunol. Rev. *246*, 254–271.

Kaltschmidt, B., and Kaltschmidt, C. (2009). NF-kappaB in the nervous system. Cold Spring Harb. Perspect. Biol. *1*, a001271.

Kaltschmidt, B., and Kaltschmidt, C. (2015). NF-KappaB in Long-Term Memory and Structural Plasticity in the Adult Mammalian Brain. Front. Mol. Neurosci. *8*, 69.

Kaltschmidt, B., Greiner, J.F.W., Kadhim, H.M., and Kaltschmidt, C. (2018). Subunit-Specific Role of NF-κB in Cancer. Biomedicines *6*, 44.

Kanduri, M., Cahill, N., Goransson, H., Enstrom, C., Ryan, F., Isaksson, A., and Rosenquist, R. (2010). Differential genome-wide array-based methylation profiles in prognostic subsets of chronic lymphocytic leukemia. Blood *115*, 296–305.

Kanduri, M., Tobin, G., Åleskog, A., Nilsson, K., and Rosenquist, R. (2011). The novel NF-κB inhibitor IMD-0354 induces apoptosis in chronic lymphocytic leukemia. Blood Cancer J. *1*, e12–e12.

Kapahnke, M., Banning, A., and Tikkanen, R. (2016). Random Splicing of Several Exons Caused by a Single Base Change in the Target Exon of CRISPR/Cas9 Mediated Gene Knockout. Cells *5*, 45.

Karin, M. (2006). Nuclear factor-κB in cancer development and progression. Nature *441*, 431–436.

Karran, P. (2001). Mechanisms of tolerance to DNA damaging therapeutic drugs. Carcinogenesis *22*, 1931–1937.

Kashyap, T., Argueta, C., Aboukameel, A., Unger, T.J., Klebanov, B., Mohammad, R.M., Muqbil, I., Azmi, A.S., Drolen, C., Senapedis, W., et al. (2016). Selinexor, a Selective Inhibitor of Nuclear Export (SINE) compound, acts through NF-κB deactivation and combines with proteasome inhibitors to synergistically induce tumor cell death. Oncotarget *7*, 78883–78895.

Kato, G.J., Barrett, J., Villa-Garcia, M., and Dang, C. V (1990). An amino-terminal c-myc domain required for neoplastic transformation activates transcription. Mol. Cell. Biol. *10*, 5914–5920.

Kawagoe, H., Kandilci, A., Kranenburg, T.A., and Grosveld, G.C. (2007). Overexpression of N-Myc rapidly causes acute myeloid leukemia in mice. Cancer Res. *67*, 10677–10685.

Keino, H., Watanabe, T., Sato, Y., Niikura, M., Wada, Y., and Okada, A.A. (2008). Therapeutic effect of the potent IL-12/IL-23 inhibitor STA-5326 on experimental autoimmune uveoretinitis. Arthritis Res. Ther. *10*, R122.

Kern, W., Bacher, U., Schnittger, S., Dicker, F., Alpermann, T., Haferlach, T., and Haferlach, C. (2014). Flow cytometric identification of 76 patients with biclonal disease among 5523 patients with chronic lymphocytic leukaemia (B-CLL) and its genetic characterization. Br. J. Haematol. *164*, 565–569.

Kikushige, Y., Ishikawa, F., Miyamoto, T., Shima, T., Urata, S., Yoshimoto, G., Mori, Y., Iino, T., Yamauchi, T., Eto, T., et al. (2011). Self-Renewing Hematopoietic Stem Cell Is the Primary Target in Pathogenesis of Human Chronic Lymphocytic Leukemia. Cancer Cell *20*, 246–259.

Kim, S., Kim, D., Cho, S.W., Kim, J., and Kim, J.-S. (2014). Highly efficient RNA-guided genome editing in human cells via delivery of purified Cas9 ribonucleoproteins. Genome Res. *24*, 1012–1019.

King, K.E., Ponnamperuma, R.M., Allen, C., Lu, H., Duggal, P., Chen, Z., Van Waes, C., and Weinberg, W.C. (2008). The p53 Homologue Np63 Interacts with the Nuclear Factor- B Pathway to Modulate Epithelial Cell Growth. Cancer Res. *68*, 5122–5131.

Klein, U., Tu, Y., Stolovitzky, G.A., Mattioli, M., Cattoretti, G., Husson, H., Freedman, A., Inghirami, G., Cro, L., Baldini, L., et al. (2001). Gene Expression Profiling of B Cell Chronic Lymphocytic Leukemia Reveals a Homogeneous Phenotype Related to Memory B Cells ✪. J. Exp. Med *121400*, 1625–1638.

Klein, U., Lia, M., Crespo, M., Siegel, R., Shen, Q., Mo, T., Ambesi-Impiombato, A., Califano, A., Migliazza, A., Bhagat, G., et al. (2010). The DLEU2/miR-15a/16-1 Cluster Controls B Cell Proliferation and Its Deletion Leads to Chronic Lymphocytic Leukemia. Cancer Cell *17*, 28–40.

Kleinstiver, B.P., Pattanayak, V., Prew, M.S., Tsai, S.Q., Nguyen, N.T., Zheng, Z., and Joung, J.K. (2016). High-fidelity CRISPR–Cas9 nucleases with no detectable genome-wide off-target effects. Nature *529*, 490–495.

Kluiver, J., Kok, K., Pfeil, I., de Jong, D., Blokzijl, T., Harms, G., van der Vlies, P., Diepstra, A., Atayar, C., Poppema, S., et al. (2007). Global correlation of genome and transcriptome changes in classical Hodgkin lymphoma. Hematol. Oncol. *25*, 21–29.

Köhnke, T., Wittmann, V.K., Bücklein, V.L., Lichtenegger, F., Pasalic, Z., Hiddemann, W., Spiekermann, K., and Subklewe, M. (2017). Diagnosis of CLL revisited: increased specificity by a modified five-marker scoring system including CD200. Br. J. Haematol. *179*, 480–487.

Komarova, N.L., Burger, J.A., and Wodarz, D. (2014). Evolution of ibrutinib resistance in chronic lymphocytic leukemia (CLL). Proc. Natl. Acad. Sci. *111*, 13906–13911.

Konermann, S., Brigham, M.D., Trevino, A.E., Hsu, P.D., Heidenreich, M., Le Cong, L., Platt, R.J., Scott, D.A., Church, G.M., and Zhang, F. (2013). Optical control of mammalian endogenous transcription and epigenetic states. Nature *500*, 472–476.

Konermann, S., Brigham, M.D., Trevino, A.E., Joung, J., Abudayyeh, O.O., Barcena, C., Hsu, P.D., Habib, N., Gootenberg, J.S., Nishimasu, H., et al. (2015). Genome-scale transcriptional activation by an engineered CRISPR-Cas9 complex. Nature *517*, 583–588.

Konopleva, M., Pollyea, D.A., Potluri, J., Chyla, B., Hogdal, L., Busman, T., McKeegan, E., Salem, A.H., Zhu, M., Ricker, J.L., et al. (2016). Efficacy and Biological Correlates of Response in a Phase II Study of Venetoclax Monotherapy in Patients with Acute Myelogenous Leukemia. Cancer Discov. *6*, 1106–1117.

Köntgen, F., Grumont, R.J., Strasser, A., Metcalf, D., Li, R., Tarlinton, D., and Gerondakis, S. (1995). Mice lacking the c-rel proto-oncogene exhibit defects in lymphocyte proliferation, humoral immunity, and interleukin-2 expression. Genes Dev. *9*, 1965–1977.

Krysko, D. V., Brouckaert, G., Kalai, M., Vandenabeele, P., and D'Herde, K. (2003). Mechanisms of internalization of apoptotic and necrotic L929 cells by a macrophage cell line studied by electron microscopy. J. Morphol. *258*, 336–345.

Krysko, D. V., Vanden Berghe, T., D'Herde, K., and Vandenabeele, P. (2008). Apoptosis and necrosis: Detection, discrimination and phagocytosis. Methods *44*, 205–221.

Kulis, M., Heath, S., Bibikova, M., Queirós, A.C., Navarro, A., Clot, G., Martínez-Trillos, A., Castellano, G., Brun-Heath, I., Pinyol, M., et al. (2012). Epigenomic analysis detects widespread gene-body DNA hypomethylation in chronic lymphocytic leukemia. Nat. Genet. *44*, 1236–1242.

Küppers, R. (2005). Mechanisms of B-cell lymphoma pathogenesis. Nat. Rev. Cancer *5*, 251–262.

Kwiecinska, A., Ichimura, K., Berglund, M., Dinets, A., Sulaiman, L., Collins, V.P., Larsson, C., Porwit, A., and Lagercrantz, S.B. (2014). Amplification of 2p as a genomic marker for transformation in lymphoma. Genes. Chromosomes Cancer *53*, 750–768.

Kyriakopoulou, C.B., Nordvarg, H., and Virtanen, A. (2001). A Novel Nuclear Human Poly(A) Polymerase (PAP), PAPγ. J. Biol. Chem. *276*, 33504–33511.

Lam, K.P., Kühn, R., and Rajewsky, K. (1997). In vivo ablation of surface immunoglobulin on mature B cells by inducible gene targeting results in rapid cell death. Cell *90*, 1073–1083.

Landau, D.A., and Wu, C.J. (2013). Chronic lymphocytic leukemia: molecular heterogeneity revealed by high-throughput genomics. Genome Med. *5*, 47.

Landau, D.A., Carter, S.L., Stojanov, P., McKenna, A., Stevenson, K., Lawrence, M.S., Sougnez, C., Stewart, C., Sivachenko, A., Wang, L., et al. (2013). Evolution and impact of subclonal mutations in chronic lymphocytic leukemia. Cell *152*.

Landau, D.A., Clement, K., Ziller, M.J., Boyle, P., Fan, J., Gu, H., Stevenson, K., Sougnez, C., Wang, L., Li, S., et al. (2014). Locally Disordered Methylation Forms the Basis of Intratumor Methylome Variation in Chronic Lymphocytic Leukemia. Cancer Cell *26*, 813–825.

Landau, D.A., Tausch, E., Taylor-Weiner, A.N., Stewart, C., Reiter, J.G., Bahlo, J., Kluth, S., Bozic, I., Lawrence, M., Böttcher, S., et al. (2015). Mutations driving CLL and their evolution in progression and relapse. Nature *526*, 525–530.

Landau, D.A., Sun, C., Rosebrock, D., Herman, S.E.M., Fein, J., Sivina, M., Underbayev, C., Liu, D., Hoellenriegel, J., Ravichandran, S., et al. (2017). The evolutionary landscape of chronic lymphocytic leukemia treated with ibrutinib targeted therapy. Nat. Commun. *8*, 2185.

Lapalombella, R., Sun, Q., Williams, K., Tangeman, L., Jha, S., Zhong, Y., Goettl, V., Mahoney, E., Berglund, C., Gupta, S., et al. (2012). Selective inhibitors of nuclear export show that CRM1/XPO1 is a target in chronic lymphocytic leukemia. Blood *120*, 4621–4634.

Laurenti, E., and Göttgens, B. (2018). From haematopoietic stem cells to complex differentiation landscapes. Nature 553(7689): 418–426

Lawrence, M.S., Stojanov, P., Mermel, C.H., Robinson, J.T., Garraway, L.A., Golub, T.R., Meyerson, M., Gabriel, S.B., Lander, E.S., and Getz, G. (2014). Discovery and saturation analysis of cancer genes across 21 tumour types. Nature ***505***, 495–501.

Lee, B.-S., Lee, B.-K., Iyer, V.R., Sleckman, B.P., Shaffer, A.L., Ippolito, G.C., Tucker, H.O., and Dekker, J.D. (2017). Corrected and Republished from: BCL11A Is a Critical Component of a Transcriptional Network That Activates RAG Expression and V(D)J Recombination. Mol. Cell. Biol. ***38***.

Lee, J.W., Park, S.H., Kang, H.J., Park, K.D., Shin, H.Y., and Ahn, H.S. (2018). ALK Protein Expression Is Related to Neuroblastoma Aggressiveness But Is Not Independent Prognostic Factor. Cancer Res. Treat. ***50***, 495–505.

Leeksma, A.C., Taylor, J., Wu, B., Gardner, J.R., He, J., Nahas, M., Gonen, M., Alemayehu, W.G., te Raa, D., Walther, T., et al. (2019). Clonal diversity predicts adverse outcome in chronic lymphocytic leukemia. Leukemia ***33***, 390–402.

Leeman, J.R., Weniger, M.A., Barth, T.F., and Gilmore, T.D. (2008). Deletion analysis and alternative splicing define a transactivation inhibitory domain in human oncoprotein REL. Oncogene *27*, 6770–6781.

Levenson, J.M., Choi, S., Lee, S.-Y., Cao, Y.A., Ahn, H.J., Worley, K.C., Pizzi, M., Liou, H.-C., and Sweatt, J.D. (2004). A bioinformatics analysis of memory consolidation reveals involvement of the transcription factor c-rel. J. Neurosci. *24*, 3933–3943.

Levin, S. (1998). Apoptosis, necrosis, or oncosis: what is your diagnosis? A report from the Cell Death Nomenclature Committee of the Society of Toxicologic Pathologists. Toxicol. Sci. *41*, 155–156.

Li, G.-M. (2008). Mechanisms and functions of DNA mismatch repair. Cell Res. *18*, 85–98.

Li, H., Zhu, H., Xu, C.J., and Yuan, J. (1998). Cleavage of BID by caspase 8 mediates the mitochondrial damage in the Fas pathway of apoptosis. Cell *94*, 491–501.

Li, L., Xu-Monette, Z.Y., Ok, C.Y., Tzankov, A., Manyam, G.C., Sun, R., Visco, C., Zhang, M., Montes-Moreno, S., Dybkaer, K., et al. (2015). Prognostic impact of c-Rel nuclear expression and <i>REL</i> amplification and crosstalk between c-Rel and the p53 pathway in diffuse large B-cell lymphoma. Oncotarget *6*, 23157–23180.

Li, M., Ke, J., Wang, Q., Qian, H., Yang, L., Zhang, X., Xiao, J., Ding, H., Shan, X., Liu, Q., et al. (2017). Upregulation of ROCK2 in gastric cancer cell promotes tumor cell proliferation, metastasis and invasion. Clin. Exp. Med. *17*, 519–529.

Li, S.-H., Li, J.-P., Chen, L., and Liu, J.-L. (2018). miR-146a induces apoptosis in neuroblastoma cells by targeting BCL11A. Med. Hypotheses *117*, 21–27.

Li, X.-T., Jun, Y., Erickstad, M.J., Brown, S.D., Parks, A., Court, D.L., and Jun, S. (2016). tCRISPRi: tunable and reversible, one-step control of gene expression. Sci. Rep. *6*, 39076.

Lia, M., Carette, A., Tang, H., Shen, Q., Mo, T., Bhagat, G., Dalla-Favera, R., and Klein, U. (2012). Functional dissection of the chromosome 13q14 tumor-suppressor locus using transgenic mouse lines. Blood *119*, 2981–2990.

Liang, M.-C., Bardhan, S., Porco, J.A., and Gilmore, T.D. (2006). The synthetic epoxyquinoids jesterone dimer and epoxyquinone A monomer induce apoptosis and inhibit REL (human c-Rel) DNA binding in an IkappaBalpha-deficient diffuse large B-cell lymphoma cell line. Cancer Lett. *241*, 69–78.

Lim, K.-H., Yang, Y., and Staudt, L.M. (2012). Pathogenetic importance and therapeutic implications of NF-κB in lymphoid malignancies. Immunol. Rev. *246*, 359–378.

Liou, H.C., Sha, W.C., Scott, M.L., and Baltimore, D. (1994). Sequential induction of NF-kappa B/Rel family proteins during B-cell terminal differentiation. Mol. Cell. Biol. *14*, 5349–5359.

Liu, F.-T., Jia, L., Wang, P., Wang, H., Farren, T.W., and Agrawal, S.G. (2016a). STAT3 and NF-κB cooperatively control in vitro spontaneous apoptosis and poor chemo-responsiveness in patients with chronic lymphocytic leukemia. Oncotarget *7*, 32031–32045.

Liu, H., Ippolito, G.C., Wall, J.K., Niu, T., Probst, L., Lee, B.-S., Pulford, K., Banham, A.H., Stockwin, L., Shaffer, A.L., et al. (2006). Functional studies of BCL11A: characterization of the conserved BCL11A-XL splice variant and its interaction with BCL6 in nuclear paraspeckles of germinal center B cells. Mol. Cancer *5*, 18.

Liu, L., Xu, F., Chang, C.-K., He, Q., Wu, L.-Y., Zhang, Z., and Li, X. (2017). MYCN contributes to the malignant characteristics of erythroleukemia through EZH2-mediated epigenetic repression of p21. Cell Death Dis. *8*, e3126.

Liu, P., Keller, J.R., Ortiz, M., Tessarollo, L., Rachel, R.A., Nakamura, T., Jenkins, N.A., and Copeland, N.G. (2003). Bcl11a is essential for normal lymphoid development. Nat. Immunol. *4*, 525–532.

Liu, X., Homma, A., Sayadi, J., Yang, S., Ohashi, J., and Takumi, T. (2016b). Sequence features associated with the cleavage efficiency of CRISPR/Cas9 system. Sci. Rep. *6*, 19675.

Lopez-Guerra, M., and Colomer, D. (2010). NF-kappaB as a therapeutic target in chronic lymphocytic leukemia. Expert Opin. Ther. Targets *14*, 275–288.

Lopez-Guerra, M., Roue, G., Perez-Galan, P., Alonso, R., Villamor, N., Montserrat, E., Campo, E., and Colomer, D. (2009). p65 Activity and ZAP-70 Status Predict the Sensitivity of Chronic Lymphocytic Leukemia Cells to the Selective I B Kinase Inhibitor BMS-345541. Clin. Cancer Res. *15*, 2767–2776.

Lozano-Santos, C., García-Vela, J.A., Pérez-Sanz, N., Nova-Gurumeta, S., Fernandez-Cuevas, B., Gomez-Lozano, N., Sánchez-Beato, M., Sanchez-Godoy, P., Bueno, J.L., and Garcia-Marco, J.A. (2017). Biallelic ATM alterations detected at diagnosis identify a subset of treatment-naïve chronic lymphocytic leukemia patients with reduced overall survival similar to patients with p53 deletion. Leuk. Lymphoma *58*, 859–865.

Luo, X., Budihardjo, I., Zou, H., Slaughter, C., and Wang, X. (1998). Bid, a Bcl2 interacting protein, mediates cytochrome c release from mitochondria in response to activation of cell surface death receptors. Cell *94*, 481–490.

Lutzny, G., Kocher, T., Schmidt-Supprian, M., Rudelius, M., Klein-Hitpass, L., Finch, A.J., Dürig, J., Wagner, M., Haferlach, C., Kohlmann, A., et al. (2013). Protein kinase

c-β-dependent activation of NF-κB in stromal cells is indispensable for the survival of chronic lymphocytic leukemia B cells in vivo. Cancer Cell *23*, 77–92.

Ma, D., Chen, Z., Patel, K.P., Mishra, B.M., Yao, H., Abruzzo, L. V, Medeiros, L.J., Wierda, W., Keating, M., Sargent, R., et al. (2011). Array comparative genomic hybridization analysis identifies recurrent gain of chromosome 2p25.3 involving the ACP1 and MYCN genes in chronic lymphocytic leukemia. Clin. Lymphoma. Myeloma Leuk. *11 Suppl 1*, S17-24.

Maddalo, D., Manchado, E., Concepcion, C.P., Bonetti, C., Vidigal, J.A., Han, Y.-C., Ogrodowski, P., Crippa, A., Rekhtman, N., de Stanchina, E., et al. (2014). In vivo engineering of oncogenic chromosomal rearrangements with the CRISPR/Cas9 system. Nature *516*, 423–427.

Maddocks, K.J., Ruppert, A.S., Lozanski, G., Heerema, N.A., Zhao, W., Abruzzo, L., Lozanski, A., Davis, M., Gordon, A., Smith, L.L., et al. (2015). Etiology of Ibrutinib Therapy Discontinuation and Outcomes in Patients With Chronic Lymphocytic Leukemia. JAMA Oncol. *1*, 80.

Maeder, M.L., Linder, S.J., Cascio, V.M., Fu, Y., Ho, Q.H., and Joung, J.K. (2013). CRISPR RNA–guided activation of endogenous human genes. Nat. Methods *10*, 977–979.

Makino, S., Fukumura, R., and Gondo, Y. (2016). Illegitimate translation causes unexpected gene expression from on-target out-of-frame alleles created by CRISPR-Cas9. Sci. Rep. *6*, 39608.

Mali, P., Yang, L., Esvelt, K.M., Aach, J., Guell, M., DiCarlo, J.E., Norville, J.E., and Church, G.M. (2013). RNA-Guided Human Genome Engineering via Cas9. Science (80-.). *339*, 823–826.

Malynn, B.A., de Alboran, I.M., O'Hagan, R.C., Bronson, R., Davidson, L., DePinho, R.A., and Alt, F.W. (2000). N-myc can functionally replace c-myc in murine development, cellular growth, and differentiation. Genes Dev. *14*, 1390–1399.

Mansouri, L., Sutton, L.-A., Ljungström, V., Bondza, S., Arngården, L., Bhoi, S., Larsson, J., Cortese, D., Kalushkova, A., Plevova, K., et al. (2015). Functional loss of IκBε leads to NF-κB deregulation in aggressive chronic lymphocytic leukemia. J. Exp. Med. *212*, 833–843.

Mansouri, L., Papakonstantinou, N., Ntoufa, S., Stamatopoulos, K., and Rosenquist, R. (2016). NF-κB activation in chronic lymphocytic leukemia: A point of convergence of external triggers and intrinsic lesions. Semin. Cancer Biol. *39*, 40–48.

Marcelis, C.L., van der Putten, H.W., Tops, C., Lutgens, L.C., and Moog, U. (2001). Chemotherapy resistant ovarian cancer in carriers of an hMSH2 mutation? Fam. Cancer *1*, 107–109.

Martín-Subero, J.I., Gesk, S., Harder, L., Sonoki, T., Tucker, P.W., Schlegelberger, B., Grote, W., Novo, F.J., Calasanz, M.J., Hansmann, M.L., et al. (2002). Recurrent involvement of the REL and BCL11A loci in classical Hodgkin lymphoma. Blood *99*, 1474–1477.

Martin, A.G., and Fresno, M. (2000). Tumor Necrosis Factor-α Activation of NF-κB Requires the Phosphorylation of Ser-471 in the Transactivation Domain of c-Rel. J. Biol. Chem. *275*, 24383–24391.

Martin, A.G., San-Antonio, B., and Fresno, M. (2001). Regulation of nuclear factor kappa B transactivation. Implication of phosphatidylinositol 3-kinase and protein kinase C zeta in c-Rel activation by tumor necrosis factor alpha. J. Biol. Chem. *276*, 15840–15849.

Martinez-Climent, J.A., Alizadeh, A.A., Segraves, R., Blesa, D., Rubio-Moscardo, F., Albertson, D.G., Garcia-Conde, J., Dyer, M.J.S., Levy, R., Pinkel, D., et al. (2003). Transformation of follicular lymphoma to diffuse large cell lymphoma is associated with a heterogeneous set of DNA copy number and gene expression alterations. Blood *101*, 3109–3117.

Martinez-Trillos, A., Pinyol, M., Navarro, A., Aymerich, M., Jares, P., Juan, M., Rozman, M., Colomer, D., Delgado, J., Gine, E., et al. (2014). Mutations in TLR/MYD88 pathway identify a subset of young chronic lymphocytic leukemia patients with favorable outcome. Blood *123*, 3790–3796.

Martyniszyn, A., Krahl, A.-C., André, M.C., Hombach, A.A., and Abken, H. (2017). CD20-CD19 Bispecific CAR T Cells for the Treatment of B-Cell Malignancies. Hum. Gene Ther. *28*, 1147–1157.

Mathews Griner, L.A., Guha, R., Shinn, P., Young, R.M., Keller, J.M., Liu, D., Goldlust, I.S., Yasgar, A., McKnight, C., Boxer, M.B., et al. (2014). High-throughput combinatorial screening identifies drugs that cooperate with ibrutinib to kill activated B-cell–like diffuse large B-cell lymphoma cells. Proc. Natl. Acad. Sci. *111*, 2349–2354.

Mato, A.R., Nabhan, C., Barr, P.M., Ujjani, C.S., Hill, B.T., Lamanna, N., Skarbnik, A.P., Howlett, C., Pu, J.J., Sehgal, A.R., et al. (2016). Outcomes of CLL patients treated with sequential kinase inhibitor therapy: a real world experience. Blood *128*, 2199–2205.

Matutes, E., and Polliack, A. (2000). Morphological and immunophenotypic features of chronic lymphocytic leukemia. Rev. Clin. Exp. Hematol. *4*, 22–47.

Matutes, E., Owusu-Ankomah, K., Morilla, R., Garcia Marco, J., Houlihan, A., Que, T.H., and Catovsky, D. (1994). The immunological profile of B-cell disorders and proposal of a scoring system for the diagnosis of CLL. Leukemia *8*, 1640–1645.

Maurano, M.T., Humbert, R., Rynes, E., Thurman, R.E., Haugen, E., Wang, H., Reynolds, A.P., Sandstrom, R., Qu, H., Brody, J., et al. (2012). Systematic Localization of Common Disease-Associated Variation in Regulatory DNA. Science (80-.). *337*, 1190–1195.

McGrath, K.E., Frame, J.M., Fromm, G.J., Koniski, A.D., Kingsley, P.D., Little, J., Bulger, M., and Palis, J. (2011). A transient definitive erythroid lineage with unique regulation of the β-globin locus in the mammalian embryo. Blood *117*, 4600–4608.

Meers, C., Keskin, H., and Storici, F. (2016). DNA repair by RNA: Templated, or not templated, that is the question. DNA Repair (Amst). *44*, 17–21.

Melo, J. V, Foroni, L., Brito-Babapulle, V., Luzzatto, L., and Catovsky, D. (1988). The establishment of cell lines from chronic B cell leukaemias: evidence of leukaemic origin by karyotypic abnormalities and Ig gene rearrangement. Clin. Exp. Immunol. *73*, 23–28.

Messina, M., Del Giudice, I., Khiabanian, H., Rossi, D., Chiaretti, S., Rasi, S., Spina,

V., Holmes, A.B., Marinelli, M., Fabbri, G., et al. (2014). Genetic lesions associated with chronic lymphocytic leukemia chemo-refractoriness. Blood *123*, 2378–2388.

Milanovic, M., Heise, N., De Silva, N.S., Anderson, M.M., Silva, K., Carette, A., Orelli, F., Bhagat, G., and Klein, U. (2017). Differential requirements for the canonical NF-κB transcription factors c-REL and RELA during the generation and activation of mature B cells. Immunol. Cell Biol. *95*, 261–271.

Miles, L.A., Garippa, R.J., and Poirier, J.T. (2016). Design, execution, and analysis of pooled *in vitro* CRISPR/Cas9 screens. FEBS J. *283*, 3170–3180.

Miller, C.R., Ruppert, A.S., Heerema, N.A., Maddocks, K.J., Labanowska, J., Breidenbach, H., Lozanski, G., Zhao, W., Gordon, A.L., Jones, J.A., et al. (2017). Near-tetraploidy is associated with Richter transformation in chronic lymphocytic leukemia patients receiving ibrutinib. Blood Adv. *1*, 1584–1588.

Milpied, P., Nadel, B., and Roulland, S. (2015). Premalignant cell dynamics in indolent B-cell malignancies. Curr. Opin. Hematol. *22*, 388–396.

Miyamoto, S., Chiao, P.J., and Verma, I.M. (1994). Enhanced I kappa B alpha degradation is responsible for constitutive NF-kappa B activity in mature murine B-cell lines. Mol. Cell. Biol. *14*, 3276–3282.

Mohammadi, S.M., Mohammadnejad, D., Hosseinpour Feizi, A.A., Movassaghpour, A.A., Montazersaheb, S., and Nozad Charoudeh, H. (2017). Inhibition of c-REL using siRNA increased apoptosis and decreased proliferation in pre-B ALL blasts: Therapeutic implications. Leuk. Res. *61*, 53–61.

Mohanraju, P., Makarova, K.S., Zetsche, B., Zhang, F., Koonin, E. V, and van der Oost, J. (2016). Diverse evolutionary roots and mechanistic variations of the CRISPR-Cas systems. Science *353*, aad5147.

Mojica, F.J.M., and Garrett, R.A. (2013). Discovery and Seminal Developments in the CRISPR Field. In CRISPR-Cas Systems, (Berlin, Heidelberg: Springer Berlin Heidelberg), pp. 1–31.

Mojica, F.J.M., Díez-Villaseñor, C., García-Martínez, J., and Soria, E. (2005). Intervening sequences of regularly spaced prokaryotic repeats derive from foreign genetic elements. J. Mol. Evol. *60*, 174–182.

Moon, E.-Y., and Lerner, A. (2002). Benzylamide sulindac analogues induce changes in cell shape, loss of microtubules and G(2)-M arrest in a chronic lymphocytic leukemia (CLL) cell line and apoptosis in primary CLL cells. Cancer Res. *62*, 5711–5719.

Moreau, E.J., Matutes, E., A'Hern, R.P., Morilla, A.M., Morilla, R.M., Owusu-Ankomah, K.A., Seon, B.K., and Catovsky, D. (1997). Improvement of the chronic lymphocytic leukemia scoring system with the monoclonal antibody SN8 (CD79b). Am. J. Clin. Pathol. *108*, 378–382.

Morgens, D.W., Deans, R.M., Li, A., and Bassik, M.C. (2016). Systematic comparison of CRISPR/Cas9 and RNAi screens for essential genes. Nat. Biotechnol. *34*, 634–636.

Morris, S.W., Kirstein, M.N., Valentine, M.B., Dittmer, K.G., Shapiro, D.N., Saltman, D.L., and Look, A.T. (1994). Fusion of a kinase gene, ALK, to a nucleolar protein gene, NPM, in non-Hodgkin's lymphoma. Science *263*, 1281–1284.

Morris, S.W., Naeve, C., Mathew, P., James, P.L., Kirstein, M.N., Cui, X., and Witte, D.P. (1997). ALK, the chromosome 2 gene locus altered by the t(2;5) in non-Hodgkin's lymphoma, encodes a novel neural receptor tyrosine kinase that is highly related to leukocyte tyrosine kinase (LTK). Oncogene.

Mossé, Y.P., Laudenslager, M., Longo, L., Cole, K.A., Wood, A., Attiyeh, E.F., Laquaglia, M.J., Sennett, R., Lynch, J.E., Perri, P., et al. (2008). Identification of ALK as a major familial neuroblastoma predisposition gene. Nature *455*, 930–935.

Mou, H., Smith, J.L., Peng, L., Yin, H., Moore, J., Zhang, X.-O., Song, C.-Q., Sheel, A., Wu, Q., Ozata, D.M., et al. (2017). CRISPR/Cas9-mediated genome editing induces exon skipping by alternative splicing or exon deletion. Genome Biol. *18*, 108.

Müller, I., Larsson, K., Frenzel, A., Oliynyk, G., Zirath, H., Prochownik, E. V., Westwood, N.J., and Henriksson, M.A. (2014). Targeting of the MYCN Protein with Small Molecule c-MYC Inhibitors. PLoS One *9*, e97285.

Munoz, D.M., Cassiani, P.J., Li, L., Billy, E., Korn, J.M., Jones, M.D., Golji, J., Ruddy, D.A., Yu, K., McAllister, G., et al. (2016). CRISPR Screens Provide a Comprehensive Assessment of Cancer Vulnerabilities but Generate False-Positive Hits for Highly Amplified Genomic Regions. Cancer Discov. *6*, 900–913.

Nakamura, T., Yamazaki, Y., Saiki, Y., Moriyama, M., Largaespada, D.A., Jenkins, N.A., and Copeland, N.G. (2000). Evi9 encodes a novel zinc finger protein that physically interacts with BCL6, a known human B-cell proto-oncogene product. Mol. Cell. Biol. *20*, 3178–3186.

Nava, V.E., Cohen, P., Kalan, M., and Ozdemirli, M. (2008). HIV-associated anaplastic large cell lymphoma: a report of three cases. AIDS *22*, 1892–1894.

Neggers, J.E., Vercruysse, T., Jacquemyn, M., Vanstreels, E., Baloglu, E., Shacham, S., Crochiere, M., Landesman, Y., and Daelemans, D. (2015). Identifying Drug-Target Selectivity of Small-Molecule CRM1/XPO1 Inhibitors by CRISPR/Cas9 Genome Editing. Chem. Biol. *22*, 107–116.

Neggers, J.E., Vanstreels, E., Baloglu, E., Shacham, S., Landesman, Y., and Daelemans, D. (2016). Heterozygous mutation of cysteine528 in XPO1 is sufficient for resistance to selective inhibitors of nuclear export. Oncotarget *7*, 68842–68850.

Neo, W.H., Lim, J.F., Grumont, R., Gerondakis, S., and Su, I.-H. (2014). c-Rel regulates Ezh2 expression in activated lymphocytes and malignant lymphoid cells. J. Biol. Chem. *289*, 31693–31707.

Ng, L.G., Mackay, C.R., and Mackay, F. (2005). The BAFF/APRIL system: life beyond B lymphocytes. Mol. Immunol. *42*, 763–772.

Ngo, V.N., Young, R.M., Schmitz, R., Jhavar, S., Xiao, W., Lim, K.-H., Kohlhammer, H., Xu, W., Yang, Y., Zhao, H., et al. (2011). Oncogenically active MYD88 mutations in human lymphoma. Nature *470*, 115.

Nguyen, P.-H., Fedorchenko, O., Rosen, N., Koch, M., Barthel, R., Winarski, T., Florin, A., Wunderlich, F.T., Reinart, N., and Hallek, M. (2016). LYN Kinase in the Tumor Microenvironment Is Essential for the Progression of Chronic Lymphocytic Leukemia. Cancer Cell *30*, 610–622.

Niemann, C.U., Mora-Jensen, H.I., Dadashian, E.L., Krantz, F., Covey, T., Chen, S.-S., Chiorazzi, N., Izumi, R., Ulrich, R., Lannutti, B.J., et al. (2017). Combined BTK

and PI3Kδ Inhibition with Acalabrutinib and ACP-319 Improves Survival and Tumor Control in CLL Mouse Model. Clin. Cancer Res. *23*, 5814–5823.

Nishimasu, H., Ran, F.A., Hsu, P.D., Konermann, S., Shehata, S.I., Dohmae, N., Ishitani, R., Zhang, F., and Nureki, O. (2014). Crystal Structure of Cas9 in Complex with Guide RNA and Target DNA. Cell *156*, 935–949.

Di Noia, J.M., and Neuberger, M.S. (2007). Molecular Mechanisms of Antibody Somatic Hypermutation. Annu. Rev. Biochem. *76*, 1–22.

Noske, A., Weichert, W., Niesporek, S., Röske, A., Buckendahl, A.-C., Koch, I., Sehouli, J., Dietel, M., and Denkert, C. (2008). Expression of the nuclear export protein chromosomal region maintenance/exportin 1/Xpo1 is a prognostic factor in human ovarian cancer. Cancer *112*, 1733–1743.

Nutt, S.L., and Kee, B.L. (2007). The Transcriptional Regulation of B Cell Lineage Commitment. Immunity *26*, 715–725.

Oakes, C.C., Claus, R., Gu, L., Assenov, Y., Hullein, J., Zucknick, M., Bieg, M., Brocks, D., Bogatyrova, O., Schmidt, C.R., et al. (2014). Evolution of DNA Methylation Is Linked to Genetic Aberrations in Chronic Lymphocytic Leukemia. Cancer Discov. *4*, 348–361.

Oakes, C.C., Seifert, M., Assenov, Y., Gu, L., Przekopowitz, M., Ruppert, A.S., Wang, Q., Imbusch, C.D., Serva, A., Koser, S.D., et al. (2016). DNA methylation dynamics during B cell maturation underlie a continuum of disease phenotypes in chronic lymphocytic leukemia. Nat. Genet. *48*, 253–264.

Oeckinghaus, A., and Ghosh, S. (2009). The NF-kappaB family of transcription factors and its regulation. Cold Spring Harb. Perspect. Biol. *1*, a000034.

Ohnuma, K., Uchiyama, M., Yamochi, T., Nishibashi, K., Hosono, O., Takahashi, N., Kina, S., Tanaka, H., Lin, X., Dang, N.H., et al. (2007). Caveolin-1 Triggers T-cell Activation via CD26 in Association with CARMA1. J. Biol. Chem. *282*, 10117–10131.

Ojha, J., Ayres, J., Secreto, C., Tschumper, R., Rabe, K., Van Dyke, D., Slager, S., Shanafelt, T., Fonseca, R., Kay, N.E., et al. (2015). Deep sequencing identifies genetic heterogeneity and recurrent convergent evolution in chronic lymphocytic leukemia. Blood *125*, 492–498.

Oku, Y., Tareyanagi, C., Takaya, S., Osaka, S., Ujiie, H., Yoshida, K., Nishiya, N., and Uehara, Y. (2014). Multimodal Effects of Small Molecule ROCK and LIMK Inhibitors on Mitosis, and Their Implication as Anti-Leukemia Agents. PLoS One *9*, e92402.

Ooi, C.Y., Carter, D.R., Liu, B., Mayoh, C., Beckers, A., Lalwani, A., Nagy, Z., De Brouwer, S., Decaesteker, B., Hung, T.-T., et al. (2018). Network Modeling of microRNA–mRNA Interactions in Neuroblastoma Tumorigenesis Identifies miR-204 as a Direct Inhibitor of MYCN. Cancer Res. *78*, 3122–3134.

Orkin, S.H., and Zon, L.I. (2008). Hematopoiesis: An Evolving Paradigm for Stem Cell Biology. Cell *132*, 631–644.

Oscier, D., Else, M., Matutes, E., Morilla, R., Strefford, J.C., and Catovsky, D. (2016). The morphology of CLL revisited: the clinical significance of prolymphocytes and correlations with prognostic/molecular markers in the LRF CLL4 trial. Br. J. Haematol. *174*, 767–775.

Palis, J., and Yoder, M.C. (2001). Yolk-sac hematopoiesis: the first blood cells of mouse and man. Exp. Hematol. *29*, 927–936.

Park, H.Y., Lee, S.-B., Yoo, H.-Y., Kim, S.-J., Kim, W.-S., Kim, J.-I., and Ko, Y.-H. (2016). Whole-exome and transcriptome sequencing of refractory diffuse large B-cell lymphoma. Oncotarget *7*, 86433–86445.

Pattanayak, V., Lin, S., Guilinger, J.P., Ma, E., Doudna, J.A., and Liu, D.R. (2013). High-throughput profiling of off-target DNA cleavage reveals RNA-programmed Cas9 nuclease specificity. Nat. Biotechnol. *31*, 839–843.

Pawluk, A., Amrani, N., Zhang, Y., Garcia, B., Hidalgo-Reyes, Y., Lee, J., Edraki, A., Shah, M., Sontheimer, E.J., Maxwell, K.L., et al. (2016). Naturally Occurring Off-Switches for CRISPR-Cas9. Cell *167*, 1829–1838.e9.

Pede, V., Rombout, A., Vermeire, J., Naessens, E., Vanderstraeten, H., Philippé, J., and Verhasselt, B. (2013). Expression of ZAP70 in chronic lymphocytic leukaemia activates NF-κB signalling. Br. J. Haematol. *163*, 621–630.

Penaloza, C., Lin, L., Lockshin, R.A., and Zakeri, Z. (2006). Cell death in development: shaping the embryo. Histochem. Cell Biol. *126*, 149–158.

Peng, M., Zhao, G., Yang, F., Cheng, G., Huang, J., Qin, X., Liu, Y., Wang, Q., Li, Y., and Qin, D. (2017). NCOA1 is a novel susceptibility gene for multiple myeloma in the Chinese population: A case-control study. PLoS One *12*, e0173298.

Perez-Pinera, P., Kocak, D.D., Vockley, C.M., Adler, A.F., Kabadi, A.M., Polstein, L.R., Thakore, P.I., Glass, K.A., Ousterout, D.G., Leong, K.W., et al. (2013). RNA-guided gene activation by CRISPR-Cas9-based transcription factors. Nat. Methods *10*, 973–976.

Perez, E.E., Wang, J., Miller, J.C., Jouvenot, Y., Kim, K.A., Liu, O., Wang, N., Lee, G., Bartsevich, V. V, Lee, Y.-L., et al. (2008). Establishment of HIV-1 resistance in CD4+ T cells by genome editing using zinc-finger nucleases. Nat. Biotechnol. *26*, 808–816.

Perkins, N.D. (2007). Integrating cell-signalling pathways with NF-κB and IKK function. Nat. Rev. Mol. Cell Biol. *8*, 49–62.

Perkins, N.D. (2012). The diverse and complex roles of NF-κB subunits in cancer. Nat. Rev. Cancer.

Perrot, A., Pionneau, C., Nadaud, S., Davi, F., Leblond, V., Jacob, F., Merle-Béral, H., Herbrecht, R., Béné, M.-C., Gribben, J.G., et al. (2011). A unique proteomic profile on surface IgM ligation in unmutated chronic lymphocytic leukemia. Blood *118*, e1-15.

Pham, L. V. (2005). Constitutive NF- B and NFAT activation in aggressive B-cell lymphomas synergistically activates the CD154 gene and maintains lymphoma cell survival. Blood *106*, 3940–3947.

Pohl, T., Gugasyan, R., Grumont, R.J., Strasser, A., Metcalf, D., Tarlinton, D., Sha, W., Baltimore, D., and Gerondakis, S. (2002). The combined absence of NF-kappa B1 and c-Rel reveals that overlapping roles for these transcription factors in the B cell lineage are restricted to the activation and function of mature cells. Proc. Natl. Acad. Sci. U. S. A. *99*, 4514–4519.

Pridans, C., Holmes, M.L., Polli, M., Wettenhall, J.M., Dakic, A., Corcoran, L.M., Smyth, G.K., and Nutt, S.L. (2008). Identification of Pax5 target genes in early B cell differentiation. J. Immunol. *180*, 1719–1728.

Puente, X.S., Pinyol, M., Quesada, V., Conde, L., Ordóñez, G.R., Villamor, N., Escaramis, G., Jares, P., Beá, S., González-Díaz, M., et al. (2011). Whole-genome sequencing identifies recurrent mutations in chronic lymphocytic leukaemia. Nature *475*, 101–105.

Puente, X.S., Beà, S., Valdés-Mas, R., Villamor, N., Gutiérrez-Abril, J., Martín-Subero, J.I., Munar, M., Rubio-Pérez, C., Jares, P., Aymerich, M., et al. (2015). Non-coding recurrent mutations in chronic lymphocytic leukaemia. Nature *526*, 519–524.

Puissant, A., Frumm, S.M., Alexe, G., Bassil, C.F., Qi, J., Chanthery, Y.H., Nekritz, E.A., Zeid, R., Gustafson, W.C., Greninger, P., et al. (2013). Targeting MYCN in Neuroblastoma by BET Bromodomain Inhibition. Cancer Discov. *3*, 308–323.

Purroy, N., and Wu, C.J. (2017). Coevolution of Leukemia and Host Immune Cells in Chronic Lymphocytic Leukemia. Cold Spring Harb. Perspect. Med. *7*, a026740.

Purroy, N., Abrisqueta, P., Carabia, J., Carpio, C., Calpe, E., Palacio, C., Castellví, J., Crespo, M., and Bosch, F. (2014). Targeting the proliferative and chemoresistant compartment in chronic lymphocytic leukemia by inhibiting survivin protein. Leukemia *28*, 1993–2004.

Qi, L.S., Larson, M.H., Gilbert, L.A., Doudna, J.A., Weissman, J.S., Arkin, A.P., and Lim, W.A. (2013). Repurposing CRISPR as an RNA-Guided Platform for Sequence-Specific Control of Gene Expression. Cell *152*, 1173–1183.

Quesada, V., Conde, L., Villamor, N., Ordóñez, G.R., Jares, P., Bassaganyas, L., Ramsay, A.J., Beà, S., Pinyol, M., Martínez-Trillos, A., et al. (2012). Exome sequencing identifies recurrent mutations of the splicing factor SF3B1 gene in chronic lymphocytic leukemia. Nat. Genet. *44*, 47–52.

Rai, K.R., and Montserrat, E. (1987). Prognostic factors in chronic lymphocytic leukemia. Semin. Hematol. *24*, 252–256.

Rai, K.R., Sawitsky, A., Cronkite, E.P., Chanana, A.D., Levy, R.N., and Pasternack, B.S. (1975). Clinical staging of chronic lymphocytic leukemia. Blood *46*, 219–234.

Ramlee, M.K., Yan, T., Cheung, A.M.S., Chuah, C.T.H., and Li, S. (2015). High-throughput genotyping of CRISPR/Cas9-mediated mutants using fluorescent PCR-capillary gel electrophoresis. Sci. Rep. *5*, 15587.

Ramos, J.C., Ruiz, P., Ratner, L., Reis, I.M., Brites, C., Pedroso, C., Byrne, G.E., Toomey, N.L., Andela, V., Harhaj, E.W., et al. (2007). IRF-4 and c-Rel expression in antiviral-resistant adult T-cell leukemia/lymphoma. Blood *109*, 3060–3068.

Ramsay, A.J., Martínez-Trillos, A., Jares, P., Rodríguez, D., Kwarciak, A., and Quesada, V. (2013). Next-generation sequencing reveals the secrets of the chronic lymphocytic leukemia genome. Clin. Transl. Oncol. *15*, 3–8.

Rassenti, L.Z., and Kipps, T.J. (1997). Lack of allelic exclusion in B cell chronic lymphocytic leukemia. J. Exp. Med. *185*, 1435–1445.

Rawlings, D.J., Schwartz, M.A., Jackson, S.W., and Meyer-Bahlburg, A. (2012). Integration of B cell responses through Toll-like receptors and antigen receptors. Nat.

Rev. Immunol. *12*, 282–294.

Refaat, A., Zhou, Y., Suzuki, S., Takasaki, I., Koizumi, K., Yamaoka, S., Tabuchi, Y., Saiki, I., and Sakurai, H. (2011). Distinct roles of transforming growth factor-beta-activated kinase 1 (TAK1)-c-Rel and interferon regulatory factor 4 (IRF4) pathways in human T cell lymphotropic virus 1-transformed T helper 17 cells producing interleukin-9. J. Biol. Chem. *286*, 21092–21099.

Rhodes, D.R., Kalyana-Sundaram, S., Mahavisno, V., Barrette, T.R., Ghosh, D., and Chinnaiyan, A.M. (2005). Mining for regulatory programs in the cancer transcriptome. Nat. Genet. *37*, 579–583.

Rieger, M.A., and Schroeder, T. (2012). Hematopoiesis. Cold Spring Harb. Perspect. Biol. *4*.

Rikova, K., Guo, A., Zeng, Q., Possemato, A., Yu, J., Haack, H., Nardone, J., Lee, K., Reeves, C., Li, Y., et al. (2007). Global survey of phosphotyrosine signaling identifies oncogenic kinases in lung cancer. Cell *131*, 1190–1203.

Rinaldi, A., Mian, M., Kwee, I., Rossi, D., Deambrogi, C., Mensah, A.A., Forconi, F., Spina, V., Cencini, E., Drandi, D., et al. (2011). Genome-wide DNA profiling better defines the prognosis of chronic lymphocytic leukaemia. Br. J. Haematol. *154*, 590–599.

Roberts, A.W., Davids, M.S., Pagel, J.M., Kahl, B.S., Puvvada, S.D., Gerecitano, J.F., Kipps, T.J., Anderson, M.A., Brown, J.R., Gressick, L., et al. (2016). Targeting BCL2 with Venetoclax in Relapsed Chronic Lymphocytic Leukemia. N. Engl. J. Med. *374*, 311–322.

Romieu-Mourez, R., Kim, D.W., Shin, S.M., Demicco, E.G., Landesman-Bollag, E., Seldin, D.C., Cardiff, R.D., and Sonenshein, G.E. (2003). Mouse mammary tumor virus c-rel transgenic mice develop mammary tumors. Mol. Cell. Biol. *23*, 5738–5754.

Roos-Weil, D., Nguyen-Khac, F., Chevret, S., Touzeau, C., Roux, C., Lejeune, J., Cosson, A., Mathis, S., Feugier, P., Leprêtre, S., et al. (2018). Mutational and cytogenetic analyses of 188 CLL patients with trisomy 12: A retrospective study from the French Innovative Leukemia Organization (FILO) working group. Genes, Chromosom. Cancer *57*, 533–540.

Rose-Zerilli, M.J.J., Forster, J., Parker, H., Parker, A., Rodríguez, A.E., Chaplin, T., Gardiner, A., Steele, A.J., Collins, A., Young, B.D., et al. (2014). ATM mutation rather than BIRC3 deletion and/or mutation predicts reduced survival in 11q-deleted chronic lymphocytic leukemia: data from the UK LRF CLL4 trial. Haematologica *99*, 736–742.

Rosenbauer, F., Owens, B.M., Yu, L., Tumang, J.R., Steidl, U., Kutok, J.L., Clayton, L.K., Wagner, K., Scheller, M., Iwasaki, H., et al. (2006). Lymphoid cell growth and transformation are suppressed by a key regulatory element of the gene encoding PU.1. Nat. Genet. *38*, 27–37.

Rosenwald, A., Alizadeh, A.A., Widhopf, G., Simon, R., Davis, R.E., Yu, X., Yang, L., Pickeral, O.K., Rassenti, L.Z., Powell, J., et al. (2001). Relation of gene expression phenotype to immunoglobulin mutation genotype in B cell chronic lymphocytic leukemia. J. Exp. Med. *194*, 1639–1647.

Rossi, D., and Gaidano, G. (2009). Richter syndrome: molecular insights and clinical perspectives. Hematol. Oncol. *27*, 1–10.

Rossi, D., and Gaidano, G. (2016a). The clinical implications of gene mutations in chronic lymphocytic leukaemia. Br. J. Cancer *114*, 849–854.

Rossi, D., and Gaidano, G. (2016b). Richter syndrome: pathogenesis and management. Semin. Oncol. *43*, 311–319.

Rossi, D., Cerri, M., Deambrogi, C., Sozzi, E., Cresta, S., Rasi, S., De Paoli, L., Spina, V., Gattei, V., Capello, D., et al. (2009). The Prognostic Value of TP53 Mutations in Chronic Lymphocytic Leukemia Is Independent of Del17p13: Implications for Overall Survival and Chemorefractoriness. Clin. Cancer Res. *15*, 995–1004.

Rossi, D., Deaglio, S., Dominguez-Sola, D., Rasi, S., Vaisitti, T., Agostinelli, C., Spina, V., Bruscaggin, A., Monti, S., Cerri, M., et al. (2011). Alteration of BIRC3 and multiple other NF- B pathway genes in splenic marginal zone lymphoma. Blood *118*, 4930–4934.

Rossi, D., Fangazio, M., Rasi, S., Vaisitti, T., Monti, S., Cresta, S., Chiaretti, S., Del Giudice, I., Fabbri, G., Bruscaggin, A., et al. (2012). Disruption of BIRC3 associates with fludarabine chemorefractoriness in TP53 wild-type chronic lymphocytic leukemia. Blood *119*, 2854–2862.

Rossi, D., Rasi, S., Spina, V., Bruscaggin, A., Monti, S., Ciardullo, C., Deambrogi, C., Khiabanian, H., Serra, R., Bertoni, F., et al. (2013). Integrated mutational and cytogenetic analysis identifies new prognostic subgroups in chronic lymphocytic leukemia. Blood *121*, 1403–1412.

Rossi, D., Khiabanian, H., Spina, V., Ciardullo, C., Bruscaggin, A., Famà, R., Rasi, S., Monti, S., Deambrogi, C., De Paoli, L., et al. (2014). Clinical impact of small TP53 mutated subclones in chronic lymphocytic leukemia. Blood *123*, 2139–2147.

Ruiz-Ballesteros, E., Mollejo, M., Rodriguez, A., Camacho, F.I., Algara, P., Martinez, N., Pollán, M., Sanchez-Aguilera, A., Menarguez, J., Campo, E., et al. (2005). Splenic marginal zone lymphoma: proposal of new diagnostic and prognostic markers identified after tissue and cDNA microarray analysis. Blood *106*, 1831–1838.

Ruiz-Lafuente, N., Alcaraz-García, M.-J., Sebastiá N-Ruiz, S., Gó Mez-Espuch, J., Funes, C., Moraleda, J.-M., García-Garay, M.-C., Montes-Barqueros, N., Minguela, A., Lvarez-Ló Pez, M.-R., et al. (2014). The Gene Expression Response of Chronic Lymphocytic Leukemia Cells to IL-4 Is Specific, Depends on ZAP-70 Status and Is Differentially Affected by an NFkB Inhibitor. PLoS One *9*.

Ruiz-Pérez, M.V., Henley, A.B., and Arsenian-Henriksson, M. (2017). The MYCN Protein in Health and Disease. Genes (Basel). *8*, 113.

Ryan, D.E., Taussig, D., Steinfeld, I., Phadnis, S.M., Lunstad, B.D., Singh, M., Vuong, X., Okochi, K.D., McCaffrey, R., Olesiak, M., et al. (2017). Improving CRISPR–Cas specificity with chemical modifications in single-guide RNAs. Nucleic Acids Res. 1–12.

Salvesen, G.S., and Riedl, S.J. (2008). Caspase Mechanisms. In Advances in Experimental Medicine and Biology, pp. 13–23.

Santiago, Y., Chan, E., Liu, P.-Q., Orlando, S., Zhang, L., Urnov, F.D., Holmes, M.C., Guschin, D., Waite, A., Miller, J.C., et al. (2008). Targeted gene knockout in mammalian cells by using engineered zinc-finger nucleases. Proc. Natl. Acad. Sci.

105, 5809–5814.

Sasaki, Y., Derudder, E., Hobeika, E., Pelanda, R., Reth, M., Rajewsky, K., and Schmidt-Supprian, M. (2006). Canonical NF-kB Activity, Dispensable for B Cell Development, Replaces BAFF-Receptor Signals and Promotes B Cell Proliferation upon Activation. Immunity *24*, 729–739.

Sashital, D.G., Jinek, M., and Doudna, J.A. (2011). An RNA-induced conformational change required for CRISPR RNA cleavage by the endoribonuclease Cse3. Nat. Struct. Mol. Biol. *18*, 680–687.

Satterwhite, E., Sonoki, T., Willis, T.G., Harder, L., Nowak, R., Arriola, E.L., Liu, H., Price, H.P., Gesk, S., Steinemann, D., et al. (2001). The BCL11 gene family: Involvement of BCL11A in lymphoid malignancies. Blood *98*, 3413–3420.

Savage, K.J., Harris, N.L., Vose, J.M., Ullrich, F., Jaffe, E.S., Connors, J.M., Rimsza, L., Pileri, S.A., Chhanabhai, M., Gascoyne, R.D., et al. (2008). ALK- anaplastic large-cell lymphoma is clinically and immunophenotypically different from both ALK+ ALCL and peripheral T-cell lymphoma, not otherwise specified: report from the International Peripheral T-Cell Lymphoma Project. Blood *111*, 5496–5504.

Scandurra, M., Rossi, D., Deambrogi, C., Rancoita, P.M. V, Chigrinova, E., Mian, M., Cerri, M., Rasi, S., Sozzi, E., Forconi, F., et al. (2010). Genomic profiling of Richter's syndrome: recurrent lesions and differences with de novo diffuse large B-cell lymphomas. Hematol. Oncol. *28*, 62–67.

Schleiss, C., Ilias, W., Tahar, O., Güler, Y., Miguet, L., Mayeur-Rousse, C., Mauvieux, L., Fornecker, L.-M., Toussaint, E., Herbrecht, R., et al. (2019). BCR-associated factors driving chronic lymphocytic leukemia cells proliferation ex vivo. Sci. Rep. *9*, 701.

Schmitz, N., Trümper, L., Ziepert, M., Nickelsen, M., Ho, A.D., Metzner, B., Peter, N., Loeffler, M., Rosenwald, A., and Pfreundschuh, M. (2010). Treatment and prognosis of mature T-cell and NK-cell lymphoma: an analysis of patients with T-cell lymphoma treated in studies of the German High-Grade Non-Hodgkin Lymphoma Study Group. Blood *116*, 3418–3425.

Schneider, G., Henrich, A., Greiner, G., Wolf, V., Lovas, A., Wieczorek, M., Wagner, T., Reichardt, S., von Werder, A., Schmid, R.M., et al. (2010). Cross talk between stimulated NF-κB and the tumor suppressor p53. Oncogene *29*, 2795–2806.

Schroeder, H.W., Cavacini, L., and Cavacini, L. (2010). Structure and function of immunoglobulins. J. Allergy Clin. Immunol. *125*, S41-52.

Schulte, J.H., Lindner, S., Bohrer, A., Maurer, J., De Preter, K., Lefever, S., Heukamp, L., Schulte, S., Molenaar, J., Versteeg, R., et al. (2013). MYCN and ALKF1174L are sufficient to drive neuroblastoma development from neural crest progenitor cells. Oncogene *32*, 1059–1065.

Seeger, R.C., Brodeur, G.M., Sather, H., Dalton, A., Siegel, S.E., Wong, K.Y., and Hammond, D. (1985). Association of Multiple Copies of the N- *myc* Oncogene with Rapid Progression of Neuroblastomas. N. Engl. J. Med. *313*, 1111–1116.

Seifert, M., Sellmann, L., Bloehdorn, J., Wein, F., Stilgenbauer, S., Dürig, J., and Küppers, R. (2012). Cellular origin and pathophysiology of chronic lymphocytic leukemia. J. Exp. Med. *209*, 2183–2198.

Sekiya, Y., Yamamoto, E., Niimi, K., Nishino, K., Nakamura, K., Kotani, T., Kajiyama, H., Shibata, K., and Kikkawa, F. (2017). c-Rel Promotes Invasion of Choriocarcinoma Cells via PI3K/AKT Signaling. Oncology *92*, 299–310.

Sen, R., and Baltimore, D. (1986b). Inducibility of kappa immunoglobulin enhancer-binding protein Nf-kappa B by a posttranslational mechanism. Cell *47*, 921–928.

Sen, R., and Baltimore, D. (1986a). Multiple Nuclear Factors Interact with the Immunoglobulin Enhancer Sequences. Cell *465716*.

Sen, J., Venkataraman, L., Shinkai, Y., Pierce, J.W., Alt, F.W., Burakoff, S.J., and Sen, R. (1995). Expression and induction of nuclear factor-kappa B-related proteins in thymocytes. J. Immunol. *154*, 3213–3221.

Senftleben, U., Cao, Y., Xiao, G., Greten, F.R., Krähn, G., Bonizzi, G., Chen, Y., Hu, Y., Fong, A., Sun, S.C., et al. (2001). Activation by IKKalpha of a second, evolutionary conserved, NF-kappa B signaling pathway. Science *293*, 1495–1499.

Shalem, O., Sanjana, N.E., Hartenian, E., Shi, X., Scott, D.A., Mikkelsen, T.S., Heckl, D., Ebert, B.L., Root, D.E., Doench, J.G., et al. (2014). Genome-scale CRISPR-Cas9 knockout screening in human cells. Science *343*, 84–87.

Shalem, O., Sanjana, N.E., and Zhang, F. (2015). High-throughput functional genomics using CRISPR-Cas9. Nat. Rev. Genet. *16*, 299–311.

Sharma, S., and Rai, K.R. (2019). Chronic lymphocytic leukemia (CLL) treatment: So many choices, such great options. Cancer.

Shehata, M., Shehata, M., Shehata, F., and Pater, A. (2004). Dual apoptotic effect of Xrel3 c-Rel/NF-κB homolog in human cervical cancer cells. Cell Biol. Int. *28*, 895–904.

Shi, J., Wang, E., Milazzo, J.P., Wang, Z., Kinney, J.B., and Vakoc, C.R. (2015). Discovery of cancer drug targets by CRISPR-Cas9 screening of protein domains. Nat. Biotechnol. *33*, 661–667.

Shiloh, Y., and Ziv, Y. (2013). The ATM protein kinase: regulating the cellular response to genotoxic stress and more. Nat. Rev. Mol. Cell Biol. *14*, 197–210.

Shono, Y., Tuckett, A.Z., Ouk, S., Liou, H.-C., Altan-Bonnet, G., Tsai, J.J., Oyler, J.E., Smith, O.M., West, M.L., Singer, N. V., et al. (2014). A Small-Molecule c-Rel Inhibitor Reduces Alloactivation of T Cells without Compromising Antitumor Activity. Cancer Discov. *4*, 578–591.

Shono, Y., Tuckett, A.Z., Liou, H.-C., Doubrovina, E., Derenzini, E., Ouk, S., Tsai, J.J., Smith, O.M., Levy, E.R., Kreines, F.M., et al. (2016). Characterization of a c-Rel Inhibitor That Mediates Anticancer Properties in Hematologic Malignancies by Blocking NF-κB-Controlled Oxidative Stress Responses. Cancer Res. *76*, 377–389.

Shukla, A., Cutucache, C.E., Sutton, G.L., Pitner, M.A., Rai, K., Rai, S., Opavsky, R., Swanson, P.C., and Joshi, S.S. (2016). Absence of caveolin-1 leads to delayed development of chronic lymphocytic leukemia in Eμ-TCL1 mouse model. Exp. Hematol. *44*, 30–37.e1.

Siebenlist, U., Brown, K., and Claudio, E. (2005). Control of lymphocyte development by nuclear factor-κB. Nat. Rev. Immunol. *5*, 435–445.

De Siervi, A., De Luca, P., Moiola, C., Gueron, G., Tongbai, R., Chandramouli,

G.V.R., Haggerty, C., Dzekunova, I., Petersen, D., Kawasaki, E., et al. (2009). Identification of new Rel/NFkappaB regulatory networks by focused genome location analysis. Cell Cycle *8*, 2093–2100.

Skowronska, A., Parker, A., Ahmed, G., Oldreive, C., Davis, Z., Richards, S., Dyer, M., Matutes, E., Gonzalez, D., Taylor, A.M.R., et al. (2012). Biallelic ATM inactivation significantly reduces survival in patients treated on the United Kingdom Leukemia Research Fund Chronic Lymphocytic Leukemia 4 trial. J. Clin. Oncol. *30*, 4524–4532.

Slotta, C., Schlüter, T., Ruiz-Perera, L.M., Kadhim, H.M., Tertel, T., Henkel, E., Hübner, W., Greiner, J.F.W., Huser, T., Kaltschmidt, B., et al. (2017). CRISPR/Cas9-mediated knockout of c-REL in HeLa cells results in profound defects of the cell cycle. PLoS One *12*, e0182373.

Soda, M., Choi, Y.L., Enomoto, M., Takada, S., Yamashita, Y., Ishikawa, S., Fujiwara, S., Watanabe, H., Kurashina, K., Hatanaka, H., et al. (2007). Identification of the transforming EML4-ALK fusion gene in non-small-cell lung cancer. Nature *448*, 561–566.

Solh, M., Rai, K.R., Peterson, B.L., Kolitz, J.E., Appelbaum, F.R., Tallman, M.S., Belch, A., Larson, R.A., and Morrison, V.A. (2013). The impact of initial fludarabine therapy on transformation to Richter syndrome or prolymphocytic leukemia in patients with chronic lymphocytic leukemia: analysis of an intergroup trial (CALGB 9011). Leuk. Lymphoma *54*, 252–254.

Soma, L.A., Craig, F.E., and Swerdlow, S.H. (2006). The proliferation center microenvironment and prognostic markers in chronic lymphocytic leukemia/small lymphocytic lymphoma. Hum. Pathol. *37*, 152–159.

Son, J.-S., Sahoo, A., Chae, C.-S., Hwang, J.-S., Park, Z.Y., and Im, S.-H. (2011). JunB and c-Rel cooperatively enhance Foxp3 expression during induced regulatory T cell differentiation. Biochem. Biophys. Res. Commun. *407*, 141–147.

Spangrude, G.J., Heimfeld, S., and Weissman, I.L. (1988). Purification and characterization of mouse hematopoietic stem cells. Science *241*, 58–62.

Speedy, H.E., Di Bernardo, M.C., Sava, G.P., Dyer, M.J.S., Holroyd, A., Wang, Y., Sunter, N.J., Mansouri, L., Juliusson, G., Smedby, K.E., et al. (2014). A genome-wide association study identifies multiple susceptibility loci for chronic lymphocytic leukemia. Nat. Genet. *46*, 56–60.

Starczynowski, D.T., Reynolds, J.G., and Gilmore, T.D. (2003). Deletion of either C-terminal transactivation subdomain enhances the in vitro transforming activity of human transcription factor REL in chicken spleen cells. Oncogene *22*, 6928–6936.

Starczynowski, D.T., Trautmann, H., Pott, C., Harder, L., Arnold, N., Africa, J.A., Leeman, J.R., Siebert, R., and Gilmore, T.D. (2007). Mutation of an IKK phosphorylation site within the transactivation domain of REL in two patients with B-cell lymphoma enhances REL's in vitro transforming activity. Oncogene *26*, 2685–2694.

Steele, A.J., Prentice, A.G., Cwynarski, K., Hoffbrand, A.V., Hart, S.M., Lowdell, M.W., Samuel, E.R., and Wickremasinghe, R.G. (2010). The JAK3-selective inhibitor PF-956980 reverses the resistance to cytotoxic agents induced by interleukin-4 treatment of chronic lymphocytic leukemia cells: potential for reversal of

cytoprotection by the microenvironment. Blood *116*, 4569–4577.

Steidl, C., Telenius, A., Shah, S.P., Farinha, P., Barclay, L., Boyle, M., Connors, J.M., Horsman, D.E., and Gascoyne, R.D. (2010). Genome-wide copy number analysis of Hodgkin Reed-Sternberg cells identifies recurrent imbalances with correlations to treatment outcome. Blood *116*, 418–427.

Stilgenbauer, S., Schnaiter, A., Paschka, P., Zenz, T., Rossi, M., Dohner, K., Buhler, A., Bottcher, S., Ritgen, M., Kneba, M., et al. (2014). Gene mutations and treatment outcome in chronic lymphocytic leukemia: results from the CLL8 trial. Blood *123*, 3247–3254.

Stoica, G.E., Kuo, A., Aigner, A., Sunitha, I., Souttou, B., Malerczyk, C., Caughey, D.J., Wen, D., Karavanov, A., Riegel, A.T., et al. (2001). Identification of anaplastic lymphoma kinase as a receptor for the growth factor pleiotrophin. J. Biol. Chem. *276*, 16772–16779.

Strati, P., Abruzzo, L. V., Wierda, W.G., O'Brien, S., Ferrajoli, A., and Keating, M.J. (2015). Second Cancers and Richter Transformation Are the Leading Causes of Death in Patients With Trisomy 12 Chronic Lymphocytic Leukemia. Clin. Lymphoma Myeloma Leuk. *15*, 420–427.

Stratowa, C., L□ffler, G., Lichter, P., Stilgenbauer, S., Haberl, P., Schweifer, N., D□hner, H., and Wilgenbus, K.K. (2001). CDNA microarray gene expression analysis of B-cell chronic lymphocytic leukemia proposes potential new prognostic markers involved in lymphocyte trafficking. Int. J. Cancer *91*, 474–480.

Suenaga, Y., Islam, S.M.R., Alagu, J., Kaneko, Y., Kato, M., Tanaka, Y., Kawana, H., Hossain, S., Matsumoto, D., Yamamoto, M., et al. (2014). NCYM, a Cis-Antisense Gene of MYCN, Encodes a De Novo Evolved Protein That Inhibits GSK3β Resulting in the Stabilization of MYCN in Human Neuroblastomas. PLoS Genet. *10*, e1003996.

Sun, S.-C. (2011). Non-canonical NF-κB signaling pathway. Cell Res. *21*, 71–85.

Sung, Y.H., Baek, I.-J., Kim, D.H., Jeon, J., Lee, J., Lee, K., Jeong, D., Kim, J.-S., and Lee, H.-W. (2013). Knockout mice created by TALEN-mediated gene targeting. Nat. Biotechnol. *31*, 23–24.

Sutton, L., Chevret, S., Tournilhac, O., Divine, M., Leblond, V., Corront, B., Lepretre, S., Eghbali, H., Van Den Neste, E., Michallet, M., et al. (2011). Autologous stem cell transplantation as a first-line treatment strategy for chronic lymphocytic leukemia: a multicenter, randomized, controlled trial from the SFGM-TC and GFLLC. Blood *117*, 6109–6119.

Swerdlow, S.H., Campo, E., Pileri, S.A., Harris, N.L., Stein, H., Siebert, R., Advani, R., Ghielmini, M., Salles, G.A., Zelenetz, A.D., et al. (2016). The 2016 revision of the World Health Organization classification of lymphoid neoplasms. Blood *127*, 2375–2390.

Tait, S.W.G., and Green, D.R. (2010). Cell survival in tough times: The mitochondrial recovery plan. Cell Cycle *9*, 4254–4255.

Takeuchi, K., Choi, Y.L., Soda, M., Inamura, K., Togashi, Y., Hatano, S., Enomoto, M., Takada, S., Yamashita, Y., Satoh, Y., et al. (2008). Multiplex reverse transcription-PCR screening for EML4-ALK fusion transcripts. Clin. Cancer Res. *14*, 6618–6624.

Tanenbaum, M.E., Gilbert, L.A., Qi, L.S., Weissman, J.S., and Vale, R.D. (2014). A protein-tagging system for signal amplification in gene expression and fluorescence imaging. Cell *159*, 635–646.

Tavian, M., Biasch, K., Sinka, L., Vallet, J., and Péault, B. (2010). Embryonic origin of human hematopoiesis. Int. J. Dev. Biol. *54*, 1061–1065.

Taylor, R.C., Cullen, S.P., and Martin, S.J. (2008). Apoptosis: controlled demolition at the cellular level. Nat. Rev. Mol. Cell Biol. *9*, 231–241.

Tees, M.T., and Flinn, I.W. (2017). Chronic lymphocytic leukemia and small lymphocytic lymphoma: two faces of the same disease. Expert Rev. Hematol. *10*, 137–146.

Terajima, M., Kaneko-Kobayashi, Y., Nakamura, N., Yuri, M., Hiramoto, M., Naitou, M., Hattori, K., Yokota, H., Mizuhara, H., and Higashi, Y. (2016). Inhibition of c-Rel DNA binding is critical for the anti-inflammatory effects of novel PIKfyve inhibitor. Eur. J. Pharmacol. *780*, 93–105.

Terns, M.P., and Terns, R.M. (2011). CRISPR-based adaptive immune systems. Curr. Opin. Microbiol. *14*, 321–327.

Thieu, V.T., Nguyen, E.T., McCarthy, B.P., Bruns, H.A., Kapur, R., Chang, C.-H., and Kaplan, M.H. (2007). IL-4-stimulated NF-κB activity is required for Stat6 DNA binding. J. Leukoc. Biol. *82*, 370–379.

Thompson, P.A., O'Brien, S.M., Wierda, W.G., Ferrajoli, A., Stingo, F., Smith, S.C., Burger, J.A., Estrov, Z., Jain, N., Kantarjian, H.M., et al. (2015). Complex karyotype is a stronger predictor than del(17p) for an inferior outcome in relapsed or refractory chronic lymphocytic leukemia patients treated with ibrutinib-based regimens. Cancer *121*, 3612–3621.

Thomson, A.W., and Lotze, M.T. (2003). The Cytokine Handbook - Volume II (Academic Press).

Tian, W., and Liou, H.-C. (2009). RNAi-Mediated c-Rel Silencing Leads to Apoptosis of B Cell Tumor Cells and Suppresses Antigenic Immune Response In Vivo. PLoS One *4*, e5028.

Tirado-Gonzalez, I., Czlonka, E., Nevmerzhitskaya, A., Soetopo, D., Bergonzani, E., Mahmoud, A., Contreras, A., Jeremias, I., Platzbecker, U., Bourquin, J.P., et al. (2017). CRISPR/Cas9 edited NSG mice as PDX models of human leukemia to address the role of niche-derived SPARC. Leukemia 1–17.

Tooze, J.A., Hamzic, E., Willis, F., and Pettengell, R. (2017). Differences between chronic lymphocytic leukaemia and small lymphocytic lymphoma cells by proteomic profiling and SNP microarray analysis. Cancer Genet. *218–219*, 20–38.

Tornatore, L., Sandomenico, A., Raimondo, D., Low, C., Rocci, A., Tralau-Stewart, C., Capece, D., D'Andrea, D., Bua, M., Boyle, E., et al. (2014). Cancer-Selective Targeting of the NF-κB Survival Pathway with GADD45β/MKK7 Inhibitors. Cancer Cell *26*, 495–508.

Tothova, Z., Krill-Burger, J.M., Popova, K.D., Landers, C.C., Sievers, Q.L., Yudovich, D., Belizaire, R., Aster, J.C., Morgan, E.A., Tsherniak, A., et al. (2017). Multiplex CRISPR/Cas9-Based Genome Editing in Human Hematopoietic Stem Cells Models Clonal Hematopoiesis and Myeloid Neoplasia. Cell Stem Cell *21*, 547–555.e8.

Treon, S.P., Xu, L., Yang, G., Zhou, Y., Liu, X., Cao, Y., Sheehy, P., Manning, R.J., Patterson, C.J., Tripsas, C., et al. (2012). MYD88 L265P Somatic Mutation in Waldenström's Macroglobulinemia. N. Engl. J. Med. *367*, 826–833.

Tsimberidou, A.-M., and Keating, M.J. (2005). Richter syndrome. Cancer *103*, 216–228.

Turner, J.G., and Sullivan, D.M. (2008). CRM1-mediated nuclear export of proteins and drug resistance in cancer. Curr. Med. Chem. *15*, 2648–2655.

Tycko, J., Hess, G.T., Jeng, E.E., Dubreuil, M., and Bassik, M.C. (2017). The expanding CRISPR toolbox. Nat. Methods.

Umapathy, G., El Wakil, A., Witek, B., Chesler, L., Danielson, L., Deng, X., Gray, N.S., Johansson, M., Kvarnbrink, S., Ruuth, K., et al. (2014). The kinase ALK stimulates the kinase ERK5 to promote the expression of the oncogene MYCN in neuroblastoma. Sci. Signal. *7*, ra102-ra102.

Vaisitti, T., Gaudino, F., Ouk, S., Moscvin, M., Vitale, N., Serra, S., Arruga, F., Zakrzewski, J.L., Liou, H.-C., Allan, J.N., et al. (2017). Targeting metabolism and survival in chronic lymphocytic leukemia and Richter syndrome cells by a novel NF-κB inhibitor. Haematologica *102*, 1878–1889.

Vangapandu, H. V., Alston, B., Morse, J., Ayres, M.L., Wierda, W.G., Keating, M.J., Marszalek, J.R., Gandhi, V., Vangapandu, H. V., Alston, B., et al. (2018a). Biological and metabolic effects of IACS-010759, an OxPhos inhibitor, on chronic lymphocytic leukemia cells. Oncotarget *9*, 24980–24991.

Vangapandu, H. V, Ayres, M.L., Bristow, C.A., Wierda, W.G., Keating, M.J., Balakrishnan, K., Stellrecht, C.M., and Gandhi, V. (2017). The Stromal Microenvironment Modulates Mitochondrial Oxidative Phosphorylation in Chronic Lymphocytic Leukemia Cells. Neoplasia *19*, 762–771.

Vangapandu, H. V, Chen, H., Wierda, W.G., Keating, M.J., Korkut, A., and Gandhi, V. (2018b). Proteomics profiling identifies induction of caveolin-1 in chronic lymphocytic leukemia cells by bone marrow stromal cells. Leuk. Lymphoma *59*, 1427–1438.

Veldurthy, A., Patz, M., Hagist, S., Pallasch, C.P., Wendtner, C.-M., Hallek, M., and Krause, G. (2008). The kinase inhibitor dasatinib induces apoptosis in chronic lymphocytic leukemia cells in vitro with preference for a subgroup of patients with unmutated IgVH genes. Blood *112*, 1443–1452.

Visco, C., Moretta, F., Falisi, E., Facco, M., Maura, F., Novella, E., Nichele, I., Finotto, S., Giaretta, I., Ave, E., et al. (2013). Double productive immunoglobulin sequence rearrangements in patients with chronic lymphocytic leukemia. Am. J. Hematol. *88*, 277–282.

Vogelstein, B., Papadopoulos, N., Velculescu, V.E., Zhou, S., Diaz, L.A., and Kinzler, K.W. (2013). Cancer genome landscapes. Science (80-.). *340*, 1546–1558.

Wang, C., Li, D., Zhang, L., Jiang, S., Liang, J., Narita, Y., Hou, I., Zhong, Q., Zheng, Z., Xiao, H., et al. (2019). RNA-seq analyses of gene expression during Epstein-Barr virus infection of primary B lymphocytes. J. Virol.

Wang, H., Hong, B., Li, X., Deng, K., Li, H., Lui, V.W.Y., and Lin, W. (2017a). JQ1 synergizes with the Bcl-2 inhibitor ABT-263 against <i>MYCN</i>-amplified

small cell lung cancer. Oncotarget *8*, 86312–86324.

Wang, J., Coombes, K.R., Highsmith, W.E., Keating, M.J., and Abruzzo, L. V. (2004). Differences in gene expression between B-cell chronic lymphocytic leukemia and normal B cells: a meta-analysis of three microarray studies. Bioinformatics *20*, 3166–3178.

Wang, L., Fan, J., Francis, J.M., Georghiou, G., Hergert, S., Li, S., Gambe, R., Zhou, C.W., Yang, C., Xiao, S., et al. (2017b). Integrated single-cell genetic and transcriptional analysis suggests novel drivers of chronic lymphocytic leukemia. Genome Res. *27*, 1300–1311.

Wang, R., Preamplume, G., Terns, M.P., Terns, R.M., and Li, H. (2011). Interaction of the Cas6 Riboendonuclease with CRISPR RNAs: Recognition and Cleavage. Structure *19*, 257–264.

Wang, T., Wei, J.J., Sabatini, D.M., and Lander, E.S. (2014). Genetic Screens in Human Cells Using the CRISPR-Cas9 System. Science (80-.).

van der Watt, P.J., Maske, C.P., Hendricks, D.T., Parker, M.I., Denny, L., Govender, D., Birrer, M.J., and Leaner, V.D. (2009). The Karyopherin proteins, Crm1 and Karyopherin β1, are overexpressed in cervical cancer and are critical for cancer cell survival and proliferation. Int. J. Cancer *124*, 1829–1840.

Watts, E., Heidenreich, D., Tucker, E., Raab, M., Strebhardt, K., Chesler, L., Knapp, S., Bellenie, B., and Hoelder, S. (2019). Designing Dual Inhibitors of Anaplastic Lymphoma Kinase (ALK) and Bromodomain-4 (BRD4) by Tuning Kinase Selectivity. J. Med. Chem. *62*, 2618–2637.

Wellmann, A., Doseeva, V., Butscher, W., Raffeld, M., Fukushima, P., Stetler-Stevenson, M., and Gardner, K. (1997). The activated anaplastic lymphoma kinase increases cellular proliferation and oncogene up-regulation in rat 1a fibroblasts. FASEB J. *11*, 965–972.

Weniger, M.A., Pulford, K., Gesk, S., Ehrlich, S., Banham, A.H., Lyne, L., Martin-Subero, J.I., Siebert, R., Dyer, M.J.S., Möller, P., et al. (2006). Gains of the proto-oncogene BCL11A and nuclear accumulation of BCL11AXL protein are frequent in primary mediastinal B-cell lymphoma. Leukemia *20*, 1880–1882.

Weniger, M.A., Gesk, S., Ehrlich, S., Martin-Subero, J.I., Dyer, M.J.S., Siebert, R., Möller, P., and Barth, T.F.E. (2007). Gains of REL in primary mediastinal B-cell lymphoma coincide with nuclear accumulation of REL protein. Genes. Chromosomes Cancer *46*, 406–415.

Wiedenheft, B., Sternberg, S.H., and Doudna, J.A. (2012). RNA-guided genetic silencing systems in bacteria and archaea. Nature *482*, 331–338.

Wiesner, T., Lee, W., Obenauf, A.C., Ran, L., Murali, R., Zhang, Q.F., Wong, E.W.P., Hu, W., Scott, S.N., Shah, R.H., et al. (2015). Alternative transcription initiation leads to expression of a novel ALK isoform in cancer. Nature *526*, 453–457.

Wiestner, A. (2015). The role of B-cell receptor inhibitors in the treatment of patients with chronic lymphocytic leukemia. Haematologica *100*, 1495–1507.

Woyach, J.A., Furman, R.R., Liu, T.-M., Ozer, H.G., Zapatka, M., Ruppert, A.S., Xue, L., Li, D.H.-H., Steggerda, S.M., Versele, M., et al. (2014). Resistance Mechanisms for the Bruton's Tyrosine Kinase Inhibitor Ibrutinib. N. Engl. J. Med. *370*, 2286–2294.

Xia, Y., Shen, S., and Verma, I.M. (2014). NF- B, an Active Player in Human Cancers. Cancer Immunol. Res. *2*, 823–830.

Xu, J., Zhou, P., Wang, W., Sun, A., and Guo, F. (2014). RelB, together with RelA, sustains cell survival and confers proteasome inhibitor sensitivity of chronic lymphocytic leukemia cells from bone marrow. J. Mol. Med. *92*, 77–92.

Xu, J., Lian, W., Jia, Y., Li, L., and Huang, Z. (2017). Optimized guide RNA structure for genome editing via Cas9. Oncotarget *8*, 94166–94171.

Xu, Z.S., Zhang, J.S., Zhang, J.Y., Wu, S.Q., Xiong, D.L., Chen, H.J., Chen, Z.Z., and Zhan, R. (2015). Constitutive activation of NF-κB signaling by NOTCH1 mutations in chronic lymphocytic leukemia. Oncol. Rep. *33*, 1609–1614.

Yanardağ Açık, D., Yılmaz, M., Sarı, İ., Öztuzcu, S., Sayıner, Z.A., Subari, S., and Demiryürek, A.T. (2016). Investigation of Rho-Kinase Expressions and Polymorphisms in Mantle Cell Lymphoma Patients. Turkish J. Hematol. *33*, 141–147.

Yang, S., Lockwood, A., Hollett, P., Ford, R., and Kao, K. (1998). Overexpression of a novel Xenopus rel mRNA gene induces tumors in early embryos. J. Biol. Chem. *273*, 13746–13752.

Yao, Y., Dong, Y., Lin, F., Zhao, H., Shen, Z., Chen, P., Sun, Y.-J., Tang, L.-N., and Zheng, S.-E. (2009). The expression of CRM1 is associated with prognosis in human osteosarcoma. Oncol. Rep. *21*, 229–235.

Yee, J.-K. (2016). Off-target effects of engineered nucleases. FEBS J. *283*, 3239–3248.

Yigit, B., Wang, N., Chen, S.-S., Chiorazzi, N., and Terhorst, C. (2017). Inhibition of reactive oxygen species limits expansion of chronic lymphocytic leukemia cells. Leukemia *31*, 2273–2276.

Yip, K.W., and Reed, J.C. (2008). Bcl-2 family proteins and cancer. Oncogene *27*, 6398–6406.

Yogev, O., Barker, K., Sikka, A., Almeida, G.S., Hallsworth, A., Smith, L.M., Jamin, Y., Ruddle, R., Koers, A., Webber, H.T., et al. (2016). p53 Loss in MYC-Driven Neuroblastoma Leads to Metabolic Adaptations Supporting Radioresistance. Cancer Res. *76*, 3025–3035.

Youle, R.J., and Strasser, A. (2008). The BCL-2 protein family: opposing activities that mediate cell death. Nat. Rev. Mol. Cell Biol. *9*, 47–59.

Zhang, J., Yin, D., and Li, H. (2014). hMSH2 expression is associated with paclitaxel resistance in ovarian carcinoma, and inhibition of hMSH2 expression in vitro restores paclitaxel sensitivity. Oncol. Rep. *32*, 2199–2206.

Zheng, Q., Cai, X., Tan, M.H., Schaffert, S., Arnold, C.P., Gong, X., Chen, C.-Z., and Huang, S. (2014). Precise gene deletion and replacement using the CRISPR/Cas9 system in human cells. Biotechniques *57*, 115–124.

Zheng, Z., Venkatapathy, S., Rao, G., and Harrington, C. (2002). Expression profiling of B cell chronic lymphocytic leukemia suggests deficient CD1-mediated immunity, polarized cytokine response, altered adhesion and increased intracellular protein transport and processing of leukemic cells. Leukemia *16*, 2429–2437.

Zhou, H.-J., Pham, L. V., Tamayo, A.T., Lin-Lee, Y.-C., Fu, L., Yoshimura, L.C., and

Ford, R.J. (2007). Nuclear CD40 interacts with c-Rel and enhances proliferation in aggressive B-cell lymphoma. Blood *110*, 2121–2127.

Zhou, H., Zhou, M., Li, D., Manthey, J., Lioutikova, E., Wang, H., and Zeng, X. (2017). Whole genome analysis of CRISPR Cas9 sgRNA off-target homologies via an efficient computational algorithm. BMC Genomics *18*, 826.

Zimmerman, K.A., Yancopoulos, G.D., Collum, R.G., Smith, R.K., Kohl, N.E., Denis, K.A., Nau, M.M., Witte, O.N., Toran-Allerand, D., Gee, C.E., et al. (1986). Differential expression of myc family genes during murine development. Nature *319*, 780–783.

Zischewski, J., Fischer, R., and Bortesi, L. (2017). Detection of on-target and off-target mutations generated by CRISPR/Cas9 and other sequence-specific nucleases. Biotechnol. Adv. *35*, 95–104.

Zito Marino, F., Rocco, G., Morabito, A., Mignogna, C., Intartaglia, M., Liguori, G., Botti, G., and Franco, R. (2016). A new look at the ALK gene in cancer: copy number gain and amplification. Expert Rev. Anticancer Ther. *16*, 493–502.

Zuo, E., Huo, X., Yao, X., Hu, X., Sun, Y., Yin, J., He, B., Wang, X., Shi, L., Ping, J., et al. (2017). CRISPR/Cas9-mediated targeted chromosome elimination. Genome Biol. *18*, 224.